

**The Role of Monoethanolamine in Hair Bleaching and Dyeing:
Mechanistic Insights from Model Formulations**

Robert A. W. Smith

Doctor of Philosophy

University of York

Chemistry

September 2014

Abstract

Primarily, the focus of this project was to investigate hair bleaching and dyeing mechanisms, in the presence of ammonia or ethanolamine (MEA), at room temperature. Firstly, the mechanism of hair bleaching by alkaline hydrogen peroxide was explored, using homogeneous solutions of *Sepia* melanin free acid (MFA) as a model for hair melanin. UV-vis spectroscopy was applied to study the rate of melanin bleaching under various conditions. It was established that both hydroxyl radicals and perhydroxyl anions are involved in the bleaching of melanin.

Hydrogen peroxide decomposition and *Sepia* melanin oxidation were then monitored using homogenous model bleaching solutions, to see if differences in hair bleaching when MEA is used instead of ammonia could be explained by a change in chemistry. Dissimilarities were found in ligand-free and etidronic acid (HEDP) systems when the base was altered, due to the presence of differing metal complexes. However, when strong chelating ligands such as ethylenediaminetetraacetic acid (EDTA) are used, no differences were apparent in homogenous model bleaching systems.

The mechanism of dye formation inside hair fibres was then investigated, due to the observation that catalase accelerates the oxidation of dye primaries in aqueous solutions. Dye formation was studied by UV-vis spectroscopy. It was shown that metal ion centres are predominantly responsible for the formation of dyes in the hair cortex. Fe(III) proved to be a more effective catalyst for dye production than Cu(II).

Finally, the effect of MEA on the rate of hair dye formation in aqueous systems was studied, using HPLC and UV-vis spectroscopy. The rate of colour formation in MEA based formulations was found to be greater than in ammonia systems, possibly due to slower degradation of the dyes in MEA systems. It was also found that nucleophilic attack of MEA on preformed dye molecules leads to the formation of different dyes, which incorporate the base into their structure. The formation of these dyes greatly changes the colour of model aqueous dye solutions.

Table of Contents

Abstract.....	ii
Table of Contents.....	iii
List of figures.....	ix
List of tables.....	xvii
Acknowledgements	xviii
Declaration.....	xx
Chapter 1 – Introduction.....	2
1.1 A brief history of hair colouring	2
1.1.1 Modern hair colouring	2
1.2 Human Hair.....	4
1.2.1 The function of human hair	4
1.2.2 The structure of human hair	4
1.3 Melanin Pigments.....	6
1.3.1 Melanogenesis.....	7
1.3.2 Structural studies of eumelanin from both human hair and cuttlefish ink	11
1.4 The chemistry of hair colouring	14
1.4.1 Hair Bleaching	14
1.4.1.1 Hair Damage.....	15
1.4.1.2 Fenton chemistry	17
1.4.1.3 The radical pathway of hydrogen peroxide decomposition	17
1.4.1.4 The non-radical pathway of hydrogen peroxide decomposition	18
1.4.1.5 Mechanism of hair fibre damage.....	21
1.4.1.6 The effect of reactive oxygen species on hair fibres	24

1.4.1.7 Preventing hair fibre damage	25
1.4.1.8 Quantifying hydroxyl radical production	30
1.4.2 Hair Dyeing.....	33
1.5 The role of water in hair colouring.....	35
1.5.1 The role of water in hair bleaching.....	35
1.5.2 The role of water in hair dyeing.....	36
1.6 The application of hair colouring products to hair.....	39
1.6.1 Hair colouring at home	39
1.6.2 Hair colouring in salons.....	40
1.7 The use of MEA in hair colouring formulations.....	41
1.7.1 The possible causes for the differences observed in bleaching systems containing MEA.....	42
1.7.1.1 Hair fibre damage.....	43
1.7.1.2 Bleaching potential	45
1.7.2 The possible causes for the differences observed in dyeing systems containing MEA.....	46
1.7.2.1 Chemical factors.....	46
1.7.2.2 Physical factors.....	48
1.8 Project Aims.....	49
Chapter 2 – Mechanistic studies of soluble melanin bleaching.....	53
2.1 Introduction.....	53
2.1.1 Human hair melanin and <i>Sepia</i> melanin.....	53
2.1.2 Melanin free acid (MFA)	54
2.1.3 The mechanism of melanin degradation.....	55
2.1.4 Possible oxidants of melanin in a Fenton-like system.....	60
2.2 Aims	65

2.3 Experimental Methods	66
2.3 Results and Discussion	69
2.3.1 Preparation of <i>Sepia</i> MFA and bleaching solutions.....	69
2.3.2 Colour fading studies of <i>Sepia</i> MFA.....	71
2.3.3 The copper atom environment during melanin bleaching.....	73
2.3.4 The effect of hydroxyl radicals on <i>Sepia</i> MFA bleaching.....	79
2.3.5 The effect of perhydroxyl anion on <i>Sepia</i> MFA bleaching.....	85
2.3.6 Time delayed chelation of metal ions during <i>Sepia</i> MFA bleaching	88
2.3.7 The role of ammonia in soluble melanin bleaching	96
2.4 Conclusions.....	100

Chapter 3 – A comparison of monoethanolamine-based and ammonia-based hair bleaching systems.....103

3.1 – Introduction.....	103
3.2 Aims	103
3.3 Results & Discussion.....	105
3.3.1 The bleaching of whole hair fibres	105
3.3.2 Hydrogen peroxide decomposition in model aqueous systems	108
3.3.3 The chemistry behind the differences observed in hydrogen peroxide decomposition	113
3.3.4 HEDP degradation.....	125
3.3.5 MEA degradation in the HEDP system.....	130
3.3.6 MEA degradation in the ligand-free formulations	135
3.3.7 The effect of MEA on soluble melanin bleaching.....	141
3.3.8 Hydrogen peroxide decomposition in solutions containing pulverised hair fibres	145

3.4 Conclusions.....	152
Chapter 4 – The Mechanism of Hair Dye Primary Oxidation in Hair Fibres.....	157
4.1 Introduction.....	157
4.1.1 The mechanism of hair dye formation	157
4.1.2 The chemistry behind the formation of dyes during hair colouring	158
4.2 The effect of catalase on dye reagent coupling in aqueous systems to form dyes.....	160
4.3 Aims	163
4.4 Results & Discussion.....	164
4.4.1 The mechanism of dye formation by catalase.....	164
4.4.2 Comparison of whole hair and pulverised hair	168
4.4.3 Dye precursor oxidation within hair fibres.....	170
4.4.4 EDTA treatment of pulverised hair	172
4.4.5 Identifying the types of metal ions that are responsible for dye formation	174
4.5 Conclusions.....	179
Chapter 5 – The effect of replacing ammonia with ethanolamine in dyeing formulations.....	182
5.1 Introduction.....	182
5.1.1 The mechanism of dye formation in binuclear systems.....	183
5.1.2 The mechanism of dye formation in trinuclear systems.....	183
5.2 Aims	186
5.3 Results & Discussion.....	187
5.3.1 Dye formation in aqueous MEA and NH ₃ solutions.....	187

5.3.2 Consumption of dye couplers.....	191
5.3.3 The formation of an additional chromophore in the PAP-MAP-MEA formulation	201
5.3.4 Identification of a new dye in MAP systems when MEA was used as a base	203
5.3.5 Analysis of the MEA incorporated dye (274).....	204
5.3.6 Systems that incorporate MEA into dyes	211
5.3.7 Mechanism of MEA incorporation.....	215
5.4 Conclusions.....	219
Chapter 6 – Conclusions and Further Work.....	222
6.1 Summary.....	222
6.2 Concluding Remarks	226
6.2.1 The mechanism of hair bleaching and dyeing.....	226
6.2.2 The Effect of MEA on hair colouring formulations.....	226
6.3 Further Work	227
Chapter 7 – Experimental.....	230
7.1 Materials and chemicals.....	230
7.2 Instrumentation / techniques	231
7.3 Preparation of buffer solutions containing either ammonia or ethanolamine	233
7.4 Isolation of <i>Sepia</i> melanin	234
7.5 Conversion of <i>Sepia</i> melanin to <i>Sepia</i> MFA	234
7.6 Monitoring the bleaching of <i>Sepia</i> Melanin by UV-vis.....	235
7.7 Monitoring the hydroxyl radical flux of Fenton-like systems	235

7.8 Determination of the hydrogen peroxide decomposition	235
7.9 Verification of hydrogen peroxide concentrations by titration	237
7.10 Phosphate ion analysis during the Fenton-like degradation of HEDP	238
7.11 GC analysis MEA degradation products	238
7.12 Binding Constants	239
7.13 Speciation curves of metal complexes	239
7.14 Monitoring dye formation in aqueous systems by UV-vis	240
7.15 HPLC analysis of dye formation	240
7.16 Separation of the MEA dye molecule in the PAP-MAP system.....	241
Appendix	242
Abbreviations.....	247
List of References	250

List of figures

Figure 1: The general structure of some semi-permanent hair dyes ^{3, 4}	3
Figure 2: Cross-section of a human hair fibre ⁷	5
Figure 3: SEM image of a human hair fibre ⁸	6
Figure 4: Scheme to show the biosynthesis of eumelanin and pheomelanin ¹⁷	8
Figure 5: The biosynthetic pathway for the production of pheomelanin from dopaquinone	9
Figure 6: The main monomer building blocks of eumelanin ^{16, 19}	10
Figure 7: The benzothiazine monomer units that are the basis of the formation of pheomelanin oligomers ^{16, 19}	10
Figure 8: The tentative structures of the eumelanin and pheomelanin oligomers ¹⁶ ..	10
Figure 9: The proposed alignment of DHICA units of eumelanin from NMR studies ²⁹ ..	12
Figure 10: The proposed structure for tyrosinase-based melanin	13
Figure 11: The formation of possible hypervalent iron complexes as intermediates of Fenton chemistry ⁶⁶	19
Figure 12: Scheme to show the catalytic pathway of hydrogen peroxide decomposition by catalase ⁷⁴	21
Figure 13: A possible mechanism of protein oxidation by hydroxyl radical and by redox metals. ⁷⁸	22
Figure 14: One of the possible mechanisms of disulphide bond cleavage in alkaline media ⁸¹	23
Figure 15: Scheme to show the possible routes of disulphide bond cleavage to form sulfonic acid, via cystine oxide intermediates ^{10, 80}	23
Figure 16: SEM images of (a) an untreated hair fibre, (b) & (c) hair fibres treated with 6% H ₂ O ₂ at pH 10.2 (21 °C) or (d) a hair fibre treated with a bleach crème treatment of 9% H ₂ O ₂ at pH 8.6 (21 °C) ⁸⁵	24
Figure 17: The structure of the chelating ligand EDTA.	27
Figure 18: Speciation plot to show the copper complexes formed in a model hair system containing 400 mM NH ₃ , 13.95 mM EDTA, 170 mM Ca ²⁺ and 1.27 mM Cu ²⁺ ⁶⁰ ..	28
Figure 19: The structure of the chelating ligand EDDS.	29
Figure 20: Speciation plot to show the copper complexes formed in a model hair system containing 400 mM NH ₃ , 13.95 mM EDDS, 170 mM Ca ²⁺ and 1.27 mM Cu ²⁺ ⁶⁰ ..	30
Figure 21: The generation of DMPO-OH adduct from the reaction of hydroxyl radical with DMPO ⁹⁸ ..	31
Figure 22: The typical EPR spectrum for the DMPO-OH adduct ⁹⁹	31

Figure 23: Mechanism to show the hydroxylation of DMPO by water in the presence of Fe(III) ⁹⁸	32
Figure 24: The colorimetric probe NPDPA.	32
Figure 25: Scheme to show the formation of permanent dye molecules by the oxidation of PPD.....	34
Figure 26: Structures of the bases ethanolamine and ammonia.....	42
Figure 27: The formation of radicals by the reaction of MEA with hydroxyl radical ¹²⁵	43
Figure 28: Some examples of the possible complexes that can form as a result of the use of MEA and ammonia in hair colouring systems.....	44
Figure 29: The speciation plot for a solution containing 400 mM MEA, 1.3 mM EDDS, 0.18 mM Cu(II) and 70 mM H ₂ O ₂	48
Figure 30: Two of the possible monomeric units (A) & (B) that are more abundant in Sepia MFA	55
Figure 31: The general reaction scheme for the breakdown of monomeric indole-based units to pyrrolic acids.	56
Figure 32: Possible mechanism of the breakdown of eumelanin oligomers by hydrogen peroxide and copper ions to form PDCA.	57
Figure 33: Possible mechanism of the breakdown of eumelanin oligomers by hydrogen peroxide and copper ions to form PTCA.....	58
Figure 34: An additional reaction pathway for the breakdown of eumelanin into alternative pyrrolic acids ^{147, 148}	59
Figure 35: Disproportionation of the melanin radical	61
Figure 36: Proposed mechanism for the production of hydrogen peroxide on the irradiation of melanin with UV radiation.	62
Figure 37: The mechanism for the metal ion oxidation of catechol, in the presence of oxygen, that could potentially be applied to melanin.....	63
Figure 38: The mechanism of hydroxylation of the colorimetric probe NPDPA	67
Figure 39: The UV-vis spectrum of (i) 0.03 mg mL ⁻¹ Sepia MFA in 400 mM NH ₄ OH at pH 10 & 20 °C, exhibiting broadband absorbance (ii) 8 mM hydrogen peroxide in water (iii) 0.03 mg mL ⁻¹ Sepia MFA that has been bleached for 120 minutes at pH 10 & 20 °C in the presence of 400 mM NH ₄ OH, 0.18 mM Cu(II) and 0.979 M H ₂ O ₂ , exhibiting a uniform decrease in absorbance in the visible region.	70
Figure 40: UV-vis spectra to show the fading of Sepia MFA over 2 hours at 20 °C where it was dissolved in 20 mM NH ₃ at pH 10 in the presence of 0.18 mM Cu(II).	72
Figure 41: The binding of metals by melanin residue at alkaline pH ¹⁵³	74
Figure 42: EPR spectra of frozen solutions at 140 K containing 20 mM NH ₄ OH, 0.18 mM Cu(II), (1.3 mM EDTA) and/or (0.06 mg mL ⁻¹ Sepia MFA at pH 10. Spectral subtraction has been used to remove the melanin signal from all spectra.	75

Figure 43: Graph to show the rates of hydrogen peroxide decomposition for the following systems: 20 mM NH ₃ , 0.18 mM Cu(II), 0.979 M H ₂ O ₂ , (0.06 mg mL ⁻¹ Sepia MFA) at pH 10 & 20 °C. 1.3 mM EDTA, added at 30 seconds.	77
Figure 44: The UV-vis spectra showing an increasing absorbance at 430 nm due to hNPDPA formation during the reaction of 20 mM MEA, 0.18 mM Cu(II) and 0.979 M H ₂ O ₂ and 1 mM NPDPA, at pH 10 & 20 °C.	81
Figure 45: Graph to show the rate of formation of hydroxyl radical, by observation of the absorbance at 430 nm in the following systems: 20 mM NH ₃ , (1.3 mM ligand), 0.18 mM Cu(II), 0.979 M H ₂ O ₂ and 1 mM NPDPA at pH 10 & 20 °C.....	82
Figure 46: Graph to show the rate of melanin bleaching in systems containing 20 mM NH ₃ , (1.3 mM ligand), 0.18 mM Cu(II), 0.979 M H ₂ O ₂ and 0.06 mg mL ⁻¹ Sepia MFA at pH 10 & 20 °C.	83
Figure 47: Graph to show melanin bleaching in the following system: 20 mM NH ₃ , (1.3 mM ligand), 0.18 mM Cu(II), 0.979 M H ₂ O ₂ and 0.06 mg mL ⁻¹ MFA at pH 10 or 7 & 20 °C.....	86
Figure 48: Graph to show hydroxyl radical flux in the following systems: 20 mM NH ₃ , (1.3 mM ligand), 0.18 mM Cu(II), 0.979 M H ₂ O ₂ and 1 mM NPDPA at pH 10 or 7 & 20 °C.	87
Figure 49: Graph to show how the time-delayed addition of 1.3 mM EDTA affects the bleaching of Sepia MFA in the following system: 20 mM NH ₃ , 0.18 mM Cu(II), 0.979 M H ₂ O ₂ and 0.06 mg mL ⁻¹ Sepia MFA at pH 10 & 20 °C.....	89
Figure 50: UV-vis spectra over the time course of melanin bleaching, showing a shoulder in the absorbance at 400 nm for the following system: 20 mM NH ₃ , 0.18 mM Cu(II), 0.979 M H ₂ O ₂ and 0.06 mg mL ⁻¹ Sepia MFA at pH 10 & 20 °C.....	90
Figure 51: UV-vis spectra over the time course of melanin bleaching, showing no shoulder in the absorbance at 400 nm for the following system: 20 mM NH ₃ , 1.3 mM EDTA, 0.18 mM Cu(II), 0.979 M H ₂ O ₂ and 0.06 mg mL ⁻¹ Sepia MFA at pH 10 & 20 °C.	91
Figure 52: Graph to show how the time-delayed addition of 1.3 mM EDTA affects the bleaching of Sepia MFA in the following composition: 20 mM NH ₃ , 0.18 mM Cu(II), 0.979 M H ₂ O ₂ and 0.06 mg mL ⁻¹ Sepia MFA at pH 7 & 20 °C.	92
Figure 53: Graph to show the effect of pH on the rate of Sepia MFA bleaching in the following compositions: 20 mM ammonia, 0.18 mM Cu(II), 0.979 M H ₂ O ₂ and 0.06 mg mL ⁻¹ Sepia MFA at pH 10 or 7 & 20 °C(1.3 mM EDTA added at 1 minute).	93
Figure 54: Mechanism to show the reactivity of hydroxyl radical towards indole-like molecules.	94
Figure 55: Potential mechanism of hydroxyl radical mediated melanin oxidation in the absence of perhydroxyl anions.....	95
Figure 56: Heterogeneous melanin bleaching (400 mM NH ₃ , 2 mg mL ⁻¹ Sepia melanin & 1.63 M H ₂ O ₂ at pH 10 & 20 °C) at (a) 0 hours and (b) 12 hours.....	97

Figure 57: Heterogeneous melanin bleaching (400 mM NaOH, 2 mg mL ⁻¹ Sepia melanin & 1.63 M H ₂ O ₂ at pH 10 & 20 °C) at (a) 0 hours and (b) 12 hours	97
Figure 58: Graph to show the differences in Sepia MFA bleaching on varying the base for the following systems: 20 mM base, (1.3 mM ligand), 0.18 mM Cu(II), 0.979 M H ₂ O ₂ and 0.06 mg mL ⁻¹ Sepia MFA at pH 10 & 20 °C.	98
Figure 59: Graph to show the effect of base on hydroxyl radical production for the following systems: 20 mM base, (1.3 mM ligand), 0.18 mM Cu(II), 0.979 M H ₂ O ₂ and 1 mM NPDPA at pH 10 & 20 °C.	99
Figure 60: The relative rates of hydrogen peroxide decomposition due to whole hair fibres dosed with copper ions for the following systems: (400 mM base, 2.5 mg mL ⁻¹ whole hair fibres and 0.979 M H ₂ O ₂ at pH 10 & 20 °C)	107
Figure 61: The level of hydroxyl radical flux in bleaching systems containing 20 mM MEA, (1.3 mM ligand), 0.18 mM Cu(II), 0.979 M H ₂ O ₂ and 1 mM NPDPA at pH 10 & 20 °C.	112
Figure 62: The relative rates of hydrogen peroxide decomposition for the following compositions: (400 mM base, 0.18 mM Cu(II) and 0.979 M H ₂ O ₂ at pH 10 & 20 °C)	114
Figure 63: The speciation plot for 400 mM NH ₃ , 0.18 mM Cu(II) and 0.979 M H ₂ O ₂ at pH 10.	115
Figure 64: The speciation plot for 400 mM MEA, 0.18 mM Cu(II) and 0.979 M H ₂ O ₂ at pH 10.	115
Figure 65: The relative rates of hydrogen peroxide decomposition for the following systems: (400 mM base, 1.3 mM HEDP, 0.18 mM Cu(II) and 0.979 M H ₂ O ₂ at pH 10 & 20 °C). Thanks to Kazim Naqvi for allowing the use of the ammonia data in this figure.	117
Figure 66: The speciation plot for 400 mM NH ₃ , 1.3 mM HEDP, 0.18 mM Cu(II) and 0.979 M H ₂ O ₂ at pH 10.	118
Figure 67: The speciation plot for 400 mM MEA, 1.3 mM HEDP, 0.18 mM Cu(II) and 0.979 M H ₂ O ₂ at pH 10.	118
Figure 68: The relative rates of hydrogen peroxide decomposition for the following systems: (20 mM base, 1.3 mM HEDP, 0.18 mM Cu(II) and 0.979 M H ₂ O ₂ at pH 10 & 20 °C). Thanks to Kazim Naqvi for allowing the use of the ammonia data in this figure.	120
Figure 69: The speciation plot for 20 mM NH ₃ , 1.3 mM HEDP, 0.18 mM Cu(II) and 0.979 M H ₂ O ₂ at pH 10.	121
Figure 70: The speciation plot for 20 mM MEA, 1.3 mM HEDP, 0.18 mM Cu(II) and 0.979 M H ₂ O ₂ at pH 10.	121
Figure 71: pH profile during hydrogen peroxide decomposition for systems containing 20 mM base, 1.3 mM HEDP, 0.18 mM Cu(II) and 0.979 M H ₂ O ₂ at pH 10 & 20 °C.	123

Figure 72: Speciation plot to show the copper complexes formed in a model hair system containing 400 mM MEA, 13.95 mM EDDS, 170 mM Ca ²⁺ and 1.27 mM Cu ²⁺ ⁶⁰	124
Figure 73: The structure of HEDP.....	125
Figure 74: ¹ H NMR spectrum of 20 mM MEA, 1.3 mM HEDP, 0.18 mM Cu(II) and 0.979 M H ₂ O ₂ for 0 minutes and for 120 minutes of reaction time.	126
Figure 75: Normalised concentration of MEA and HEDP during the reaction of 20 mM MEA, 1.3 mM HEDP, 0.18 mM Cu(II) and 0,979 M H ₂ O ₂	127
Figure 76: UV spectrum of the molybdenum blue complex, showing the peak at 882 nm that is used for phosphate analysis.	128
Figure 77: The production of phosphate, as a result of HEDP degradation, for formulations containing 20 mM base, 1.3 mM HEDP, 0.18 mM Cu(II) and 0.979 M H ₂ O ₂ at pH 10 & 20 °C. Thanks to Kazim Naqvi for allowing the use of the ammonia data in this figure.	129
Figure 78: ¹ H NMR spectra of the –CH ₂ peaks of MEA.....	130
Figure 79: The possible mechanistic pathways of MEA degradation by single electron oxidants ^{182, 183}	132
Figure 80: The experimental titrations and the predicted titrations of a 20 mL solution of 8.83 mM MEA, 4.21 mM acetic acid, 0.18 mM Cu(II) and 2.26 mM phosphate and 1.4 mM formic acid against 30 mM HCl, as well as the equivalence points of the titrations.	134
Figure 81: The pH profile during hydrogen peroxide decomposition for systems containing 20 mM MEA, (1.3 mM ligand), 0.18 mM Cu(II) and 0.979 M H ₂ O ₂ at 20 °C.	135
Figure 82: The increasing absorbance at 365 nm observed during the reaction of 400 mM MEA, 0.18 mM Cu(II) and 0.979 M H ₂ O ₂ at pH 10 & 20 °C.....	136
Figure 83: Chromatogram of a solution of 400 mM MEA, 0.18 mM Cu(II), 0.979 M H ₂ O ₂	137
Figure 84: Mass spectrum (EI) of the peak at 6.022 minutes	138
Figure 85: The proposed structure of the peak at 6.022 minutes in Figure 83.	138
Figure 86: The possible mechanism of HEI formation ^{181, 183, 186}	139
Figure 87: The rate of degradation of MEA in a solution containing 400 mM MEA, 0.18 mM Cu(II) and 0.979 M H ₂ O ₂ at pH 10 & 20 °C.....	140
Figure 88: Graph to show the rate of melanin bleaching in the following systems: 20 mM MEA or 20 mM ammonia, (1.3 mM ligand), 0.18 mM Cu(II), 0.979 M H ₂ O ₂ and 0.06 mg mL ⁻¹ Sepia MFA at pH 10 & 20 °C.	143
Figure 89: Heterogeneous melanin bleaching for systems containing 400 mM base, 2.5 mg mL ⁻¹ Sepia melanin & 1.63 M H ₂ O ₂ at pH 10 & 20 °C. (a) ammonia, 0 h, (b) MEA, 0 h, (c) ammonia, 12 h & (d) MEA, 12 h.	144

Figure 90: The effect of changing the base on hydrogen peroxide decomposition for systems containing 400 mM base, 2.5 mg mL ⁻¹ pulverised hair and 0.979 M H ₂ O ₂ at pH 10 & 20 °C.	147
Figure 91: The effect of pulverised and whole hair fibres on hydrogen peroxide decomposition for systems containing 400 mM NH ₃ , 2.5 mg mL ⁻¹ hair and 0.979 M H ₂ O ₂ at pH 10 & 20 °C.	149
Figure 92: The effect of pulverised hair on the decomposition of hydrogen peroxide for systems containing 400 mM NH ₃ , (n) mM Cu(II), 0.979 M H ₂ O ₂ and (2.5 mg mL ⁻¹ pulverised hair) at pH 10 & 20 °C.	150
Figure 93: Oxidation of the aromatic amine PPD to QDI	157
Figure 94: Mechanism to show the coupling of AHT to QDI to form indamine dye molecules	158
Figure 95: Graph to show the increase in dye coupling on addition of 0.1 mL catalase to the following composition: 400 mM NH ₃ , 1.3 mM EDDS, 0.18 mM Cu(II), 70 mM H ₂ O ₂ , 1 mM PAP and 1 mM AHT at pH 10 and 20 °C.	161
Figure 96: (Above left) the structure of human erythrocyte catalase (The four porphyrin heme groups are shown in blue). (Above right) the structure of each heme group ^{203, 204}	162
Figure 97: Graph to show the increase in dye reagent coupling on addition of 0.1 mL catalase to the following system: 400 mM base, 1.3 mM EDDS, 0.18 mM Cu(II), 70 mM H ₂ O ₂ , 1 mM primary and 1 mM coupler at pH 10 & 20 °C.	165
Figure 98: Graph to show the effect of 0.1 mL catalase on the coupling of PAP-AHT, with and without the hydrogen peroxide in the following system: 400 mM NH ₃ , 1.3 mM EDDS, 0.18 mM Cu(II), 0.07 M H ₂ O ₂ , 1 mM PAP and 1 mM AHT at pH 10 & 20 °C.	167
Figure 99: Graph to show the effect of adding pulverised hair or whole hair to an aqueous system containing 400 mM NH ₃ , 1.3 mM EDDS, 0.18 mM Cu(II), 70 mM H ₂ O ₂ , 1 mM PAP and 1 mM AHT at pH 10 & 20 °C.	169
Figure 100: Graph to show the effect of pulverised hair and EDTA rinsed pulverised hair on the coupling of PAP-AHT in the following system: 400 mM NH ₃ , 1.3 mM EDDS, 0.18 mM Cu(II), 0.07 M H ₂ O ₂ , 1 mM PAP and 1 mM AHT at pH 10 & 20 °C.	173
Figure 101: The rate of primary species oxidation in formulations containing 400 mM NH ₃ , 1.3 mM EDDS, 0.18 mM Cu(II), 70 mM H ₂ O ₂ , 1 mM PAP and 1 mM AHT at pH 10 & 20 °C when 10 mg pulverised hair (218.0 or 13.1 ppm Cu(II)) is added at 25 minutes.	175
Figure 102: The effect of metal ion dosed pulverised hair fibres on primary oxidation in systems containing 400 mM NH ₃ , 1.3 mM EDDS, 0.18 mM Cu(II), 70 mM H ₂ O ₂ , 1 mM PAP and 1 mM AHT at pH 10 & 20 °C.	177
Figure 103: Possible mechanisms for the formation of trinuclear dye species from PPD and from MAP. (a) nucleophilic attack of PPD on a binuclear dye (b) electrophilic attack of QDI on a leuco dye intermediate.	184

Figure 104: Examples of UV-vis spectra for the following dye formulations, 400 mM NH ₃ , 1.3 mM EDDS, 0.18 mM Cu(II), 70 mM H ₂ O ₂ , 1 mM primary and 1 mM coupler at pH 10 & 20 °C.	189
Figure 105: The relative rates of dye formation in aqueous dye baths containing 400 mM base, 1.3 mM EDDS, 0.18 mM Cu(II), 70 mM H ₂ O ₂ , 1 mM primary and 1mM coupler at pH 10 & 20 °C. (The base used is MEA or ammonia, the primary used is PAP or PPD and the coupler used is MAP or AHT).....	190
Figure 106: Chromatogram to show dye formation after 2 hours for the following system: 400 mM NH ₃ , 1.3 mM EDDS, 0.18 mM Cu(II), 70 mM H ₂ O ₂ , 1 mM PPD and 1 mM MAP at pH 10 & 20 °C.....	192
Figure 107: The ESI mass spectrum of the peak at 31.2 minutes.....	193
Figure 108: UV-vis spectrum of the peak at 31.2 minutes (λ_{\max} = 506 nm).....	194
Figure 109: The ESI mass spectrum of the peak at 42.2 minutes.....	194
Figure 110: UV-vis spectrum of the peak at 42.2 minutes.	195
Figure 111: Chromatogram to show dye formation after 30 minutes for the following system: 400 mM NH ₃ , 1.3 mM EDDS, 0.18 mM Cu(II), 70 mM H ₂ O ₂ , 1 mM PPD and 1 mM AHT at pH 10 & 20 °C.	196
Figure 112: Calibration curve to show how the HPLC peak areas at ~11 minutes changes with concentration of the coupler MAP.	197
Figure 113: Calibration curve to show how the HPLC peak area at ~19 minutes changes with concentration of the coupler AHT.	198
Figure 114: Chart to show a relative estimate of the amount of non-specific dye formed after 30 minutes of the following reaction: 400 mM base, 1.3 mM EDDS, 0.18 mM Cu(II), 70 mM H ₂ O ₂ , 1 mM primary and 1 mM coupler at pH 10 & 20 °C.....	198
Figure 115: Chart to show a relative estimate of the amount of non-specific dye formed after 2 hours of the following reaction: 400 mM base, 1.3 mM EDDS, 0.18 mM Cu(II), 70 mM H ₂ O ₂ , 1 mM primary and 1 mM coupler at pH 10 & 20 °C.....	199
Figure 116: Chromatogram to show the dyes formed in the following system: 400 mM MEA, 1.3 mM EDDS, 0.18 mM Cu(II), 70 mM H ₂ O ₂ , 1 mM PAP and 1 mM MAP at pH 10 & 20 °C.	202
Figure 117: Mass spectrum of peak 1 from the chromatogram shown in Figure 116.	203
Figure 118: The possible structure of the dye formed in the PAP-MAP dyeing reaction when MEA is used as a base.	203
Figure 119: ¹ H NMR spectrum for dye molecule 274	205
Figure 120: The proposed structure of the dye molecule 274	205
Figure 121: ¹ H COSY spectrum for dye molecule 274.....	206
Figure 122: HSQC spectrum for dye molecule 274.....	207
Figure 123: The proposed structure for dye molecule 274 with labelled carbons .	208
Figure 124: HMBC spectrum for dye molecule 274.....	209
Figure 125: An alternative isomer for dye molecule 274	211

Figure 126: UV-vis spectrum for PAP-MAP dimer in H ₂ O.	214
Figure 127: UV-vis spectrum of the MEA incorporated PAP-MAP dimer in H ₂ O.....	214
Figure 128: Mechanism to show the possible formation of dye molecule 274 by nucleophilic attack of MEA on PPD-MAP dimer.	216
Figure 129: Mechanism to show the possible generation of a protonated imine electrophile from MEA that could then react with leuco dye to give an MEA incorporated dye.....	216
Figure 130: MS to show the formation of dyes in the following system: 400 mM NH ₃ , 1.3 mM EDDS, 0.18 mM Cu(II), 70 mM H ₂ O ₂ , 1 mM PPD and 1 mM MAP at pH 10 & 20 °C	217
Figure 131: MS to show the formation of dyes in the following system: 400 mM NH ₃ , 1.3 mM EDDS, 0.18 mM Cu(II), 70 mM H ₂ O ₂ , 1 mM PPD and 1 mM MAP at pH 10 & 20 °C (+800 mM MEA).....	218
Figure 132: Diagram to show the experimental setup that was used to monitor hydrogen peroxide decomposition in Fenton(-like) reactions.	236
Figure 133: Mass spectrum for the product of a reaction solution containing 400 mM MEA, 1.3 mM EDDS, 0.18 mM Cu(II), 70 mM H ₂ O ₂ , 1 mM MBB and 1 mM MAP, at pH 10, after 2 h at 20 °C.....	242
Figure 134: Mass spectrum for a reaction solution containing 400 mM MEA, 1.3 mM EDDS, 0.18 mM Cu(II), 70 mM H ₂ O ₂ , 1 mM PPD and 1 mM MAP, at pH 10, after 2 h at 20 °C.	243
Figure 135: MS/MS of the molecular ion peak at 273.1370 shown in the mass spectrum in Figure 134.	244
Figure 136: Mass spectrum for a reaction solution containing 400 mM MEA, 1.3 mM EDDS, 0.18 mM Cu(II), 70 mM H ₂ O ₂ , 1 mM PAP and 1 mM NAP, at pH 10, after 2 h at 20 °C.	245
Figure 137: Mass spectrum for a reaction solution containing 400 mM NH ₃ , 1.3 mM EDDS, 0.18 mM Cu(II), 70 mM H ₂ O ₂ , 1 mM PPD and 1 mM MAP, at pH 10, after 2 h at 20 °C.	246
Figure 138: Mass spectrum for a reaction solution containing 400 mM NH ₃ , 1.3 mM EDDS, 0.18 mM Cu(II), 70 mM H ₂ O ₂ , 1 mM PAP and 1 mM NAP, at pH 10, after 2 h at 20 °C.	246

List of tables

Table 1: The mean levels of exogenous metal ions found on the surface of human hair samples from around the globe ⁴⁷	16
Table 2: The binding constants of EDTA with the metal ions found in hair ⁹⁵	28
Table 3: The binding constants of EDDS with the metal ions found in hair ⁹⁵	29
Table 4: The measured stability constants of ammonia and MEA copper complexes compared with EDTA and EDDS copper complexes ^{95, 130}	45
Table 5: Partial elemental analysis of Sepia melanin and of Sepia MFA, compared to literature values.	70
Table 6: The hyperfine (A) and g tensors for copper-EDTA and copper-MFA complexes.	75
Table 7: The stability constants of various Cu(II) complexes ^{95, 130}	78
Table 8: The extent of hydrogen peroxide decomposition after 2 hours for the general reaction, 20 mM base, (1.3 mM ligand), 0.18 mM Fe(III) and 0.979 M H ₂ O ₂ at pH 10 & 20 °C.	110
Table 9: The extent of hydrogen peroxide decomposition after 2 hours for the general reaction, 20/400 mM base, (1.3 mM ligand), 0.18 mM Cu(II) and 0.979 M H ₂ O ₂ at pH 10 & 20 °C.	110
Table 10: Retention times and peak identities for the chromatogram shown in Figure 83.....	137
Table 11: The binding constants of some copper complexes ^{95, 130}	188
Table 12: The elution times and identities for the peaks of the chromatogram shown in Figure 106.....	192
Table 13: The elution times and identities for the peaks of the chromatogram shown in Figure 111.....	197
Table 14: The elution times and identities for the peaks of the chromatogram shown in Figure 116.....	202
Table 15: The shifts for the carbons in dye molecule 274 as revealed by HSQC.....	208
Table 16: The HSQC and HMBC interactions with all proton environments for dye molecule 274.....	210
Table 17: Proposed structures of dye products detected by MS on oxidation of dye systems containing MAP	212
Table 18: Proposed dye products detected by MS on oxidation of the precursors PAP and NAP	213
Table 19: The conditions used to obtain chromatograms for solutions of degraded MEA.	239

Acknowledgements

I would like to extend my gratitude to a number of people, without whom the production of this thesis would not have been possible. Thank you so much for going above and beyond for me.

Firstly, my thanks go to my supervisor Victor Chechik, who supported me throughout this project. I am extremely grateful for all the help and encouragement he has given me over the past 4 years. I would also like to express my appreciation to Simon Godfrey, Jennifer Marsh and Procter & Gamble for providing funding, materials and many valuable discussions. I am also appreciative of the help from my IPM, Paul Walton with MATLAB and copper EPR.

I am indebted to Kazim Naqvi for the help that he has given me throughout this project with the development of methods, the countless important discussions we have shared and for allowing me to use some of his data (*Figure 45* and the data shown for ammonia systems in *Figures 65, 68 & 77*). I would also like to acknowledge Robert Thatcher for his help and expertise in the field of 2D NMR, Jamie Gould for his assistance in the lab, as well as Brendan Garrett for all his help and knowledge about melanin.

Thanks also to the rest of the VC group (present and past), particularly Chiara Baldassarri, Zhou Lu, Thomas Newby and Sindhu Krishna for useful conversations and help in the lab. Thanks to the technicians and stores guys for all their support and the DKS group for providing shelter in their lab, after a small fire. The technical support staff at York have been invaluable. Thanks to Karl Heaton and Helen Robinson for their expertise and help with MS, HPLC-MS and GC-MS, Graeme McCallister for performing CHN analysis, Heather Fish and Pedro Aguiar for their help with 1D & 2D NMR and Jin Guo Wang for his help with EPR.

Finally, thank you to all my family and friends, particularly my parents, sister and grandparents, for providing funding and support when times were hard. I would like to acknowledge Anthony Woodhead and Rob Mitchell, who made sure I had a roof

over my head and also helped sink a few ales with me over the last 4 years. Lastly, thank you Laura for your support while I've been writing. You have done extremely well to put up with me.

Declaration

Except where specific reference is made to other sources, the work presented in this thesis is the work of the author. It has not been submitted, in whole or part, for any other degree.

Rob Smith

Chapter 1

Chapter 1 – Introduction

1.1 A brief history of hair colouring

Humans are perhaps the vainest of all the mammals. For over 4000 years various techniques have been employed to alter the natural colour of human hair fibres. There is now evidence to suggest that hair colouring started with the ancient Egyptians, who went as far as using nanotechnology to cover up their grey hairs. This is the first documented use of hair dyes and it involves the uptake of black PdS nanoparticles by hair, which masks the natural colour¹. Since then, different methods have been used to alter the colour of hair fibres, including the use of organic dyes from henna, marigolds and hibiscus.

In approximately 1860, it was discovered that hydrogen peroxide could be used to lighten the natural colour of hair in a bleaching process. This started a prolonged period of hair loss and scalp burns, but also led to the development of permanent hair dyes, in the early 20th century, which use phenylenediamine and hydrogen peroxide².

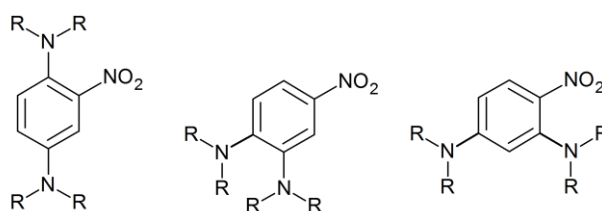
From the time that these colouring systems containing hydrogen peroxide were introduced and marketed, there has been a host of research dedicated to their improvement. This thesis contributes to this research.

1.1.1 Modern hair colouring

Today millions of people worldwide use hair colouring products, which can be separated into 2 major categories, besides bleaching.

1. Semi-permanent dyes

Semi-permanent dyes, as the name suggests, alter the colour of the hair fibre but these dyes can be eventually washed off the hair fibre. The hair will at this point return to its natural colour as the treatment does not chemically alter the natural shade of the hair fibre. Generally, temporary colouring of hair is achieved by the use of pre-formed dyes, based on aromatic nitro compounds that are relatively low in molecular weight, compared to those formed in permanent dye systems³. An example of the structure that these semi-permanent dyes are based on is shown in *Figure 1*. The R groups are changed between hydrogen atoms, alkyl groups and hydroxyethyl groups to achieve a range of colours across the entire visible spectrum^{3, 4}.



R = H, alkyl or hydroxyalkyl

Figure 1: The general structure of some semi-permanent hair dyes^{3, 4}.

2. Permanent dyes

In contrast to semi-permanent dyes, permanent dyes involve the formation of dye molecules within the hair fibre, where they are trapped and prevented from being washed out. As mentioned earlier they are based on systems that use precursors, such as *p*-phenylenediamine, and hydrogen peroxide to generate dye molecules that have a relatively high molecular weight, when compared with the semi-permanent dyes. Some examples of the structures of the dyes produced during this treatment are shown in *Figure 94* and *Figure 103*. Again, by varying functional

groups on the precursors, a range of colours across the entire visible spectrum can be produced.

This work focuses on systems that make use of hydrogen peroxide to alter hair colour permanently either through bleaching and/or permanent oxidative dyeing. The chemistry of these processes will be discussed in more detail later. Before the chemistry behind hair colouring can be discussed, it is important to appreciate the structure and function of hair fibres and also to understand what is responsible for the natural colour of such fibres.

1.2 Human Hair

1.2.1 The function of human hair

The two major functions of hair in non-human primates are camouflage and thermoregulation. Undoubtedly, these are important factors for the survival of primates in the wild. However, for humans, changing selection pressures over time has generally led to a decrease in hair cover, due to the change in the structure of hairs. Generally, less of a change has been observed for human head hair. It is thought that this is due to the role scalp hair plays in the thermoregulation of the brain. Human hair can also serve many other purposes including, protecting the body from harmful UV rays, helping with touch and sense and excreting toxic substances, such as arsenic^{5,6}.

1.2.2 The structure of human hair

The structure of a human head hair fibre is shown in *Figure 2*. The sheath that surrounds the whole hair structure forms part of the hair follicle. This is where hair cells are originally made and then die as they are pushed upwards by newly formed

hair cells, to form the hair shaft. The outer layer of the hair shaft is formally considered to be the cuticle.

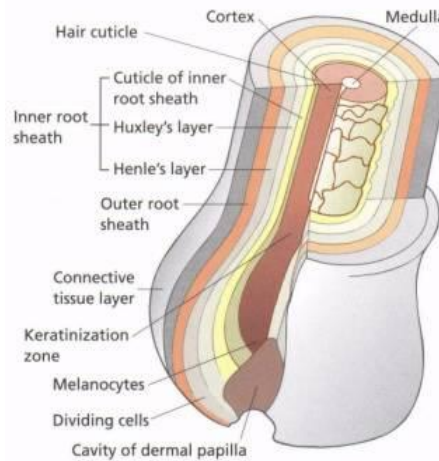


Figure 2: Cross-section of a human hair fibre⁷

The cells in the cuticle layer are flat, square sheets that overlap each other extensively, as shown in *Figure 3*. This arrangement of these cells protects the hair from mechanical stress and ensures that as the hair fibre grows, any dirt and old cells are removed⁸. In addition to this, the hydrophobic molecule 18-methyleicosanoic acid is bound to surface proteins of the cuticle⁹. This is thought to provide a water repellent layer that assists with the drying of the hair fibre⁸. In short, this layer is essentially designed to protect the inner layers of the hair shaft.

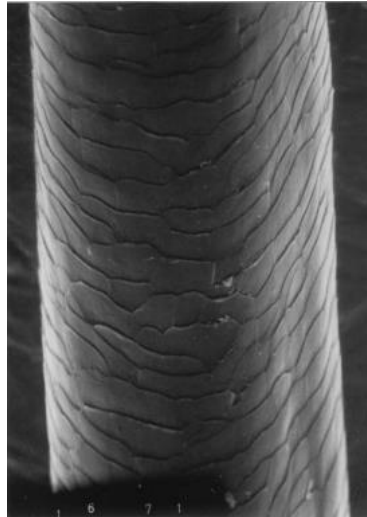


Figure 3: SEM image of a human hair fibre⁸

The cuticle cells are firmly attached to the cortex. This layer is made up of elongated cells that are orientated along the fibre, to provide further mechanical strength⁸. It is here where melanin granules can be found within the hair shaft¹⁰. It is thought that melanin produced by the melanocytes in the hair follicle is ingested into cortical cells by phagocytosis¹¹. It is the melanin pigment in the hair cortex that is responsible for the natural colour of hair fibres^{12, 13}. The function of the final part of the hair shaft, the medulla, is currently unknown.

1.3 Melanin Pigments

As mentioned above, it is the pigment melanin that is responsible for the natural shade of human hair. Melanin predominantly exists in two forms in human hair, eumelanin is brownish black and pheomelanin is reddish yellow^{14, 15}. The exact colour of hair fibres depends on the exact ratios of these melanins within the hair fibre.

1.3.1 Melanogenesis

As mentioned earlier, melanin is made in the melanocytes before it is transferred to the hair cortex. The biosynthesis of melanin is referred to as melanogenesis.

The primary building block of both pheomelanin and eumelanin is the amino acid tyrosine. Inside the melanosome, the enzyme tyrosinase converts the tyrosine to dopaquinone, through dopa. At this stage the incorporation of cysteine into the biosynthetic pathway can lead to the formation of pheomelanin. However, if cysteine is not included, the dopaquinone is cyclised to form cyclodopa. Cyclodopa can also be converted to dopachrome, with the simultaneous transformation of dopaquinone to dopa. Finally, the tautomerisation of dopachrome by dopachrome tautomerase leads to the formation of DHI (5,6-dihydroxyindole) and DHICA (5,6-dihydroxyindole-2-carboxylic acid). Eumelanin is a complex mixture of oligomers, of varying chain length and branching, which are comprised of cyclodopa, dopachrome, DHI and DHICA. This synthetic pathway is outlined in *Figure 4*^{16, 17}.

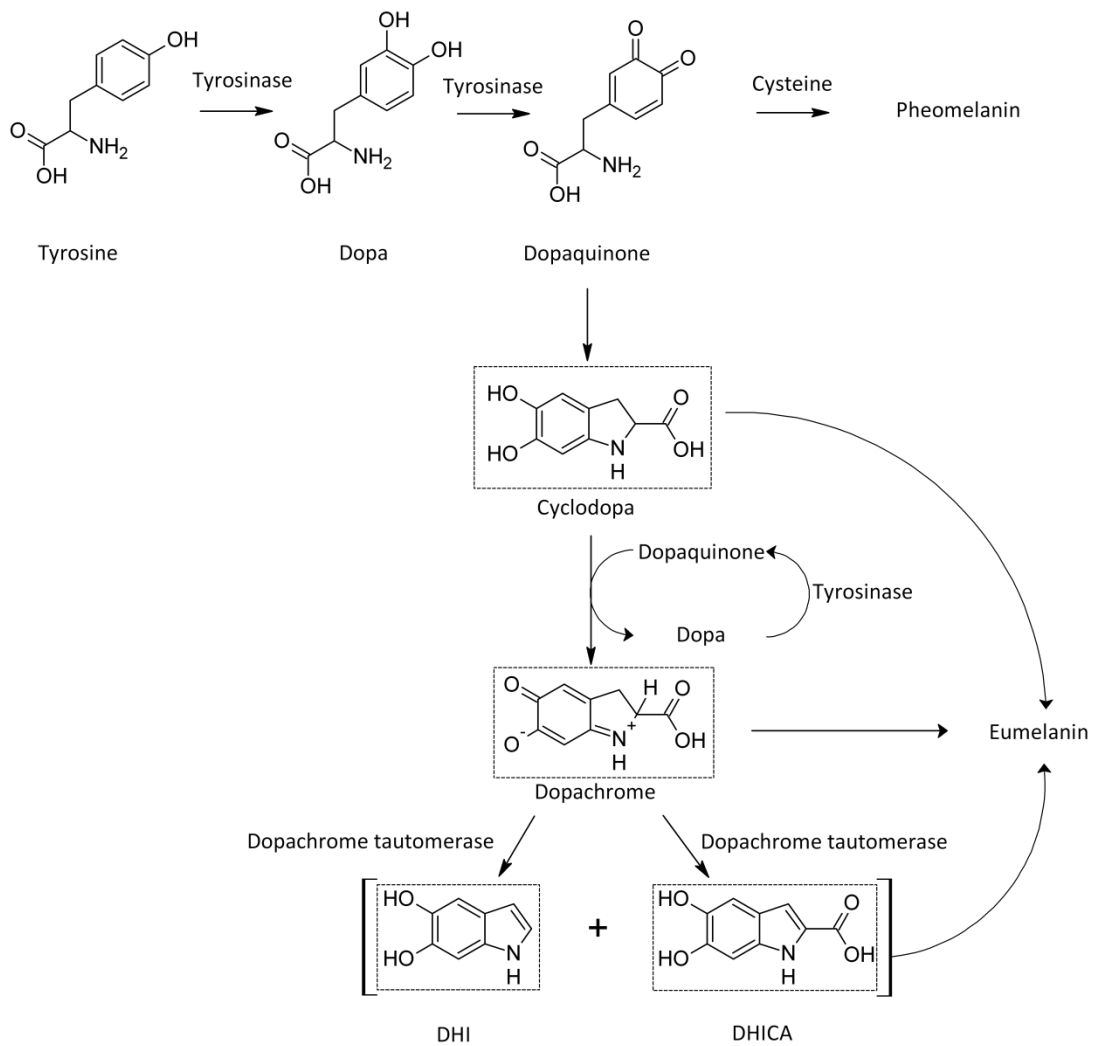


Figure 4: Scheme to show the biosynthesis of eumelanin and pheomelanin¹⁷

When cysteine is incorporated into the melanogenesis, this leads to the production of pheomelanin by melanocytes. This occurs because of a mutation of the melanocortin 1 receptor (MC1R) gene, which is responsible for the variation of skin and hair colour in humans¹⁸. The biosynthetic pathway for the production of pheomelanin is outlined in *Figure 5*. As is shown, cysteine reacts rapidly with dopaquinone to form 5-S-cysteinyl-dopa predominantly with a small amount of 2-S-cysteinyl-dopa being formed. These cysteinyl-dopas are then oxidised by dopaquinone to form cysteinyl-quinones and dopa. The cysteinyl-quinones are then cyclised to form benzothiazine intermediates, which are further oxidised to make up pheomelanin¹⁹.

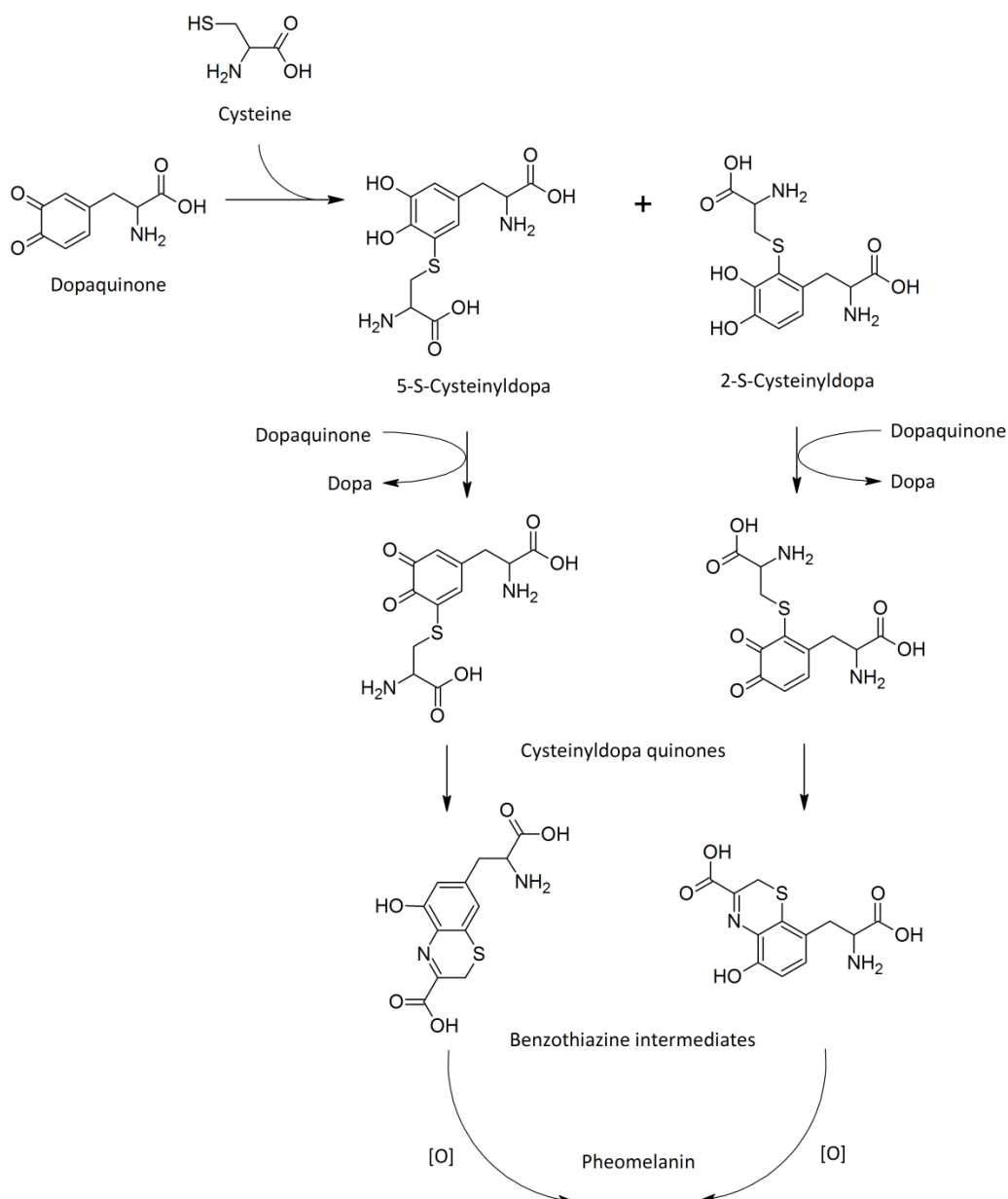


Figure 5: The biosynthetic pathway for the production of pheomelanin from dopaquinone

These biosynthetic pathways result in the monomers that make up eumelanin and pheomelanin oligomeric chains. The main monomers associated with each melanin are shown in Figure 6 and Figure 7, whilst the tentative structures of eumelanin and pheomelanin oligomers are represented in Figure 8. However, in reality, melanin oligomers that are produced are a complex mixture of pheomelanin and eumelanin units¹⁶. This results in a wide variation of human hair colours.

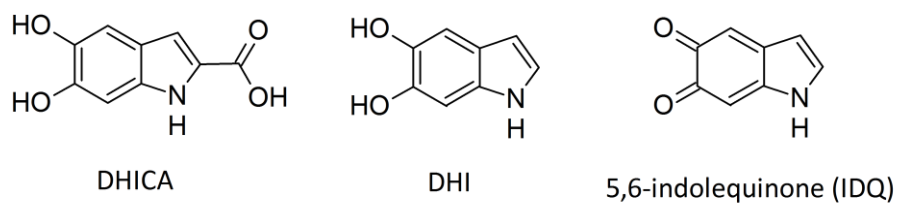


Figure 6: The main monomer building blocks of eumelanin^{16, 19}.

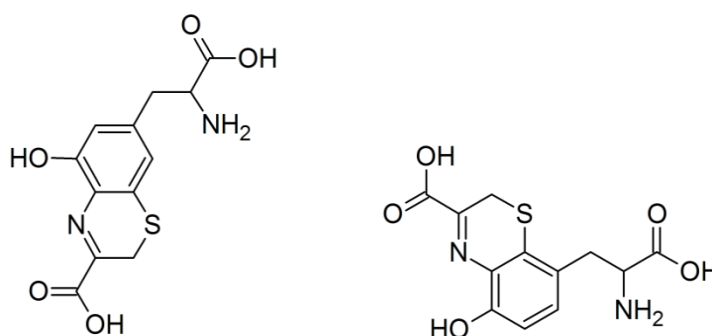


Figure 7: The benzothiazine monomer units that are the basis of the formation of pheomelanin oligomers^{16, 19}.

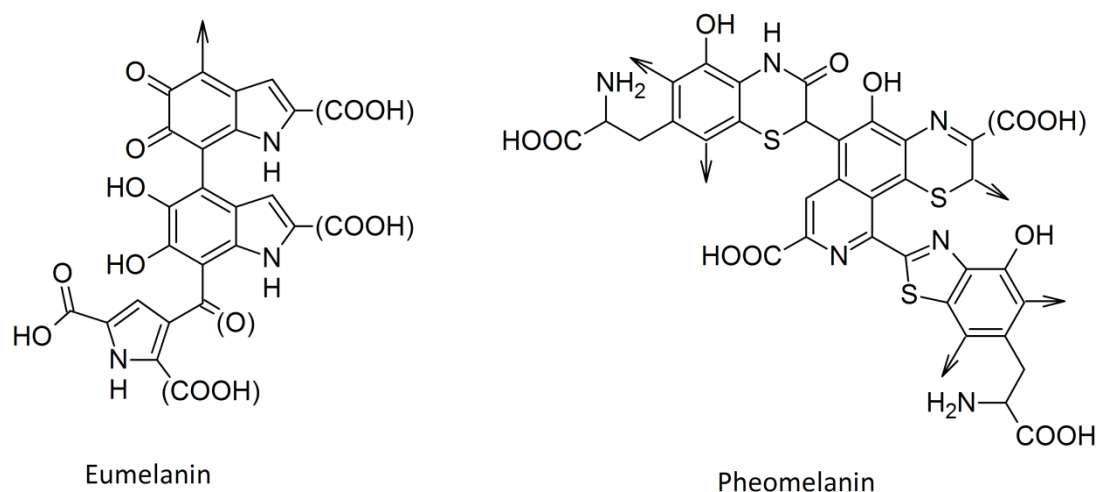


Figure 8: The tentative structures of the eumelanin and pheomelanin oligomers¹⁶.

1.3.2 Structural studies of eumelanin from both human hair and cuttlefish ink

The tentative structure of eumelanin is shown in *Figure 8*. It is worth noting that linkages between monomeric units may also be present between the 2 and 3 positions of the indole ring, if carboxylate groups are not present in these positions. This leads to complex mixtures of randomly organised oligomeric chains, coupled with the fact that these are relatively insoluble in practically all solvents, the structures are very difficult to ascertain²⁰.

Various studies have been attempted, with the intention of clarifying the structure of eumelanin in more detail. For several years the oxidative degradation of melanin was studied using various methods, including acidic permanganate oxidation and alkaline hydrogen peroxide oxidation²¹⁻²³. Using these methods the degradation products can be separated and quantified using HPLC. Under these conditions, eumelanin breaks down to form pyrrolic acids²⁴. Pyrrole-2,3,5-tricarboxylic acid (PTCA) and pyrrole-2,3-dicarboxylic acid (PDCA) can be used as specific markers for the detection of dihydroxyindole carboxylic acid (DHICA) and dihydroxyindole (DHI) monomeric units (*Figure 6*) of eumelanin, respectively²⁵. Although these methods serve to give an indication of the quantities and types of units present, they do not give any indication as to how they are linked together.

NMR is generally a powerful tool for determining the structure of complex molecules. However, the low solubility and irregular arrangement of oligomeric chains leads to broad lines in the NMR spectra of melanins²⁶. Nevertheless, various types of NMR experiments have been employed in order to gain more insight into how the monomeric units of melanin are bound together, including solid-state cross-polarization magic angle spinning (for ¹³C and ¹⁵N NMR)²⁷, water suppression experiments for 2S homo-nuclear decoupled ¹H NMR experiments²⁶ as well as 2D INEPT solid state (¹H-¹³C) NMR²⁸.

The studies yield spectra that are still rather broad, however some useful information has been determined from the data acquired, including the amount of

protons per structural unit and estimations of unit molecular weight. Attempts have also been made to determine the relative DHI and DHICA content of melanins, as well as the preferred positions of substituents on the indole ring. The linkages between DHI units are still unresolved even with these results. However, it is proposed that DHICA units are mainly aligned in a linear manner, due to the carboxylate substituent on the 2 position of the indole ring, which prevents linkages at this position (*Figure 9*)²⁹. If DHICA units are adjacent to each other in the melanin oligomer then this could be the preferred linkage of the monomers. However, the presence of DHI units in melanin will disrupt the sequence of DHICA units connected together.

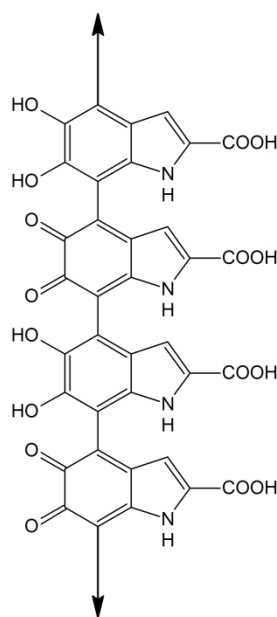


*Figure 9: The proposed alignment of DHICA units of eumelanin from NMR studies*²⁹.

Linkages between DHI units have been visualised using STM and molecular modelling. The structure in *Figure 10* was determined to be viable for synthetic, tyrosinase-based melanin (DHI units only)³⁰. The presence of DHICA units would interrupt this arrangement of DHI monomers. However, the study showed that DHI can form linkages between the 2,3,4 and 7 positions of the indole ring.

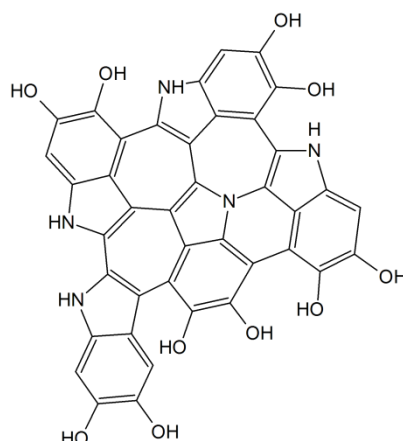


Figure 10: The proposed structure for tyrosinase-based melanin

Unfortunately, the structures shown in *Figure 9* and *Figure 10* cannot exist exclusively for biosynthesised eumelanin, as it contains mixtures of DHICA and DHI units. Therefore, the tentative structure in *Figure 8* is currently the most accepted picture of the possible linkages between monomers.

In addition to providing the natural pigmentation of hair, melanin also plays a vital role in mammalian skin. Again it provides the pigment, but eumelanin can also act as a powerful antioxidant in order to protect cells from damage by reactive oxygen species (ROS), such as hydroxyl radicals and superoxide anions, formed on exposure to UV radiation¹⁷. The reaction of melanin with the superoxide anion is outlined on page 60. By contrast, pheomelanin has been the subject of multiple studies that suggest it behaves as a prooxidant, leading to cell damage in the skin that results in sun burn and melanoma³¹⁻³³. The antioxidant activity of eumelanin means it is also suited to a protective role in the retina³⁴. Additionally, structurally similar neuromelanin is present in the human brain, the biological role of which is not fully understood³⁵⁻³⁷. However, a link has been shown between Parkinson's disease and lower neuromelanin levels, demonstrating the potential importance of neuromelanin in the prevention of cell death³⁸.

1.4 The chemistry of hair colouring

By studying the structure of hair and how natural colour arises, the process of hair colouring can be understood in greater detail. This thesis focuses on “permanent” hair colour changes, including bleaching and oxidative dyeing.

1.4.1 Hair Bleaching

As mentioned earlier, hydrogen peroxide has been used to lighten the natural shade of hair for almost 150 years. In order for this chemically induced hair bleaching to occur it is necessary to break down the melanin granules in the hair cortex that are responsible for the natural colour of the hair³⁹. This poses a significant challenge when the structure of hair fibres is considered.

Firstly, the cuticle is protected by the hydrophobic layer consisting of lipids, including 18-methyleicosanoic acid. This may help to prevent the diffusion of oxidants within aqueous dye baths into the hair cortex. Additionally, the structure of the cuticle itself forms a barrier, which also helps prevent the diffusion of substances into the hair cortex⁸. It is therefore important to discuss how the diffusion of aqueous solutions of hydrogen peroxide into the hair cortex can be facilitated.

On immersion in water, hair fibres are known to swell. This is due to the disruption of hydrogen bonds within proteins inside the hair⁴⁰. However, Wolfram has shown a relationship exists between the pH and the extent of swelling that occurs⁴¹. This could be rationalised by the deprotonation of protein side-chains at high pH, leading to a build-up of negative charges that repel each other. Additionally, the cleavage of disulphide bonds may contribute to the expansion of fibres^{10, 42}. Swelling of hair fibres facilitates the diffusion of hydrogen peroxide through the cuticle layers. Therefore, ammonia can be used to assist diffusion, as it will result in an alkaline pH that leads to significant hair swelling^{43, 44}. A combination of ammonia

and hydrogen peroxide has also been shown to break up and solubilise heterogeneous melanin granules effectively. This occurs as melanin is converted into melanin free acid (MFA), which is a more soluble form of melanin. Conversion of melanin into MFA is accompanied by a slight structural change, discussed in chapter 2. It does not result in substantial colour change of the hair. However, solubilisation of the pigment is sometimes a prerequisite for bleaching to occur. The oxidative breakdown of melanin that follows during bleaching has been proposed to lead to voids within the hair fibre, which also contribute to hair fibre swelling⁴¹.

As well as facilitating diffusion, the alkaline pH (usually this is approximately pH 10) results in the deprotonation of hydrogen peroxide ($pK_a = 11.65$) to generate the perhydroxyl anion⁴⁵. This is a critical function of ammonia in bleaching systems, as the perhydroxyl anion is thought to be an active oxidant in the melanin bleaching process⁴⁶.

Unfortunately, the combination of ammonia and hydrogen peroxide on the human hair leads to complications with the bleaching procedure, that lead to the hair fibres becoming damaged due to the presence of metals on hair fibres.

1.4.1.1 Hair Damage

Hair fibres naturally contain an abundance of endogenous metal ions, within the hair fibre and exogenous metal ions bound to the surface of hair fibres. Endogenous metal ions enter the hair when it is made in the follicle. Exogenous metal ions are present when hair comes into contact with the local environment, for example when the hair is washed. Water is the biggest factor that influences the type and quantity of exogenous metal ions found on the surface of hair. Obviously the types and amounts of metal ions that are transferred from water to hair fibres varies greatly depending on geographical location, as the global distribution of metal ions in water itself differs⁴⁷. Other factors that influence the amounts of metal ions found both within hair fibres and on the surface of fibres include, age, ethnicity,

condition of the hair and any pretreatments that the hair has been exposed to. *Table 1* shows the results from a recent global study by Godfrey, which determined the mean amounts of some metal ions found on hair fibres.

Metal ions	Mean concentration / ppm
Ca ²⁺	4625
Mg ²⁺	302
Cu ²⁺	45
Fe ³⁺	27

Table 1: The mean levels of exogenous metal ions found on the surface of human hair samples from around the globe⁴⁷

The study also compared metal levels on hair fibres of both colourant and non-colourant users. It was seen that the amounts of Mg²⁺ and Ca²⁺ rise for individuals that colour their hair. However, the amounts of Cu²⁺ and Fe³⁺ remained similar. The authors concede that these results may underestimate the actual amounts present during the colouring process, as it is thought metal ions may be complexed by components within the formulations and rinsed out after application. The greater metal ion contents on the hair fibres of hair colourant users may be attributed to the formation of carboxylate anions and sulfonic acids during protein oxidation (discussed on page 22). These acids can also bind metal ions upon washing, thus increasing the amounts found on hair fibres that have been damaged by colouring^{10, 48-50}.

Whilst the literature shows a correlation between copper levels and the level of hair damage caused by UV radiation⁵¹, it is also known that the presence of copper and iron cause complications in the presence of alkaline hydrogen peroxide, as this leads to Fenton(-like) chemistry⁵².

1.4.1.2 Fenton chemistry

In 1894 Fenton discovered that a mixture of an iron salt with hydrogen peroxide resulted in the oxidation of tartaric acid⁵². It was later proposed that iron salts lead to the decomposition of hydrogen peroxide to form reactive intermediates that are responsible for the oxidation⁵³. To this day the exact mechanism by which hydrogen peroxide is decomposed by metal ions, such as Cu^{2+} and Fe^{3+} is not fully understood, despite knowledge of the chemistry dating back to 1894. There are currently two proposed mechanisms by which the hydrogen peroxide is suggested to decompose, the radical pathways and the non-radical pathways.

1.4.1.3 The radical pathway of hydrogen peroxide decomposition

The radical pathway of hydrogen peroxide decomposition was the first mechanism suggested by Haber and Willstätter in 1931⁵⁴. Since then continuous publications have arisen, suggesting different or additional steps to the mechanism⁵³. The key steps are outlined in the scheme below^{55, 56}.



Step 1 is responsible for the production of the superoxide anion. However, it also gives Fe(II) , which reacts very quickly with hydrogen peroxide to give the hydroxyl

radical (HO^\bullet) in step 2. Generation of the superoxide anion is also possible under basic conditions, when hydrogen peroxide is deprotonated to give the perhydroxyl anion. Electron transfer between redox metal ions and the perhydroxyl anion gives the perhydroxyl radical, which is deprotonated to give superoxide anion (step 3). Superoxide anions can either react with hydrogen peroxide to generate hydroxyl radicals (step 5), or they can react with metal ions to regenerate Fe(II) (step 4), allowing for the efficient redox cycling of the metal ions.

The hydroxyl radical is highly reactive and known to react with biomolecules, such as proteins, at diffusion-controlled rates^{57, 58}. Oxidation of proteins in this manner is thought to result in aging and loss of cellular function⁵⁹.

As a result of Fenton chemistry therefore, vulnerable hair colouring treatments lead to the generation of hydroxyl radicals. The hydroxyl radical has been linked with protein loss in hair fibres and may be a cause of hair damage⁶⁰. This is discussed in more detail from page 21.

1.4.1.4 The non-radical pathway of hydrogen peroxide decomposition

The non-radical pathway was postulated later as an alternative to the radical mechanism⁶¹. Highly reactive hypervalent metal intermediates, such as Fe(IV) and Cu(III) have been proposed to form instead of radical species, such as hydroxyl radicals⁶²⁻⁶⁴. These hypervalent intermediates show similar reactivity to that of the hydroxyl radical, meaning that distinguishing between the two pathways is difficult. However, regardless of the pathway, the formation of either intermediate during Fenton(-like) reactions leads to the potential oxidation of hair proteins⁶⁵. A scheme representing the possible reaction pathways and reaction intermediates for the Fe(II)-catalysed Fenton reaction is summarised below⁶⁶.

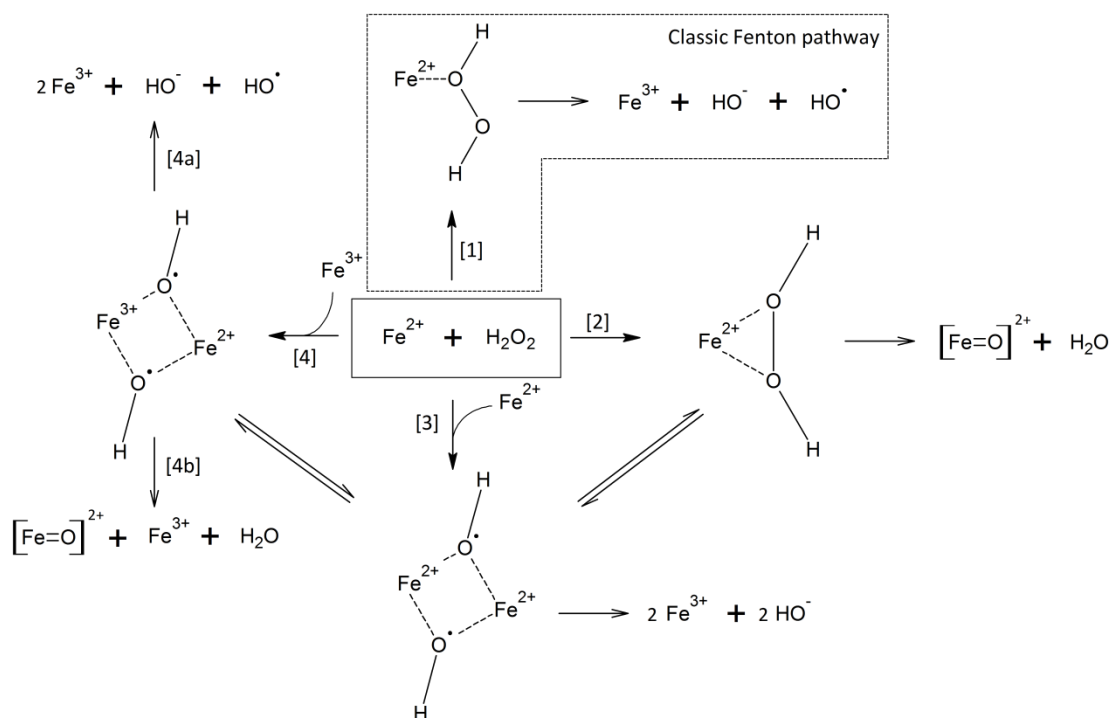


Figure 11: The formation of possible hypervalent iron complexes as intermediates of Fenton chemistry⁶⁶.

It can be seen in the above pathways that radical generation may occur from the non-radical complexes formed; particularly in pathway 4 there are two outcomes. Production of either the non-radical ferryl ion (Fe^{IV}) (4b) or the hydroxyl radical (4a) is possible. In fact the reaction pathway and intermediates involved have long been the subject of intense debate.

The chemistry is affected by the presence of oxygen, pH and any chelating ligands that are present in the system^{63, 67, 68}. At low pH, it is thought that the reduction of hydrogen peroxide results in the production of hydroxyl radicals⁶⁹. Attempts to determine the reduction potential of the metal species involved in the reaction have been made, in order to establish whether or not the ferryl ion is involved⁶⁵. There are many variables associated with the determination of reduction potentials, for instance, effective charge and pH. This makes identification of the species involved very difficult^{63, 64}.

Studies of reaction kinetics have also been used in order to determine whether or not the intermediate involved is the ferryl ion or the hydroxyl radical under certain reaction conditions. This is again dependent upon many variables such as, hydrogen peroxide concentration, pH and ligands present. Due to all these variables there is discrepancy amongst the literature over values of rate constants. Many assumptions have to be made with regards to which reactions are occurring when the conditions are changed⁶⁸.

Efforts have also been made to discount the non-radical pathway by incorporating ¹⁷O labelled H₂O₂ into a Fenton system. The idea was to try and trap the resulting HO[•] using DMPO and detecting by EPR⁷⁰. However, the non-radical iron-peroxide complex is capable of producing similar results⁷¹. Experimentally it has been proven to be very difficult to distinguish between the possible intermediates. However, a recent DFT study proposed that the ferryl ion intermediate was most likely to be formed in aqueous solutions, when water was the only ligand. This finding was based on the activation energies of oxygen-oxygen bond breaking, for both hydrogen peroxide bound to iron ions and free hydrogen peroxide. It was then proposed that there exists a very small energy barrier for the transformation of the intermediate iron complexes formed, into the ferryl ion, in the presence of a non-coordinated water molecule⁷².

Several enzymes in mammals, including catalases, peroxidases and cytochrome c make use of ferryl ion intermediates to break down hydrogen peroxide, without generating highly damaging radical species^{73, 74}. In the case of catalase, multiple studies have confirmed that the breakdown of hydrogen peroxide proceeds via the formation of a ferryl ion intermediate^{75, 76}. The catalytic pathway of hydrogen peroxide decomposition by catalase is shown in *Figure 12*. Catalase is discussed in further detail in Chapter 4.

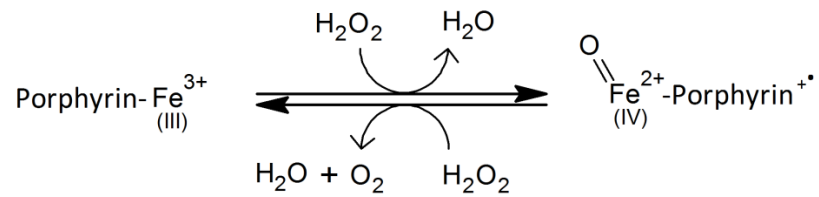


Figure 12: Scheme to show the catalytic pathway of hydrogen peroxide decomposition by catalase⁷⁴.

Regardless of which intermediates exist in Fenton chemistry, they are likely to be highly reactive. Indeed both the ferryl ion and the hydroxyl radical have the potential to damage proteins⁷⁷.

1.4.1.5 Mechanism of hair fibre damage

As mentioned earlier, reactive oxygen species (ROS) from the metal ion catalysed decomposition of hydrogen peroxide are prone to oxidise biomolecules such as lipids and proteins. This is thought to be one of the mechanisms of the aging process. Therefore, in hair colouring processes if ROS, such as the hydroxyl radical, are produced, they can react with lipids and proteins in the hair. This reaction can occur if formulations do not contain radical scavengers or anti-oxidants. As the hydroxyl radical is so reactive, its reaction with proteins occurs when metal ions are bound to the proteins directly. Decomposition of the hydrogen peroxide by these ions then generates hydroxyl radical directly at the site of the proteins.

Figure 13 shows how protein oxidation and peptide bond cleavage is possible⁷⁸. In this example the major species responsible for protein oxidation is the hydroxyl radical, which forms a carbon centred radical. Oxygen can then react to form the peroxy radical, followed by further oxidation by either redox metals or ROS to give an alkoxy radical. This then leads to peptide bond cleavage, which ultimately results in the breakdown of proteins.

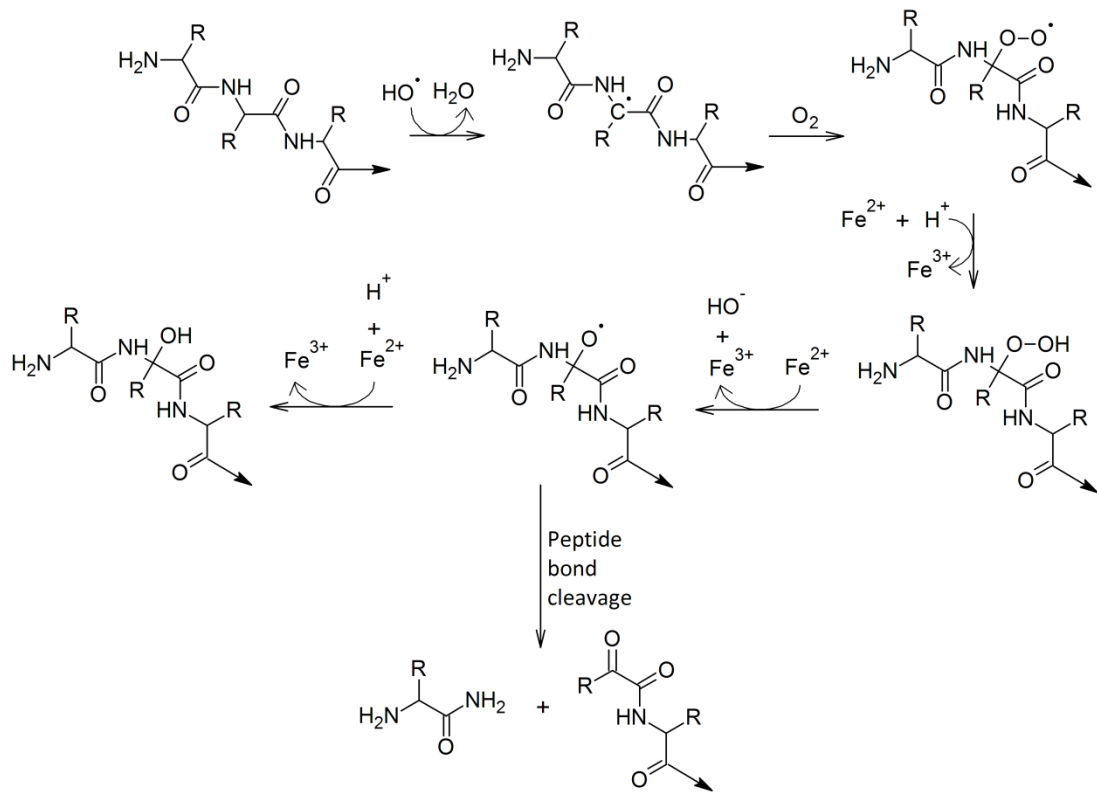


Figure 13: A possible mechanism of protein oxidation by hydroxyl radical and by redox metals.⁷⁸

Cleavage and formation of disulphide bonds is another problem associated with protein damage. ROS are capable of cleaving disulphide bonds, as well as oxidising cysteine and methionine units in proteins, leading to the formation of these bonds. This leads to structural modifications of the proteins⁷⁸. Figure 14 shows how the cleavage of disulphide bonds can also occur under alkaline conditions used for hair bleaching⁷⁹. The oxidation and hydrolysis of disulphides leads to the production of sulfonates, such as cysteic acid, as shown in Figure 15^{10, 80}. These sulfonates assist in the binding of metals, which in turn contributes to further protein damage of the hair⁴⁸.



Figure 14: One of the possible mechanisms of disulphide bond cleavage in alkaline media⁸¹

It is worth noting that this is not the only postulated mechanism of disulphide bond cleavage at alkaline pH. Hydrogen elimination from both the α or β carbon is plausible, followed by the subsequent cleavage of a sulphur-sulphur or carbon-sulphur bond^{81, 82}. However during hair bleaching, it is thought that S-S bond fission is the predominant mechanism of disulphide bond cleavage^{10, 83}.

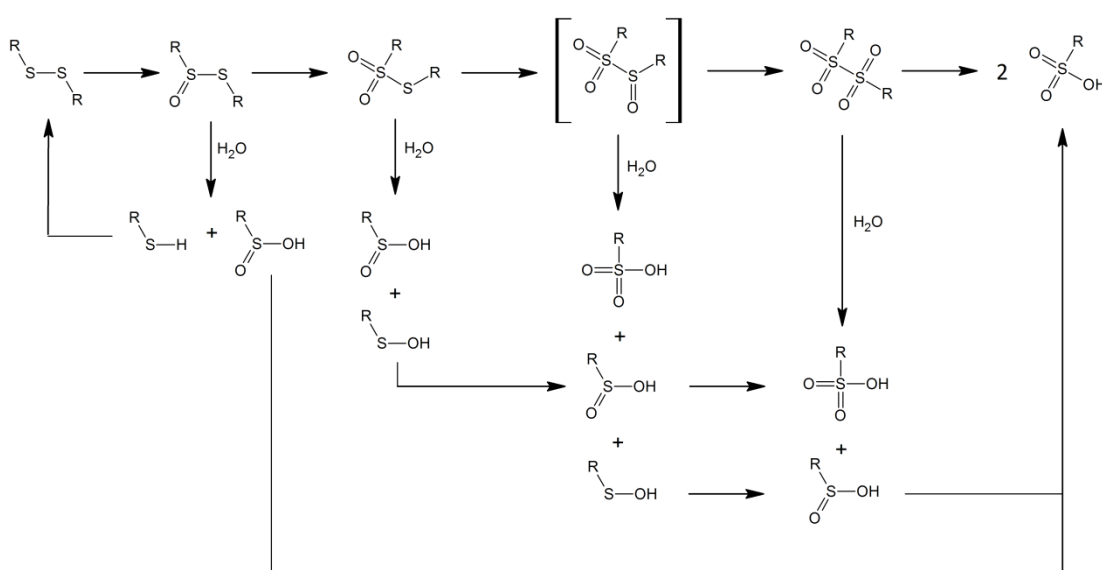


Figure 15: Scheme to show the possible routes of disulphide bond cleavage to form sulfonic acid, via cystine oxide intermediates^{10, 80}.

The oxidation of proteins within hair fibres in these ways leads to hair damage. Several studies have examined hair samples after various treatments to observe and/or quantify the extent of damage that may occur.

1.4.1.6 The effect of reactive oxygen species on hair fibres

In the hair, protein oxidation leads to increased hair fibre damage and a feeling of dryness, due to cuticles lifting from the hair shaft. After several bleaching or dyeing cycles, holes may form in the outer layer of the cuticle and eventually the complete removal of some layers is observable⁸⁴. The SEM images in *Figure 16* show this clearly⁸⁵.

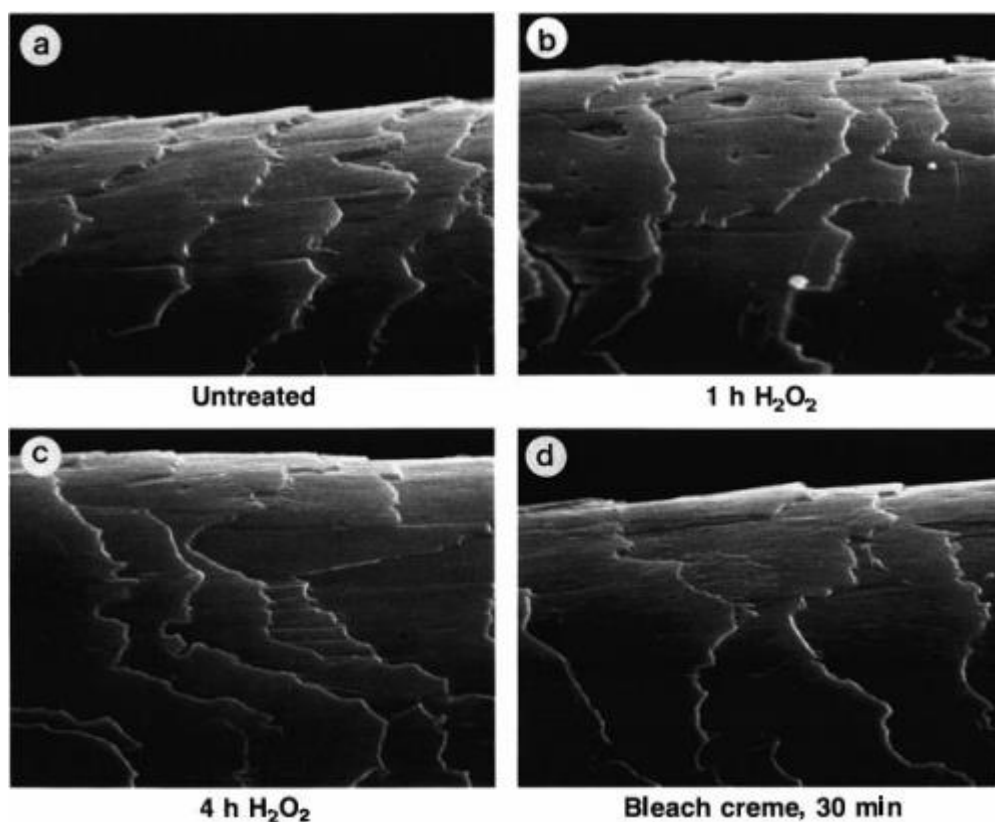


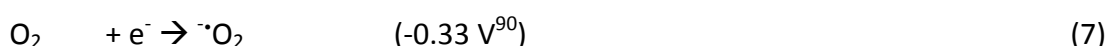
Figure 16: SEM images of (a) an untreated hair fibre, (b) & (c) hair fibres treated with 6% H_2O_2 at pH 10.2 (21 °C) or (d) a hair fibre treated with a bleach crème treatment of 9% H_2O_2 at pH 8.6 (21 °C)⁸⁵.

Although this damage appears extensive, it has been shown that this does not affect the tensile properties of the hair fibre, probably because the cortex is primarily responsible for the mechanical strength of hair^{10, 86}. It does however, lead

to a decline in the appearance and feel of the hair, which is not ideal for a cosmetic treatment. As a result, a large amount of research has gone into attempting to prevent damage to hair fibres that can occur during permanent hair colouring procedures.

1.4.1.7 Preventing hair fibre damage

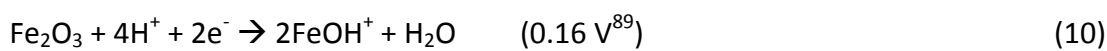
Ordinarily the Fenton reaction relies on a transition metal ion to catalyse the decomposition of hydrogen peroxide. For decomposition to occur spontaneously, the metal ion needs to cycle between two oxidation states, as shown by reactions (1) – (4) on page 17. In the Fenton reaction the metal ion centre would be expected to have a redox potential that fits between the values $-0.33 - 0.46 \text{ V}^{87}$, that correspond to the half-equations (6) & (7) at pH 7⁸⁸. This allows the metal to cycle between oxidation states, whilst hydrogen peroxide is decomposed through reactions, (2) & (4) on page 17. It should be noted that this redox window is based on standard oxidation potentials that have been acquired at pH 7. These oxidation potentials may vary for Fenton reactions that occur at alkaline pH.



The redox potential of $\text{Cu}^{2+}/\text{Cu}^+$ is 0.161 V , shown in half equation (8). This makes it able to catalyse the decomposition reaction. Moreover, as this value is in the middle of the redox window it allows for fast decomposition of the peroxide. If the oxidation potential lies towards the edge of this window it will lead to slower decomposition, as the rate of either reaction (2) or (4) will decrease⁸⁸.



The situation is more complex for iron ions. The oxidation potential of $\text{Fe}^{3+}/\text{Fe}^{2+}$ (half equation (9)) is 0.771 V, which lies outside the redox window. However, pH plays an important role in the Fenton reaction. It has been suggested that, at pH 10, Fe(II) could exist as the $[\text{Fe}(\text{OH})]^{+}$ complex, whilst Fe(III) is generally insoluble and exists as Fe_2O_3 ^{91, 92}. The redox potential associated with these species (half-equation (10)) lies in the redox window and could explain the catalytic behaviour of iron⁸⁹. On the other hand, it is more likely that Fe(III) is bound to substances within the hair fibre, which could alter redox potentials sufficiently to allow iron ions to catalyse the Fenton reaction.



Understanding the redox potentials behind Fenton chemistry has enabled the development of technology to stabilise hydrogen peroxide and hence prevent decomposition. One of the more effective ways to achieve this is by the use of chelating ligands to sequester the metals⁸⁸. Ligands can alter the redox potential of the metal centre to a value that lies outside (or closer to the edge) of the redox window. Hence, they reduce the rate of either reaction (2) or (4) substantially enough to prevent decomposition. Additionally, ligands coordinatively saturate the metal centre, preventing hydrogen peroxide from binding and thus decomposing⁹³. This has been applied successfully to hair colouring systems. Chelating ligands are now commonly used in formulations to prevent the damage of hair fibres by hydroxyl radicals, as a result of hydrogen peroxide decomposition⁵⁰.

One of the more effective chelants for inhibiting hydrogen peroxide decomposition by copper is ethylenediaminetetraacetic acid (EDTA) (*Figure 17*)⁹⁴. However, as mentioned on page 16, hair fibres contain significant levels of other metals.

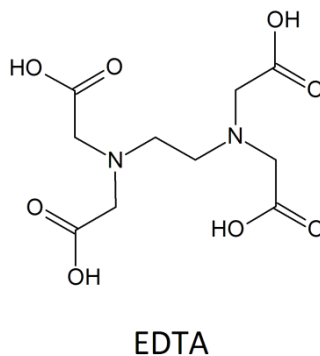


Figure 17: The structure of the chelating ligand EDTA.

The presence of such a high concentration of calcium ions causes problems that are associated with the use of EDTA. Despite the much lower stability constant of the Ca(EDTA) complex, when compared with those of the Cu(EDTA) or Fe(EDTA) complexes (*Table 2*), the large excess of calcium results in the majority of EDTA being complexed to the calcium ion at pH 10. This leaves the redox active metal ions unbound, leading to Fenton(-like) chemistry and hence hair fibre damage. Chapter 7 describes how speciation plots could be predicted based on the stability constants of the metal complexes. The speciation plot in *Figure 18* shows the possible copper complexes that form in an aqueous model system containing 400 mM NH₃, 13.95 mM EDTA, 170 mM Ca²⁺ and 1.27 mM Cu²⁺. These simplified conditions represent the environment found on the surface of hair fibres during bleaching⁶⁰. Under realistic bleaching conditions, the relatively low concentration of EDTA means that copper does not bind to the ligand, resulting in the formation of copper-ammonia complexes. However, in real hair systems proteins are likely to compete with ammonia to bind the copper.

Metal	LogK
Ca^{2+}	10.81
Mg^{2+}	8.96
Cu^{2+}	18.78
Fe^{3+}	25.10

Table 2: The binding constants of EDTA with the metal ions found in hair⁹⁵.

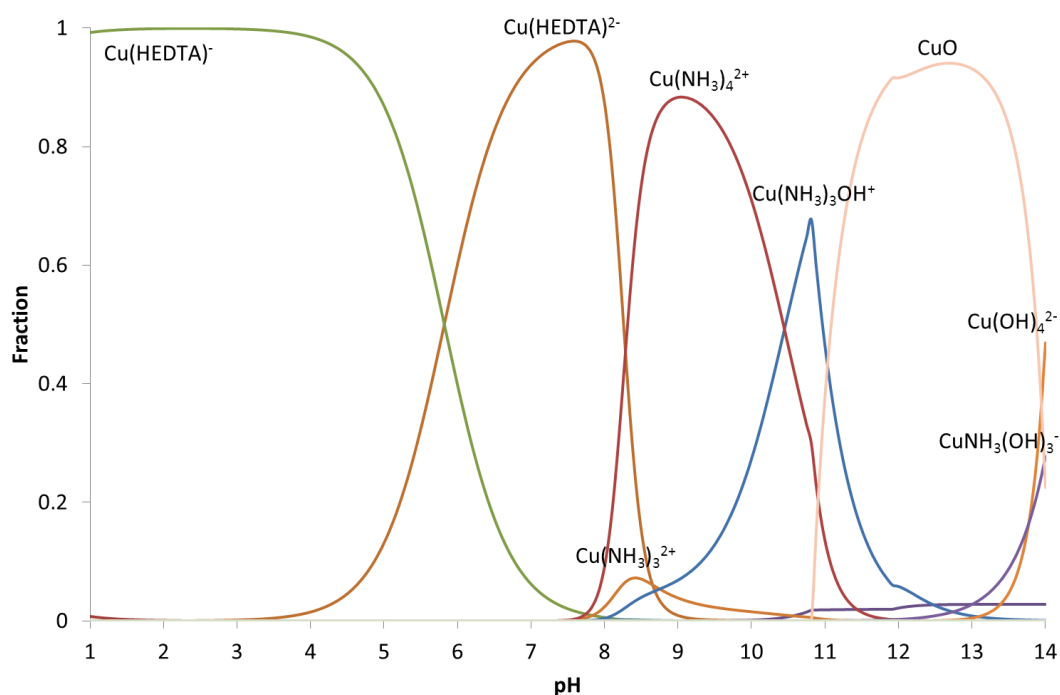


Figure 18: Speciation plot to show the copper complexes formed in a model hair system containing 400 mM NH_3 , 13.95 mM EDTA, 170 mM Ca^{2+} and 1.27 mM Cu^{2+} ⁶⁰.

Chelating the calcium ions is not desired as it does not catalyse the Fenton reaction. Chelation of this ion essentially uses up the chelating agent, so that iron ions and copper ions remain unbound. Thus, the transition metal ions are free to catalyse the decomposition of hydrogen peroxide, generating hydroxyl radicals.

This observation led to the use of the ligand ethylenediamine-*N,N'*-disuccinic acid (EDDS), which has a much higher specificity for the copper ion over the calcium ion

(Table 3). It has been suggested that this selectivity is determined by the size of the central metal ions. Ca^{2+} has an ionic radius of 0.099 nm, which is much larger than the radius of Cu^{2+} (0.073 nm)⁹⁶. EDTA can accommodate both Ca^{2+} and Cu^{2+} easily, leading to stable complexes. However, whilst copper ions are small enough to form a stable complex with EDDS, it is thought that the Ca^{2+} ion is too large. The distortion of the complex that must occur for EDDS to bind calcium ions, leads to a relatively unstable complex⁹⁷. Therefore, EDDS binds copper ions much more effectively in the presence of other metals, as shown by the speciation plot for a system containing 400 mM NH_3 , 13.95 mM EDDS, 170 mM Ca^{2+} and 1.27 mM Cu^{2+} (Figure 20). This leads to a system that produces fewer hydroxyl radicals, thereby being likely to reduce hair fibre damage in colouring systems⁵⁰.

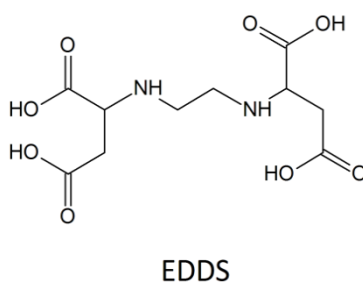


Figure 19: The structure of the chelating ligand EDDS.

Metal	LogK
Ca^{2+}	4.58
Mg^{2+}	6.01
Cu^{2+}	18.40
Fe^{3+}	22.00

Table 3: The binding constants of EDDS with the metal ions found in hair⁹⁵.

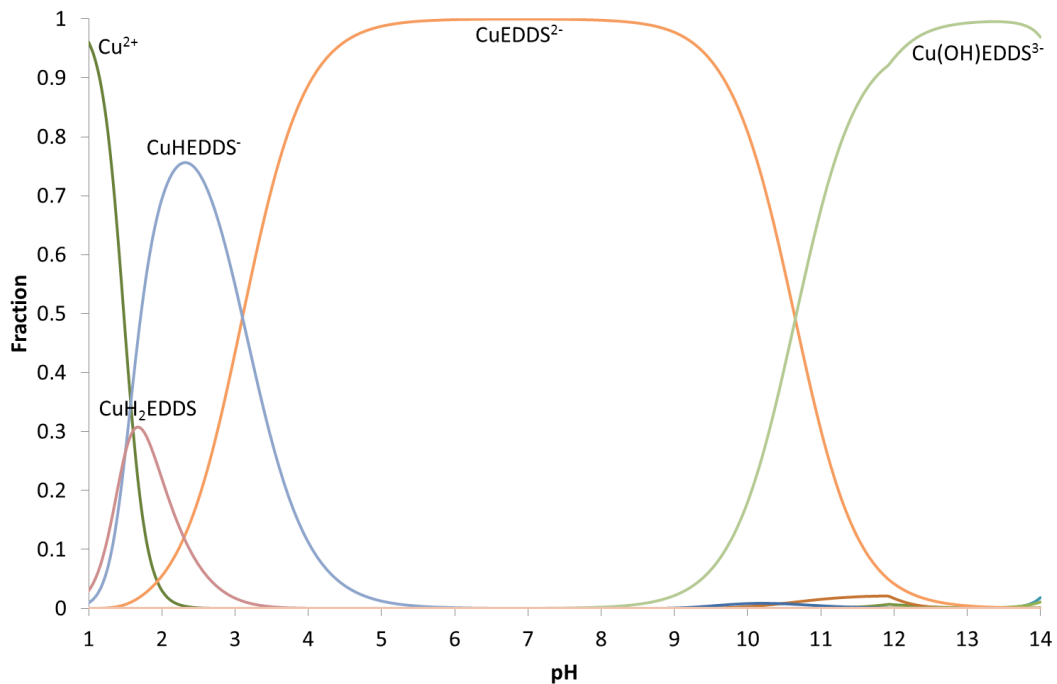


Figure 20: Speciation plot to show the copper complexes formed in a model hair system containing 400 mM NH_3 , 13.95 mM EDDS, 170 mM Ca^{2+} and 1.27 mM Cu^{2+60} .

1.4.1.8 Quantifying hydroxyl radical production

As the amount of hydroxyl radicals produced in hair colouring systems has been linked with hair fibre damage, it is useful to be able to quantify hydroxyl radical production in these systems. One of the more used methods of hydroxyl radical quantification involves the reaction of the hydroxyl radical with a spin trap and subsequent detection using electron paramagnetic resonance (EPR).

The hydroxyl radical is an extremely reactive and short-lived species, thus it is difficult to detect. Spin traps are molecules that may react with reactive radical species to form more stable radicals that exist for long enough periods of time to be detected by EPR. Dimethyl-1-pyrroline-N-oxide (DMPO) is an example of a spin trap that can react with the hydroxyl radical to form the DMPO-OH adduct, the spectrum of which is shown in Figure 22.

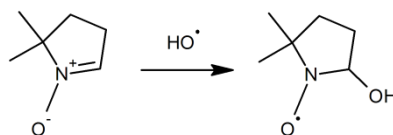


Figure 21: The generation of DMPO-OH adduct from the reaction of hydroxyl radical with DMPO⁹⁸.

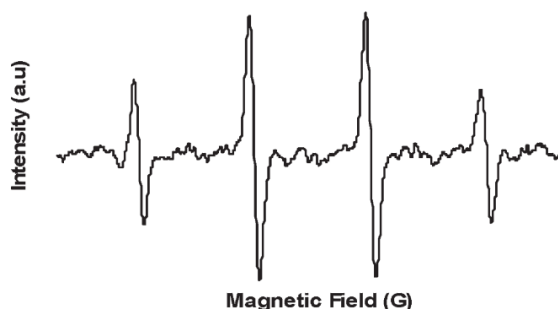


Figure 22: The typical EPR spectrum for the DMPO-OH adduct⁹⁹

In the presence of redox metal ions it has been shown that the formation of the DMPO-OH adduct is possible in aqueous media in the absence of hydroxyl radicals. This occurs by the formation of the DMPO-Fe³⁺ complex, which allows electron transfer from DMPO to the metal ion. Nucleophilic attack of water may then occur resulting in the hydroxylated probe and Fe²⁺, as shown by the mechanism in *Figure 23*⁹⁸. This could potentially lead to a misrepresentation of hydroxyl radicals amounts that are produced in systems.

Alternatively, using EPR to measure the decay of the nitroxide radicals, such as 2,2,6,6-tetramethylpiperidine-1-oxyl (TEMPO) may lead to an overestimation of the hydroxyl radicals. This is because redox metal ions easily reduce the radical to hydroxylamine in the absence of the hydroxyl radical¹⁰⁰.

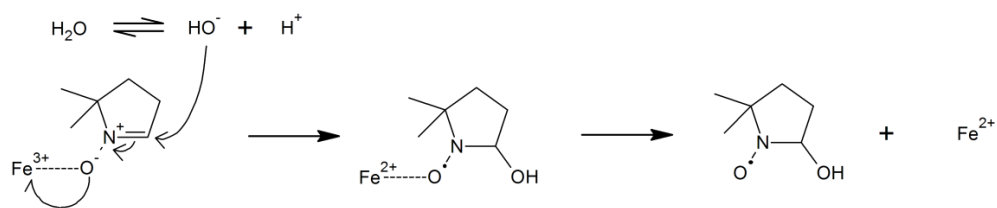


Figure 23: Mechanism to show the hydroxylation of DMPO by water in the presence of Fe(III) ⁹⁸

To avoid the problems associated with spin traps, the use of colorimetric probes is another technique that can be used to measure hydroxyl radical concentrations in Fenton systems. Hydroxyl radicals can react with aromatic substrates to produce hydroxylated adducts, which can then be monitored by UV-vis spectroscopy or HPLC to give an estimate of the amount of hydroxyl radical flux in certain systems. Probes that are commonly used include nitrobenzene, benzoic acid, terephthalic acid and salicylic acid¹⁰¹⁻¹⁰³. It is documented that the hydroxylation of these probes may occur at multiple locations around the aromatic ring, as the hydroxyl radical is highly reactive and non-selective¹⁰². The multiple products of hydroxylation can lead to problems associated with quantifying the amount of hydroxyl radical that is produced¹⁰¹.

Additionally, salicylic acid is known to bind to metal ions, which will affect the extent of hydrogen peroxide decomposition that occurs in certain systems. Thus, the amount of hydroxyl radical may be altered by the presence of this probe¹⁰⁴.

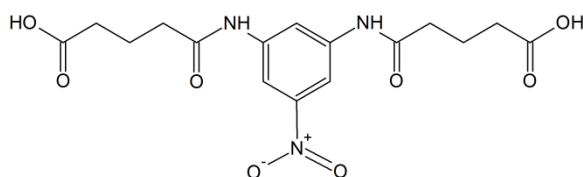


Figure 24: The colorimetric probe NPDPA.

The problem of metal ion chelation NPDPA may be overcome by the use of the colorimetric probe 5,5'-[(5-nitro-1,3-phenylene)diimino]bis(5-oxopentanoic acid) (NPDPA) (*Figure 24*). NPDPA is more suitable for use in monitoring hydroxyl radical production in Fenton(-like) systems, as it will not bind metals strongly. Hydroxylation of the probe at the ortho position and the para position is possible and the ratio of products has been documented¹⁰⁴. The nitrophenol adducts that are formed absorb strongly in the visible region, under basic conditions, allowing for a quantitative estimation of hydroxyl radicals by UV-vis spectroscopy. As a result, NPDPA has been used throughout this project to measure hydroxyl radical formation in various systems. The mechanism of NPDPA hydroxylation is discussed in more detail in chapter 2.

1.4.2 Hair Dyeing

The process of hair dyeing initially makes use of the principles behind hair bleaching, to degrade the melanin in hair that is responsible for the natural colour of the fibres. This requires the use of hydrogen peroxide, which may also play a role in the production of dye molecules.

Generally, these permanent dye molecules are produced by the oxidation of smaller dye precursors, which first diffuse into the cortex of the hair fibre, along with hydrogen peroxide. Once inside the hair cortex they may then be oxidised by the hydrogen peroxide to form larger dye molecules that are trapped permanently within the hair fibres.

Hair dye precursors that are used are para-substituted aromatic amines or phenols that are susceptible to oxidation. Typically the size of these precursors is approximately 0.5 nm¹⁰⁵, allowing them to diffuse into the hair fibres through "pores", thought to have a size of up to 3.5 nm¹⁰⁶. Phenylenediamine (PPD) is a common precursor that is used in dye formulations. In the presence of alkaline hydrogen peroxide it is oxidised to the reactive quinone diimine intermediate (QDI),

as shown in *Figure 25*. It has been observed that PPD can cause contact dermatitis¹⁰⁷. When ingested in sufficient quantities PPD can also cause renal failure¹⁰⁸. For these reasons, alternatives to PPD may be used in hair colouring formulations, such as 2,5-diaminotoluene sulfate (DTS) or 1,4-diamino-2-methoxymethyl-benzene (MBB)¹⁰⁹.

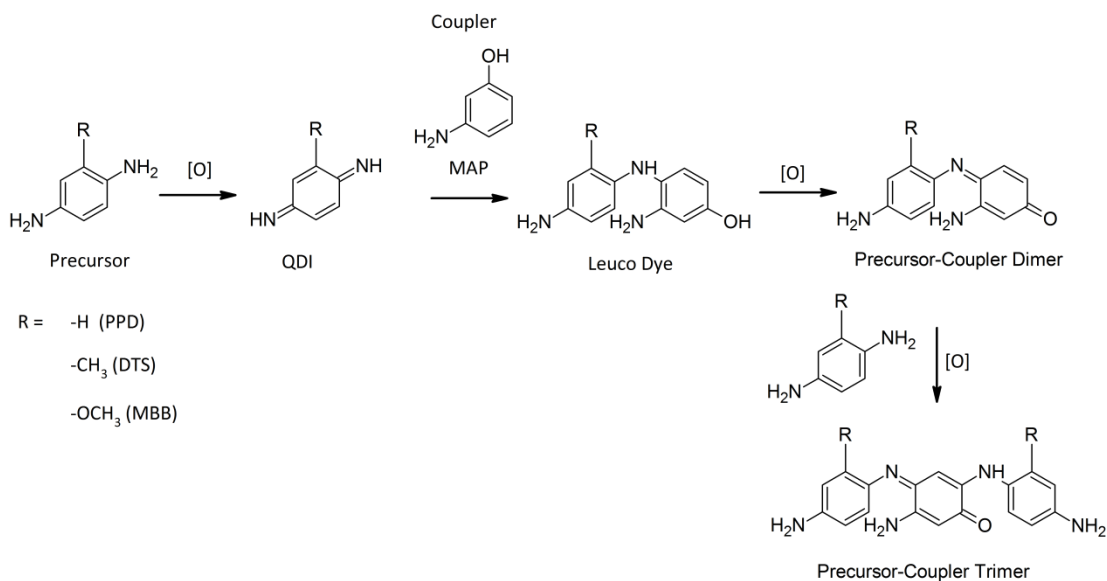


Figure 25: Scheme to show the formation of permanent dye molecules by the oxidation of PPD.

QDI can then react with couplers, which are typically meta-substituted aromatic amines or phenols, such as meta-aminophenol (MAP). This reaction forms colourless leuco dye intermediates, which can then be further oxidised to form indophenol and indamine-based dye molecules that are responsible for the final colour of the formulation³. The mechanism of dye formation is discussed in more detail in chapter 4.

1.5 The role of water in hair colouring

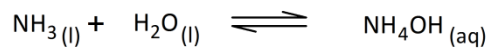
The major component of hair colouring formulations is water. It is primarily used as a biologically suitable solvent, which contains all of the ingredients that make up hair bleaching and hair colouring formulations. Therefore, water allows hair formulations to be applied easily to the hair. However, in addition to acting as a solvent, water plays several roles during the process of hair colouring.

1.5.1 The role of water in hair bleaching

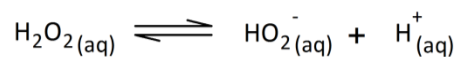
As discussed in section 1.4.1, the process of hair bleaching relies on the hydrogen peroxide-mediated oxidation of melanin. Melanin is found in the cortex of hair fibres. Therefore, diffusion of the hydrogen peroxide from the formulation into the hair fibres is necessary, for bleaching to occur. Water facilitates this process in multiple ways. Firstly, it provides a transport medium for the hydrogen peroxide, as keratin, which is present throughout the hair fibre cortex, is hydrophilic and can absorb large amounts of water¹¹⁰. Thus, aqueous formulations are absorbed into the hair cortex. However, the hair surface is hydrophobic and this provides a substantial barrier for aqueous-based formulations to initially overcome¹⁰. The use of surfactants in formulations is designed to tune the hydrophilicity and surface tension of the hair fibres so that formulations can be applied effectively¹¹¹. Additionally, these surfactants assist in the solubilisation of components within the formulation that have limited solubility in water.

Secondly, as mentioned in section 1.4.1, water facilitates the diffusion of molecules, such as hydrogen peroxide, into the hair cortex, by swelling the hair fibres^{10, 110}. This swelling probably arises as a consequence of the cleavage of hydrogen bonds between the protein chains that make up the hair fibre¹⁰. Hair fibre swelling is greatly increased by alkaline pH. Therefore, water is again critical for allowing the dissociation of bases that are used to generate this high pH. For example, the

equation below represents the formation of ammonium hydroxide in water, resulting in an alkaline solution.



Penetration of molecules, such as hydrogen peroxide, into hair fibres is accelerated as a consequence of increased hair fibre swelling. It is not sufficient that hydrogen peroxide reaches the cortex for hair bleaching to occur. It is also essential that dissociation of the hydrogen peroxide occurs, to form the perhydroxyl anion⁴¹, as shown by the equation below. Again, this dissociation requires an aqueous medium.



Due to the factors discussed above, aqueous formulations are necessary for hair colouring procedures. However, there are also problems associated with the use of water. Firstly, hair swelling is known to make the hair fibres more susceptible to damage, as the cuticle is lifted and more susceptible to fragmentation¹⁰. This leads to a dry and damaged feel to the hair. It is also recommended that hair colouring treatments should not be applied to wet hair. If colouring formulations are applied to wet hair, it is difficult to control where the colour forms on the hair. This is due to the fact that the ingredients in formulations are free to diffuse throughout the water on the surface of the hair. Therefore, it is important for formulations to contain the appropriate amount of water and to use hair colouring formulations under the correct conditions.

1.5.2 The role of water in hair dyeing

Water often plays the same roles in hair dyeing as hair bleaching, as the first step of dyeing hair can involve melanin bleaching (when a lighter hair shade than the natural colour is desired). Additionally, water also contributes to the oxidation of

dyes that are used to colour hair. Corbett has shown that by bubbling oxygen through aqueous alkaline solutions, mixtures of PPD and MAP can react to form indoaniline dyes, which are used to colour hair¹¹². This is important to bear in mind, as oxygen is dissolved in water. Thus, as it diffuses into the cortex water transports oxygen into the hair fibres. Oxygen saturation levels of water vary depending on many factors, including temperature and the salinity of the water. In the case of hair colouring procedures that use hydrogen peroxide, the decomposition of hydrogen peroxide in the hair cortex releases oxygen, which can further increase the oxygen saturation levels of water¹¹³. Direct oxidation of dye precursors by oxygen is not the only way that oxygen contributes to dye formation. During the Fenton reaction, oxygen is required for the redox cycling of metal ions, which catalyses the decomposition of hydrogen peroxide (half-equation 7 – page 25). This leads to the production of ROS, which are also able to oxidise dye precursors or melanin during hair colouring, as well as causing protein oxidation and hair damage. Therefore, the fact that oxygen can be transported into the cortex by water potentially leads to both positive and negative aspects of hair colouring procedures.

Another transient species that can become involved in redox chemistry in aqueous media is the hydrated electron ($e^-_{(aq)}$). When metal ions lose electrons in water they release electrons that can be solvated by water molecules. Solvated electrons are powerful reducing agents in solutions $> \text{pH } 7.85$ (oxidation potential of $e^-_{(aq)}$ is -2.77 V^{114}). Therefore, they could play a role in the reduction of Fe(III) to Fe(II), which would increase the rate of hydrogen peroxide decomposition, during hair colouring procedures. The rate of decomposition not only affects the extent of hair damage that can arise, but also how much dye is degraded by hydroxyl radicals. There is little literature available that discusses the role of solvated electrons in Fenton reactions. However, the transfer of an aqueous electron to a metal ion centre is an outer-sphere process¹¹⁵. There is evidence that has shown that inner-sphere electron transfer during Fenton reactions is more favoured^{56, 116}. Therefore, it is currently unclear what role the hydrated electron plays during Fenton chemistry. Thus, its role in hair dyeing and melanin bleaching is also unknown.

Inner-sphere electron transfer during Fenton chemistry involves the direct bonding of hydrogen peroxide to the metal ion centre. This is achievable when the metal ion is bound to labile ligands, such as water. Water can diffuse easily into the hair fibres, making this a possibility. Most hair colouring formulations use less labile chelating ligands, such as EDTA, to prevent hydrogen peroxide from binding to the metal ion and decomposing. However, it is unclear whether these ligands can diffuse into the hair fibre, due to their large size and the negative charge that they carry. This could result in the types of complexes shown in *Figure 28* forming in the hair cortex, which would lead to more extensive decomposition than if the less labile EDTA ligand was bound. Thus, more hair damage could result.

It can be seen that water plays several important roles (both positive and potentially negative) during the process of hair colouring. Throughout this thesis aqueous solutions are used as a model for the study of the reactions that occur during the course of hair bleaching and hair dyeing. Due to the importance of water in hair colouring processes the use of aqueous model solutions was considered to be appropriate. The biggest limitation of their use as models is that diffusion rates of substances into hair fibres are not accounted for. Although, for many of the studies, this was considered to be an advantage (discussed in the relevant sections). It was also recognised that the concept of localised pH could not be replicated by the use of aqueous formulations. During hair bleaching, aqueous formulations diffuse into the hair at varying rates, due to the inconsistent structure of hair fibres. For example, the cuticle of hair that has been pre-treated with colouring formulations tends to be more damaged than untreated hair. Often, holes appear in the cuticle as a result of this damage (*Figure 16 (b)*). This can lead to faster diffusion rates of hydrogen peroxide into the hair fibre, where these holes exist. The diffusion rates of formulations into the hair are important to consider. The less time formulations spend on the surface of the hair, the less time there is for volatile bases to evaporate, due to heat from the scalp. This would lead to localised areas with different pH values within the hair cortex. Despite these limitations, aqueous model solutions were considered to be suitable for many of the reactions studied throughout this work.

1.6 The application of hair colouring products to hair

People who desire to change the natural colour of their hair tend to have two options. They can choose to get it coloured by a stylist in a salon, or they can buy colouring kits to use at home themselves. Nowadays, permanent hair colouring formulations for use at home are readily available for consumers. They are a cheaper alternative to salons. Thus, they are a popular choice for many people.

1.6.1 Hair colouring at home

Typically, home hair colouring kits are comprised of 3 separate components¹¹⁷:

1. Colour – The colouring agent is an aqueous solution, containing a variety of dye precursors that will form the indamine or indophenol dyes, such as PPD and MAP. They also contain ligands, such as EDTA, and radical scavengers, such as sulphites, to prevent hair damage. Finally, as an alkaline pH is required for this chemistry, they contain a base, for example ammonia (up to 0.5 M)⁴⁷.
2. Activator – The activator contains aqueous hydrogen peroxide ($\sim 1\text{ M}$)⁴⁷, to lighten the natural shade of the hair by oxidising melanin. The hydrogen peroxide also oxidises the dye precursors, to form the dyes responsible for the final colour.
3. Conditioner – The conditioner is an aqueous-based mixture of predominantly alcohols and oils, designed to keep the hair hydrated after the colouring process.

Instructions for the application of these home colouring kits dictate that the colouring agent and activator be mixed thoroughly, until the colour has completely

blended and the mixture has thickened. This should then be applied to dry hair, which has not been shampooed (conditioner should be applied to the ends of the hair if they are too dry). This mixture should then be applied to hair for approximately 25 minutes. This time is dependent on the type of colour that is desired. However, the mixture should not be left on for more than 45 minutes, to prevent extensive fibre damage. Previous users of colouring formulations are advised to pay particular attention to their roots in this step. After the appropriate amount of time the mixture should be rinsed off with warm water. The conditioner should then be applied for 2 minutes to hydrate the hair¹¹⁸.

1.6.2 Hair colouring in salons

A similar process is used in salons to colour hair, whereby the colouring agent is mixed with activator and applied to the hair. However, there are some subtle differences used by professional stylists, depending on the type of hair that is being coloured. These differences result in a change to the conditions used to colour the hair, for example, depending on several factors such as, ethnicity, initial shade or age, varying concentrations of hydrogen peroxide will be used. Generally, higher concentrations of hydrogen peroxide are used if the initial shade of the hair is darker and the desired shade is relatively light. However, the most important difference is the temperature at which the hair is coloured. Stylists often use heat lamps to increase the rate of colour development during the application of the activated colouring mixture. Typically, heat is applied to virgin hair or darker shades of hair, where it is more difficult to lighten the natural shade of the fibres. This results in a wide range of conditions that are used in hair colouring procedures, which need to be tailored to the individual.

Throughout this thesis, reactions are studied at a temperature of 20 °C (unless otherwise stated). Therefore, the data were acquired under conditions that are

most comparable to those that exist during colouring at home, where the temperature that is generated during the reaction is sufficient to drive the colouring process. As mentioned in the previous section, a higher temperature is often used during salon procedures, to facilitate colour formation. This higher temperature may lead to changes to the chemistry that is discussed. The concentrations of hydrogen peroxide used in commercial formulations are also likely to vary from the concentrations used in this thesis, depending on the type of hair and the colouring procedure that is desired. Typically, in salons this concentration varies between approximately 0.9 M and 2.5 M. The concentration of hydrogen peroxide used in the presented work is predominantly at the lower end of this range, focussing on less harsh bleaching conditions.

1.7 The use of MEA in hair colouring formulations

Ammonia is typically used for hair colouring systems in order to provide an alkaline pH and to facilitate the diffusion of oxidants and dye precursors into hair fibres, (page 14). However, the use of ammonia results in formulations with bad odours. Consequently, alternative bases have been investigated for their potential use in hair colouring formulations.

Monoethanolamine (MEA) (*Figure 26*) is one of the more promising bases that can be used in hair colouring formulations as an alternative to ammonia. In fact, it is used in several products that are currently on the market, due to the similar properties of the molecule to ammonia. Both ammonia and ethanolamine are water soluble bases that have similar pK_a values, (9.21) and (9.50), respectively. Therefore, similar concentrations can be used in order to achieve the same final pH of formulations¹¹⁹. Both compounds also have the ability to interfere with hydrogen bonding throughout the hair fibre¹¹⁰. Thus they can assist with the diffusion of dye precursors and oxidants into the fibre. There are however some differences between the two bases that may lead to a change in the behaviour of colouring formulations. As a result, there are several problems associated with the use of

MEA in colouring formulations. Firstly, MEA may cause contact dermatitis, which can affect the scalp of users¹²⁰. In addition to this, less extensive bleaching of hair fibres is associated with the use of MEA-based compositions and finally increased fibre damage and hair loss has been observed^{43, 121, 122}.

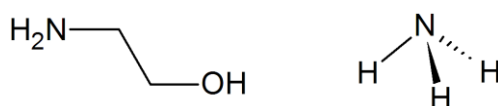


Figure 26: Structures of the bases ethanolamine and ammonia

1.7.1 The possible causes for the differences observed in bleaching systems containing MEA

When MEA is used in hair colouring formulations, instead of ammonia, two major differences arise. The first is that a higher concentration of MEA is required to achieve the same level of hair bleaching that is observed when ammonia formulations are used⁴³. The second is that up to 85% more hair damage (protein loss and cuticle damage) is observed when formulations containing MEA are used. This has been studied using SEM, protein loss studies and by monitoring cysteic acid formation, using Fourier transform infrared spectroscopy (FTIR)⁴³.

Currently, the reasons for the differences observed in hair colouring formulations containing MEA are unknown. Any of the following physical or chemical factors may play a role in the increased level of fibre damage, or decreased extent of melanin bleaching that is observed in these systems.

1.7.1.1 Hair fibre damage

MEA is a much less volatile molecule than ammonia. The vapour pressure of a 34.5% solution of ammonia is roughly 111 kPa at 20°C¹²³, whilst the value for MEA is much lower at 0.03 kPa at 21°C¹²⁴. This means that MEA is much more likely to remain on the hair fibre for a longer period of time than ammonia. Thus, when MEA-containing formulations are used, hair proteins may be exposed to the base for a longer period of time and more hair fibre damage may occur⁴³.

The increased fibre damage that was observed in the MEA-containing formulations (page 42) could also occur as a result of the formation of MEA radicals. It has been shown that two major radical species form as a result of the reaction between MEA and the hydroxyl radical. The majority of radical formation is thought to occur at the amino site, whilst carbon-centred radicals are also possible at the α -carbon to the alcohol (Figure 27)¹²⁵.

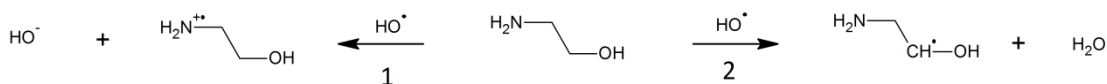


Figure 27: The formation of radicals by the reaction of MEA with hydroxyl radical¹²⁵

The fact that MEA forms such radicals, as well as remaining on hair fibres for a longer period of time, would be expected to contribute to the increased level of hair fibre damage that is observed in these systems.

The presence of metals on hair fibres also leads to the formation of various metal-ligand complexes, in the presence of bases. Copper ions in particular have been shown to bind the bidentate MEA ligand and the monodentate ammonia ligand¹²⁶.

The metal centres of copper(II) complexes have electron configurations of d^9 . The lowest energy conformation of these complexes is a distorted octahedral geometry, as they are affected by Jahn-Teller distortion. This is due to the presence of an

unpaired electron in the e_g orbitals. As a result, the complex distorts to give a tetragonal geometry in order to encourage the removal of degeneracy. Thus, the ligands in the axial positions are bound further from the metal centre than those in the equatorial positions and, hence, they are more weakly bound¹²⁷⁻¹²⁹. When this is taken into account along with the different binding shown by MEA and ammonia ligands, this influences the stability constants of the metal complexes that are formed (*Table 4*). The structures of some of the Cu(II) complexes that form in the presence of ammonia and MEA are shown in *Figure 28*¹²⁶. The presence of these different complexes could affect the rate or extent of hydrogen peroxide decomposition in Fenton-like systems. Thus, a difference in the extents of protein oxidation may be observed, as a result of the varying hydroxyl radical flux of the colouring formulations.

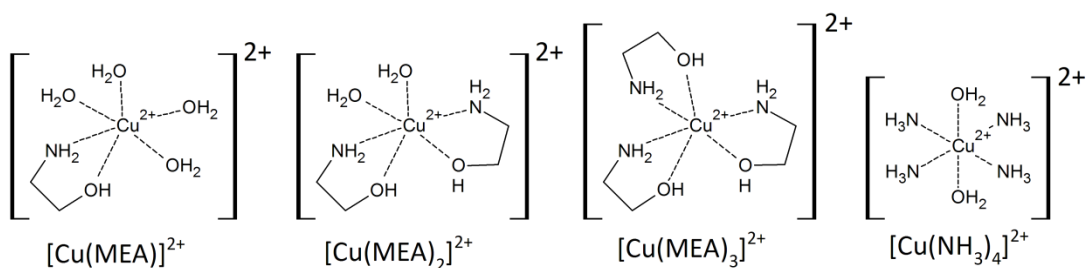


Figure 28: Some examples of the possible complexes that can form as a result of the use of MEA and ammonia in hair colouring systems

It should be noted at this point that most hair colouring formulations use chelating ligands, such as EDTA, which has a higher binding affinity for metal ions than the bases themselves (*Table 4*). However, it is debated whether or not chelating ligands, can diffuse into the hair fibre, due to their size and the large amount of negative charge that they carry. Inside the hair fibres, therefore, the base could become a factor that influences the types of metal complexes that form.

Metal-ligand complex	Stability Constants (LogK)
$[\text{Cu}(\text{MEA})]^{2+}$	4.60
$[\text{Cu}(\text{MEA})_2]^{2+}$	8.25
$[\text{Cu}(\text{MEA})_3]^{2+}$	10.80
$[\text{Cu}(\text{NH}_3)_4]^{2+}$	12.50
$[\text{Cu}(\text{EDDS})]^{2-}$	18.40
$[\text{Cu}(\text{EDTA})]^{2-}$	18.78

Table 4: The measured stability constants of ammonia and MEA copper complexes compared with EDTA and EDDS copper complexes^{95, 130}.

1.7.1.2 Bleaching potential

The lower bleaching potential of MEA formulations could be attributed to the differences in the structure of the bases (*Figure 26*). Although both of these molecules have the ability to swell hair fibres by disrupting hydrogen bonding and cleaving disulphide bonds between proteins, the extent to which this occurs could vary, once formulations containing either ethanolamine or ammonia have been applied. This in turn would affect the rate of diffusion of oxidants into the hair fibres and the extent of melanin bleaching could vary as a result.

The surface tension of hair fibres is another factor that can influence the diffusion of oxidants into the cortex of hair fibres. On changing the base in formulations, the surface tension of the formulations can change^{131, 132}. This difference is more noticeable at higher temperatures, which exist during some salon treatments. The surface tension of the hair fibre is affected, as a result of the variation of formulation surface tension. Thus, the permeability of the hair fibre is in turn affected and the rate of diffusion of molecules into hair fibres will change¹³³. Throughout this thesis the difference in surface tension of model formulations was minimised by studying compositions of relatively low base concentration, at temperatures of 20 °C.

As mentioned above, MEA can form complexes with metal ions, such as copper ions^{126, 134}. This could lead to a change in the redox potential of metal centres. Thus, affecting the kinetics of hydrogen peroxide decomposition, resulting in differences to the extent of bleaching that is observed. It is generally accepted that an increased concentration of MEA is required to achieve the same level of bleaching as that obtained in ammonia-based formulations^{43, 135}.

1.7.2 The possible causes for the differences observed in dyeing systems containing MEA

As well as the differences that are apparent in the bleaching systems, producers of hair dye formulations visually observe changes to the final colours that are obtained from dyeing systems, when ammonia is replaced with MEA. The possible causes of colour changes can again be categorised as either chemical or physical factors (or both).

1.7.2.1 Chemical factors

The differences that manufacturers observe in dye formulations could be due to the change in base affecting the pH. As mentioned on page 41, the two bases NH_3 and MEA have different pK_a values. As manufacturers do not buffer their formulations, this could lead to changes in the pH. Some components of commercial formulations could act as buffers to minimise the differences in pH between MEA-based formulations and ammonia-based formulations. However, if the pH of solutions does change this could have a number of effects on dye formation.

The pH directly affects the rate of oxidation of hair dye primaries in a number of ways. Firstly, it is a key factor in hydrogen peroxide decomposition. Thus, the concentration of oxidants that are available for reaction with the precursor varies with changing pH^{56, 136}. Furthermore, changing the base alters the ratio of the metal

complexes in solution. *Figure 29* shows the speciation plot for an aqueous solution containing 400 mM MEA, 1.3 mM EDDS, 0.18 mM Cu(II) and 70 mM H₂O₂. These conditions were chosen to mimic the concentrations of active species found inside hair fibres. The speciation plots of the equivalent NH₃ solutions are identical. However, if the change in base results in a change in pH, the ratio of CuEDDS²⁻ and Cu(OH)EDDS³⁻ complexes will vary between the systems. These different metal complexes will catalyse dye formation at different rates, due to a change in the redox potential of the metal ion centre. Therefore, a variation in the ratio of these complexes would result in a change in the rate of dye production. Faster rates of dye production would lead to a greater amount of the dyes forming, for similar treatment times. Thus, a darker or bolder shade would be achieved using such a formulation.

Secondly, for systems that involve precursors such as PPD, an increase in pH results in an inhibition of the rate of dye formation³. Corbett proposes the main reason for this is because a high pH affects the concentration of the reactive quinone diimine intermediate ($pK_a = 5.75^3$) that is present in its protonated form. Corbett also suggests that the pH affects the proportion of coupler that can react in its deprotonated form. However, these may not be the reasons for the change in kinetics, as the initial oxidation of PPD is thought to be the rate-determining step. It seems more likely that pH affects the types and quantities of oxidants, such as hydroxyl radical, that are formed during the Fenton reaction, or simply the amount of perhydroxyl anion that is available to oxidise PPD to QDI. Regardless of the reasoning it has been shown that a change in pH does affect the rate of dye formation and this could be an important factor in the quantities of dyes that are produced when different bases are used in formulations.

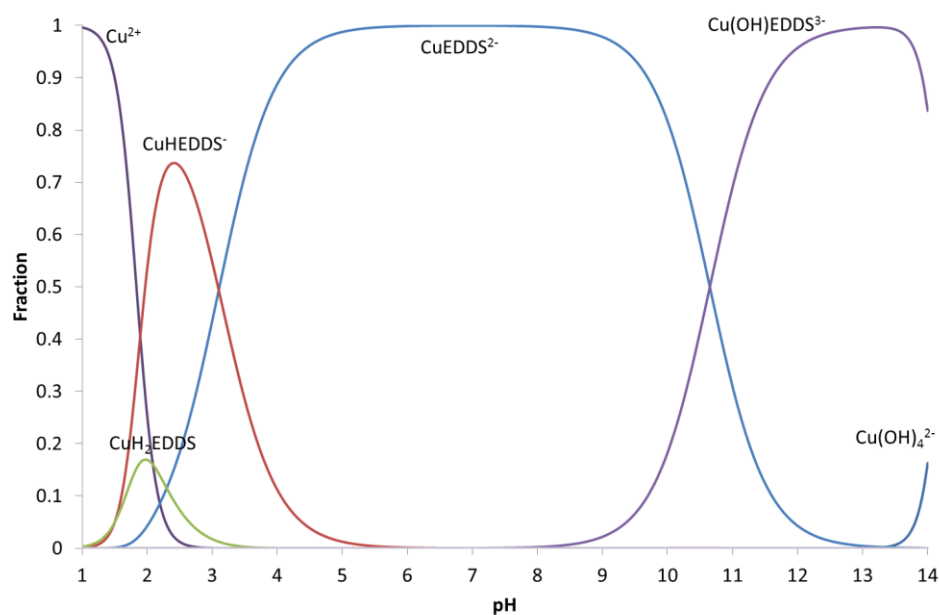


Figure 29: The speciation plot for a solution containing 400 mM MEA, 1.3 mM EDDS, 0.18 mM Cu(II) and 70 mM H₂O₂.

Finally, the pH also affects the overall charge on the final dye molecules, due to the presence of oxygen atoms and nitrogen atoms in the molecules. This too affects the final colour of the system¹¹³.

As a result of these factors, the pH has an effect on the rate of dye formation and hence the final colour of dye formulations¹³⁷. In addition to this, the base may also affect the structure of dye molecules that are produced. For example, MEA is more nucleophilic than NH₃. Therefore, it may be able to react with dye molecules⁴³.

1.7.2.2 Physical factors

In addition to the chemical factors described above, there are several physical factors that may affect hair colouring when MEA is used. Firstly, changing the base could affect the extent of hair fibre swelling. As discussed on page 14, hair fibre swelling is affected by the cleavage of hydrogen bonds and disulphide bridges between hair proteins. This process could be affected by a change in base, which

will initially disrupt the hydrogen bonding and disulphide bridges between proteins to differing extents. As a result, the rate of diffusion of oxidants, such as the perhydroxyl anion, into hair fibres would be affected by the variation in hair fibre swelling. This in turn leads to a variation in the rate or extent of melanin bleaching that occurs when the base is changed, as mentioned in chapter 2. If less melanin bleaching occurs, then more of the natural pigmentation of the hair will be evident in the final shade, after the formulation has been applied. Less melanin degradation further decreases hair fibre swelling, due to fewer voids forming within the fibres (page 15), leading to an even greater effect on the diffusion rates of oxidants. The rate of dye precursor diffusion into the hair fibre will also change as a result of the variation in hair fibre swelling. This is likely to affect the final shade of products, due to differing concentrations of dye forming inside the hair.

Other physical factors that affect the final shade achieved by colouring formulations include temperature, the amount of water present and how hair fibres are pre-treated. However, during this study model aqueous formulations were used, at a constant temperature (20 °C) to account for these factors. The concentrations of active species were also controlled carefully. These conditions were used to ensure that any differences that were observed between the model formulations could be attributed to the change in base.

1.8 Project Aims

The use of MEA in hair colouring formulations results in changes to both the colour that is obtained from using the formulations and the damage that can occur to hair fibres, as mentioned above. These differences could be due to physical effects, such as the volatility of the base or the effect it has on facilitating diffusion of reactants into hair fibres. Alternatively, these differences could be observed because of chemical effects, such as the formation of different radical species or metal-ligand complexes, once formulations have been applied to the hair. The primary aim of this project is to use aqueous model solutions of hair dye formulations in order to

observe the changes in model hair colouring compositions that occur as a result of chemical differences, when the base is changed. By using aqueous solutions, factors such as volatility and varying diffusion rates of active species into hair fibres, will not contribute to any changes that may be observed. As water is the one of the main components of hair colouring formulations, aqueous model solutions can be considered to be a viable model. Any intermolecular forces that play a role in the science behind formulations, such as hydrogen bonding, will play the same role in the model compositions. Importantly, the physical properties of MEA-H₂O based compositions and NH₃-H₂O based compositions are also comparable at 20 °C, for the concentrations of base used in these studies (20 mM – 400 mM). Surface tension and solubility are both equivalent under these conditions (discussed on page 186). Freezing point measurements for both MEA solutions and NH₃ solutions are also equivalent at a concentration of 400 mM (~-1 °C)^{138, 139}. Finally, the refractive index measurements of MEA-water mixtures and ammonia-water mixtures at 400 mM are comparable at 20 °C (1.3371 n_D and 1.3333 n_D respectively^{140, 141}). Taking all of these physical factors into account, it was considered to be appropriate to use aqueous model solutions for the study of reactions that occur during hair colouring, in the presence of MEA or ammonia.

Before the effect of MEA on hair bleaching is investigated, the mechanism of melanin bleaching will be studied. As discussed in chapter 2, it is unclear which oxidants are responsible for melanin oxidation. The work in this chapter will therefore look to identify oxidants of melanin, providing insights into the roles of these oxidants, during the bleaching of the more water-soluble *Sepia* MFA, in model compositions.

Chapter 3 concerns the differences in chemistry when MEA is used in bleaching formulations. Of particular interest is the amount of hydroxyl radical flux in model aqueous bleaching formulations that contain MEA. This provides an indication of the level of protein damage or melanin bleaching that can occur in these systems, when compared with those that contain ammonia.

After discussing the bleaching systems, the mechanism of hair dye precursor oxidation is discussed in chapter 4. It is unclear from the literature which species are responsible for hair dye formation within hair fibres. Therefore, the potential oxidants of dye precursors will be investigated in both aqueous model systems and in systems that contain hair.

Generating hair dye formulations that produce consistent colours can be difficult. Many factors are responsible for slight changes in the final shades of products. This point is discussed in more detail in chapter 5. As a result, changing the base from ammonia to MEA leads to changes to the final colour of dye formulations. Again, in chapter 5, consideration is given to an investigation of aqueous model dye formulations that contain MEA. The chemical reasons for any differences that may be observed are discussed.

Chapter 2

Chapter 2 – Mechanistic studies of soluble melanin bleaching

2.1 Introduction

Bleaching of melanin is an important step in the hair colouring process when consumers desire a colour that is lighter than the natural shade of their hair. Despite it being well known that the process requires hydrogen peroxide at an alkaline pH, there are some areas of the procedure that remain mechanistically unclear. The largest complication is due to the presence of endogenous metal ions in hair fibres, which leads to the decomposition of hydrogen peroxide, via a Fenton(-like) reaction. The resulting mixture of reactive oxygen species (ROS) (See chapter 1) can lead to the bleaching of melanin inside the hair fibre, which lightens the natural shade of the hair. However, the extent to which each individual species contributes to bleaching is not known^{46, 47, 50, 52}. The work in this chapter looks at the mechanistic aspects of melanin bleaching.

2.1.1 Human hair melanin and *Sepia* melanin

As discussed in chapter 1, melanin in the hair fibre is present in two forms. Eumelanin is responsible for the brown-black pigmentation of hair and pheomelanin for the yellow-red pigmentation^{14, 142}. The overall colour of human hair that is observed is predominantly determined by the ratio of these two types of melanin. This ratio is determined by many factors including geography, genetics and ethnicity^{143, 144}. The chemistry of melanin bleaching will change depending on the types of melanin that are present in the hair fibre. This variation in the types of melanin could affect the consistency of bleaching studies if the melanin was extracted from human hair. Additionally, melanin is difficult to extract from hair fibres. Different methods have been used to isolate melanin from hair fibres, resulting in the coextraction of varying levels of proteins and metal ions from the

hair^{145, 146}. To avoid the difficulties associated with melanin isolation from hair fibres, studies in the literature have used *Sepia* melanin (from the ink sacs of *Sepia Officinalis*) as a model for black human hair²⁰. It is possible to precipitate large quantities of *Sepia* melanin from cuttlefish ink in one batch, minimising any inconsistencies in protein and metal ion content, which may arise during the preparation of melanin over multiple extractions.

The comparison between *Sepia* melanin and black human hair melanin can be made, as both pigments are predominantly eumelanin in character, and both thought to consist mainly of DHICA units²³. The main difference between melanin extracted from cuttlefish ink and black human hair is the size of the melanosomes, *Sepia* melanosomes being much larger. This size difference has been shown to affect the rate of melanin bleaching of heterogeneous melanin²⁰. The work in this thesis was based on comparing the rate of a more soluble form of the melanin, minimising the effect that the size of aggregates would have on the rate of melanin bleaching. The added solubility of melanin in this study results in another limitation of the reliability of this model study to commercial bleaching formulations. During hair bleaching treatments it is necessary for oxidants to diffuse into the hair cortex. However, diffusion of oxidants through the hair cuticle to bleach melanin was not necessary in these soluble model compositions. Therefore, this would lead to an apparent increase in rate of bleaching, when compared with that in heterogeneous commercial bleaching formulations. Despite this limitation, the bleaching in model soluble *Sepia* melanin formulations could be studied to provide insights into the role that oxidants play during the oxidation of melanin for individuals that have black hair.

2.1.2 Melanin free acid (MFA)

As mentioned in the previous section, to study the bleaching of melanin it was decided to use the more water-soluble form of *Sepia* melanin, *Sepia* melanin free acid (MFA). Using aqueous model bleaching formulations, containing MFA, it was

possible to monitor its bleaching by UV-vis spectroscopy. Studies by NMR have shown that the monomeric units of MFA are different to those of *Sepia* melanin¹⁴² (Figure 8). There are more quaternary aromatic carbons. Additionally, there is rearrangement involving the C-N bond of the indolic moiety. As such the authors propose that whilst *Sepia* MFA is similar to *Sepia* melanin, it contains more of the monomeric units shown in Figure 30¹⁴⁷.

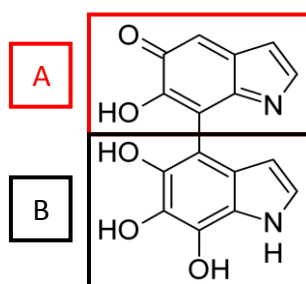


Figure 30: Two of the possible monomeric units (A) & (B) that are more abundant in *Sepia* MFA

As discussed in chapter 1, a large amount of data has been acquired on the structure of melanins. However, the monomeric units of melanin free acid have not been identified. Additionally, it is unclear how these monomers are linked together. This in turn makes determining a mechanism for the degradation of the material difficult.

2.1.3 The mechanism of melanin degradation

Melanin degradation by various oxidants has been the subject of investigation for several years and an exact mechanism has not been determined. Several studies have postulated mechanisms based on the general scheme shown in Figure 31.⁴⁶

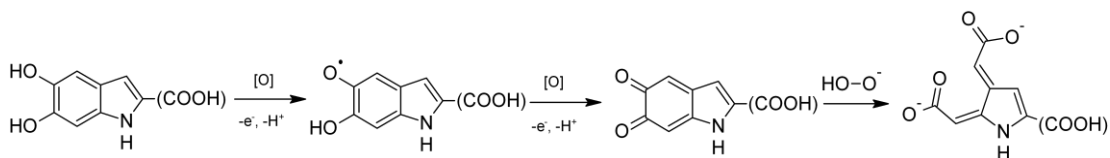


Figure 31: The general reaction scheme for the breakdown of monomeric indole-based units to pyrrolic acids.

This reaction scheme was further explored and more detailed steps are suggested in figures 32-34²⁴. As can be seen, the initial step is the single-electron oxidation of hydroquinone units to *o*-quinone moieties (theoretically feasible with redox metal ions, such as Fe^{III} or Cu^{II}, or by ROS such as HO[•]). This proceeds via the eumelanin radical, as is also shown in Figure 31. The *o*-quinone units are then subject to attack by perhydroxyl anions in a variety of possible ways. The attack may proceed via either of the reaction pathways shown in Figure 32 and 33.

Figure 32 depicts the initial cleavage of the oligomer backbone, in this case the 2,4 linkage, to yield the hydroxylated *o*-quinone (**4**), via a 1,2-dioxetane-mediated C-C cleavage. This *o*-quinone can be further oxidised by the perhydroxyl anion, followed by copper ions or hydroxyl radicals to form PDCA (**5**) and oxalic acid.

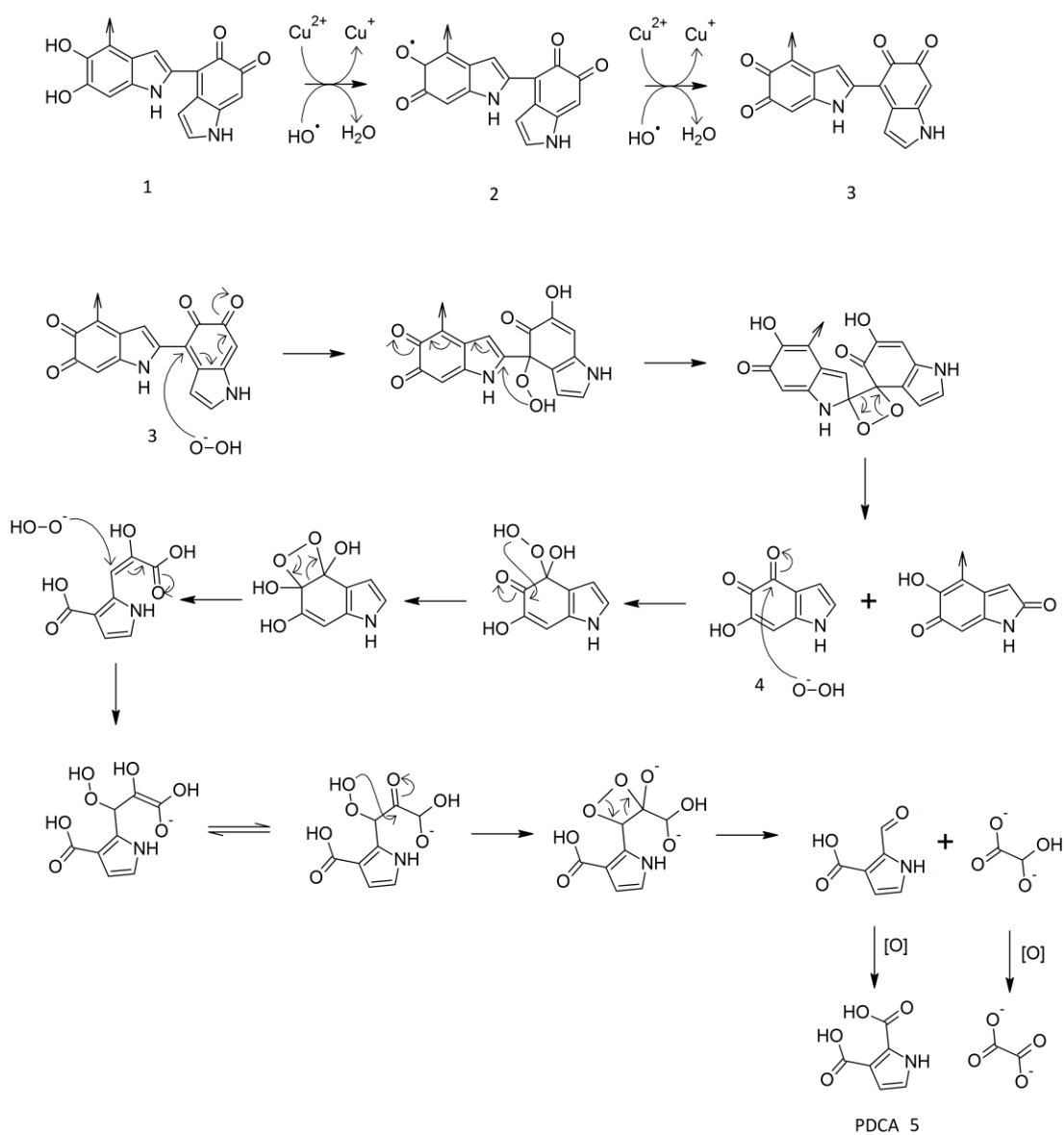


Figure 32: Possible mechanism of the breakdown of eumelanin oligomers by hydrogen peroxide and copper ions to form PDCA.

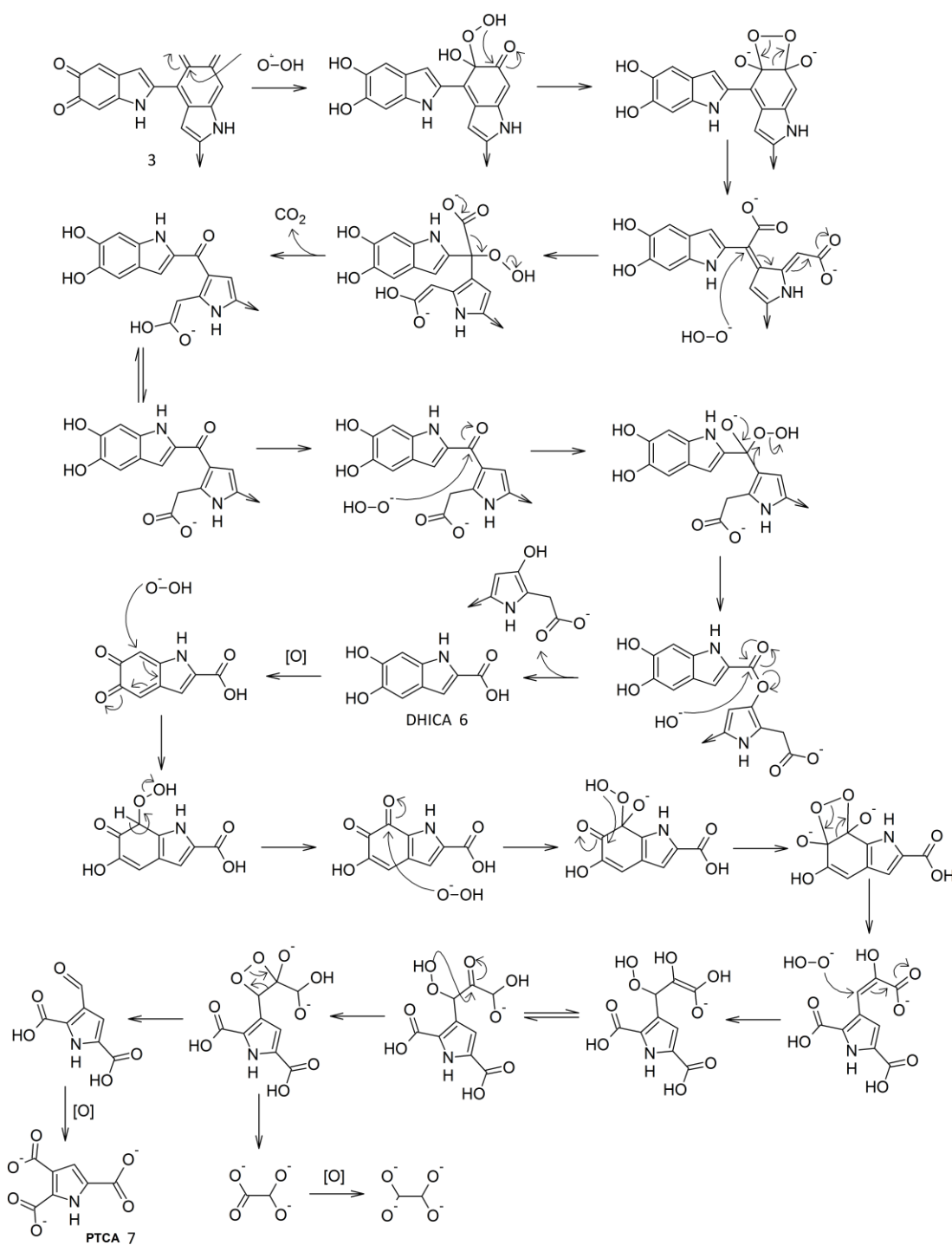


Figure 33: Possible mechanism of the breakdown of eumelanin oligomers by hydrogen peroxide and copper ions to form PTCA.

Figure 33 indicates that one of the *o*-quinone units of **3** is first oxidised via a muconic-type C-C cleavage to the dicarboxylic acid^{24, 148}. Decarboxylation to form a

carbonyl, followed by a Baeyer-Villiger oxidation, allows cleavage of the oligomer backbone to form DHICA (**6**) (Though this is not the only possible mechanism). Further breakdown of DHICA by perhydroxyl anions, followed by single electron oxidants, such as redox metals or hydroxyl radicals, leads to the formation of PTCA (**7**).

Later it was proposed that there may be an alternative reaction pathway, via the epoxide intermediate shown in *figure 34*¹⁴⁹.

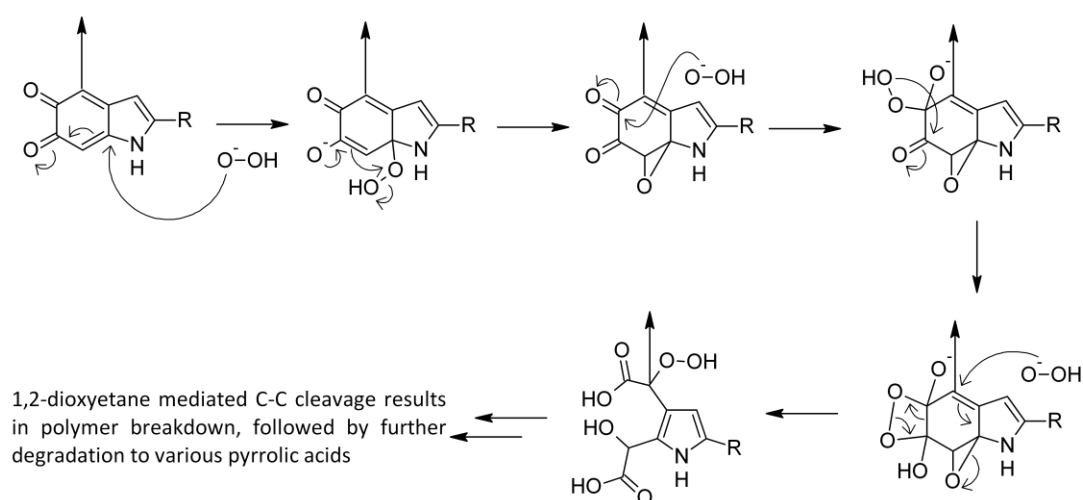


Figure 34: An additional reaction pathway for the breakdown of eumelanin into alternative pyrrolic acids^{150, 151}.

More pyrrolic acids can be formed via this epoxide intermediate. Attempts to interconvert between all the pyrrolic acids by decarboxylation were unsuccessful, showing that the various reaction pathways outlined are independent of each other.

There are several suspected oxidants for the steps shown in *Figure 31* and *Figure 32*. Some of the major species that could potentially contribute towards the oxidation of melanin are discussed in the next section.

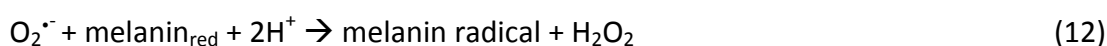
2.1.4 Possible oxidants of melanin in a Fenton-like system

As discussed in chapter 1, the presence of metal ions on the surface and inside hair fibres leads to the catalytic decomposition of hydrogen peroxide, when hydrogen peroxide is used to bleach hair. This leads to the formation of a variety of different reactive oxygen species (ROS), which potentially contribute in some way to the oxidative degradation of melanin, as outlined in *Figure 32*. These ROS include the superoxide anion, hydroxyl radical and perhydroxyl anion. Other possible oxidants may include molecular oxygen and the metal ions themselves. The roles of these oxidants have been studied to some extent in previous work^{46, 149}. However, the relative roles of these oxidants in melanin bleaching remain unknown.

Superoxide anion

The superoxide anion is likely to be formed in H₂O₂-based bleaching systems by a couple of pathways. The first is the oxidation of hydrogen peroxide by metal ions, as in Fenton(-like) chemistry, as discussed in chapter 1. The second is the reduction of molecular oxygen by metal ions.

It has been shown that melanin can oxidise the majority of superoxide anions to form molecular oxygen. The remainder is reduced to form hydrogen peroxide, as shown in reactions (11) and (12). As a result, monomeric melanin units are converted to melanin radicals¹⁵².



When melanin reacts with a superoxide anion, little change is observed in the optical spectrum¹⁵². This is possibly due to the disproportionation of melanin

radicals, yielding *o*-quinone units and hydroquinone units (*Figure 35*), without the oligomeric structure being broken down.

However, when the superoxide anion is produced in a Fenton(-like) system, the presence of other oxidants complicates matters. This results in the further oxidation of the melanin radical or *o*-quinone units, thus degrading the oligomer (*Figure 31*) and leading to a loss of colour.

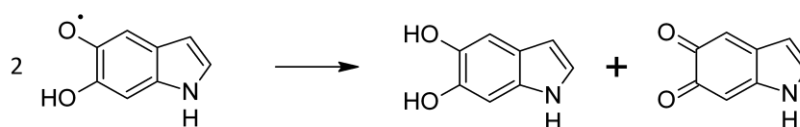


Figure 35: Disproportionation of the melanin radical

UV Radiation

Exposure to radiation has been shown to result in the bleaching of melanin pigments⁴⁶. This has been proposed to be due to the formation of hydrogen peroxide from melanin, in the presence of oxygen, when it is irradiated with UV radiation. *Figure 36* shows how this is possible through the excitation of melanin, to form the melanin radical. This radical can then react with oxygen to form a superoxide anion, which can dismutate in the presence of water to form hydrogen peroxide^{39, 152, 153}. UV radiation or metal ions in the hair fibre may then decompose hydrogen peroxide, to produce ROS, such as the hydroxyl radical, which is implicated in the bleaching of melanin pigments¹⁵⁴. Alternatively, under basic conditions the perhydroxyl anion could attack the quinine moieties of the melanin⁴⁶.

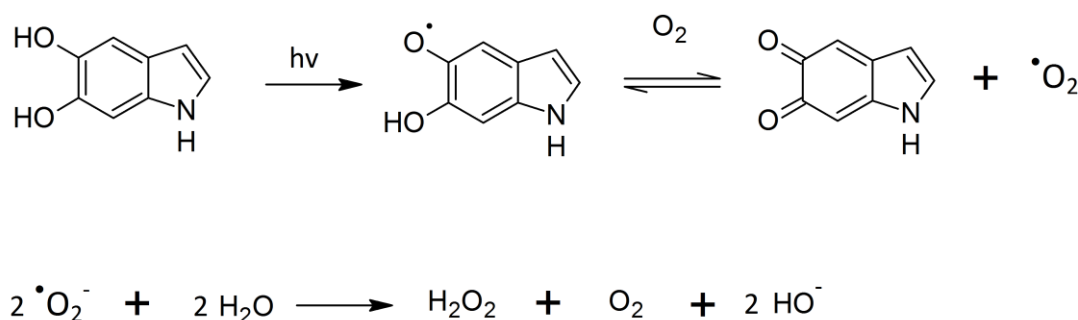


Figure 36: Proposed mechanism for the production of hydrogen peroxide on the irradiation of melanin with UV radiation.

Metal ions

Metal ions can bind directly to melanin units via the hydroxyl groups on DHI units or by the carboxylate groups on DHICA units^{155, 156}. The effect of melanin bound metal ions is complex and the majority of studies have focussed on iron ions. Recent work has shown that the concentration and oxidation state of the metals play important roles in the decomposition of hydrogen peroxide by the melanin-iron complexes^{157, 158}. At high enough concentrations of Fe(III) ions an increase in the production of hydroxyl radicals is evident, compared with that which occurs in melanin-free systems. It has been proposed that this is because the reduction of Fe(III) to Fe(II) is accelerated by melanin, thus increasing the rate of hydrogen peroxide decomposition. At high concentrations, the Fe(III) ions may then displace bound Fe(II) ions from melanin and the solvated Fe(II) can then catalyse the production of hydroxyl radicals. By contrast, when Fe(II) systems were used, hydroxyl radical production appeared to be inhibited in the presence of melanin, potentially as the Fe(II) ions are effectively sequestered¹⁵⁹. Little information is available on the effect of copper ions. However, Korytowksi proposes that a similar situation may exist for the reduction of Cu(II) to Cu(I) by melanin⁴⁶.

Previous work has demonstrated a correlation between the concentration of copper ions and the level of melanin bleaching that is observed for a system, though it is unclear whether this is a direct result of the metal ions themselves or the ROS

that are formed from the decomposition of hydrogen peroxide³⁷. It is possible that metal complex centres could bind to hydroquinone moieties of the melanin. In the presence of oxygen, this could lead to the degradation of melanin, as shown in *Figure 37*^{160, 161}.

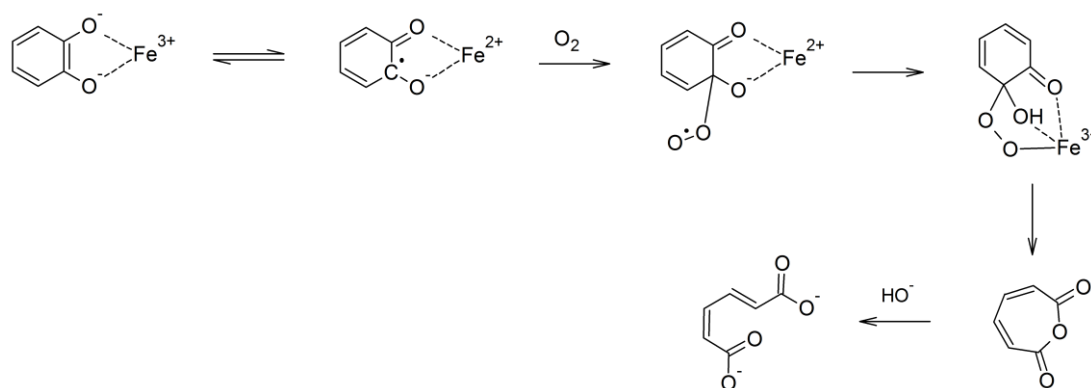


Figure 37: The mechanism for the metal ion oxidation of catechol, in the presence of oxygen, that could potentially be applied to melanin.

Perhydroxyl anion

Typical bleaching systems have a pH of approximately 10. Therefore, as aqueous hydrogen peroxide has a pK_a of 11.65, a substantial concentration of perhydroxyl anion will exist, due to the deprotonation of hydrogen peroxide^{45, 50}. It has been suggested that perhydroxyl anion may cleave carbon-carbon single bonds via nucleophilic addition to *o*-quinone type monomeric units, formed by the reversible oxidation of the hydroquinone monomer units, by other oxidants, as shown in *Figure 31*^{46, 149}. Previous work has indicated that the perhydroxyl anion may also be involved in the solubilisation of melanin, which is a prerequisite for bleaching⁴¹. However, there is no conclusive evidence that proves melanin is bleached by the perhydroxyl anion.

Hydroxyl radical

Hydroxyl radicals can be formed by the metal ion catalysed decomposition of hydrogen peroxide in a Fenton(-like) reaction, as discussed in chapter 1. It is possible that hydroxyl radicals are involved in the initial single electron oxidation steps that are responsible for the reversible conversion of hydroquinone melanin units into *o*-quinone units. It has been shown that phenol is subject to oxidation by hydroxyl radicals to form phenoxy radicals.¹⁶² Similarly, melanin radicals could disproportionate to form *o*-quinone units (*Figure 35*), which are then subject to nucleophilic attack by the perhydroxyl anion^{46, 149}.

Previous work has attempted to use radical scavengers, such as salicylate based compounds in order to inhibit bleaching. However, it was rationalised that this would not provide much information, as hydroxyl radicals would be produced at the metal centres that are bound to melanin. Due to their high reactivity, hydroxyl radicals are more likely to react with the melanin than with the scavenger, at the site of their production⁴⁶. Thus, the exact role of hydroxyl radical in melanin bleaching remains unconfirmed.

The hydroxyl radical is known to react with most organic molecules at diffusion-controlled rates¹⁶³. This causes problems when trying to monitor melanin bleaching in heterogeneous systems. It is likely that the hydroxyl radicals generated in heterogeneous bleaching baths will react with the outer cuticles of hair fibres or with melanosome membranes of isolated heterogeneous melanin, rather than diffuse through these structures to oxidise the melanin itself. In fact, it is the reaction of hydroxyl radicals with hair cuticles that is thought to contribute to hair fibre damage⁵⁰. Homogeneous aqueous bleaching systems could be used to gain a representation of the effect that the hydroxyl radical has on melanin bleaching. This would avoid the problems that are associated with the diffusion of oxidants into hair fibres, as mentioned above.

If the relative concentrations of oxidants, such as hydroxyl radical, present in various bleaching systems can be determined, then the roles of certain species

involved in the oxidation of melanin may be investigated for soluble melanin bleaching systems.

2.2 Aims

The primary aim of the work that is addressed in this chapter was to establish the mechanism of soluble melanin bleaching in aqueous solutions. The use of these aqueous compositions was to ensure that bleaching solutions could be monitored by UV-vis spectroscopy. It also served to remove problems associated with the diffusion of highly reactive species into hair fibres or through melanosome membranes of heterogeneous melanin, as mentioned on pages 14 and 64²⁰.

Studying the role of the hydroxyl radical in melanin bleaching would be beneficial, as melanin is known to bind metals^{155, 156, 164}. Any perhydroxyl anion or hydrogen peroxide that diffuses into the hair fibre may be decomposed directly at the melanin, due to bound redox metal ions. Therefore, site-specific oxidation of melanin may occur. By studying the effect of hydroxyl radicals on melanin oxidation in soluble solutions, it was hoped that some insight into the process of hair bleaching might be forthcoming.

Additionally, the perhydroxyl anion has been postulated to play an important role in melanin bleaching⁴⁶. By studying bleaching systems at varying pH values, the role of the perhydroxyl anion in melanin bleaching could be investigated.

Also of interest is the role that ammonia plays as a base, in the bleaching of soluble melanin. It was thought that by comparing systems that used NaOH or NH₃, buffered to the same pH, the rates of melanin oxidation could yield information on the role of bases in the chemistry of hair bleaching processes.

2.3 Experimental Methods

All the melanin bleaching reactions that were carried out in this work were performed in the laboratory, in the presence of light. The metal ion concentration of bleaching solutions was carefully controlled.

Hydroxyl radical concentration and perhydroxyl anion concentration were varied to observe their effect on melanin bleaching. To determine the relative concentrations of each of these oxidants, the following procedures were used.

Perhydroxyl anion

The perhydroxyl anion concentration is easily calculated using the Henderson-Hasselbalch equation, given the pK_a of hydrogen peroxide (11.65)⁴⁵:

$$pH = pK_a + \log_{10} \frac{[A^-]}{[HA]}$$

For an initial hydrogen peroxide concentration of 0.979 M, the concentration of perhydroxyl anion is 1000 times greater in a system at pH 10 compared with one at pH 7:

At pH 7, $[HOO^-] = 0.022 \text{ mM}$

At pH 10, $[HOO^-] = 21.92 \text{ mM}$

It is important to remember that in certain Fenton(-like) systems, extensive decomposition of hydrogen peroxide occurs, which will obviously affect the concentration of perhydroxyl anion that is available for bleaching over the course of time.

Hydroxyl radical

As mentioned in chapter 1, the hydroxyl radical can be quantitatively estimated for each individual system using the UV active probe NPDPA, which has been synthesised by Singh and Hider¹⁰⁴. The structure of NPDPA and the mechanism of hydroxylation are shown in *Figure 38*.

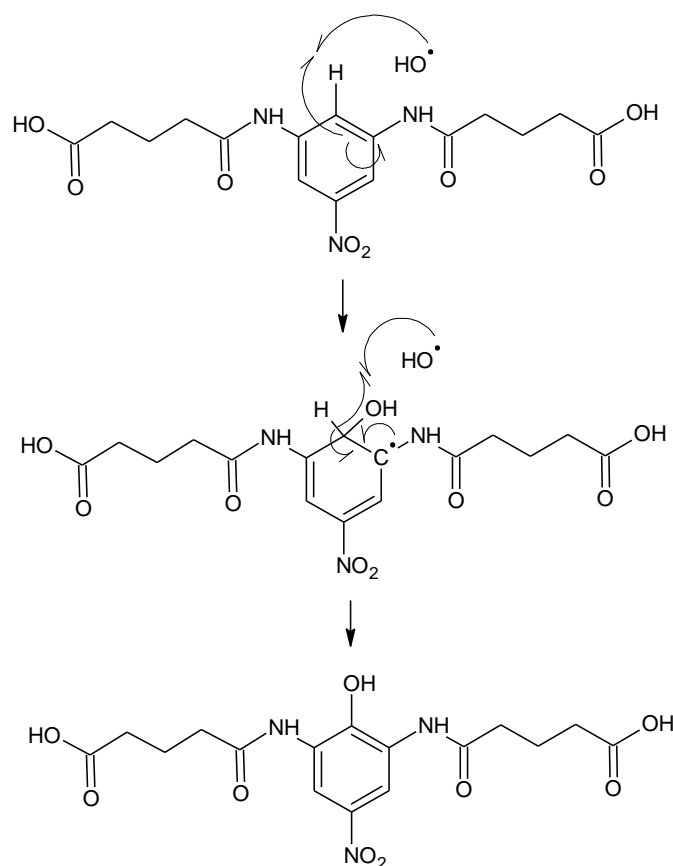


Figure 38: The mechanism of hydroxylation of the colorimetric probe NPDPA

As can be seen from the mechanism, the hydroxyl radical reacts with NPDPA, to yield a hydroxylated carbon-centred radical. Aromaticity is regenerated by the loss of a hydrogen atom. This could occur due to the single-electron oxidation of the intermediate by a number of species, including redox metal ions or the hydroxyl radical. The hydroxylated product that is formed has a strong absorbance at 430 nm (λ_{max}). By monitoring the absorbance at this wavelength during a Fenton(-like) reaction, a relative quantitative estimation of the concentration of hydroxyl radicals

produced in each system can be measured. This method cannot give an absolute concentration of hydroxyl radicals, as the selectivity of the reaction of NPDPA with hydroxyl radicals is unknown.

It's important to bear in mind that this method measures the hydroxylation of the NPDPA probe. Whether this is due to the hydroxyl radical or a non-radical species, such as the ferryl ion (See page 18) is unclear. Both of these reactive oxygen species have similar reactivity. Attempts to distinguish between them have been made for years. However, it is very difficult to make clear distinctions. Some studies suggest that both species may be present in a way that is dependent on the exact reaction conditions^{71, 165}.

2.3 Results and Discussion

It is unclear from the literature which oxidants play a role in the breakdown of melanin during hair bleaching. It was therefore decided to focus on identifying the roles and relative importance of oxidants, such as the hydroxyl radical and the perhydroxyl anion, in melanin bleaching. It was thought that the relative rates of melanin bleaching under various conditions could yield information on the roles of these oxidants. With this in mind it was decided that a study of the oxidation of soluble melanin in homogeneous model hair bleaching solutions should be undertaken. By using homogeneous solutions, physical factors such as the diffusion of hydrogen peroxide into hair fibres, or the solubilisation of melanin, should not interfere with the observed rate of melanin bleaching.

When dissolved in aqueous solutions, melanin gives a broadband absorbance when observed by UV-vis spectroscopy. As melanin is bleached and degraded it becomes colourless and there is a uniform decrease of the broadband absorbance, as shown in *Figure 51*. Therefore UV-vis spectroscopy is an appropriate method for monitoring the bleaching. Though the spectrum of melanin lacks defined peaks, bleaching can be monitored by following an arbitrary wavelength. With this in mind, several experiments were designed whereby aqueous solutions of melanin were bleached with hydrogen peroxide under varying conditions. The effect of the hydroxyl radicals and perhydroxyl anions on soluble melanin bleaching was the primary area of focus.

2.3.1 Preparation of *Sepia* MFA and bleaching solutions

Sepia melanin was isolated from the ink of *Sepia Officinalis* and converted to Melanin Free Acid (MFA), as described in work by Magarelli and Aime^{147, 166}. The electronic spectrum of *Sepia* MFA in NH₄OH is shown in spectrum (i) (*Figure 39*). The elemental analysis of *Sepia* melanin and MFA are shown in *Table 5*, both analyses compare well with the literature values^{147, 166}. *Sepia* MFA was then dissolved in a

base (NH_3 , MEA or NaOH) and the rate of bleaching by hydrogen peroxide was monitored using UV-vis spectroscopy.

Element	% C	% H	% N	% Rest
<i>Sepia</i> melanin observed	54.54	3.85	9.18	32.44
<i>Sepia</i> melanin theoretical ²⁶	53.64	2.80	8.52	35.04
<i>Sepia</i> MFA observed	42.15	4.96	9.13	43.76
<i>Sepia</i> MFA theoretical ²⁶	44.62	3.39	7.60	44.39

Table 5: Partial elemental analysis of *Sepia* melanin and of *Sepia* MFA, compared to literature values.

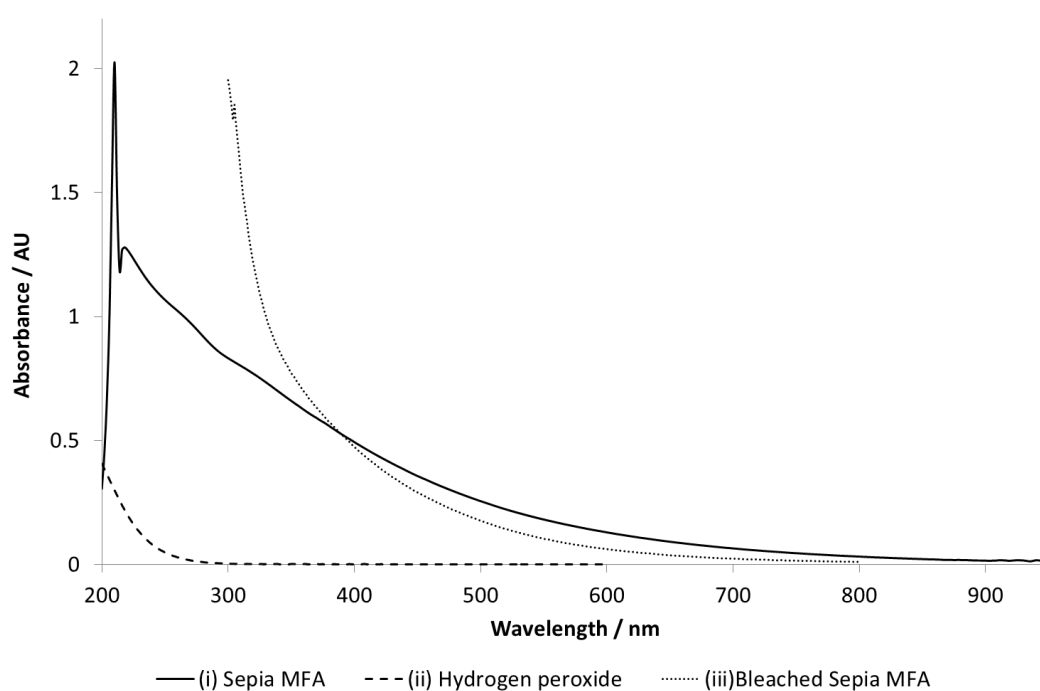


Figure 39: The UV-vis spectrum of (i) 0.03 mg mL^{-1} *Sepia* MFA in $400 \text{ mM NH}_4\text{OH}$ at $\text{pH } 10$ & $20 \text{ }^\circ\text{C}$, exhibiting broadband absorbance (ii) 8 mM hydrogen peroxide in water (iii) 0.03 mg mL^{-1} *Sepia* MFA that has been bleached for 120 minutes at $\text{pH } 10$ & $20 \text{ }^\circ\text{C}$ in the presence of $400 \text{ mM NH}_4\text{OH}$, 0.18 mM Cu(II) and $0.979 \text{ M H}_2\text{O}_2$, exhibiting a uniform decrease in absorbance in the visible region.

A substantial absorbance is present between 200 - 300 nm in the spectra of bleaching solutions (spectrum (iii) in *Figure 39*). This absorbance was shown to be caused by the high concentration of hydrogen peroxide in the solutions (spectrum (ii) *Figure 39*). This high concentration of hydrogen peroxide makes the UV region of MFA spectra difficult to analyse. However, it is apparent that during bleaching there is a uniform decrease in the broadband absorbance at wavelengths higher than 450 nm. This decrease in absorbance occurs as a result of the degradation of the oligomeric chains that comprise the melanin. Therefore, it was considered to be necessary to choose a wavelength above 450 nm to monitor the relative concentration of melanin during bleaching. For the sake of this study a wavelength of 532 nm was chosen, as melanin shows broad band absorbance and no wavelength of maximum absorbance is apparent. As a control it was necessary to monitor colour fading of the *Sepia* MFA, once it had been dissolved in solution. This was to ensure that bleaching in the formulations occurred as a direct result of the oxidants being studied, preventing any misrepresentations.

2.3.2 Colour fading studies of *Sepia* MFA

Monitoring the fading of the solubilised melanin was achieved by dissolving 0.06 mg mL⁻¹ *Sepia* MFA in 20 mM NH₃ at pH 10 and adding 0.18 mM Cu(II). These conditions were chosen as they represent the conditions used for bleaching throughout this work, before hydrogen peroxide is added (see section 2.3.4 for a detailed rationalisation of the conditions). Colour fading was then monitored by UV-vis spectroscopy at 20 °C for 2 hours. The electronic spectra are shown in *Figure 40*.

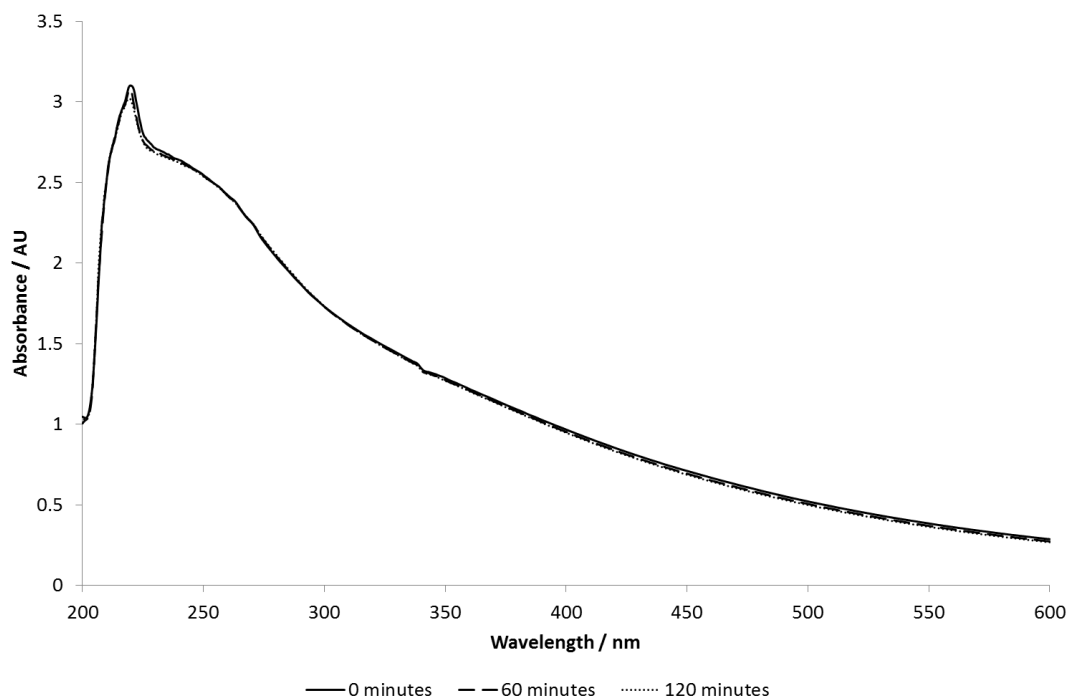


Figure 40: UV-vis spectra to show the fading of *Sepia* MFA over 2 hours at 20 °C where it was dissolved in 20 mM NH_3 at pH 10 in the presence of 0.18 mM Cu(II) .

It can be seen that over the course of 2 hours, under conditions that were used for bleaching (before hydrogen peroxide is added), there is negligible fading of colour. This is evident as there is very little change to the intensity of the UV-vis spectra over the course of 2 hours. Therefore, it follows that under basic conditions, in the presence of copper ions and oxygen, very little melanin is oxidised at 20 °C over the course of 2 hours.

Having demonstrated that the solubilisation of the *Sepia* MFA itself did not lead to substantial colour loss, the rate of melanin bleaching by hydrogen peroxide could then be monitored with confidence, using UV-vis spectroscopy. It was of considerable interest to study the effect of hydroxyl radicals on melanin bleaching, as it is not clear from the literature whether this ROS contributes to the breakdown of melanin. In order to investigate the effect of hydroxyl radicals on *Sepia* MFA bleaching, it was decided to use Fenton(-like) systems containing the soluble melanin. This provided model homogeneous solutions that were similar to the

environment that exists during hair bleaching procedures. In order to control the flux of hydroxyl radicals during bleaching, a variety of chelating ligands were used.

Before this bleaching was monitored, it was necessary to quantify the extent of hydroxyl radical production in the systems containing ligands, using UV-vis spectroscopy and the colorimetric probe NPDPA. Due to the broadband absorbance of melanin it was necessary to omit it from solutions, when using NPDPA to monitor the hydroxyl radical flux (in order to prevent the convolution of UV-vis spectra). However, as melanin is known to bind metals, its omission from Fenton-like solutions could lead to a change in the environment of metal ion centres. This could then affect the amount of hydroxyl radicals that is produced, when compared with systems containing melanin. It was therefore considered to be necessary to determine whether or not the copper ion environment changes on the removal of the melanin from the bleaching solutions.

2.3.3 The copper atom environment during melanin bleaching

Many types of melanin have been shown to be effective at binding redox metals, such as Cu(II) and Fe(III), predominantly by the hydroxyl groups of multiple hydroquinone moieties in the melanin, as shown in (*Figure 41*)^{155, 156, 160, 167}. The carboxylic acid group of DHICA units has been shown to bind Ca²⁺ and Mg²⁺¹⁶⁷. However, binding in this manner has only been demonstrated for Fe(III) at acidic pH¹⁶⁰. Due to this tendency of melanin to bind to metal ions, it was important to determine whether chelating ligands, such as EDTA, bind the metal centres effectively in the presence of *Sepia* MFA. The effect of the metal-ligand complex on hydrogen peroxide decomposition and hydroxyl radical production in a Fenton-like system could then be determined.

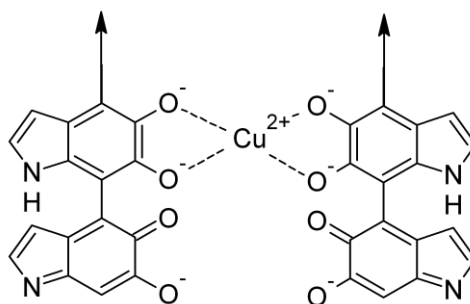


Figure 41: The binding of metals by melanin residue at alkaline pH¹⁵⁶

Figure 42 shows the EPR spectra of frozen solutions, at 140 K, containing 20 mM NH_4OH , 0.18 mM Cu(II), (1.3 mM EDTA and/or 0.06 mg mL⁻¹ *Sepia* MFA). The hyperfine (A) and g-tensors for each spectrum were simulated using EasySpin in MATLAB and are shown in Table 6. It is apparent that in the presence of EDTA and *Sepia* MFA, Cu(II) is bound to EDTA. The addition of *Sepia* MFA to a solution containing 0.18 mM Cu(II) and 1.3 mM EDTA in 20 mM NH_4OH makes little difference to the EPR spectrum that is observed. The simulated parameters of the Cu(II)-EDTA spectrum compare well to values from the literature ($g_{\parallel} = 2.337$, $g_{\perp} = 2.09$ & $A_{\parallel} = 431.58$ MHz^{168, 169}).

Both of these spectra vary significantly from the spectrum of Cu^{II} in ligand-free solutions containing *Sepia* MFA, showing that the copper is not bound to the melanin. 0.06 mg mL⁻¹ *Sepia* MFA is roughly equivalent to a concentration of 0.36 mM, based on the unit molecular weight of 164.4 g mol⁻¹ proposed by Katritzky²⁶. Therefore, *Sepia* MFA should not be saturated with copper ions. Additionally, the EPR spectrum of copper in solutions of *Sepia* MFA shows that only one copper species exists in solution under these conditions. Presumably, this is a Cu(II)-*Sepia* MFA complex, based on previous studies on the affinity of various melanins for copper^{155, 156}. The simulated parameters of the Cu(II)-MFA complex do not compare well with literature values for Cu(II)-catechol melanin, at pH 9.9 ($g_{\parallel} = 2.271$ & $A_{\parallel} = 575.00$ MHz¹⁵⁵), though this could be due to the structural differences between the *Sepia* MFA and catechol melanin (Figure 30 & Figure 10). Despite this, it can be

concluded from these EPR spectra that Cu(II) is not bound to *Sepia* MFA in the presence of EDTA.

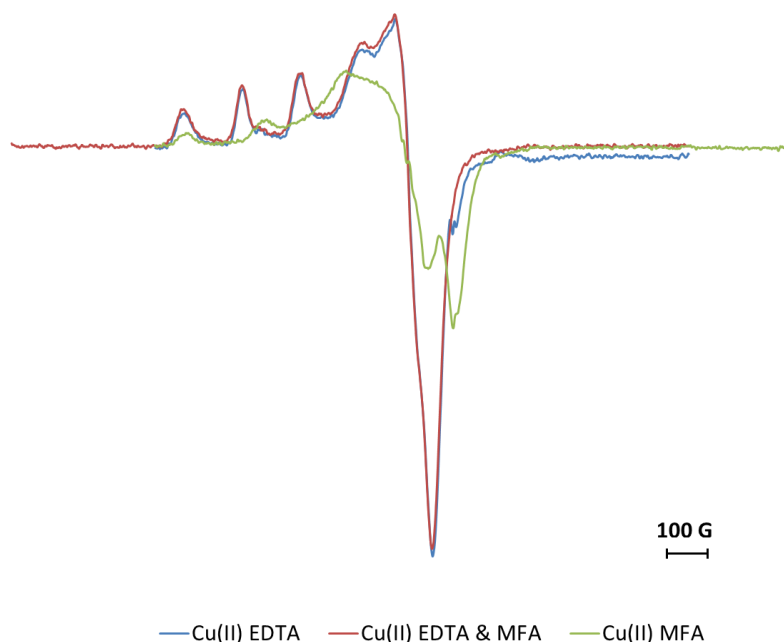


Figure 42: EPR spectra of frozen solutions at 140 K containing 20 mM NH_4OH , 0.18 mM Cu(II), (1.3 mM EDTA) and/or (0.06 mg mL^{-1} *Sepia* MFA at pH 10. Spectral subtraction has been used to remove the melanin signal from all spectra.

Complex	g_{\parallel}	g_{∞}	$A_{\parallel} / \text{MHz}$	A_{∞} / MHz
Cu(II)-EDTA	2.307	2.065	434.39	39.23
Cu(II)-MFA	2.395	2.055	599.73	120.51

Table 6: The hyperfine (A) and g tensors for copper-EDTA and copper-MFA complexes.

These results are consistent with the literature data on binding constants of synthetic DHI-melanin, which show that copper bound to the hydroxyl groups of

hydroquinone moieties has a binding constant of $\log k = 15.6$.¹⁵⁶ EDTA has a higher binding constant for Cu(II) (*Table 7*), confirming that any metal ions present in solution will be chelated to the ligand. It is important to note that the binding constant of the Cu(II)-MFA complex will be slightly different to the value shown for Cu(II)-synthetic melanin, as there are some structural differences between the two melanins (*Figure 10* and *Figure 30*). However, synthetic melanin provides a good model to make an estimate of the binding constant of Cu(II)-MFA complex.

In order to determine the time taken for ligands, such as EDTA, to chelate the copper ions that are bound to *Sepia* MFA. It was decided to study the change in kinetics of hydrogen peroxide decomposition, when EDTA is added to a solution of a Cu(II)-MFA complex in alkaline conditions. Hydrogen peroxide decomposition is thought to occur in the presence of the copper-melanin complex⁴⁶. By contrast, the EDTA-Cu(II) complex is known to result in negligible hydrogen peroxide decomposition, (see chapter 3). Thus, the time taken for the change in the kinetics of hydrogen peroxide decomposition to occur should provide an indication of the time taken for EDTA to chelate copper centres from *Sepia* MFA.

The rate of hydrogen peroxide decomposition can be studied by measuring the volume of oxygen evolved during the Fenton-like reaction, (see chapter 7). Using this method the percentage peroxide decomposition was calculated for a system containing 20 mM NH₃, 0.18 mM Cu(II) and 0.979 M H₂O₂ at pH 10 & 20 °C with 1.3 mM EDTA added at a reaction time of 30 seconds. By delaying the addition of EDTA by 30 seconds the rate of hydrogen peroxide can be observed before the addition of ligand. The change in the kinetics of the decomposition can thus be observed on the addition of the ligand.

Figure 43 shows that for a Fenton(-like) system containing 20 mM NH₄OH, 0.18 mM Cu(II) and 0.979 M H₂O₂ at pH 10 & 20 °C, the rate of decomposition proceeds at a relatively slow rate, before the addition of 1.3 mM EDTA. Upon the addition of the ligand, the rate of decomposition becomes negligible, showing that Cu(II)-EDTA complex is effective at inhibiting the breakdown of hydrogen peroxide.

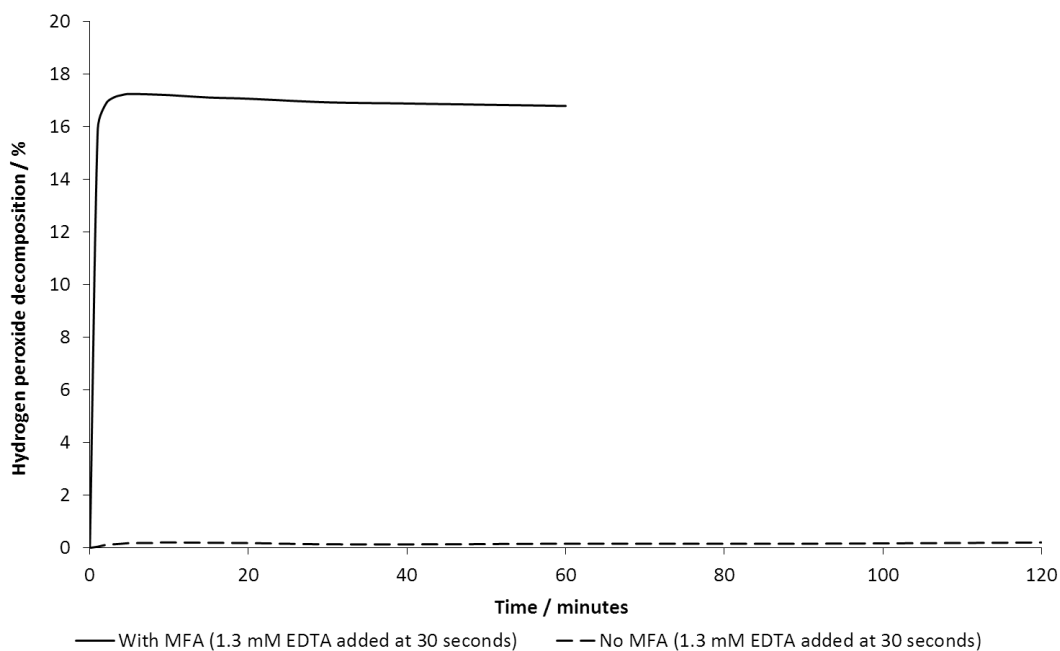


Figure 43: Graph to show the rates of hydrogen peroxide decomposition for the following systems: 20 mM NH_3 , 0.18 mM Cu(II) , 0.979 M H_2O_2 , (0.06 mg mL^{-1} *Sepia* MFA) at pH 10 & 20 °C. 1.3 mM EDTA, added at 30 seconds.

For a system containing *Sepia* MFA (20 mM NH_3 , 0.18 mM Cu(II) , 0.979 M H_2O_2 and 0.06 mg mL^{-1} *Sepia* MFA, at pH 10 & 20 °C, with the addition of 1.3 mM EDTA, at a reaction time of 30 seconds), the initial rate of hydrogen peroxide decomposition, before EDTA addition, is much greater than the corresponding system without *Sepia* MFA. This suggests that the Cu(II) -melanin complex may catalyse hydrogen peroxide decomposition, initially in a similar manner to that of the Fe(III) -melanin complex, where the metal ion centre is reduced by melanin (Page 62)¹⁵⁸. Korytowski proposes that this is also a possibility for Cu(II) -melanin. Furthermore, it has been shown that Cu(I) -melanin is readily oxidised by hydrogen peroxide or oxygen⁴⁶, whereas this has not been shown for Fe(II) -melanin complexes. Therefore, the catalytic activity of bound-to-melanin copper ions appears to differ to iron ions and can efficiently decompose hydrogen peroxide.

Upon the addition of EDTA, at 30 seconds the rapid inhibition of peroxide decomposition is observed, as in the MFA-free system. This is evidence for the rapid

binding of copper by EDTA, in aqueous systems that contain soluble *Sepia* MFA. Additionally, it was shown that the EDTA-Cu(II) complex is the only copper ion environment that will exist in these bleaching solutions. Thus, it can be assumed that the concentration of hydroxyl radical flux, measured in the absence of melanin, will be similar to systems that contain melanin. Although the extraction of copper from melanin was only investigated for EDTA, it can be reasonably assumed that EDDS and DTPMP would behave in a similar manner due to the high stability constants of the Cu(II) complexes (*Table 7*). When HEDP is added to solutions of melanin and copper at a basic pH, Cu(II) is likely to remain bound to the melanin due to the low affinity of HEDP for Cu(II) ions under alkaline conditions (See *Figure 69*).

Ligand	Stability Constant / logK
EDTA	18.78
EDDS	18.50
DTPMP	19.50
HEDP	12.10

Table 7: The stability constants of various Cu(II) complexes^{95, 130}.

Using the colorimetric probe NPDPA, the production of hydroxyl radicals as a result of hydrogen peroxide decomposition by these copper-ligand complexes, could be measured. As discussed, it was necessary to omit melanin from these experiments, as the broad band absorbance it exhibits interferes with the absorbance due to the hydroxylated NPDPA probe. However, for the EDTA, EDDS and DTPMP systems melanin is unlikely to make a difference to the extent of hydroxyl radical production observed. This may not be the case for the ligand-free and the HEDP systems, as the presence of melanin appears to accelerate hydrogen peroxide decomposition in the absence of strong ligands (*Figure 43*). Therefore, when melanin is omitted from HEDP and ligand-free systems, an underestimation of the level of hydroxyl radical

production may result. By measuring the relative concentrations of the hydroxyl radical flux in the various Fenton-like systems described in section 2.3.4, one can provide information to help to determine the effect that the radical has on melanin bleaching.

2.3.4 The effect of hydroxyl radicals on *Sepia* MFA bleaching

It is unclear from the literature if hydroxyl radicals play a role in melanin bleaching. Thus, it was decided to use a range of Fenton-like systems, which result in various concentrations of hydroxyl radicals, to observe the effect that the radical has on the breakdown of the melanin. Fenton-like systems that contain ligands, such as EDTA, are known to result in a low hydroxyl radical flux, whereas ligand-free systems result in much more hydroxyl radical production, due to extensive hydrogen peroxide decomposition, (see chapter 3). As discussed in the previous section, when chelating ligands are not added to melanin/copper solutions the copper will be bound by melanin. Therefore, these systems are not truly ligand-free, but are referred to as such for the sake of simplicity. By comparing the extent of melanin oxidation in ligand-free compositions to those that contain ligands, the effect of the hydroxyl radical on bleaching can be observed.

First it was necessary to determine the hydroxyl radical flux, in the various Cu(II) formulations, that could be used to bleach *Sepia* MFA. To do this the following composition was monitored at 430 nm by UV-vis spectroscopy, 20 mM NH₄OH, (1.3 mM ligand), 0.18 mM Cu(II), 0.979 M H₂O₂ and 1 mM NPDPA at pH 10 & 20 °C.

These conditions can be considered to be a model, to simulate the conditions used in commercial hair bleaching formulations. The concentration of ammonia used was substantially lower than that used in commercial formulations to avoid complications with the UV-vis spectra, as discussed in chapter 3. However, solutions were still buffered to pH 10. This is typical of the pH that is provided by bleaching formulations. A copper ion concentration of 0.18 mM Cu(II) was used to mimic the

concentration of copper ions found in the hair cortex, where melanin bleaching occurs. The hydrogen peroxide concentration used is also representative of the concentration found in commercial formulations. Finally, NPDPA was used to quantitatively estimate the amount of hydroxyl radical produced by these model bleaching formulations. Once the amount of hydroxyl radical had been estimated, the NPDPA was replaced with 0.06 mg mL^{-1} *Sepia* MFA, to provide a model composition that would represent the typical environment found during the bleaching of black hair. It was thought that in particular these model compositions could provide information on the bleaching of hair in individuals from Asia, where black hair is common.

As discussed on page 67, the colorimetric probe NPDPA is hydroxylated in the presence of hydroxyl radicals. The hydroxylated adduct (hNPDPA) has a strong absorbance at 430 nm (*Figure 44*). Thus, by monitoring the absorbance at 430 nm, a relative quantitative estimate can be made for the amounts of hydroxyl radical that are produced by the various Fenton-like systems.

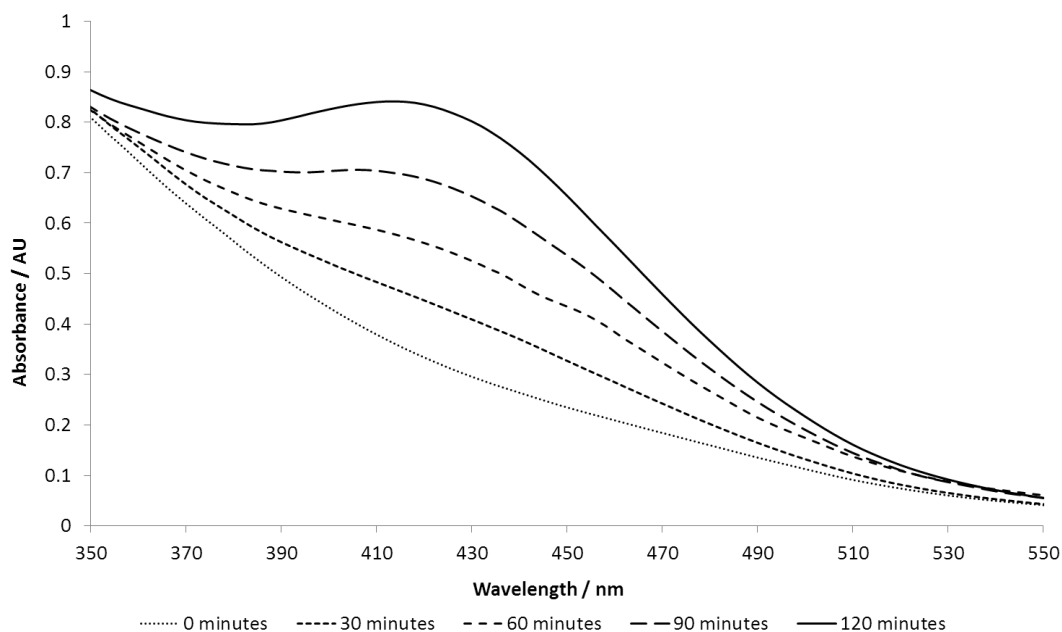


Figure 44: The UV-vis spectra showing an increasing absorbance at 430 nm due to hNPDPA formation during the reaction of 20 mM MEA, 0.18 mM Cu(II) and 0.979 M H₂O₂ and 1 mM NPDPA, at pH 10 & 20 °C.

The results in *Figure 45* show that for systems containing ligands, there is generally a very low hydroxyl radical flux, when compared with the ligand-free system, which shows a steady increase in hydroxyl radical production across 2 hours. One exception is the HEDP system, which shows a rapid generation of the hydroxyl radical inside the first 20 minutes, at which point the production of hydroxyl radical levels off. The seemingly odd behaviour of this system can be explained by recognising the formation of copper nanoparticles in Fenton-like systems that contain HEDP. These nanoparticles initially catalysed the decomposition of hydrogen peroxide, generating a high quantity of hydroxyl radical. After a reaction time of 20 minutes, the nanoparticles aggregated, leading to an abrupt decrease in the rate of hydrogen peroxide decomposition¹⁷⁰.

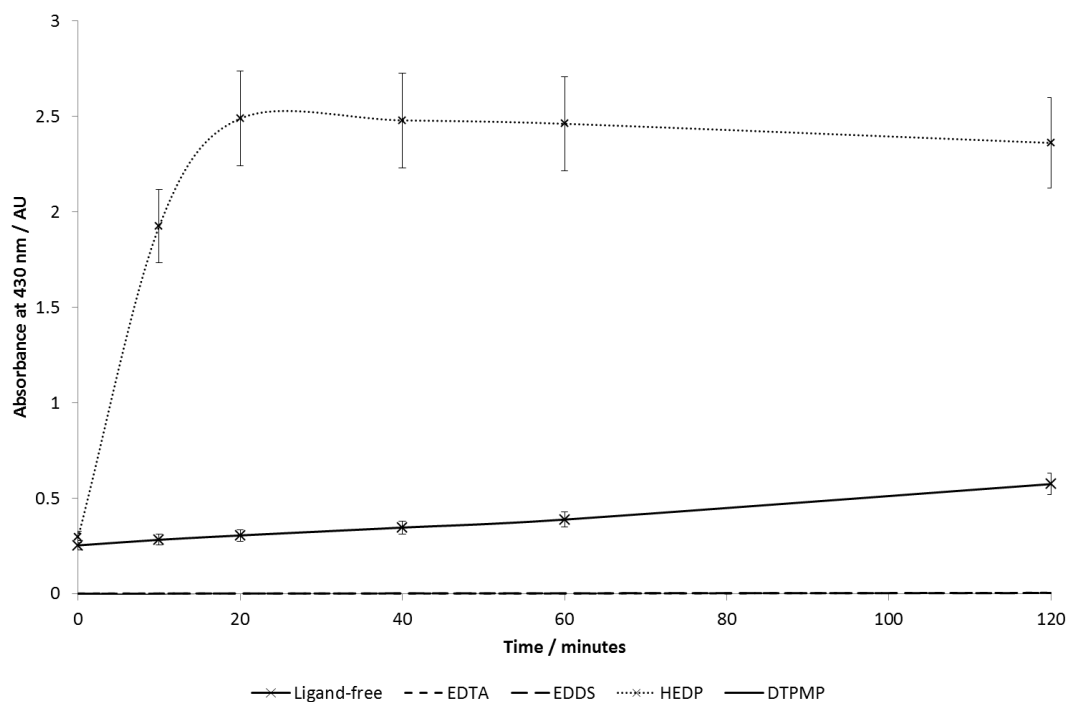


Figure 45: Graph to show the rate of formation of hydroxyl radical, by observation of the absorbance at 430 nm in the following systems: 20 mM NH_3 , (1.3 mM ligand), 0.18 mM Cu(II) , 0.979 M H_2O_2 and 1 mM NPDPA at pH 10 & 20 °C

For the ligand-free and HEDP systems there is already a substantial absorbance at the beginning of the reaction. This is due to the rapid generation of the hydroxyl radical in these systems. This, coupled with the high reactivity of the hydroxyl radical, results in an immediate hydroxylation of the NPDPA probe and hence a considerable absorbance is evident immediately after the reaction is initiated.

Using this information concerning hydroxyl radical production, it was next decided to use the same conditions to bleach melanin. It would thus be obvious if there was a correlation between the amount of hydroxyl radicals produced by a formulation and the extent of melanin bleaching that occurs.

The general reaction studied involved the use of 20 mM NH_3 , (1.3 mM ligand), 0.18 mM Cu(II) , 0.979 M H_2O_2 and 0.06 mg mL⁻¹ *Sepia* MFA, at pH 10 & 20 °C. These are the same conditions that were used to monitor the hydroxyl radical formation, with the substitution of NPDPA for *Sepia* MFA. A concentration of 0.06 mg mL⁻¹ MFA was

used, as this provided the absorbance that could be monitored reliably by UV-vis spectroscopy without any solubility issues arising. The rate of soluble *Sepia* MFA bleaching by hydrogen peroxide and Cu(II), with and without ligands, is shown in Figure 46.

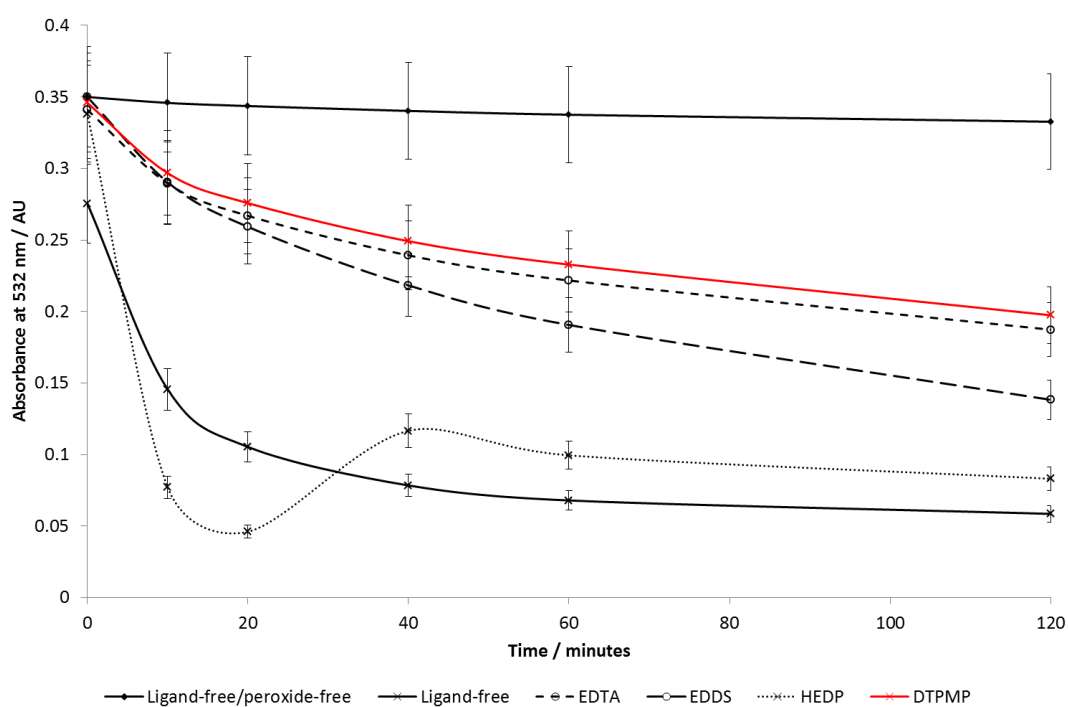


Figure 46: Graph to show the rate of melanin bleaching in systems containing 20 mM NH_3 , (1.3 mM ligand), 0.18 mM Cu(II), 0.979 M H_2O_2 and 0.06 mg mL^{-1} *Sepia* MFA at pH 10 & 20 °C.

Generally, for all the systems studied, the rate of bleaching is relatively high initially. However, this rate slows down over the course of the reaction. This could be due to the fact that melanin oligomers naturally contain *o*-quinone units, which can be oxidised by the perhydroxyl anion directly leading to the immediate breakdown of the melanin. However, once these units have been oxidised, bleaching relies on the formation of more *o*-quinone units from hydroquinone moieties before the melanin can continue to be broken down. Hence, the rate of bleaching decreases.

For the systems when a negligible hydroxyl radical flux is observed by NPDPA, such as the EDTA system, less bleaching occurs over 2 h reaction than for the ligand-free system, where the hydroxyl radical flux is high. This could be due to the fact that there are less hydroxyl radicals available in EDTA systems to convert the hydroquinone moieties to *o*-quinone units, for breakdown by perhydroxyl anions. For these systems, the majority of bleaching that is observed could be attributed to oxidants other than the hydroxyl radical, such as radiation, metal ions or perhydroxyl anion.

The ligand-free composition displayed a greater rate of hydrogen peroxide decomposition than is observed in formulations that contain strong ligands. This confirms that there is a correlation between the hydroxyl radical flux and the rate of melanin bleaching. The decrease in absorbance due to melanin was so fast in the ligand-free system that it degraded a substantial amount before the first reading was taken, hence the lower initial absorbance at the start of the reaction. This data immediately suggest that in soluble melanin systems, the hydroxyl radical could play an important role in bleaching.

Although the amount of hydroxyl radical flux appears to correlate with the extent of melanin bleaching that is observed, it is important to note that when the ligands bind to metal centres, they alter their redox potentials. On chelating the metal ion centres with ligands, such as EDTA, the decrease in melanin bleaching could be due to the inability of the metal ions to directly oxidise the melanin itself, because of its altered redox potential. However, on removing hydrogen peroxide from ligand-free bleaching solutions, the extent of melanin bleaching was negligible. This confirms that it is the hydroxyl radical and not the metal centres that are responsible for the majority of bleaching in these compositions.

In the combinations studied, the formulation containing HEDP is unique in its behaviour. The absorbance at 532 nm increased approximately 20 minutes into the reaction. It has been shown in previous work that this increase in absorbance is due to the formation of copper nanoparticles, in Fenton-like systems that contain HEDP¹⁷⁰. The bleaching of melanin appears to be complete before formation of

these nanoparticles occurs. The high rate of bleaching that was observed in this system again correlates with the extensive hydroxyl radical flux.

Having observed that hydroxyl radicals contribute to soluble melanin bleaching, as postulated in the literature⁴⁶, it was decided to investigate the role that perhydroxyl anions play in bleaching. By altering the pH of the bleaching systems, the concentration of perhydroxyl anions that are available for bleaching changes. Thus, the effect that the anion has on melanin oxidation can be observed.

2.3.5 The effect of perhydroxyl anion on *Sepia* MFA bleaching

As for the hydroxyl radical, it is unclear from the literature whether the perhydroxyl anion plays an important role in melanin bleaching. It was therefore decided to investigate the role of the anion in melanin oxidation, by varying the pH of bleaching systems. When the pH is increased in bleaching systems that contain hydrogen peroxide, the concentration of perhydroxyl anion that is available for bleaching is also increased. In order to determine if perhydroxyl anion plays an active role in the bleaching of soluble *Sepia* MFA, several experiments were set up using the general conditions 20 mM NH₃, (1.3 mM ligand), 0.18 mM Cu(II), 0.979 M H₂O₂, 0.06 mg mL⁻¹ *Sepia* MFA at pH 10 or 7 & 20 °C.

The presence of ligand gives a system which has a negligible hydroxyl radical flux. When ligand is not used there is plenty of hydroxyl radical available to contribute to bleaching. Bleaching systems with and without ligand were analysed for at pH 7 and pH 10. At pH 7 there is roughly 0.022 mM perhydroxyl anion available for bleaching, whereas at pH 10 this concentration rises to 22 mM (See page 66). By studying systems that contain ligand and those that are ligand-free at both pH values, the relative importance of perhydroxyl anion and hydroxyl radical can be compared. The extent of bleaching for these systems can be seen in *Figure 47*.

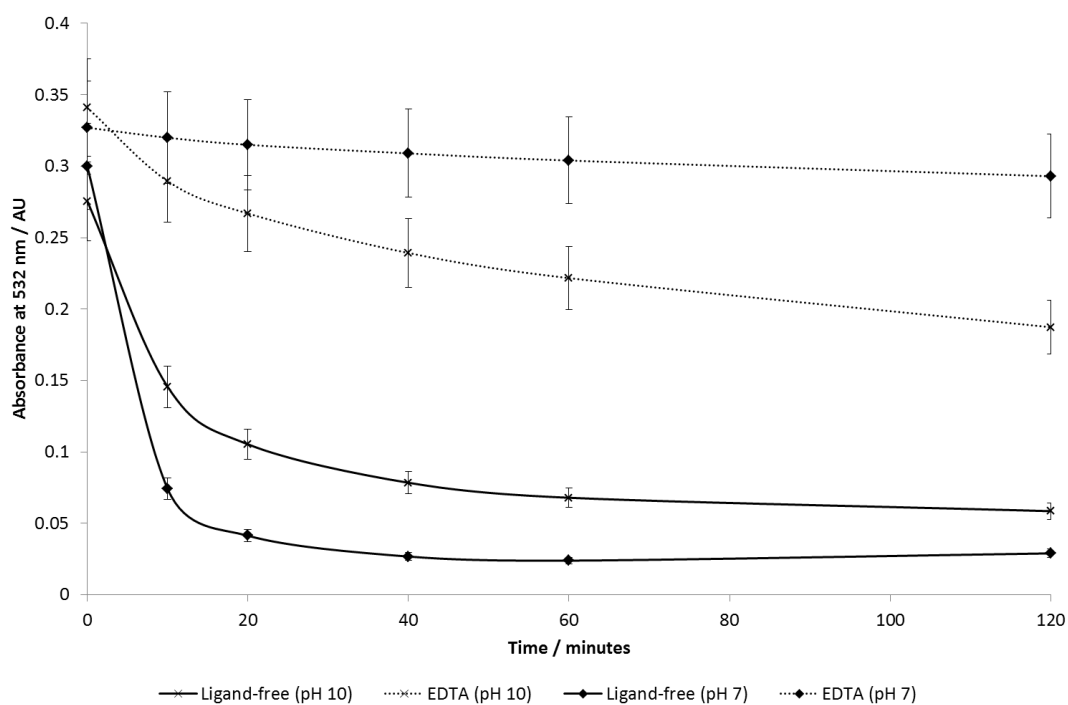


Figure 47: Graph to show melanin bleaching in the following system: 20 mM NH_3 , (1.3 mM ligand), 0.18 mM Cu(II) , 0.979 M H_2O_2 and 0.06 mg mL^{-1} MFA at pH 10 or 7 & 20 °C.

It is apparent that there is extensive bleaching of *Sepia* MFA in ligand-free systems at both pH 10 and 7. Despite the differences in perhydroxyl anion concentrations that are expected for these compositions, the amount of melanin bleaching is quite similar. Figure 48 shows that the level of hydroxyl radical flux in the pH 7 ligand-free system is much greater than for the corresponding pH 10 system. This not only compensates for the lesser amounts of perhydroxyl anions available for bleaching at neutral pH, it actually results in faster bleaching overall. This again confirms that the hydroxyl radical plays an important role in the oxidation of melanin in soluble systems. Although, ammonia is required in commercial formulations to provide an alkaline pH to bleach hair, these results show that once the melanin is solubilised, the hydroxyl radical is able to bleach melanin even at neutral pH. This confirms that ammonia is needed to solubilise the melanin in order for rapid bleaching to occur, as discussed on page 96.

Figure 48 also shows that the hydroxyl radical flux in EDTA systems is similar at both pH 7 and pH 10. However, the extent of melanin bleaching that is observed is much greater in the system at pH 10. This is due to the higher concentration of perhydroxyl anions that are available in the pH 10 system. It is also possible that the deprotonation of groups within melanin could contribute to the increased rate of oxidation, once bleaching is initiated by perhydroxyl anion. The EDTA containing formulations demonstrate the ability of the perhydroxyl anion to bleach melanin in the presence of negligible amounts of hydroxyl radicals. However, it appears that the hydroxyl radical is a much more effective oxidant of soluble melanin than the perhydroxyl anion, as the bleaching in the ligand-free systems at both high and neutral pH values is far more extensive.

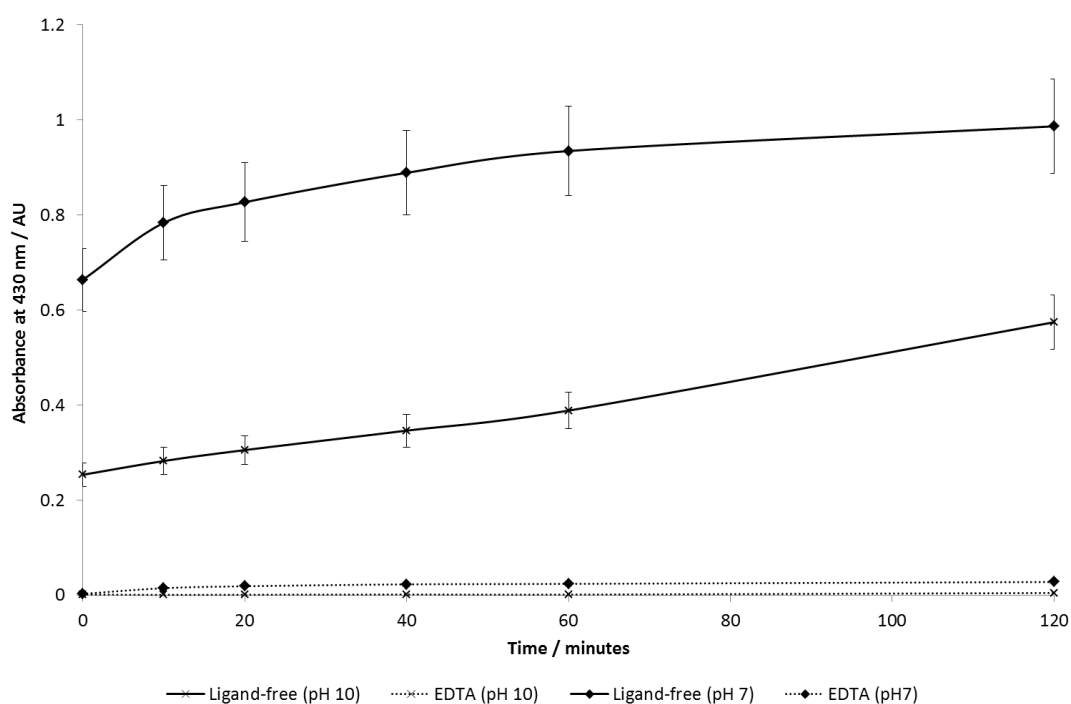


Figure 48: Graph to show hydroxyl radical flux in the following systems: 20 mM NH_3 , (1.3 mM ligand), 0.18 mM Cu(II) , 0.979 M H_2O_2 and 1 mM NPDPA at pH 10 or 7 & 20 °C.

It is also evident from *Figure 47* that rapid melanin bleaching occurs in the ligand-free system at pH 7, where there is a high flux of hydroxyl radicals and the concentration of perhydroxyl anion is negligible. This indicates that the mechanism of melanin oxidation shown in *Figure 31* is not the only possibility at a neutral pH. An additional mechanism may exist whereby the hydroxyl radicals are capable of bleaching melanin, without the need for perhydroxyl anions. (This is discussed further on page 94).

This data provide novel proof that both the hydroxyl radical and the perhydroxyl anion contribute to the mechanism of soluble melanin bleaching, as hypothesised by Korytowski⁴⁶. In order to gain further mechanistic insights into the exact roles of both these oxidants in melanin bleaching, the time-delayed addition of a chelating ligand to a soluble melanin bleaching system was investigated.

2.3.6 Time delayed chelation of metal ions during *Sepia* MFA bleaching

Existing studies of melanin bleaching propose that hydroxyl radicals could be an initial oxidant of the DHI units in melanin to form *o*-quinone units, which may then be subject to nucleophilic attack by perhydroxyl anions⁴⁶.

In order to probe this mechanism, the addition of a chelating ligand was delayed during the bleaching of *Sepia* MFA systems so that, initially, there would be a ligand-free environment to generate an abundance of hydroxyl radicals. Thus, a high number of DHI and DHICA units may be converted to *o*-quinone units. After chelation, the rate of bleaching of these *o*-quinone units, by the perhydroxyl anions, can then be compared to the rate of bleaching of melanin that has not been pre-oxidised by hydroxyl radicals.

Importantly, *Figure 43* shows that the chelation of metal ions by EDTA, in *Sepia* MFA-Cu(II) systems, is very fast and as the reactivity of the hydroxyl radical is so great, there would be no hydroxyl radicals available for bleaching almost immediately after chelation.

Alkaline pH

A ligand-free bleaching formulation containing 20 mM NH_3 , 0.18 mM Cu(II) , 0.979 M H_2O_2 and 0.06 mg mL^{-1} *Sepia* MFA, at pH 10 & 20 °C, was set up. The absorbance was monitored by UV-vis spectroscopy at 532 nm. 1.3 mM EDTA was added after various time periods. The effect on bleaching can be observed in *Figure 49*.

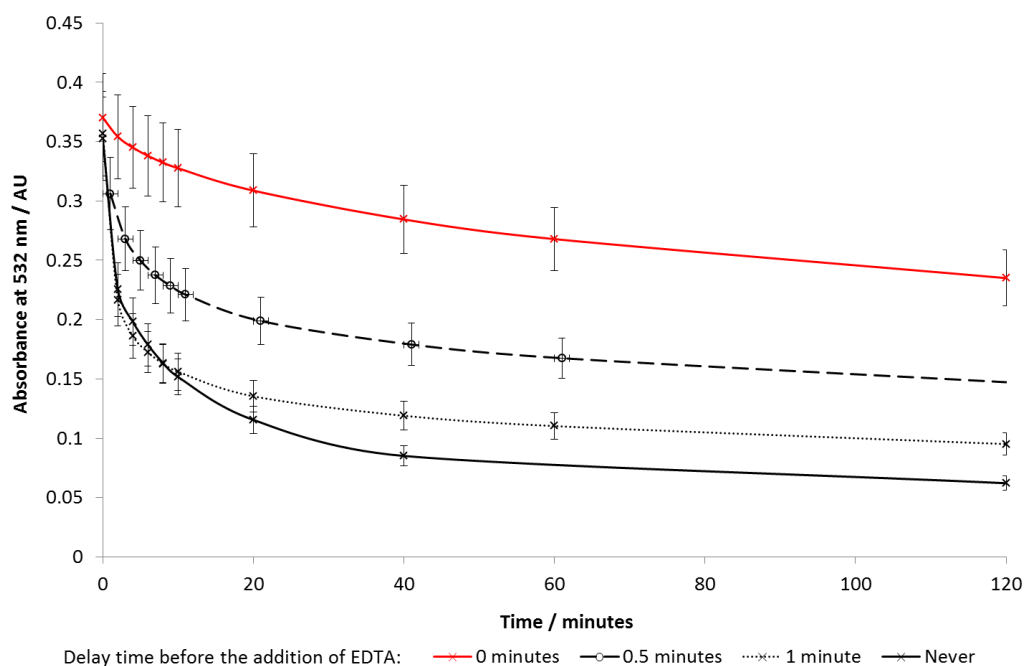


*Figure 49: Graph to show how the time-delayed addition of 1.3 mM EDTA affects the bleaching of Sepia MFA in the following system: 20 mM NH_3 , 0.18 mM Cu(II) , 0.979 M H_2O_2 and 0.06 mg mL^{-1} *Sepia* MFA at pH 10 & 20 °C.*

The rate of bleaching before the addition of EDTA is relatively high because there are plenty of hydroxyl radicals available for oxidation. Upon the addition of EDTA, the metal ions are chelated quickly yet the rate of melanin bleaching remains relatively high. This suggests that the general mechanism suggested by Korytowski, in *Figure 31*,⁴⁶ is viable. An oxidant, in this case the hydroxyl radical, converts the

melanin to an intermediate, such as *o*-quinone, that is then readily bleached by the perhydroxyl anion.

Further to this, in ligand-free bleaching systems, the UV-vis spectra show a shoulder in the absorbance, at approximately 400 nm, (*Figure 50*). This could correspond to a build-up of *o*-quinone units in the melanin¹⁷¹, as a result of a large quantity of the DHI and DHICA units being oxidised, by the high concentration of hydroxyl radical.

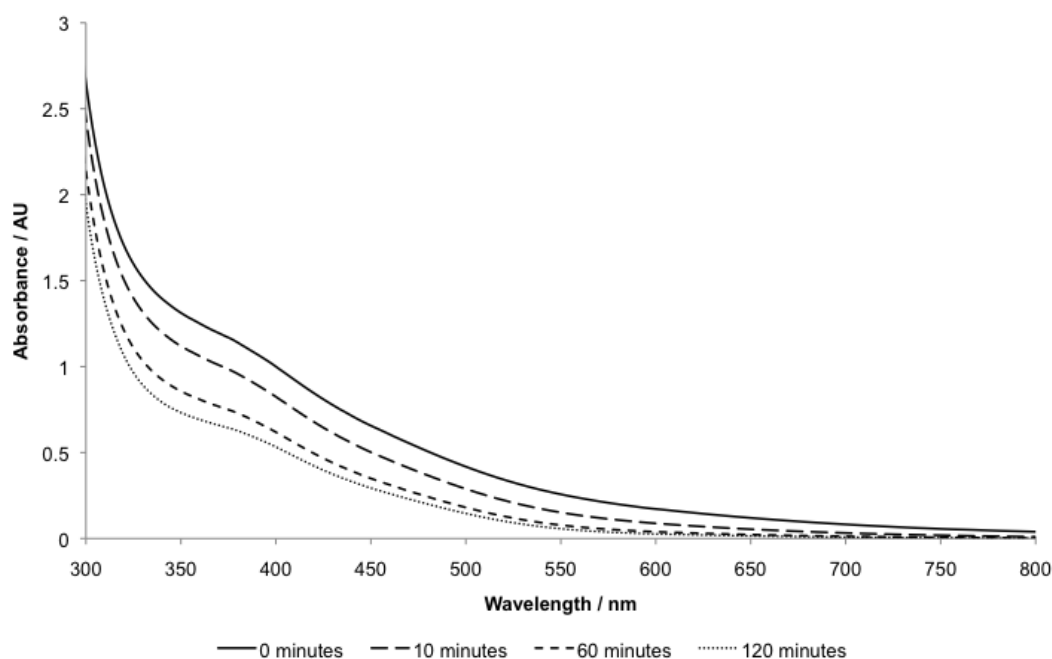
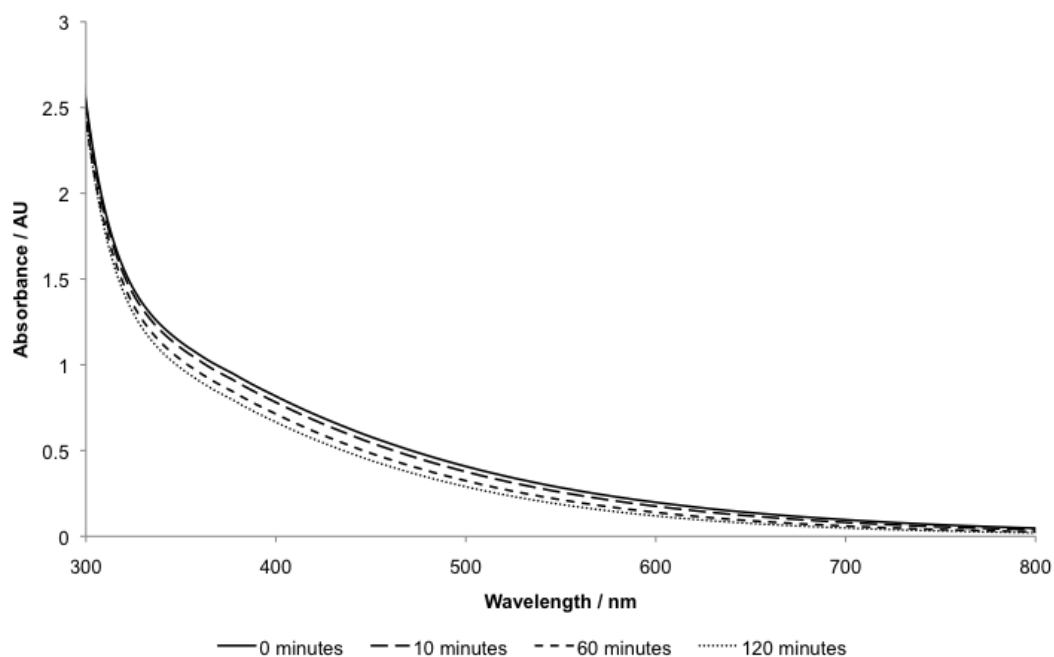


Figure 50: UV-vis spectra over the time course of melanin bleaching, showing a shoulder in the absorbance at 400 nm for the following system: 20 mM NH₃, 0.18 mM Cu(II), 0.979 M H₂O₂ and 0.06 mg mL⁻¹ Sepia MFA at pH 10 & 20 °C.

This shoulder in the absorbance, at approximately 400 nm, is not present in the composition containing EDTA, where very little hydroxyl radical is produced (*Figure 51*). This could be further evidence that, when there is lower hydroxyl radical flux, the lesser amounts of bleaching are due to less DHI/DHICA oxidation by the hydroxyl radical. Hence, this explains the lack of evidence of accumulation of *o*-quinone units in the UV-vis spectra.

By using IR to quantify the concentration of hydroxyl groups and the carbonyl environments, in both ligand-free melanin and EDTA bleached melanin, further evidence for this suggested mechanism could be acquired.



*Figure 51: UV-vis spectra over the time course of melanin bleaching, showing no shoulder in the absorbance at 400 nm for the following system: 20 mM NH_3 , 1.3 mM EDTA, 0.18 mM Cu(II) , 0.979 M H_2O_2 and 0.06 mg mL⁻¹ *Sepia* MFA at pH 10 & 20 °C.*

This data suggest that the mechanism depicted in *Figure 31* could be correct for pH 10 conditions. However, to confirm this, it was necessary to study the time-delayed chelation of metal ions in ligand-free bleaching systems, at pH 7. The effect of the perhydroxyl anions on bleaching, after the addition of EDTA, can thus be observed by comparing the rate for the pH 10 systems and the pH 7 systems. Additionally, the possibility of an alternative mechanism of melanin bleaching existing at pH 7 can be confirmed, as mentioned on page 88.

Neutral pH conditions

Bleaching experiments were performed at a neutral pH of 7. The ligand-free bleaching system was set up with 20 mM ammonia, 0.18 mM Cu(II), 0.979 M H₂O₂ with 0.06 mg mL⁻¹ *Sepia* MFA. 1.3 mM EDTA was added to the solution at various time points, to chelate the metal ions. The bleaching of melanin was monitored at 532 nm by UV-vis spectroscopy at 20 °C. The results are shown in *Figure 52*.

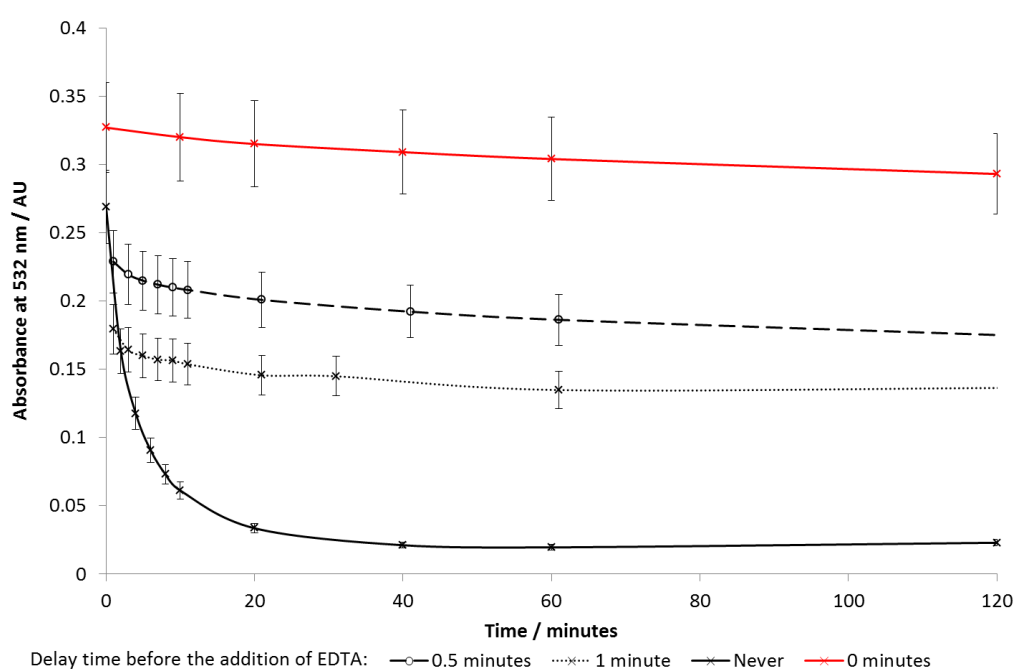


Figure 52: Graph to show how the time-delayed addition of 1.3 mM EDTA affects the bleaching of Sepia MFA in the following composition: 20 mM NH₃, 0.18 mM Cu(II), 0.979 M H₂O₂ and 0.06 mg mL⁻¹ Sepia MFA at pH 7 & 20 °C.

A similar trend can be observed for the bleaching experiments that were performed at pH 7 as for those experiments performed at pH 10. Initially there is a rapid rate of melanin bleaching due to the high hydroxyl radical flux. Upon chelation of the metal centres, by EDTA, the rate of melanin bleaching is inhibited.

However, for the bleaching systems studied at pH 7 it is apparent that the rate of bleaching after EDTA addition is different to the rate with the pH 10 systems. Firstly, bleaching is inhibited more rapidly after the EDTA addition than for the pH 10 system. Secondly, there is much less overall bleaching when EDTA is added at pH 7. *Figure 53* clearly shows an example of the lower rate of melanin bleaching that was observed for a pH 7 system, compared with a pH 10 system, after the addition of EDTA.

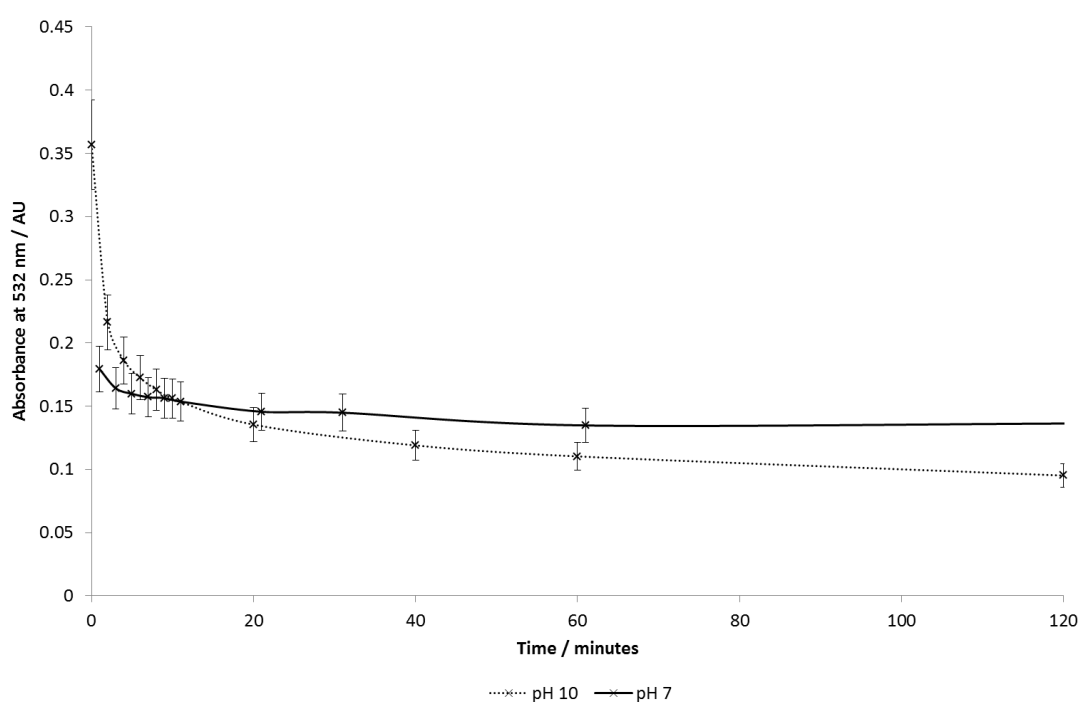


Figure 53: Graph to show the effect of pH on the rate of Sepia MFA bleaching in the following compositions: 20 mM ammonia, 0.18 mM Cu(II), 0.979 M H₂O₂ and 0.06 mg mL⁻¹ Sepia MFA at pH 10 or 7 & 20 °C (1.3 mM EDTA added at 1 minute).

The initial rate of bleaching (prior to EDTA addition) is much faster in the ligand-free system at pH 7, due to higher hydroxyl radical flux, before the addition of EDTA at 1 minute. Upon the addition of the chelating ligand, the rate of bleaching in the pH 7 composition is reduced almost immediately. At this point, the rate of bleaching is greater in the pH 10 composition. The lower rate of bleaching in the pH 7

composition is due to the fact that there is very little perhydroxyl anion available to bleach any *o*-quinone units that are generated. This appears to add further confidence in the mechanism proposed in *Figure 31*, giving further evidence for the role that hydroxyl radicals play in accelerating the rate of *Sepia* MFA bleaching due to the perhydroxyl anions. It also confirms that another rapid mechanism of bleaching, caused by the hydroxyl radicals in the pH 7 system.

In a ligand-free composition at pH 7, melanin bleaching by hydroxyl radicals may proceed via a similar mechanism to the one suggested by Poeggeler et al, for the degradation of melatonin.¹⁷² They propose that indoles may be oxidised to the indolyl cation radical. This radical is then degraded by superoxide anions to form the kynuramine metabolite shown in *Figure 54*.¹⁷² Breakdown of the oligomeric backbone could also occur as a result of hydroxyl radical oxidation to form a carbon centred radical on the indole ring which, in the presence of oxygen, would lead to peroxy radicals¹⁷³ and a 1,2-dioxetane mediated cleavage of carbon-carbon single bonds that link monomeric units (*Figure 55*). This additional mechanism could be verified by analysis of the type and the quantity of degradation products obtained in the pH 7 ligand-free formulation and in the pH 10, EDTA formulation.

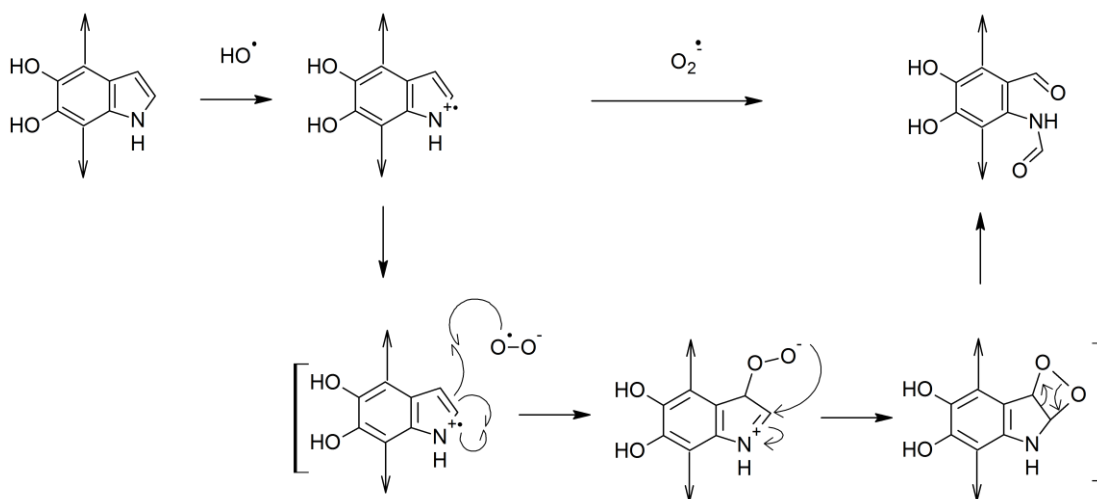


Figure 54: Mechanism to show the reactivity of hydroxyl radical towards indole-like molecules.

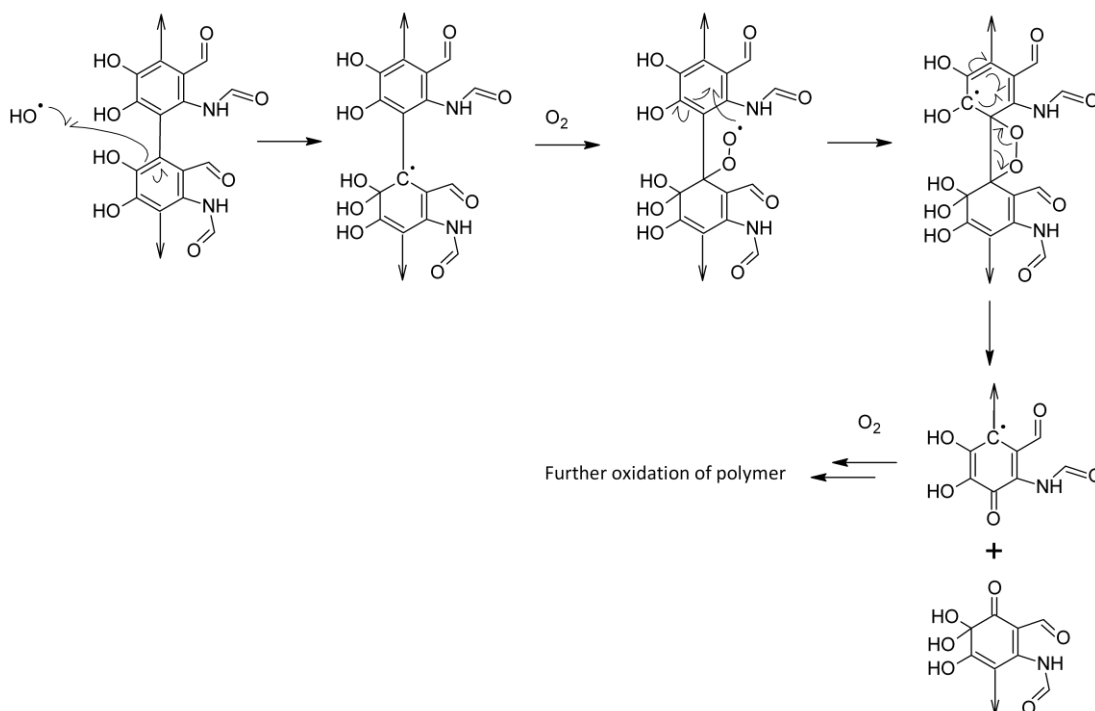


Figure 55: Potential mechanism of hydroxyl radical mediated melanin oxidation in the absence of perhydroxyl anions.

This degradation by hydroxyl radicals may occur at pH 7 when there is no perhydroxyl anion available. However, there is nothing to stop this sequence occurring at pH 10, as well as the mechanism suggested by Korytowski. The extent to which each mechanism contributes to bleaching may alter significantly depending on the pH of the bleaching system. The degradation by hydroxyl radical may dominate at a neutral pH. However, as the pH increases, the mechanism involving the perhydroxyl anion could start to play a more important role, as the concentration of perhydroxyl anion increases.

Having confirmed the importance and roles of perhydroxyl anions and hydroxyl radicals in melanin bleaching, it was considered to be desirable to establish the effect that the base has on the chemistry of soluble *Sepia* MFA bleaching. Ammonia is thought to facilitate the diffusion of oxidants into the hair fibre, where melanin bleaching can occur. Diffusion is not a factor in homogeneous systems. In this way whether or not ammonia plays a role in the chemistry of melanin bleaching can be

established. It was thought that this approach could help to explain why a change in base leads to varying levels of hair bleaching.

2.3.7 The role of ammonia in soluble melanin bleaching

Ammonia is used in hair bleaching systems in order to provide an alkaline pH for the generation of the perhydroxyl anion, which is necessary for melanin bleaching in heterogeneous systems. Ammonia is used as the base in particular is because it effectively swells hair fibres. This allows oxidants into the cortex of the hair fibre, where they can then bleach the melanin¹⁷⁴.

Ammonia also plays a role in heterogeneous melanin bleaching. *Figure 56* and *Figure 57* demonstrate the differences in heterogeneous melanin bleaching that are apparent when the base is changed from ammonia to sodium hydroxide. When ammonia is used as a base, the colour of the bleaching solution changes from dark brown to orange-brown, as the melanin is bleached. However, when sodium hydroxide is used, the initial appearance of the bleaching solution is different. *Figure 57 (a)* shows that the melanin granules are not solubilised in the same way. As a result, the solution appears slightly lighter in colour initially. Despite this, after 12 hours of bleaching, the solution is still dark-brown, demonstrating that NaOH is not as effective as ammonia in heterogeneous bleaching systems. Ammonia could potentially interfere with hydrogen bonding within melanin and allow faster oxidation, resulting in the differences that are observed.

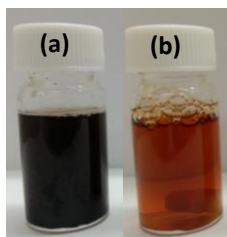


Figure 56: Heterogeneous melanin bleaching (400 mM NH_3 , 2 mg mL^{-1} *Sepia melanin* & $1.63 \text{ M H}_2\text{O}_2$ at pH 10 & $20 \text{ }^\circ\text{C}$) at (a) 0 hours and (b) 12 hours

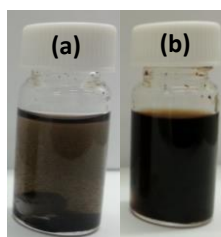


Figure 57: Heterogeneous melanin bleaching (400 mM NaOH , 2 mg mL^{-1} *Sepia melanin* & $1.63 \text{ M H}_2\text{O}_2$ at pH 10 & $20 \text{ }^\circ\text{C}$) at (a) 0 hours and (b) 12 hours

These physical factors make ammonia a suitable base for hair bleaching formulations. However, in order to establish whether or not ammonia also plays a role in the chemistry of melanin bleaching, it was decided to investigate the role of ammonia in homogeneous solutions. Diffusion of the oxidants and the solubilisation of melanin will not affect the rates of bleaching in homogeneous solutions. Any differences in the rate of bleaching that are observed when the base is changed can therefore be attributed to differences in chemistry.

In order to determine the role of ammonia, homogeneous bleaching systems were set up that used NaOH buffered to pH 10, instead of ammonia. The rate of melanin oxidation was then compared to the systems that contained ammonia. The kinetics of bleaching for the systems containing 20 mM base, (1.3 mM ligand), 0.18 mM Cu(II), 0.979 M H_2O_2 and 0.06 mg mL^{-1} *Sepia* MFA at pH 10 & $20 \text{ }^\circ\text{C}$ are shown in Figure 58.

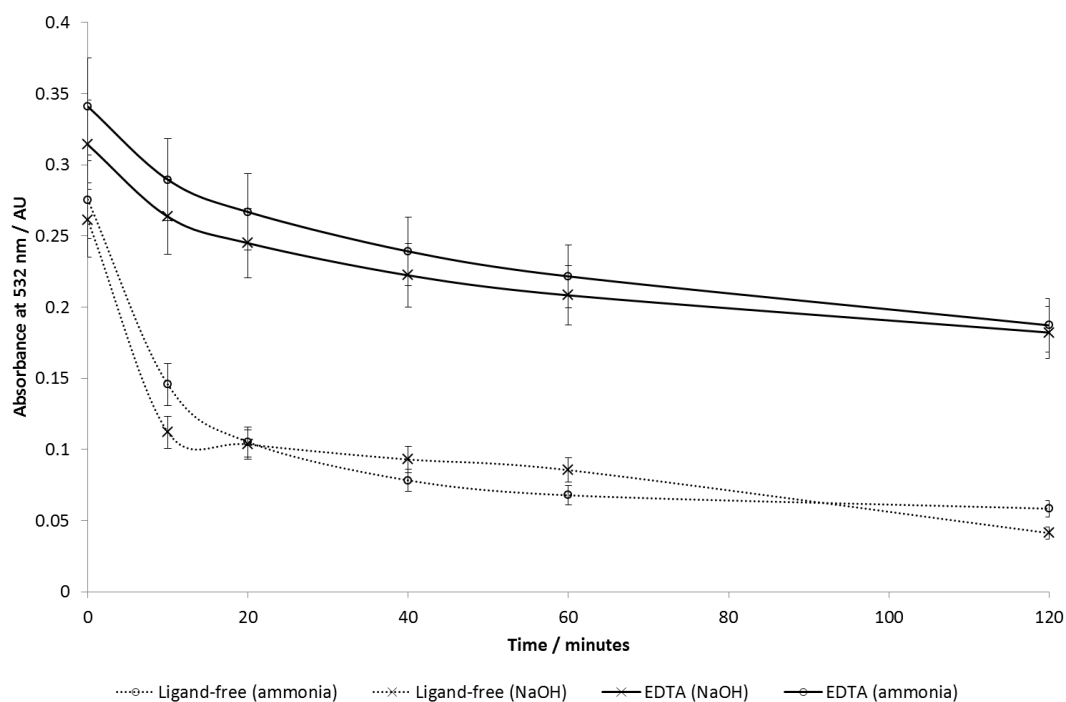


Figure 58: Graph to show the differences in Sepia MFA bleaching on varying the base for the following systems: 20 mM base, (1.3 mM ligand), 0.18 mM Cu(II), 0.979 M H₂O₂ and 0.06 mg mL⁻¹ Sepia MFA at pH 10 & 20 °C.

It is evident that the general trend in oxidation is similar, regardless of the base that is used to generate the perhydroxyl anions. When EDTA is used as a ligand there arises a negligible hydroxyl radical flux in both NH₃ and NaOH systems (Figure 59) and the rate of melanin bleaching is similar for both systems. This indicates that in soluble melanin bleaching, the type of base does not play an important role at 20 °C.

There are some slight differences in the rate of oxidation in the case of the ligand-free systems. These differences are recognised by observing the hydroxyl radical flux in these systems, as shown in Figure 59. It is clear that there is a greater hydroxyl radical concentration produced in the NaOH system by 10 minutes reaction time, so it is logical that more bleaching should have occurred by this time point. After this point bleaching is nearly complete, so any colorimetric differences between the systems are relatively minor.

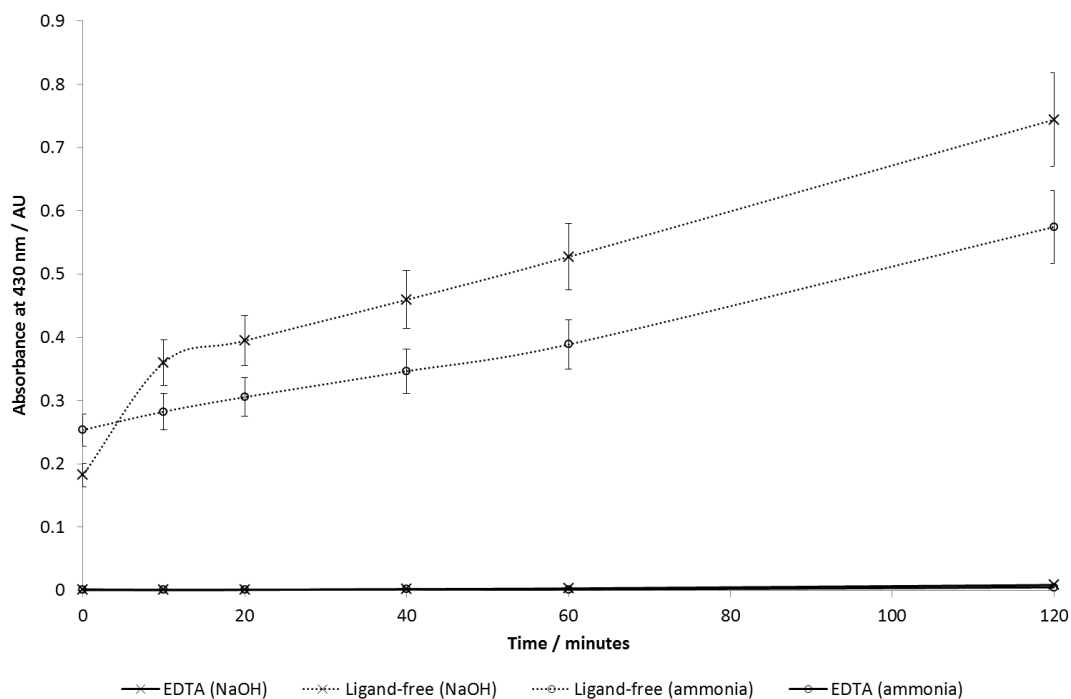


Figure 59: Graph to show the effect of base on hydroxyl radical production for the following systems: 20 mM base, (1.3 mM ligand), 0.18 mM Cu(II), 0.979 M H₂O₂ and 1 mM NPDPA at pH 10 & 20 °C.

Overall, the effect on soluble melanin bleaching of changing the base is minor. The only differences that are observed are when the base results in a change in the flux of hydroxyl radical. This suggests that these results depend on the concentration of base that was used. This also suggests that the role of the base in hair bleaching is purely a physical one, in that it allows oxidants such as the perhydroxyl anion to diffuse into the hair cortex, where melanin is situated and bleaching can occur.

2.4 Conclusions

The primary purpose of the work that was described in this chapter was to unravel the roles of hydroxyl radicals and perhydroxyl anions in the chemistry of melanin bleaching and the consequences. This was achieved by studying the bleaching of soluble *Sepia* MFA-based compositions by UV-vis spectroscopy at 20 °C. These model formulations provided mechanistic insights into the bleaching of hair from an Asian demographic, due to the comparable eumelanin content of the *Sepia* MFA and black hair. These more soluble compositions resulted in environments where the diffusion of oxidants into hair fibres was not a factor that influenced the rate of melanin bleaching. This meant the effect of individual oxidants on the chemistry of bleaching could be directly observed. However, the fact that there is no diffusion needs to be taken into account when comparing bleaching in these model formulations to commercial ones. During the bleaching of whole hair fibres diffusion of oxidants into the hair cortex will influence the rate of bleaching, as well as the role that each oxidant might play in the process.

Importantly, there was evidence to show a relatively high rate of melanin bleaching occurs in systems where a high level of hydroxyl radical flux was observed, due to extensive hydrogen peroxide decomposition.

When formulations that contained chelants, such as EDTA, were studied, the metal ion was shown to bind effectively, less melanin bleaching being observed. For these compositions, more bleaching was observed at pH 10 than under neutral pH due to the greater concentration of perhydroxyl anion. This provided novel evidence for the role that the perhydroxyl anion plays in melanin bleaching, as has been hypothesised in the literature⁴⁶.

Bleaching in the ligand-free systems occurred more rapidly at pH 7. This effect could be attributed to the fact that there is a greater hydroxyl radical flux in the ligand-free system, at pH 7. This also implies that there is a mechanism for soluble melanin bleaching that does not involve the perhydroxyl anion, (outlined in *Figure 54* and *Figure 55*).

The time-delayed chelation of metal ions, using EDTA, during melanin bleaching revealed that pre-treatment of the melanin with hydroxyl radicals increased the rate of oxidation by the perhydroxyl anion, when compared with equivalent formulations that were not pre-treated with hydroxyl radicals.

The UV-vis spectra of the ligand-free bleaching formulations showed that the absorbance at approximately 400 nm remained relatively high compared to the absorbance obtained with other formulations. This may occur as a result of the greater hydroxyl radical flux, leading to a build-up of *o*-quinone units in the melanin. These units may then be oxidised by perhydroxyl anions, which would provide further evidence for the mechanism shown in *Figure 31*. It may be possible to use IR studies to confirm the greater concentration of *o*-quinone units in the ligand-free systems to confirm that the mechanism of oxidation proposed by Korytowski is correct, at alkaline pH.

In addition to this work, ammonia was determined to have no significant effect on the chemistry of soluble melanin bleaching, despite having been shown to be important for heterogeneous melanin bleaching compositions²⁰. This is further evidence to suggest that the role of ammonia in hair bleaching is purely a physical one, in that it assists the diffusion of oxidants into hair fibres and helps in the bleaching of heterogeneous melanin.

Chapter 3

Chapter 3 – A comparison of monoethanolamine-based and ammonia-based hair bleaching systems

3.1 – Introduction

Bleaching formulations that contain MEA show three major differences to those that use ammonia. The main problem is that increased damage to hair fibres is observed when MEA formulations are used⁴³. The second is that MEA-based formulations have a lower bleaching potential than systems that use ammonia⁴³. Finally, increased foaming is observed when MEA formulations are applied. It is not clear if this may in some way be responsible for either of the first two observations.

Chapter 1 discusses the possible physical and chemical causes of the differences that are observed when MEA is used in both the bleaching formulations and the dyeing formulations. This chapter relates to the potential factors that could cause the differences observed in bleaching formulations that contain MEA.

3.2 Aims

The primary aim of the work that underpins this chapter was to establish whether or not any of the chemical factors discussed in chapter 1 might be responsible for differences seen in hair bleaching when ammonia is replaced with ethanolamine in bleaching formulations. The magnitude of these differences is also important, as it could indicate whether or not physical factors contribute to these variations in melanin bleaching and hair damage.

As discussed on page 21, hair damage can occur as a result of protein oxidation by hydroxyl radicals. However, the information given in chapter 2 shows that greater amounts of hydroxyl radical can also result in more effective melanin bleaching. In order to approximate the relative amounts of hydroxyl radicals produced in

systems, the decomposition of hydrogen peroxide can be monitored. Additionally, a colorimetric probe can be used to estimate directly the relative hydroxyl radical amounts.

When the base in commercial bleaching formulations is altered, the diffusion rates of hydrogen peroxide into hair fibres will vary, as a result of changes in hair fibre swelling and surface tension (discussed in chapter 1)^{10, 110, 175}. Hair swelling and surface tension are affected by factors such as pH, temperature, solvent polarity and relative air humidity. This could affect the rate of peroxide decomposition due to the ions of endogenous metals. Thus, the extent of melanin bleaching that occurs would vary.

Therefore, in addition to monitoring the occurrence of hydrogen peroxide decomposition, in solutions containing whole hair fibres, it was also decided that a study of various types of replica bleaching formulations to remove the problem of varying peroxide diffusion rates. Firstly, model aqueous formulations that were designed to represent the environment inside hair fibres were studied. By using homogeneous systems, diffusion rates of peroxide species into hair fibres are no longer a factor. Any differences in the rate of decomposition in these compositions should therefore be a direct result of changes in the chemistry, when the base is altered. Attempts were made to identify and to explain these changes in chemistry in model hair bleaching solutions, which represent the internal environment of hair fibres.

The rate of bleaching in soluble melanin solutions containing MEA and ammonia was also directly investigated. As with the homogeneous model peroxide decomposition formulations, there were no problems associated with diffusion. Therefore, any differences in the rate of melanin bleaching would be a result of changes in the chemistry that arises when the base is altered. As solubilisation of melanin granules is a prerequisite to bleaching, heterogeneous melanin bleaching was also studied in order to determine whether or not the extent of solubilisation is affected by the change in base.

Peroxide decomposition was then also studied in solutions containing pulverised hair. This adds to the complexity of the model systems, by representing a more realistic environment of the hair fibre cortex. Hydrogen peroxide decomposition in these compositions may be affected by the presence of heterogeneous melanin and the presence of hair fibre keratins, which are made accessible to bleaching solutions by pulverisation. However, endogenous metal ions are now also readily accessible to the bleaching solutions. Therefore once again, the diffusion rates of the peroxide will not affect the rate of decomposition. Any differences in peroxide decomposition, in these more realistic conditions, can be attributed to changes in chemistry when the base is altered. Any differences between these more representative compositions and the homogeneous model systems will also be highlighted.

By studying all these compositions, in the presence of either MEA or ammonia, it was hoped to identify and to explain any differences in the chemistry of hair bleaching. Additionally, further information may be provided on the role of base in hair fibre swelling and melanin solubilisation, by studying the bleaching of heterogeneous melanin granules.

3.3 Results & Discussion

3.3.1 The bleaching of whole hair fibres

According to the literature, when ammonia is substituted for MEA in hair bleaching formulations different extents of hair damage and bleaching are observed. Up to 85% more protein loss (damage) from hair fibres has been observed, by protein loss studies, for 0.82 M MEA formulations than with the equivalent NH_4OH based formulations⁴³. This difference in hair damage was observed for compositions containing 6% H_2O_2 that were used to bleach hair for 30 minutes at 30 °C. It is also

generally accepted that primary amines, such as ethanolamine, result in a lower bleaching potential than ammonia¹³⁵.

As discussed in chapter 1, reactive oxygen species (ROS) from the decomposition of hydrogen peroxide can cause hair fibre damage. Therefore, initially it was decided to monitor the extent of hydrogen peroxide decomposition, during the bleaching of whole hair fibres. It was thought that if the relative levels of ROS produced in the presence of either MEA or ammonia varied, this could explain the decreased levels of melanin bleaching in MEA systems.

In order to indirectly determine the levels of ROS produced, the volume of oxygen evolved from hydrogen peroxide decomposition can be monitored, as described in chapters 2 and 7. Oxygen production was therefore measured for bleaching systems containing 400 mM base, 2.5 mg mL⁻¹ whole hair fibres and 0.979 M H₂O₂ at pH 10. The concentrations of base and hydrogen peroxide were chosen to reflect the concentrations that are found in typical level 3 hair colouring formulations⁴³. The base used was either MEA or ammonia to determine the effect of base on hydrogen peroxide decomposition. The whole hair fibres that were used were either dosed with copper ions (218.1 ppm Cu(II)) or only contained natural levels of copper ions (13.0 ppm Cu(II)). This was in order to determine whether or not the concentration of copper atoms present on hair fibres affects the hydrogen peroxide decomposition when the base is varied.

The relative extents of hydrogen peroxide decomposition are shown in *Figure 60*. It is immediately obvious that the systems with greater concentrations of copper ions result in much more oxygen evolution, as is expected for Fenton-like systems. In addition to this, the rate of decomposition in these systems is greater when ammonia is used than when MEA is used. This suggests that at greater copper concentrations there is more extensive hydrogen peroxide decomposition in ammonia-containing formulations and hence more melanin bleaching could occur.

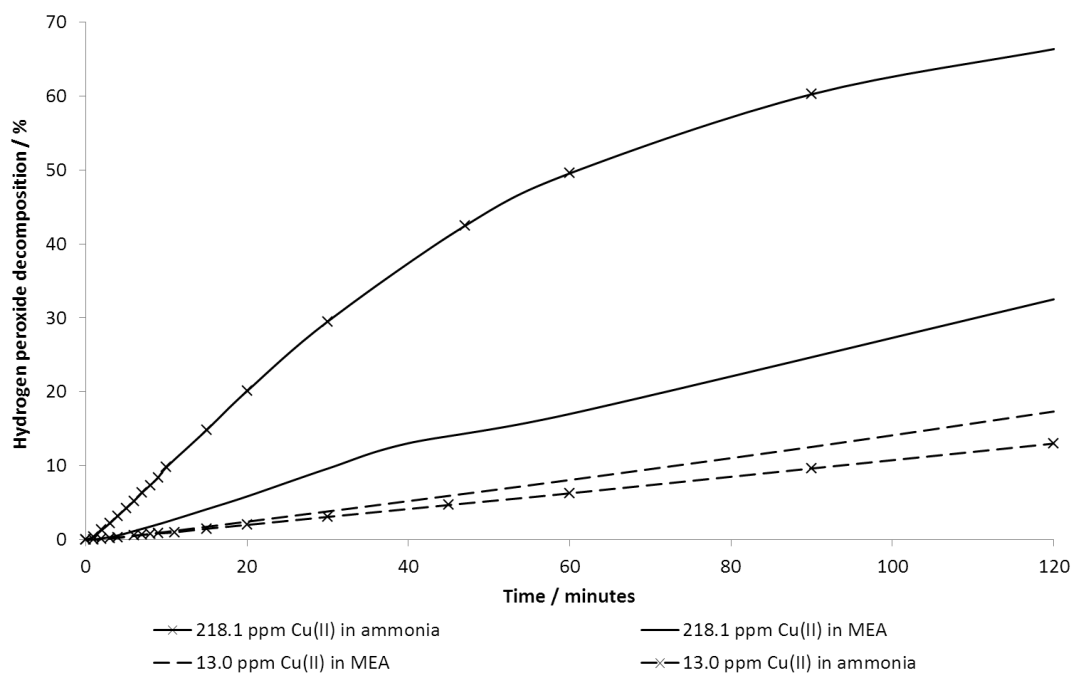


Figure 60: The relative rates of hydrogen peroxide decomposition due to whole hair fibres dosed with copper ions for the following systems: (400 mM base, 2.5 mg mL^{-1} whole hair fibres and $0.979 \text{ M H}_2\text{O}_2$ at pH 10 & 20°C)

When the whole hair fibres are not dosed with added copper ions, i.e. the copper ion concentration is representative of typical bleaching environments; the extent of oxygen evolution is greater in the MEA system, suggesting more melanin bleaching by ROS. However, this is not the case in real formulations. Primary amines generally result in less hair bleaching than does ammonia. Commercial formulations tend to include more ingredients than just base and hydrogen peroxide. This may explain any differences in peroxide decomposition between these whole hair model bleaching solutions and commercial formulations. Components such as chelating ligands need to be taken into account, as this will minimise the extent of hydrogen peroxide decomposition that is observed. In commercial formulations, radical scavengers also need to be considered as they will prevent radical mediated hair damage. For the purposes of this study, the relative rates of hydrogen peroxide decomposition were monitored as an indicator for differences that may arise in the chemistry of model formulations when the base is changed.

As discussed on page 104, the diffusion of hydrogen peroxide into hair fibres occurs at different rates when the base is altered. This will affect the rate of its decomposition by endogenous metals. If any chemical reasons for differences in peroxide decomposition (and thus melanin bleaching) are to be identified, then model systems need to be developed to remove diffusion as a factor that interferes with the decomposition rates of the peroxide. The conditions would also need to be varied to investigate more complex solutions, which include chelating ligands. It was thus decided to monitor hydrogen peroxide decomposition in various homogeneous systems where the base is varied from ammonia to MEA, in order to indirectly observe the relative amounts of ROS that are produced by monitoring the hydrogen peroxide decomposition. It was considered to be important to keep the temperature constant at 20 °C during the reaction, as varying temperatures affect the rate of the decomposition.

3.3.2 Hydrogen peroxide decomposition in model aqueous systems

Aqueous model systems were setup to replicate the conditions found inside hair fibres during hair bleaching. The extent of hydrogen peroxide decomposition was therefore monitored for reactions with the general conditions, 20/400 mM base, (1.3 mM ligand), 0.18 mM metal salt, 0.979 M H₂O₂ at pH 10 & 20 °C. Components were added to the reaction vessel in the order that they are listed. They were mixed thoroughly throughout the reaction, using a stirrer hotplate. This also allowed for the control of the temperature at 20 °C.

Chapter 1 states how chelating ligands are used in hair bleaching formulations in order to minimise the extent of hydrogen peroxide decomposition that is observed. Therefore, hydrogen peroxide decomposition was measured for systems that contain various ligands, as well as ligand-free systems, to determine whether or not a change in base resulted in different behaviour in any of these systems.

The metal ions used were either copper ions or iron ions, as these are the two most abundant metals in hair that can catalyse hydrogen peroxide decomposition. The concentrations of metal ions that are used are an approximation of the natural levels found in hair fibres of an Asian demographic, more specifically Japan¹⁷⁶. 400 mM base was used, as this is typical of the concentration used in level 3 colouring formulations⁴³. However, this was varied to 20 mM to observe the effect that the concentration of base has on hydrogen peroxide decomposition.

The extent of iron(III) catalysed hydrogen peroxide decomposition, after 120 minutes can be seen *Table 8*. Interestingly, the presence of chelating ligands does not necessarily inhibit the decomposition of hydrogen peroxide. There was no significant change in the level of decomposition when EDTA was added to a composition. Furthermore, when EDDS was added, the breakdown of hydrogen peroxide actually accelerated.

These changes in decomposition can be explained by a number of factors. In ligand-free formulations, the precipitation of iron atoms at high pH leads to a heterogeneous system, which can result in low rates of hydrogen peroxide decomposition. The addition of some chelants prevents this by solubilising the metal ions. Additionally, it has been shown that hydrogen peroxide can still bind to Fe(III)-EDTA complexes, resulting in an increased rate of peroxide breakdown¹⁷⁷. The increased rate of decomposition in the EDDS system can be attributed to a change in the redox potential of the metal complex, which increases the rate of Fe(III)-EDDS reduction to Fe(II)-EDDS by superoxide anions¹⁷⁸. It is also obvious that there are no substantial differences in the extent of iron atom catalysed hydrogen peroxide decomposition, when the base is varied from ammonia to MEA.

Ligand	20mM MEA	20mM NH ₃
None	5.0%	5.0%
EDTA	4.5%	4.5%
EDDS	10%	9.0%
HEDP	1.1%	0.4%
DTPMP	0.4%	0.7%

Table 8: The extent of hydrogen peroxide decomposition after 2 hours for the general reaction, 20 mM base, (1.3 mM ligand), 0.18 mM Fe(III) and 0.979 M H₂O₂ at pH 10 & 20 °C.

Cu(II) systems were similarly studied, as Cu(II) ions are abundant in hair fibres, which can lead to peroxide decomposition. The extent of Cu(II)-catalysed hydrogen peroxide decomposition after 120 minutes of reaction is shown in *Table 9*. Generally, the greater the concentration of base the more hydrogen peroxide decomposition is observed, the reasoning behind this is explained in further detail on page 113.

Ligand	20 mM MEA	20 mM NH ₃	400 mM MEA	400 mM NH ₃
None	4.5%	4.5%	<u>70%</u>	<u>100%</u>
EDTA	0.1%	0.06%	0.04%	
EDDS	0.1%	0.8%	2.0%	1.87%
HEDP	<u>8.0%</u>	<u>30%</u>	<u>40%</u>	<u>90%</u>
DTPMP	0.1%	0.05%	0.8%	0.06%

Table 9: The extent of hydrogen peroxide decomposition after 2 hours for the general reaction, 20/400 mM base, (1.3 mM ligand), 0.18 mM Cu(II) and 0.979 M H₂O₂ at pH 10 & 20 °C.

Unlike the iron(III) compositions, major differences exist between some of the MEA compositions and the equivalent NH_3 compositions when copper ions are used to catalyse a Fenton-like reaction. These compositions are highlighted in *Table 9*. When 20 mM base was used, the HEDP system was the only case where decomposition varied on changing the base. When the concentration of base was increased to 400 mM, differences became apparent in the ligand-free system, in addition to the HEDP one. The causes for the differences in these particular model systems are discussed further from page 113.

In addition to measuring the rates of hydrogen peroxide decomposition in these aqueous formulations, the hydroxyl radical production was monitored for these systems. This enabled the direct detection of one of the ROS that is responsible for melanin bleaching.

In order to observe the hydroxyl radical flux in these formulations, the colorimetric probe NPDPA was used, as described in chapter 2. The general reaction conditions used were 20 mM base, (1.3 mM ligand), 0.18 mM Cu(II), and 0.979 M H_2O_2 at pH 10 & 20 °C, with the addition of 1 mM NPDPA. Iron(III) systems could not be monitored due to problems with the solubility of iron atoms. Additionally, when the concentration of base was raised to 400 mM, the electronic spectra from some formulations became convoluted, as discussed on page 135.

The absorbance at 430 nm, due to the hydroxylated probe hNPDPA, was monitored over 2 hours to determine the relative amounts of hydroxyl radical produced over the course of the reaction. The rate of hydroxyl radical production is shown for 20mM MEA-based compositions with ligands and without ligands in *Figure 61*.

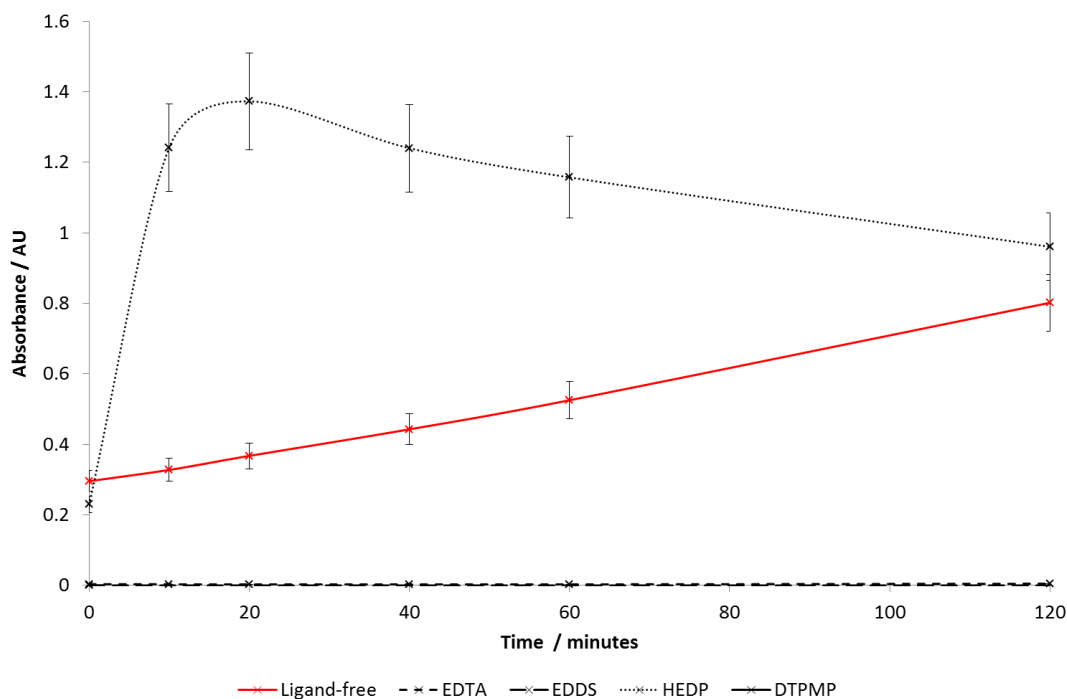


Figure 61: The level of hydroxyl radical flux in bleaching systems containing 20 mM MEA, (1.3 mM ligand), 0.18 mM Cu(II), 0.979 M H₂O₂ and 1 mM NPDPA at pH 10 & 20 °C.

As expected, for the ligand-free and the HEDP formulations, where more extensive hydrogen peroxide decomposition occurs, the amount of hydroxyl radicals that are produced is also greater. Generally, the ligand-containing systems result in negligible hydroxyl radical formation with the exception of the HEDP system. This is explained from page 119.

It is also evident that for the HEDP-based formulation there is a decline in the absorbance that would be due to hydroxylated NPDPA (hNPDPA), after 20 minutes reaction. This is possibly due to the large concentration of hydroxyl radicals, resulting in the degradation of the probe. This does not appear to be a problem for systems that produce a small amount of the radical.

If the strength of the hydroxyl radical flux is compared with the equivalent 20 mM NH₃ systems (Figure 45), it can be seen that similar amounts of hydroxyl radical are produced. However, the HEDP system does produce substantially more hydroxyl

radicals when ammonia is used, though this was expected due to the much more extensive decomposition that occurs in such formulations (*Table 9*).

Despite observing a similar extent of peroxide decomposition for the ligand-free systems, when 20 mM base was used, there appears to have been a greater hydroxyl radical flux in the MEA-based formulations. The change in the absorbance due to hNPDPA, over 120 minutes, is 0.25 for the ammonia-containing formulation and 0.51 for the MEA-containing formulation. This could be because the MEA influences the pathway by which hydrogen peroxide is decomposed and the system could produce a greater concentration of radicals as a result. This could potentially be a reason for the increased amount of hair damage that was observed in MEA-containing formulations. However, a greater concentration of base and of chelating ligands is used in commercial formulations.

These results give a partial overview of the appropriate peroxide decomposition and radical formation for various model bleaching systems. It has been shown, within the limited range studied, that differences only exist when strong ligands are not used in solutions. This mimics the situation that arises during the bleaching of whole hair fibres. However, it was necessary to establish in more detail why differences existed in the behaviour of formulations that did not contain strong ligands, when MEA was used as a base. The approach was designed to provide more evidence for the role that chemistry plays in varying bleaching potentials when the base is altered.

3.3.3 The chemistry behind the differences observed in hydrogen peroxide decomposition

Table 9 indicates that both the ligand-free and HEDP formulations show differences in behaviour when the concentration of the base is raised to 400 mM. As discussed on page 106, this represents a typical concentration of base found in level 3 colouring formulations. *Figure 62* shows the rate of hydrogen peroxide

decomposition in the ligand-free systems for reactions containing 400 mM base, 0.18 mM Cu(II) and 0.979 M H₂O₂ at pH 10 & 20 °C. It can be seen that for the ammonia-based formulation the decomposition is complete within 5 minutes, whereas a much lower rate of hydrogen peroxide decomposition is evident in the MEA formulation. The different metal complexes present in these ligand-free solutions can explain why this disparity exists when the base is changed. In contrast to the 20 mM base systems, the speciation curves in *Figure 63* and *Figure 64* show that the base becomes an important ligand when the concentration is increased to 400 mM.

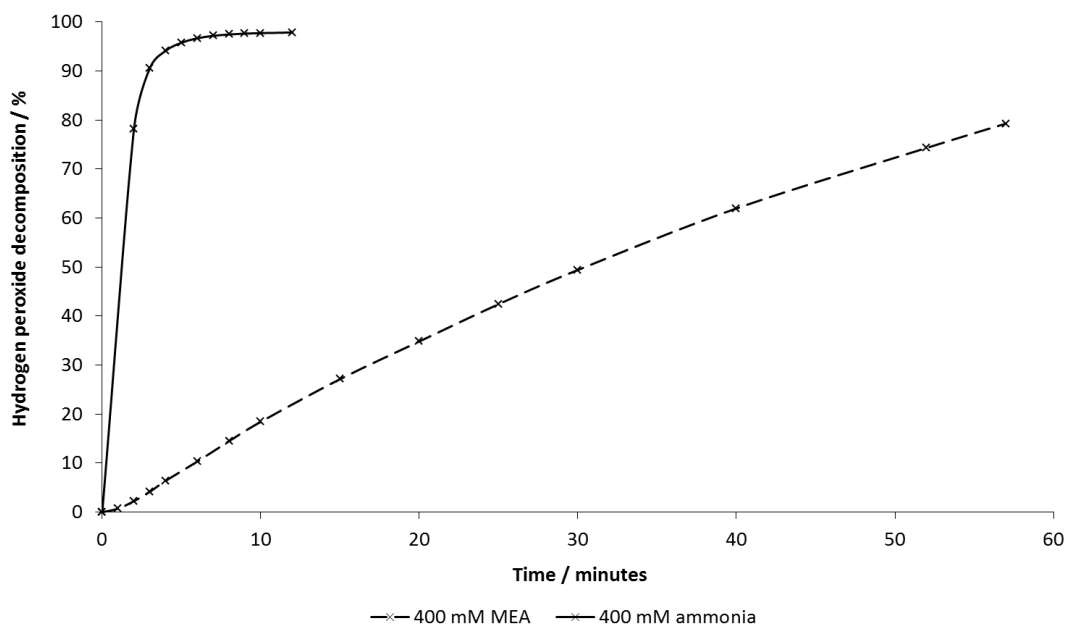


Figure 62: The relative rates of hydrogen peroxide decomposition for the following compositions: (400 mM base, 0.18 mM Cu(II) and 0.979 M H₂O₂ at pH 10 & 20 °C)

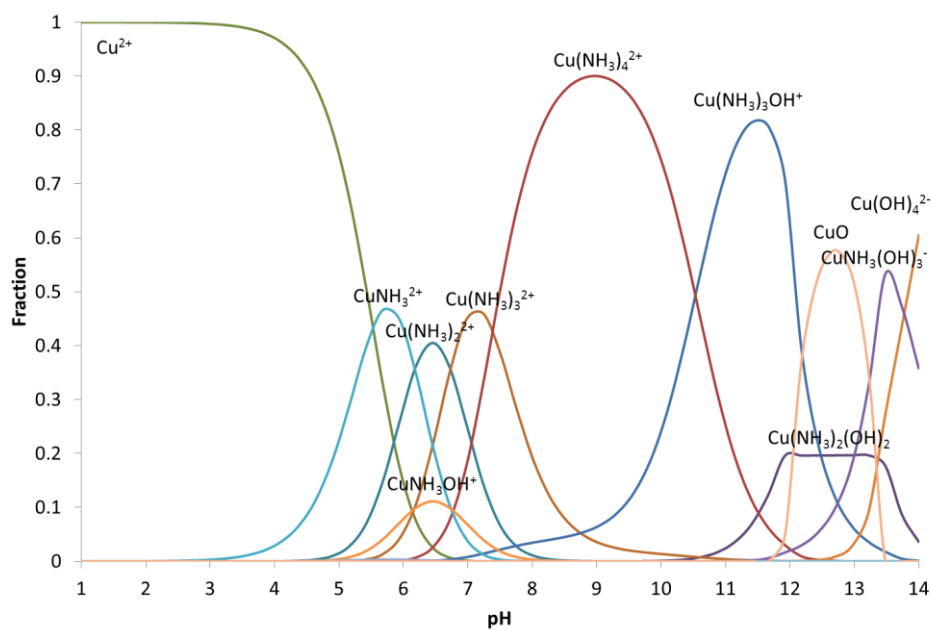


Figure 63: The speciation plot for 400 mM NH_3 , 0.18 mM Cu(II) and 0.979 M H_2O_2 at pH 10.

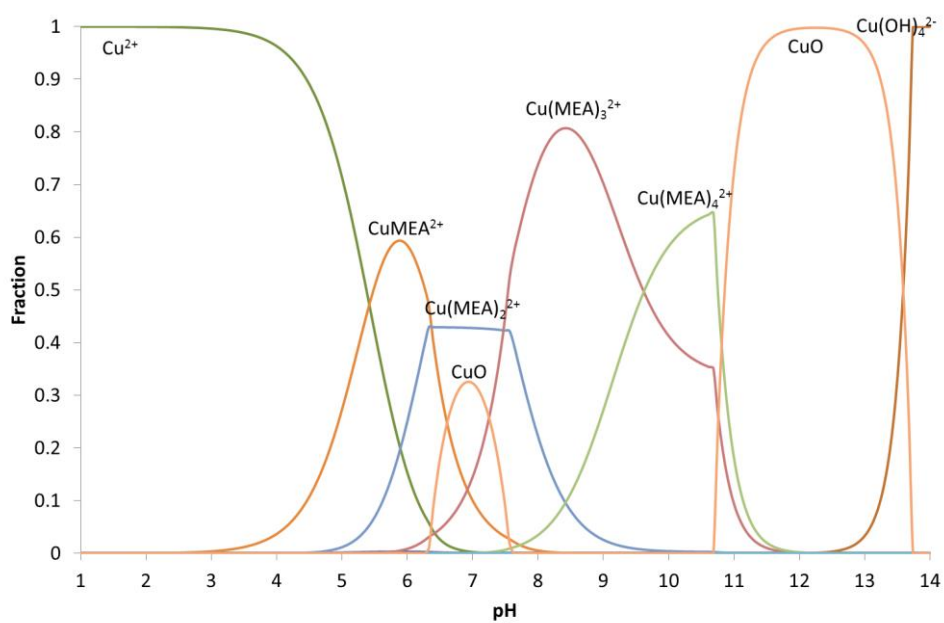


Figure 64: The speciation plot for 400 mM MEA , 0.18 mM Cu(II) and 0.979 M H_2O_2 at pH 10.

The speciation curves for the ammonia-based formulation predict that the main complexes present in solution at pH 10 are $[\text{Cu}(\text{NH}_3)_4]^{2+}$ and $[\text{Cu}(\text{NH}_3)_3\text{OH}]^+$, in addition to a small proportion of $[\text{Cu}(\text{NH}_3)_3]^{2+}$. In the MEA-based formulation $[\text{Cu}(\text{MEA})_4]^{2+}$ and $[\text{Cu}(\text{MEA})_3]^{2+}$ become the prevalent species. This could explain the differences in hydrogen peroxide decomposition that were observed when the base was altered, as the change in ligands will alter the redox potentials of the metal atom centres. For example, the NH_3 -based complexes may have redox potentials that are in the centre of the effective redox window for the Fenton-like reaction ($-0.33 - 0.46 \text{ V}^{87}$), theoretically allowing the rapid redox cycling of the copper atoms between +1 and +2 oxidation states. It is important to note that redox potentials provide information concerning the feasibility of reactions. The rates of reaction cannot be deduced from redox potentials. Rates of hydrogen peroxide decomposition are more likely to be influenced by the ability of hydrogen peroxide or perhydroxyl anion to coordinate to the metal atom centre.

When the base is changed, the redox potentials of the MEA complexes may lie closer to the edge of this redox "window". This could result in the inhibition of either the oxidation or reduction of the metal centre, which in turn may lead to a decrease in the rate of the steps of peroxide decomposition shown as reactions 1-5 on page 17, the slowest of which becomes rate-determining. Alternatively, hydrogen peroxide or the perhydroxyl anion may not coordinate as easily to the metal atom centre, when the ligand is bidentate, as is MEA, thus decreasing the rate at which it is broken down.

In addition to the difference observed in the ligand-free environment, there is also a substantial difference in peroxide decomposition for the HEDP system, when the base is changed from ammonia to MEA, for mixtures that contain both 400 and 20 mM base. For the general reaction containing 400 mM base, 1.3 mM HEDP, 0.18 mM Cu(II) and 0.979 M H_2O_2 at pH 10 & 20 °C, the difference in the rate of decomposition on altering the base can be seen in *Figure 65*. Similarly to the ligand-free solutions, it is the system that contains ammonia that results in a higher rate of peroxide decomposition. The types of complex that are present in solution can

again explain this observation. The speciation plots for the HEDP systems in the presence of 400 mM base are shown in *Figure 66* and *Figure 67*.

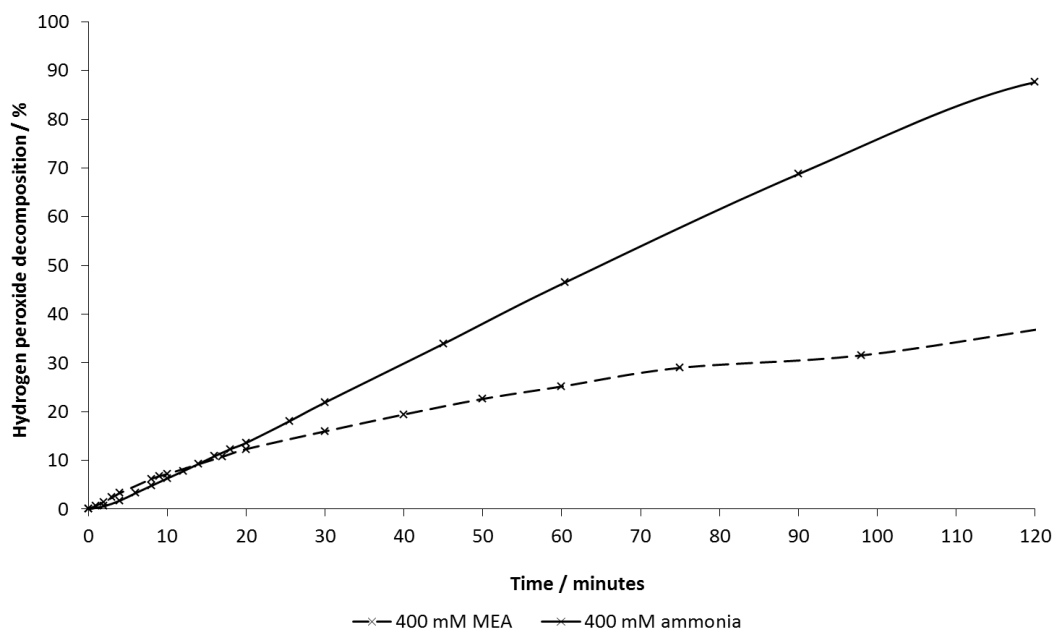


Figure 65: The relative rates of hydrogen peroxide decomposition for the following systems: (400 mM base, 1.3 mM HEDP, 0.18 mM Cu(II) and 0.979 M H₂O₂ at pH 10 & 20 °C). Thanks to Kazim Naqvi for allowing the use of the ammonia data in this figure.

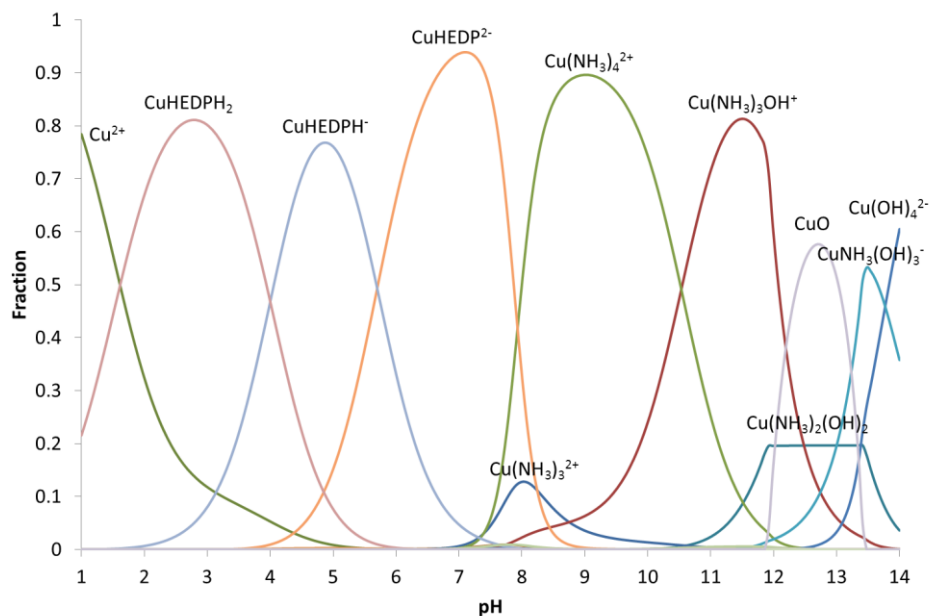


Figure 66: The speciation plot for 400 mM NH_3 , 1.3 mM HEDP, 0.18 mM Cu(II) and 0.979 M H_2O_2 at pH 10.

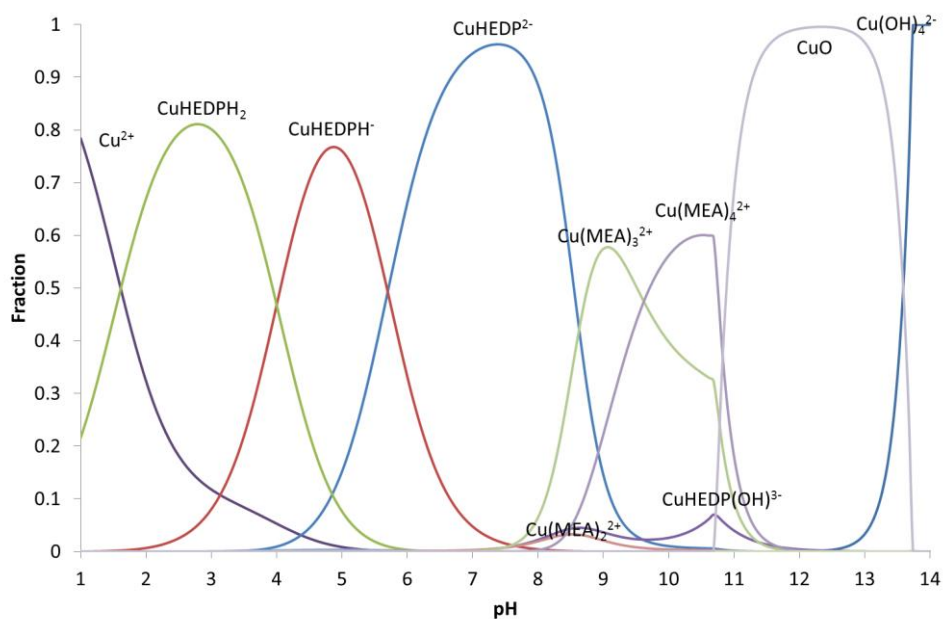


Figure 67: The speciation plot for 400 mM MEA, 1.3 mM HEDP, 0.18 mM Cu(II) and 0.979 M H_2O_2 at pH 10.

At pH 10, the types and relative amounts of complexes that are present in both the MEA and ammonia solutions are similar for both the ligand-free and HEDP systems. This explains the similar trend in peroxide decomposition for the two systems. However, it does not explain why the overall rates of hydrogen peroxide decomposition are lower for the HEDP systems compared with the ligand-free systems, if the same complexes are present. This difference in rate may be due to the fact that HEDP is susceptible to extensive degradation under these conditions, as discussed on page 125. As a result oxygen could react with any organic radicals that are formed during this degradation, as shown in reaction 13. Oxygen consumption by the potential degradation of MEA is also a possibility, as outlined on page 132. This could lead to a reduction in the volume of oxygen that is measured. However, at the end of decomposition reactions volumetric titrations were used to determine the concentration of remaining hydrogen peroxide in solution (details of the titrations are shown in chapter 7). In this way it was shown that reaction 13 does not contribute significantly to oxygen consumption. A negligible oxygen consumption can be expected due to the low extents of MEA degradation and the relatively small concentration of HEDP compared to the concentration of base, as shown in *Figure 75*.



Phosphate ions are known to cause the precipitation of soluble metal ions. Thus, the metal ions are not free to cause the metal-catalysed decomposition of hydrogen peroxide. A high enough concentration of phosphate ions could also lead to the formation of stable complexes with metal ions^{179, 180}. It is therefore possible that HEDP may degrade to form phosphate ions that would prevent any resulting decomposition. This possibility is discussed further on page 129.

When 20 mM base is used there is also a large difference in both the extent and rate of hydrogen peroxide decomposition in solutions that contain HEDP, as can be

seen from *Figure 68*. The solution that contains ammonia shows a rapid acceleration in the rate of decomposition for the first 20 minutes of the reaction, at which point no more oxygen is evolved. In contrast, the MEA system provides a much steadier rate of peroxide decomposition over the course of 2 hours.

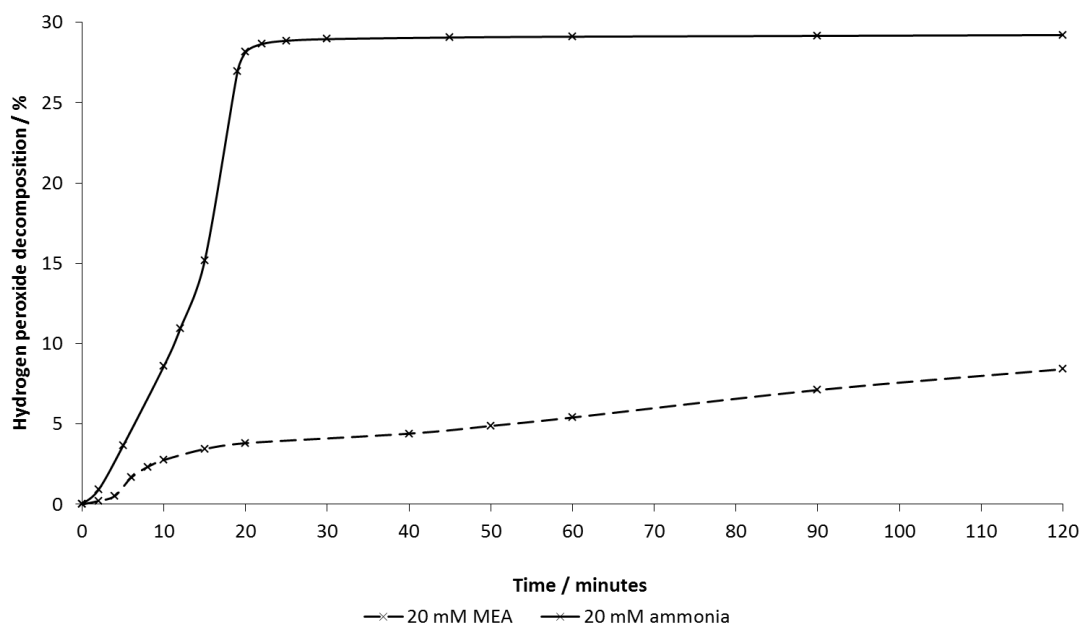


Figure 68: The relative rates of hydrogen peroxide decomposition for the following systems: (20 mM base, 1.3 mM HEDP, 0.18 mM Cu(II) and 0.979 M H₂O₂ at pH 10 & 20 °C). Thanks to Kazim Naqvi for allowing the use of the ammonia data in this figure.

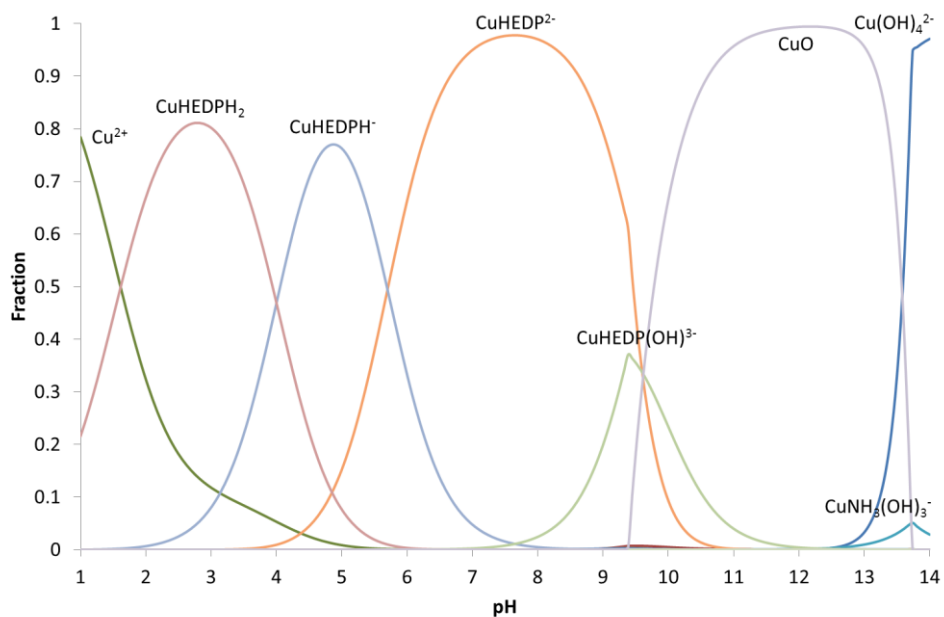


Figure 69: The speciation plot for 20 mM NH_3 , 1.3 mM HEDP, 0.18 mM Cu(II) and 0.979 M H_2O_2 at pH 10.

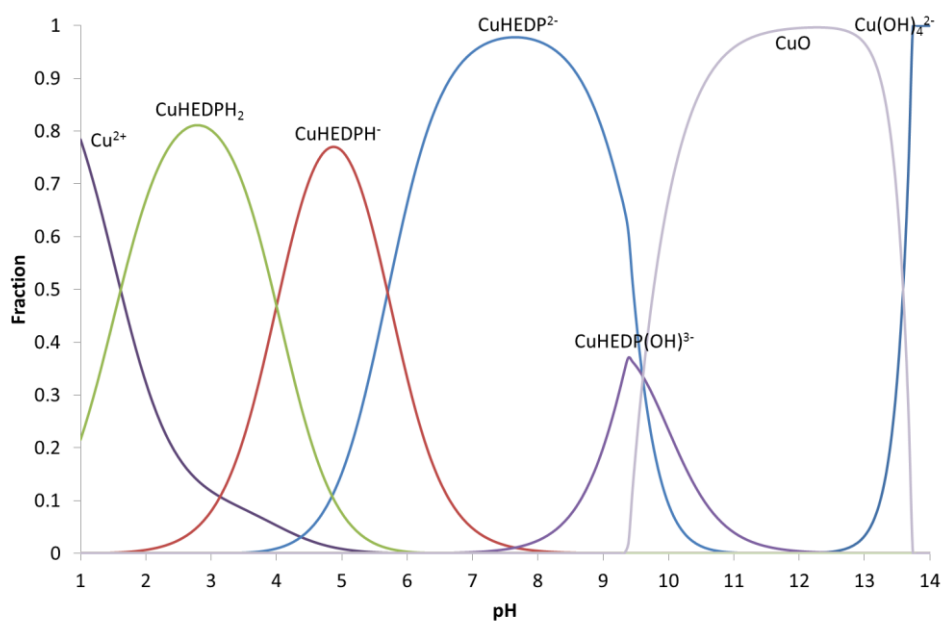


Figure 70: The speciation plot for 20 mM MEA, 1.3 mM HEDP, 0.18 mM Cu(II) and 0.979 M H_2O_2 at pH 10.

It is difficult to identify why there is such a difference in the peroxide decomposition between the MEA and NH_3 systems by simply looking at the speciation plots in *Figure 69* and *Figure 70*. The ratio of CuO , $[\text{Cu}(\text{HEDP})(\text{OH})]^{3-}$ and $[\text{Cu}(\text{HEDP})]^{2-}$ complexes is predicted to be similar in both MEA and NH_3 solutions. Whilst the speciation curves provide a rough estimation of the complexes present, undiscovered complexes may exist in the system that cannot be predicted. Additionally, when CuO is formed, the compositions become much more complex, because heterogeneous materials may be capped by ligands or by base. These factors could potentially explain the differences observed between the formulations. However, it has been shown that HEDP degrades in the ammonia system, resulting in the formation of basic $\text{Cu}(\text{II})$ phosphate/carbonate nanoparticles¹⁷⁰. These nanoparticles appear to inhibit peroxide decomposition, explaining the plateau in the rate of oxygen evolution for the ammonia-based composition¹⁷⁰. There is no evidence for the formation of these nanoparticles in the MEA composition, which could also explain the differing rate of peroxide decomposition that is observed. Furthermore, when the pH of both the ammonia solution and the MEA solution is monitored over the course of the reaction (*Figure 71*), the underlying reason for this difference in behaviour becomes clear.

The pH of both the 20 mM MEA and the ammonia buffer solutions was recorded as the individual components that make up the model system were added. On the addition of 1.3 mM HEDP, 0.18 mM $\text{Cu}(\text{II})$ and 0.979 M H_2O_2 the pH decreases from 10 to roughly 9. The pH was monitored throughout the course of the reactions. *Figure 71* shows that there is no substantial change in the pH during the reaction in the presence of ammonia. However, the pH in the solution containing MEA drops below pH 7 after approximately 30 minutes. The reason for this pH drop is discussed from page 125 onwards.

The change in pH when MEA is used may explain why there are differences in the rate of peroxide decomposition for the HEDP systems. As the pH decreases, the proportion of $[\text{Cu}(\text{HEDP})]^{2-}$ and $[\text{Cu}(\text{HEDPH})]^-$ complexes that are present in the MEA solutions will become greater than for the equivalent ammonia system. This change

in the ratio of complexes present in solution is likely to affect the level of hydrogen peroxide decomposition.

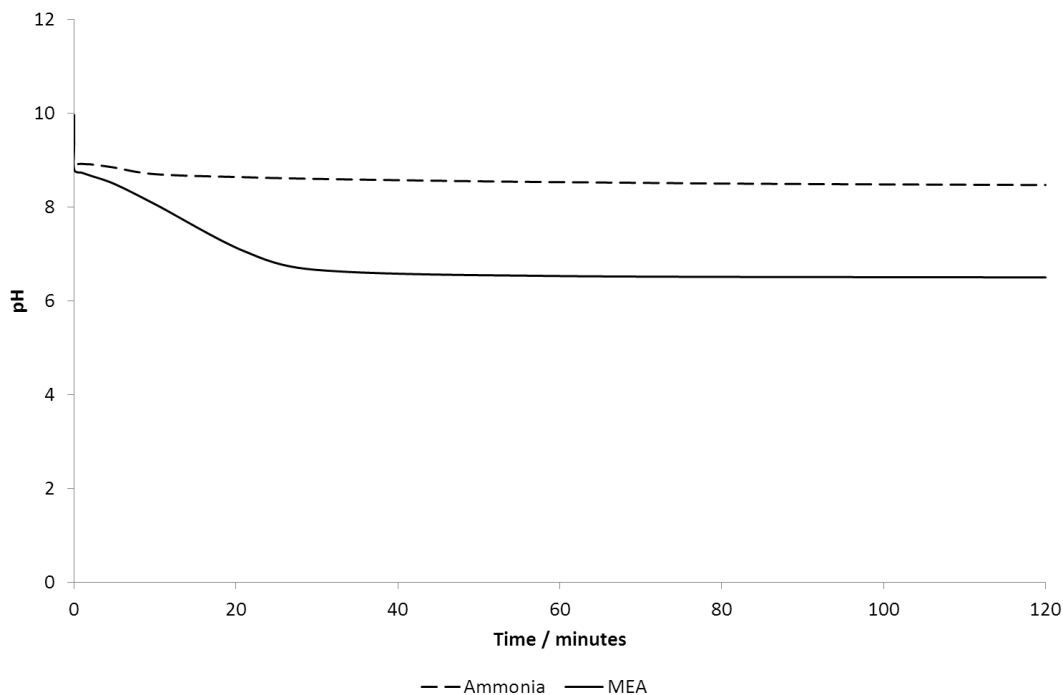


Figure 71: pH profile during hydrogen peroxide decomposition for systems containing 20 mM base, 1.3 mM HEDP, 0.18 mM Cu(II) and 0.979 M H₂O₂ at pH 10 & 20 °C.

In summary, when the base is changed in aqueous model bleaching systems, the major differences in hydrogen peroxide decomposition and hydroxyl radical production are generally due to the presence of different complexes in solution. This feature is observed for the ligand-free formulations, where the base is present at a great enough concentration to bind copper ions. Different complexes are also present in the HEDP system as speciation plots show that HEDP is an ineffective ligand at alkaline pH. Therefore, the base also plays a role in the types of complex that are present in this system. However, in commercial formulations strong chelating ligands are used, such as EDTA or EDDS. By comparing the speciation plots

in *Figure 20* and *Figure 72*, it can be seen that the complexes that are formed in these formulations are the same regardless of whether MEA or ammonia is used.

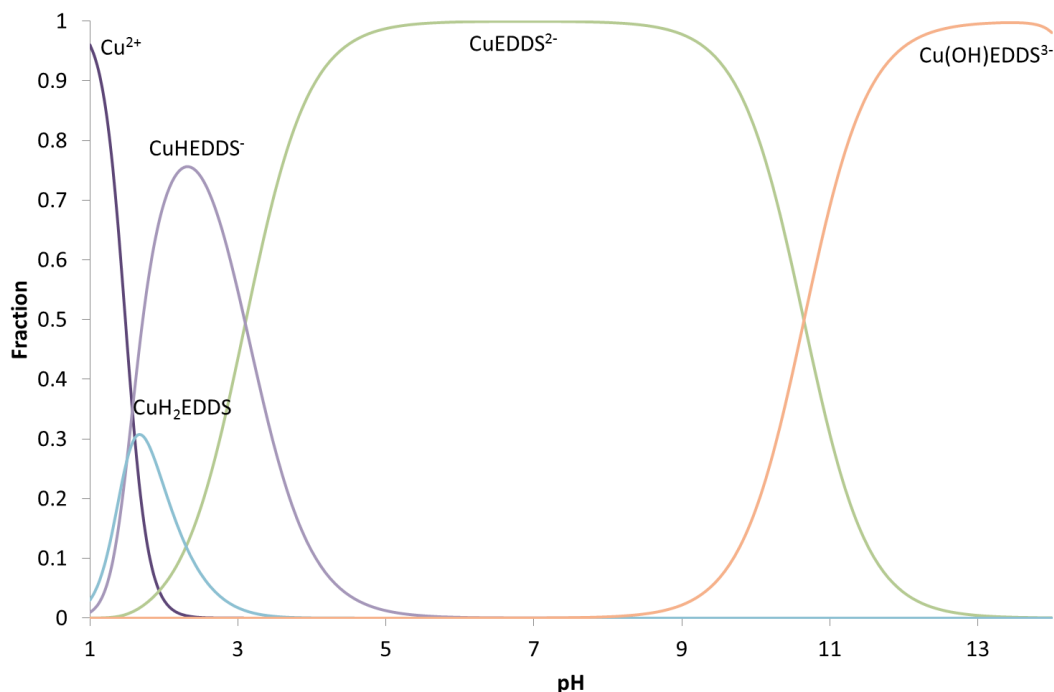


Figure 72: Speciation plot to show the copper complexes formed in a model hair system containing 400 mM MEA, 13.95 mM EDDS, 170 mM Ca²⁺ and 1.27 mM Cu²⁺

The pH decrease that is evident in solutions containing HEDP, when 20 mM MEA is used, also results in different complexes being formed compared with those developed using the ammonia-based formulations. This leads to differences in the extent of hydrogen peroxide decomposition. Although this concentration of base is not representative of bleaching formulations, it led to the investigation of the reason for the pH drop, as the observed chemistry may also be present in formulations with a greater concentration of base. Two potential causes of the pH drop were investigated. The first was the possibility of HEDP degradation, and the second was the potential oxidation of MEA.

3.3.4 HEDP degradation

The structure of HEDP is shown in *Figure 73*. It is known that these phosphonates can degrade under Fenton-like conditions to produce carbonates and phosphates^{170, 181}. It was therefore considered to be necessary to check the concentration of HEDP over the course of the reaction.

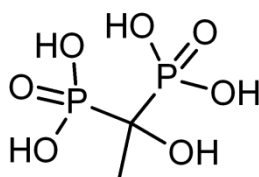


Figure 73: The structure of HEDP

In order to monitor the HEDP concentration initially over the course of a bleaching reaction, ¹H NMR of HEDP in D₂O was used. This should give a singlet at approximately 1.25 ppm, the intensity of which can be measured over the course of the reaction, in order to determine the change in concentration of the ligand.

A composition containing 20 mM MEA, 1.3 mM HEDP, 0.18 mM Cu(II), 0.979 M H₂O₂ at pH 10 & 20 °C was setup in D₂O. Samples were taken at 0, 20, 60 and 120 minutes. Catalase was added to the sample to decompose hydrogen peroxide and stop any further degradation of the ligand. 100 mM of dichloroacetic acid (DCA) was added as an internal standard. Catalase was centrifuged out of solution and a ¹H NMR spectrum of the supernatant was acquired.

Figure 74 shows the singlet at 1.25 ppm due to the methyl group of the HEDP, at a reaction time of 0 minutes. This singlet appears to be very broad due to the presence of Cu(II). In the presence of paramagnetic Cu(II) protons will have a substantially increased rate of spin-lattice relaxation via dipolar interactions^{182, 183}. This peak broadening affects the integration of peak areas significantly. However, it is clear from the spectrum that the broad peak that was present at the beginning of

the reaction had completely disappeared after 120 minutes. In fact the degradation of HEDP was so rapid that it had completely reacted within 20 minutes, as the data in *Figure 75* show.

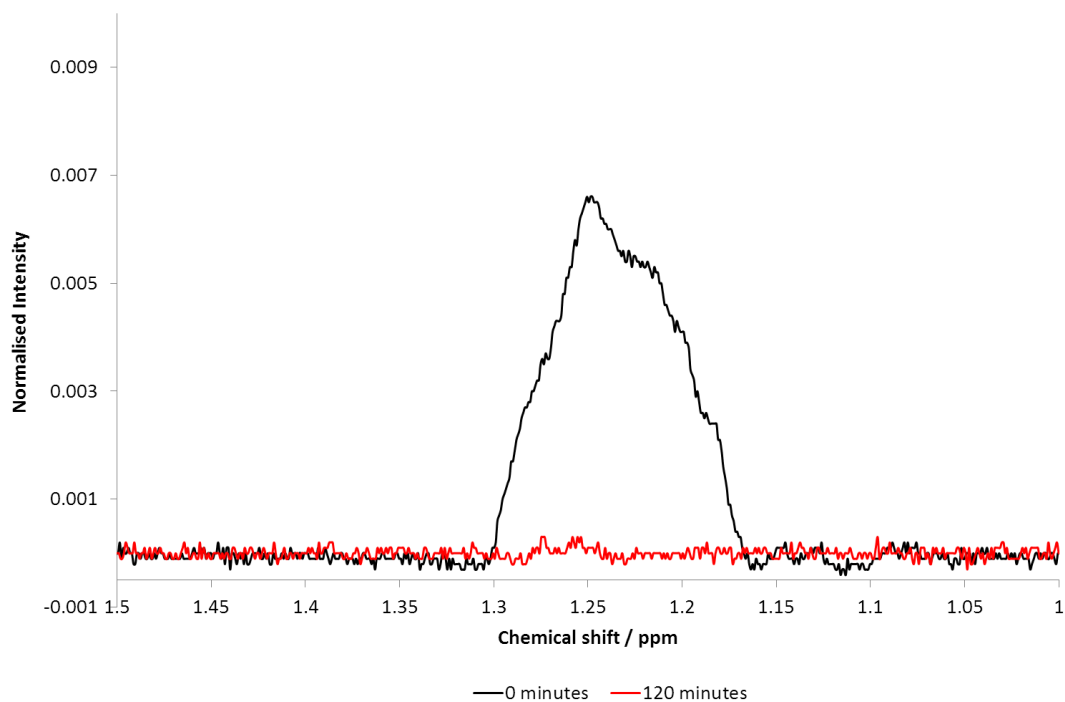


Figure 74: ^1H NMR spectrum of 20 mM MEA, 1.3 mM HEDP, 0.18 mM Cu(II) and 0.979 M H_2O_2 for 0 minutes and for 120 minutes of reaction time.

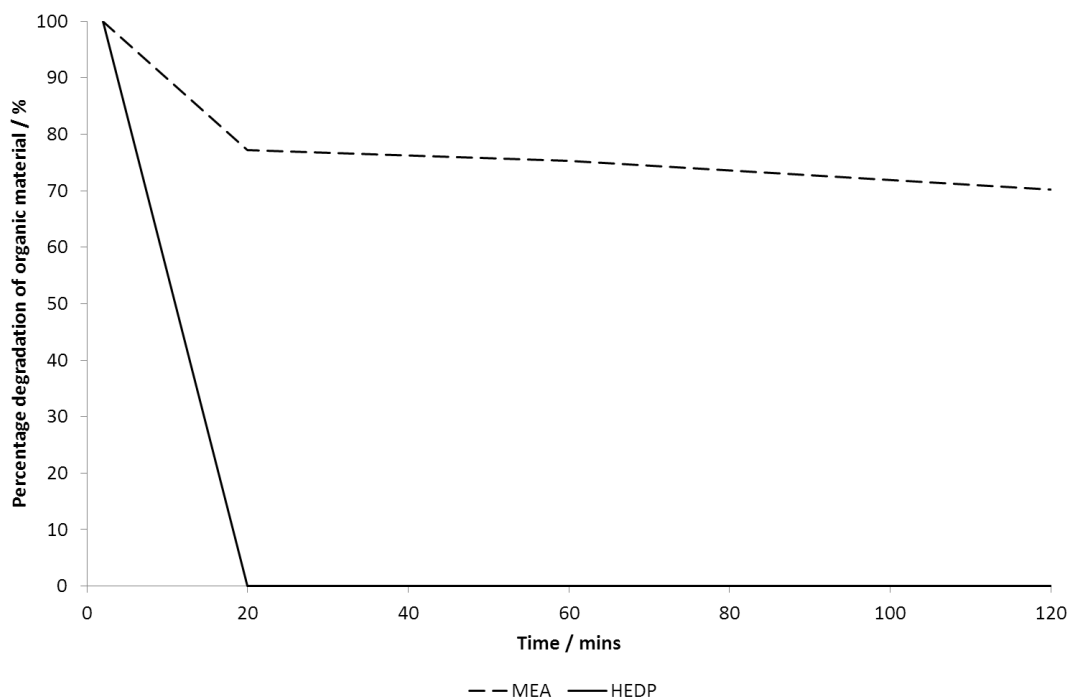


Figure 75: Normalised concentration of MEA and HEDP during the reaction of 20 mM MEA, 1.3 mM HEDP, 0.18 mM Cu(II) and 0,979 M H₂O₂.

In addition to the NMR study, which shows that the HEDP completely degraded within the first twenty minutes of the reaction, an analysis of phosphate loadings during the reaction also confirmed the degradation of HEDP in a similar time frame.

Phosphate ion analysis was carried out using a combined molybdenum reagent and UV-vis spectroscopy, as described in chapter 7. Using this reagent, a molybdenum-blue complex is formed in the presence of phosphate. A typical spectrum, showing the absorbance at 882 nm, which forms as a result of this complex, is shown in *Figure 76*. This absorbance was used to determine the concentration of phosphate ions produced during the degradation of HEDP, in the presence of MEA.

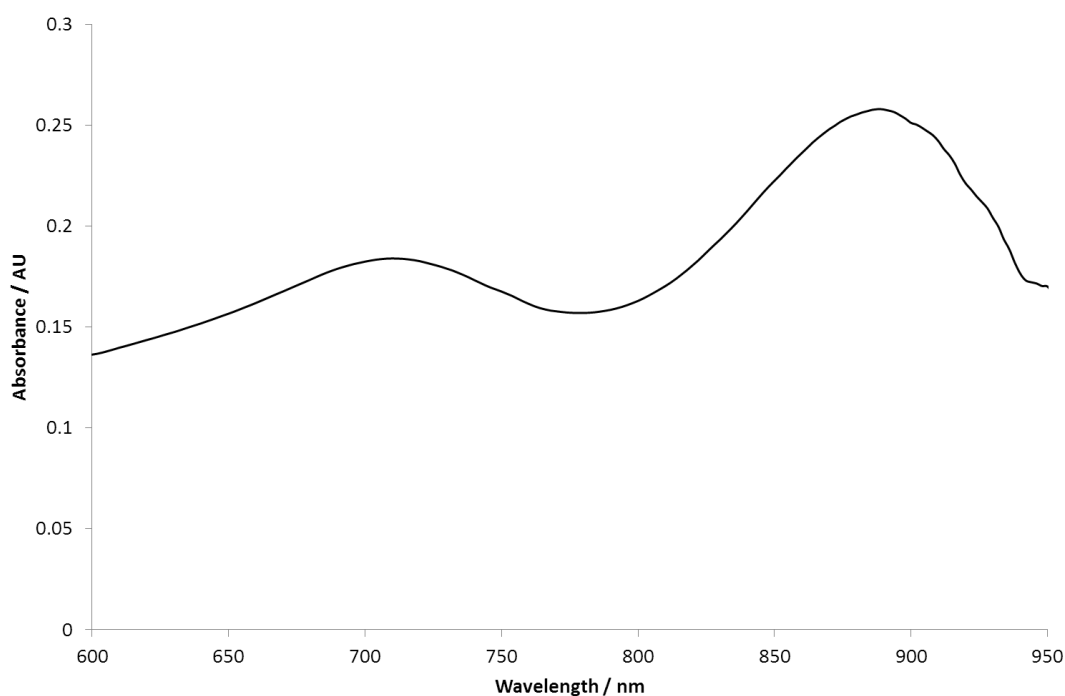


Figure 76: UV spectrum of the molybdenum blue complex, showing the peak at 882 nm that is used for phosphate analysis.

A solution consisting of 20 mM MEA, 1.3 mM HEDP, 0.18 mM Cu(II) and 0.979 M H_2O_2 , at pH 10, was set up and samples were taken at 0, 20, 60 and 120 minutes. Catalase was added to decompose the hydrogen peroxide, preventing further HEDP degradation. Samples were then treated with the combined molybdenum reagent. The absorbance at 882 nm was studied by UV-vis spectroscopy, after 15 minutes. A calibration curve was then used to determine the concentration of phosphate ions at each time point. The results are shown in *Figure 77*. These can be and are compared to the concentration of phosphate ions in the corresponding 20 mM NH_3 system, containing 1.3 mM HEDP, 0.18 mM Cu(II), 0.979 M H_2O_2 at pH 10 & 20 °C.

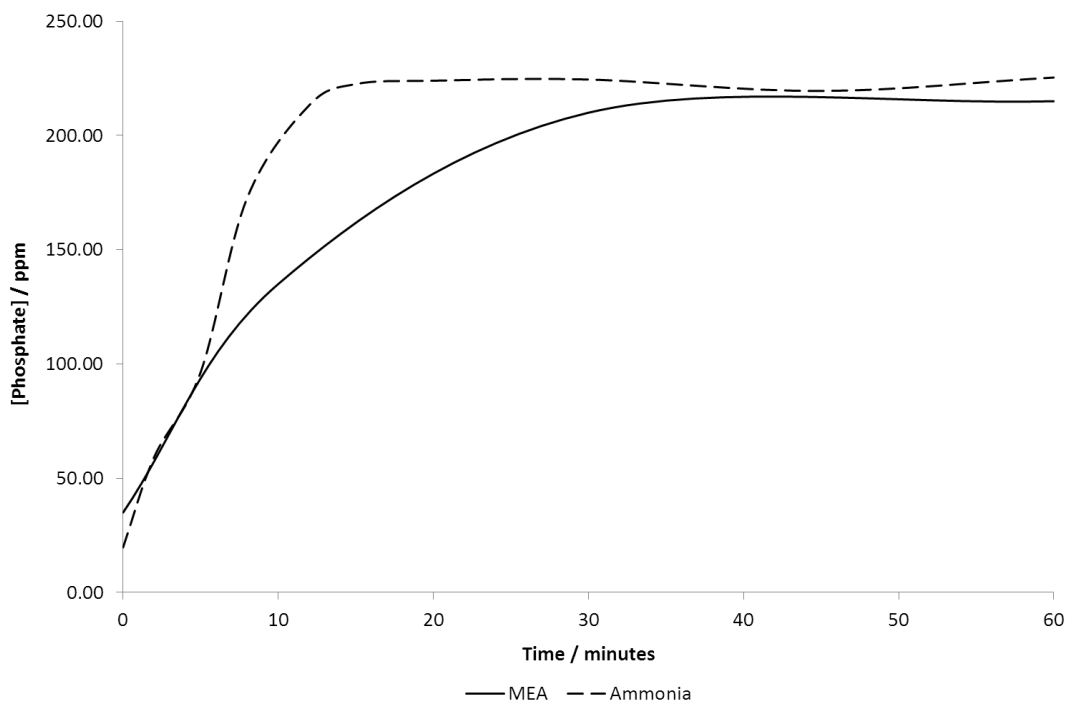


Figure 77: The production of phosphate, as a result of HEDP degradation, for formulations containing 20 mM base, 1.3 mM HEDP, 0.18 mM Cu(II) and 0.979 M H₂O₂ at pH 10 & 20 °C. Thanks to Kazim Naqvi for allowing the use of the ammonia data in this figure.

If 1.3 mM HEDP fully degrades into phosphate ions with a yield of 100%, the expected concentration of phosphate ions produced would be 2.6 mM (246.92 ppm). It is evident from *Figure 77* that the majority of the HEDP is degraded within the 30 minutes of reaction commencement when MEA is used. In the ammonia-based composition the rate at which HEDP is degraded is much greater, most of the HEDP having been degraded within 15 minutes. However, after 40 minutes the extents of phosphate production due to HEDP degradation are similar in both the ammonia-based composition and the MEA-based composition. However, it is only in the MEA system that a pH decrease is observed. Therefore, despite the degradation of HEDP to form phosphate ions, there must be another reason for the pH decrease in the MEA system when HEDP is used as a ligand.

When determining the concentration of HEDP during the Fenton-like reaction, by NMR, it was also possible to estimate the concentration of MEA over the course of the reaction. *Figure 75* shows the fall in concentration of MEA at the same time as the HEDP is degraded. It was thought that degradation of the base could potentially cause the decline in pH that was observed in this system.

3.3.5 MEA degradation in the HEDP system

MEA degradation was initially suspected due to a decrease in the intensity of $-\text{CH}_2$ signals in the ^1H NMR spectra, from the reaction of 20 mM MEA, 1.3 mM HEDP, 0.18 mM Cu(II) and 0.979 M H_2O_2 at pH 10 & 20 °C (*Figure 78*).

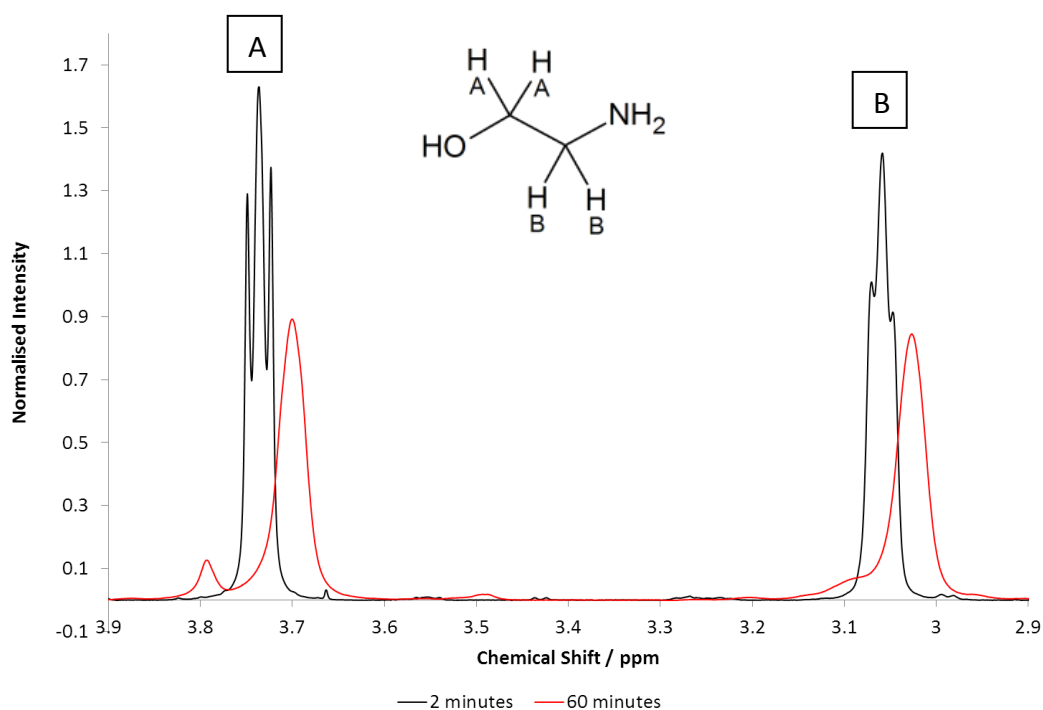


Figure 78: ^1H NMR spectra of the $-\text{CH}_2$ peaks of MEA.

The NMR data in *Figure 75* show that approximately 30% of MEA was degraded under Fenton-like conditions after 2 hours. The presence of paramagnetic Cu(II) in

this reaction has an interesting effect on the shape of the triplets that correspond to the $-\text{CH}_2$ protons of MEA. At the start of the reaction, before HEDP is degraded, the splitting of the triplets can be clearly seen. However, by 20 minutes the peaks become broadened and the chemical shift changes. As mentioned on page 125, peak broadening occurs due to the decreased relaxation time of the protons in the presence of paramagnetic material. The metal also can cause a change in the chemical shifts of the $-\text{CH}_2$ peaks, possibly by shielding the proton nuclei. It is however unclear why these effects emerge after HEDP is degraded. The emergence may be due to the change of the copper ion environment after the ligand is broken down. In ligand-free systems, for this concentration of MEA, copper is thought to exist as CuO. However, this does not exclude the possibility that Cu(II) may actually bind to the base and cause the broadening of $-\text{CH}_2$ peaks. The formation of phosphate ions in this system also complicates matters, as they may bind to Cu(II) or cause precipitation of the metal, which could also affect the NMR spectra.

Due to the effect of these paramagnetic centres, there is uncertainty over how reliable this quantification of MEA loss is, over the course of the reaction. Nevertheless, these results appear to indicate that degradation is a possibility. In addition to this interpretation, a singlet at approximately 8.2 ppm is present in these ^1H NMR spectra, which suggests the production of formic acid during this reaction. There is evidence in the literature for the formation of several acids, including formic acid, due to the oxidation of MEA¹⁸⁴, providing further evidence for the degradation of MEA under these conditions. The potential mechanism of formic acid production from the degradation of MEA by single electron oxidants is shown in *Figure 79*^{185, 186}.

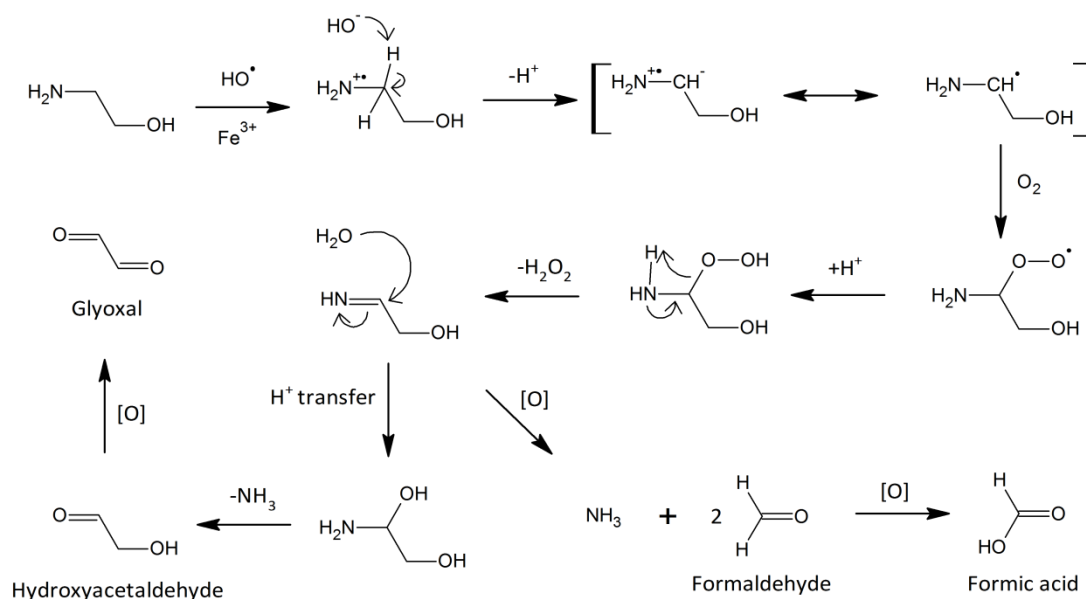


Figure 79: The possible mechanistic pathways of MEA degradation by single electron oxidants^{185, 186}.

Single electron oxidants such as the hydroxyl radical or transition metal cations may lead to the oxidation of MEA to form the MEA radical cation, which is then deprotonated and a carbon centred radical may result. This can then react with oxygen to form the peroxy radical, which can abstract a hydrogen atom from another molecule of MEA to yield the aminoperoxide. Loss of hydrogen peroxide then affords the imine. Hydrolysis of the imine by water, followed by the loss of ammonia, leads to the formation of hydroxyacetaldehyde, the oxidation of which gives glyoxal. Alternatively, radical mediated oxidative fragmentation of the imine may occur, resulting in the production of ammonia and formaldehyde, which can be further oxidised to formic acid¹⁸⁷.

CurTiPot software can be used to predict the pH of mixtures and to simulate titrations, using concentrations and pK_a values of the components¹⁸⁸. This approach was used in order to determine whether or not the combined degradation of MEA and HEDP could account for the pH drop observed in a system initially containing 20 mM MEA, 1.3 mM HEDP, 0.18 mM Cu(II) and 0.979 M H_2O_2 at 20 °C

During this reaction, HEDP has been shown to degrade completely to produce phosphate species. It is worth noting that the organic fragment of the molecule may potentially lead to the production of acetic acid, although this organic material could also be consumed during the formation of secondary MEA oxidation products. Therefore, it is difficult to say with certainty whether or not there is a net production of acetic acid due to HEDP degradation. The oxidation of MEA, generating formic acid, is also a possibility. However, other acids may also be produced as a result of degradation. Taking all of this into account, CurTiPot was used to match the final pH of the reaction solution (6.72) to that of a theoretical solution containing 8.83 mM MEA, 4.21 mM acetic acid (used to buffer MEA to pH 10), 0.18 mM Cu(II), 2.26 mM phosphate and 1.4 mM formic acid. These conditions assume that 30% of MEA has been degraded over the course of 2 hours, to produce 1.4 mM formic acid (the real concentration of MEA at the beginning of the reaction was determined to be 12.615 mM, after the base was buffered to pH 10 with acetic acid and other reactants were added to the solution). It is also assumed that 100% HEDP degrades to give 2.6 mM phosphate and no additional acetic acid. Additionally, a simulated titration curve of this theoretical final solution against 30 mM HCl can be matched closely to an experimental titration, as shown in *Figure 80*.

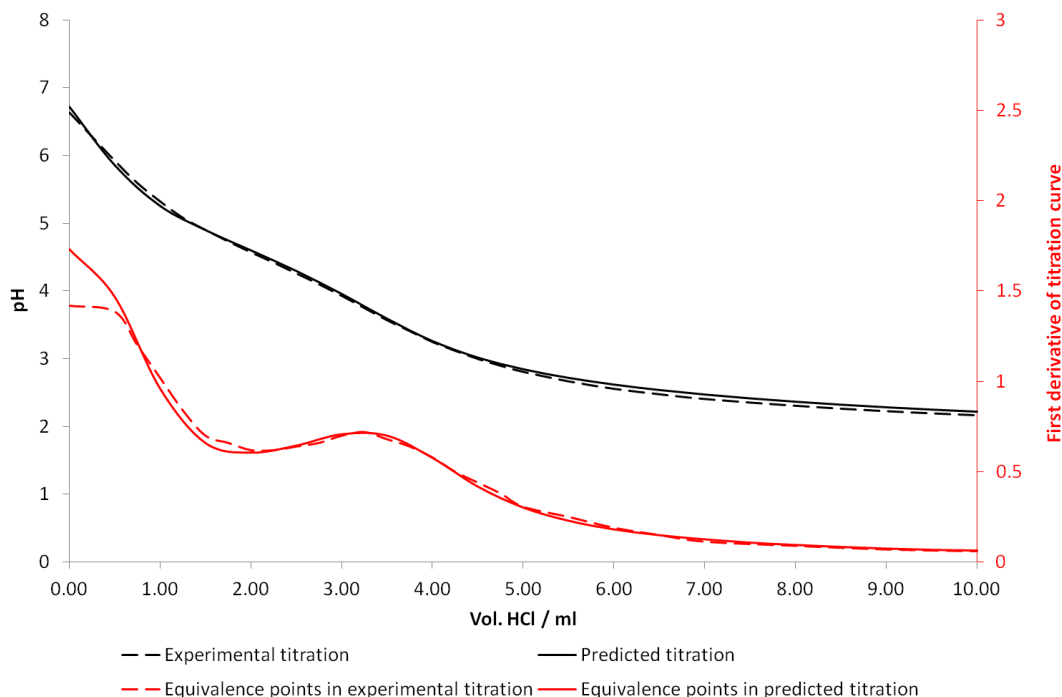


Figure 80: The experimental titrations and the predicted titrations of a 20 mL solution of 8.83 mM MEA, 4.21 mM acetic acid, 0.18 mM Cu(II) and 2.26 mM phosphate and 1.4 mM formic acid against 30 mM HCl, as well as the equivalence points of the titrations.

It can be seen that there is a good fit between the predicted and the experimental titration curves when it is assumed 1.4 mM formic acid is produced as a result of 30% MEA degradation. An exact match of these predicted and experimental curves is not seen because other acids, such as nitrous, oxalic and acetic acid that may be produced from MEA oxidation, have not been quantified under these experimental conditions.

In summary, it seems likely that the major reasons for the pH drop in the HEDP system is the complete degradation of HEDP to form phosphate ions, as well as the partial degradation of MEA to form formic acid. This would explain why the same drop in pH is not observed in systems that contain ammonia (*Figure 71*) or in systems that do not contain HEDP (*Figure 81*).

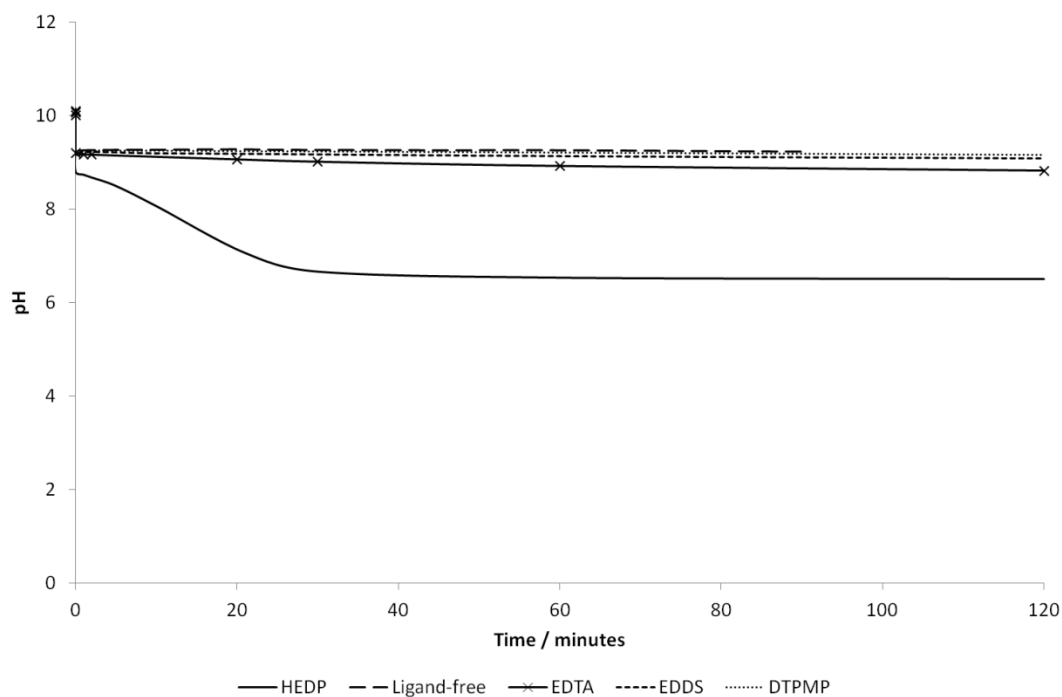


Figure 81: The pH profile during hydrogen peroxide decomposition for systems containing 20 mM MEA, (1.3 mM ligand), 0.18 mM Cu(II) and 0.979 M H₂O₂ at 20 °C.

To conclude, MEA degradation and HEDP degradation result in a significant decrease in the pH, affecting hydrogen peroxide decomposition. However, for bleaching systems that use other ligands, hydrogen peroxide decomposition is not affected by the same phenomenon. Additionally, as most bleaching systems contain at least 400 mM base they will have a much greater buffering capacity than the 20 mM compositions. Degradation of MEA would therefore not be expected to contribute to a similar pH drop for these systems. However, by varying the conditions of MEA oxidation, the formation of different products becomes possible.

3.3.6 MEA degradation in the ligand-free formulations

The formation of an unknown product, potentially due to MEA degradation, was observed over the course of a reaction composition containing 400 mM MEA, 0.18 mM Cu(II) and 0.979 M H₂O₂ at pH 10 & 20 °C. This was indicated by an increasing

absorbance at 365 nm, during the spectrophotometric detection of hydroxyl radical, described on page 111. This increasing absorbance, shown in *Figure 82*, led to the investigation of MEA degradation under these conditions.

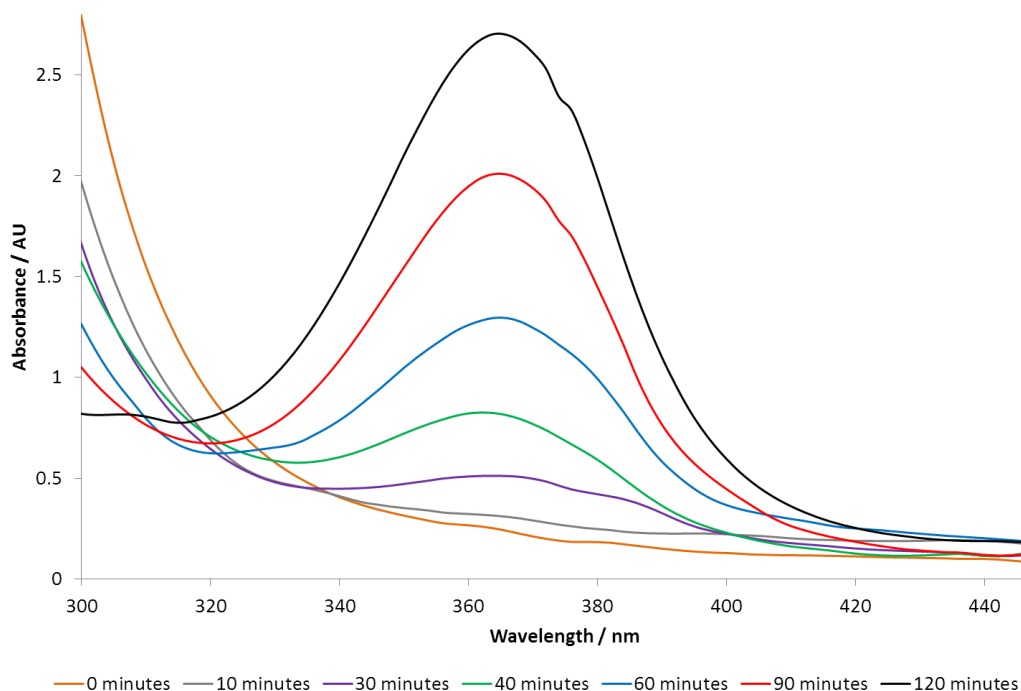


Figure 82: The increasing absorbance at 365 nm observed during the reaction of 400 mM MEA, 0.18 mM Cu(II) and 0.979 M H₂O₂ at pH 10 & 20 °C.

Due to the complexity of the NMR spectra and the presence of paramagnetic Cu(II), which further convolutes NMR spectra, it was decided to investigate the formation of any potential products of MEA degradation by gas chromatography (GC).

A mixture containing 400 mM MEA, 0.18 mM Cu(II) and 0.979 M H₂O₂ was reacted for 120 minutes. The reaction was stopped after 120 minutes, using catalase. Glycerol was added to the sample as an internal standard and the catalase was centrifuged out. The supernatant was injected for GC analysis using the method described in chapter 7. The chromatogram obtained is shown in *Figure 83*.

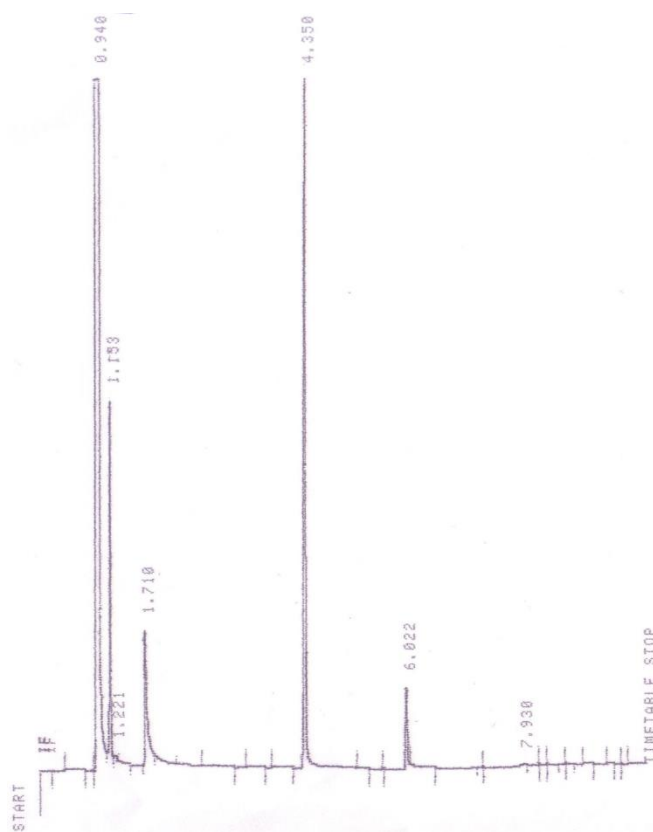


Figure 83: Chromatogram of a solution of 400 mM MEA, 0.18 mM Cu(II), 0.979 M H_2O_2 .

Retention time	Peak identity
0.940	Methanol
1.153	Acetic acid
1.710	MEA
4.350	Glycerol
6.022	Unknown

Table 10: Retention times and peak identities for the chromatogram shown in Figure 83.

All the peaks depicted in Figure 83 were identified by their retention time, except for the peak at 6.022 minutes. In order to identify this peak, GC-EI was used to

obtain a mass spectrum of the compound. The acquired mass spectrum is shown in *Figure 84*.

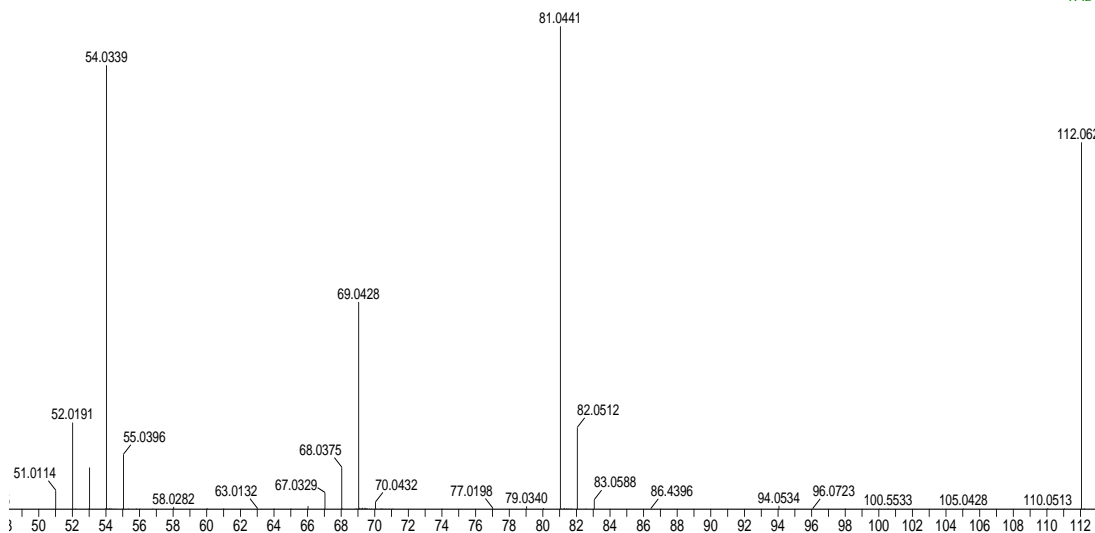


Figure 84: Mass spectrum (EI) of the peak at 6.022 minutes

A molecular ion peak is evident at 112.0621, which suggests the compound has a molecular formula of $C_5H_8N_2O$. This could correspond to the structure shown in *Figure 85*. This compound, *N*-(2-hydroxyethyl) imidazole (HEI), is also suggested as a product of MEA degradation in the literature¹⁸⁹.

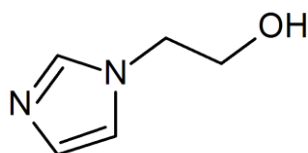


Figure 85: The proposed structure of the peak at 6.022 minutes in Figure 83.

The formation of HEI can potentially occur by the mechanism shown in *Figure 86*^{184, 186, 189}. Initially, MEA is broken down into glyoxal, formaldehyde and ammonia by the mechanism given in *Figure 79*. MEA can then react with formaldehyde and, with

the loss of water, form 2-hydroxyethylisocyanide. Alongside this, the reaction of ammonia with glyoxal forms 2-iminoacetaldehyde, after the loss of water. Cyclisation of 2-hydroxyethylisocyanide and 2-iminoacetaldehyde then affords HEI, with the loss of a proton to ammonia.

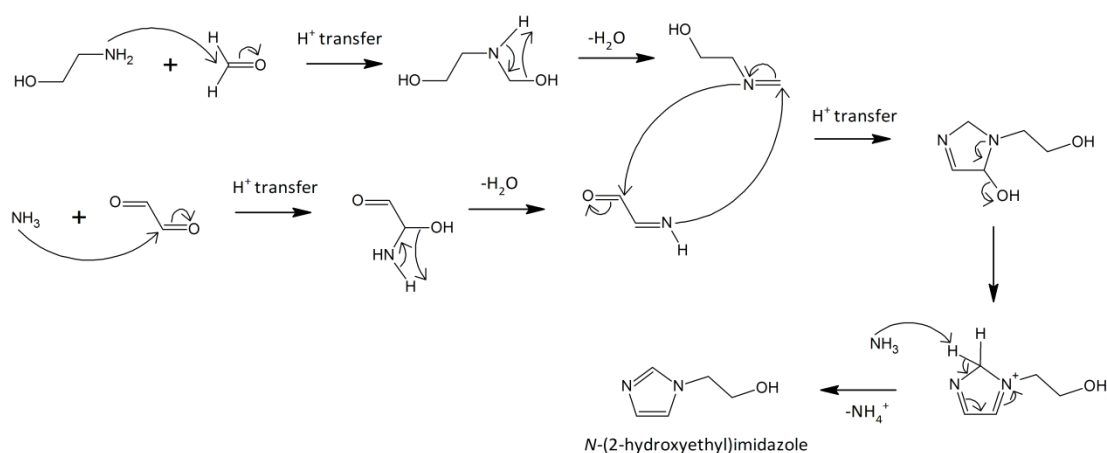


Figure 86: The possible mechanism of HEI formation^{184, 186, 189}.

HEI appears to be the major product of MEA degradation in solutions containing 400 mM MEA, 0.18 mM Cu(II) and 0.979 M H₂O₂ at pH 10 & 20 °C. Although no other products are detected by GC or GC-MS, this does not rule out the possibility of the formation of multiple products of MEA degradation.

Using GC, the extent of MEA degradation during this reaction could be estimated. The degree of degradation is shown in Figure 87. During the first 30 minutes of reaction the rate of MEA oxidation is relatively high, due to the high concentration of hydrogen peroxide, which decomposes quickly to give hydroxyl radicals. At this point, degradation levels off, possibly due to the falling concentration of hydrogen peroxide. The chromatogram also shows that the rate of HEI production increases at roughly 30 minutes. This suggests that it is possible that the remaining hydrogen peroxide is consumed during the oxidation of intermediates to form HEI, rather than oxidising more MEA. This could account for the levelling off of MEA degradation at this point.

Interestingly, *Figure 82* also shows that the absorbance due to the suspected product of MEA degradation increases rapidly at 30 minutes, suggesting this absorbance might be due to HEI. Although it appears that MEA is reformed after 30 minutes, it is likely that this effect is due to experimental error. Overall, it can be seen that approximately 25% of MEA is oxidised over the course of the reaction (a similar level of degradation to that observed in the HEDP system). This leaves a substantial amount of MEA present in solution. As a result, a significant pH drop is not evident during this reaction. The decomposition of hydrogen peroxide is therefore unlikely to be affected by the degradation of MEA.

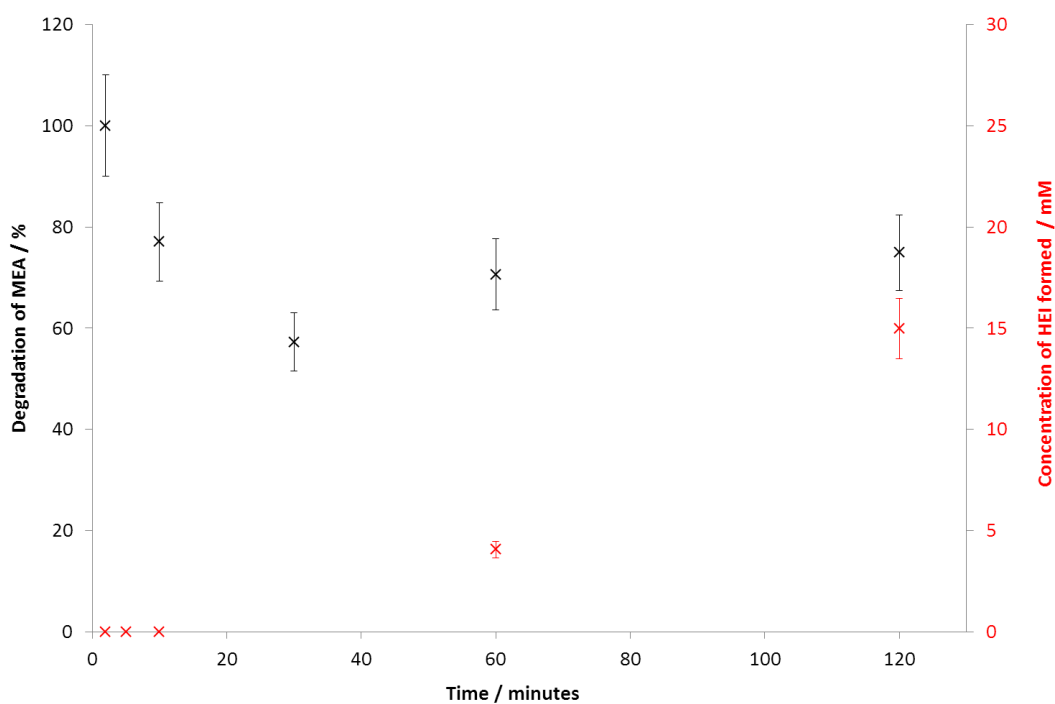


Figure 87: The rate of degradation of MEA in a solution containing 400 mM MEA, 0.18 mM Cu(II) and 0.979 M H₂O₂ at pH 10 & 20 °C.

The exact conditions of the reaction will play some role in the extent of MEA degradation that occurs and in the products that form as a result. Thus different model bleaching systems may result in the formation of different products of MEA degradation, as has been observed by this work.

The formation of HEI and formic acid in these model bleaching systems implies that radical mediated oxidation of MEA may occur, resulting in carbon-centred radicals. Such radical species are longer lived than the hydroxyl radical and may contribute to increased amounts of hair fibre damage when they are produced in bleaching formulations, as observed in a previous study⁴³.

In summary, differences in hydrogen peroxide decomposition were identified for aqueous ligand-free compositions and HEDP model bleaching compositions. The major reason for these differences has been determined to be the presence of different metal complexes in solution when the base is varied. In the ligand-free composition, this was due to the chelation of the different bases to the metal atom centre, whilst for the HEDP system it was because of a pH drop, as a result of the degradation of MEA and HEDP.

For formulations that contain ligands such as EDTA or EDDS, which are commonly used in bleaching formulations, no major differences in chemistry were found when the base was altered. This indicates that the main reason for the observed decrease in hair bleaching when MEA formulations are used is likely to be due to be the result of a physical factor, such as diffusion of hydrogen peroxide into the hair cortex. In order to confirm this, the rate of soluble melanin bleaching was directly studied in MEA solutions and the results compared with those arising from the use of solutions containing ammonia.

3.3.7 The effect of MEA on soluble melanin bleaching

Homogeneous melanin bleaching systems, containing *Sepia* MFA, were studied using UV-vis spectroscopy, in order to confirm that no chemical reasons exist for the differences observed in hair bleaching when MEA formulations are used. When pre-solubilised melanin is used, differing rates of melanin solubilisation will not affect the rate of melanin bleaching when the base is changed. By avoiding the use of hair, the rate of melanin oxidation will not be affected by varying diffusion rates of

oxidants into hair fibres, when the base is changed¹⁷⁵. Therefore, any differences in bleaching that may be observed between solutions containing MEA and those containing ammonia can be attributed to changes in chemistry. However, based on the extent of peroxide decomposition that was observed in the model systems (Page 110), HEDP and ligand-free systems are the only cases where a variation of melanin bleaching may be expected.

Using the method discussed in chapter 2, UV-vis spectroscopy was employed to monitor the decrease in the broadband absorbance due to the presence of melanin during bleaching reactions. In this way, the rates of melanin bleaching in MEA systems was observed and the results compared to data that were collected for the equivalent NH_3 systems, chapter 2.

Bleaching solutions containing 20 mM MEA, (1.3 mM ligand), 0.18 mM Cu(II) and 0.979 M H_2O_2 , at pH 10 & 20 °C were prepared. The decrease in absorbance at 532 nm indicates the rate of bleaching over the course of 2 hours at 20 °C, shown in *Figure 88*.

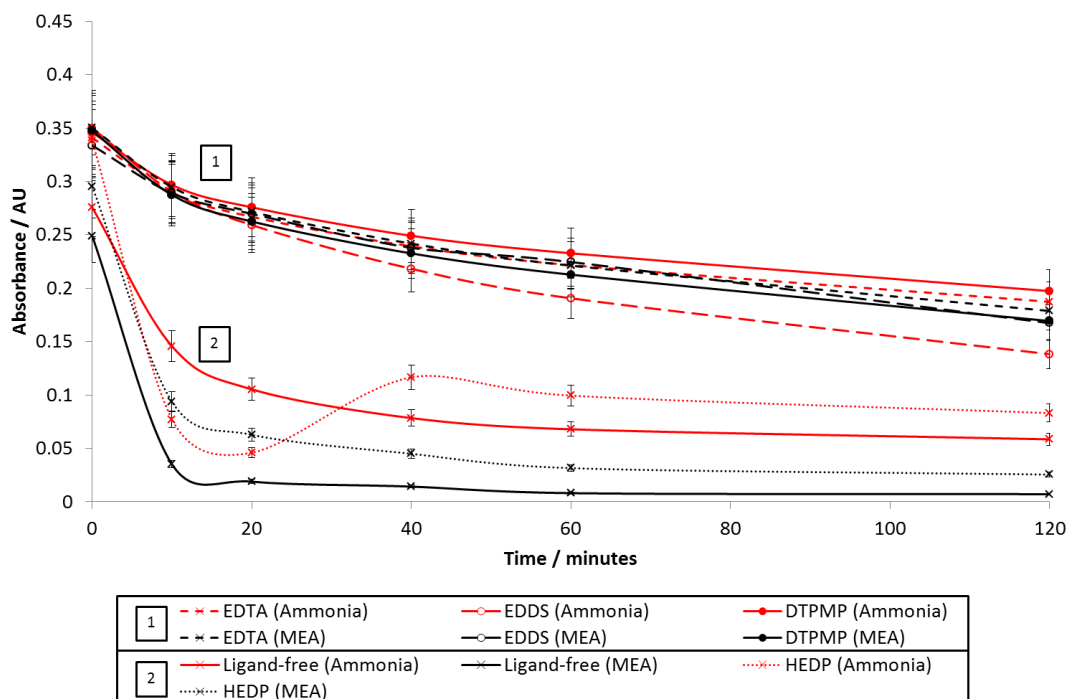


Figure 88: Graph to show the rate of melanin bleaching in the following systems: 20 mM MEA or 20 mM ammonia, (1.3 mM ligand), 0.18 mM Cu(II), 0.979 M H₂O₂ and 0.06 mg mL⁻¹ Sepia MFA at pH 10 & 20 °C.

The rates of melanin bleaching in these MEA-based formulations are comparable with those of the NH₃ compositions, which contained equivalent concentrations of reagents, shown in Figure 46. As with the ammonia-based formulations, a relatively high rate of bleaching is observed in the HEDP and in the ligand-free systems (Group 2) compared with the systems that contain strong ligands (Group 1) (See chapter 2). As expected, there is some disparity between group 2 formulations when the base is changed, due to the different rates of hydrogen peroxide decomposition in HEDP and ligand-free systems, when MEA is used. There is also no increase in absorbance after 20 minutes, in the MEA system containing HEDP. The copper nanoparticle formation, observed in the ammonia system, does not occur when MEA is used.

The EDTA, EDDS and DTPMP-containing formulations show relatively low levels of bleaching due to the lower concentration of hydroxyl radical that become available. This is explained in more detail in chapter 2. The reality that the rates of melanin

oxidation are the same in these homogeneous bleaching solutions, regardless of the base used, confirms that the differences observed in hair bleaching formulations are due to physical factors.

It is possible in heterogeneous bleaching systems that the base plays a role in disrupting hydrogen bonding within the melanin, assisting the solubilisation of melanin and allowing faster bleaching. Additionally, the base could assist with the diffusion of oxidants into the hair fibre, by changing the extent to which hair fibres swell. By changing the base, these processes could be affected and the extent of melanin bleaching that occurs could vary. A quick visual assessment of the level of bleaching in heterogeneous melanin bleaching systems could be used in attempts to identify whether or not the base affects the rate of this process.

Figure 89 shows two bleaching solutions containing 400 mM base, 2.5 mg mL⁻¹ *Sepia* melanin from cuttlefish ink & 1.63 M H₂O₂, at pH 10 & 20 °C before and after 12 hours of continuous mixing. Sample (a) contained NH₃ whilst sample (b) contained MEA. The difference in colour after 12 hours is represented by samples (c) & (d), for the ammonia and the MEA systems respectively. There appears to be no visual difference between the samples, indicating that the base does not affect the extent to which heterogeneous melanin is bleached.

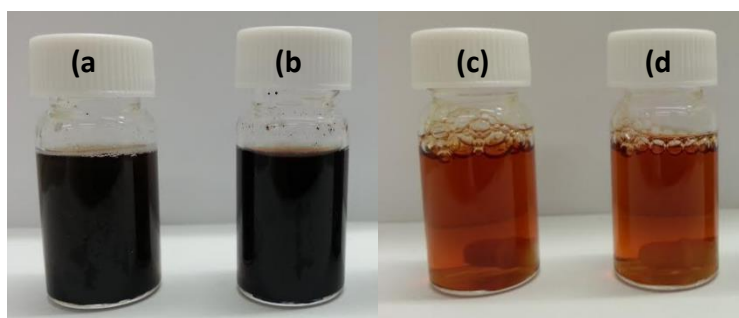


Figure 89: Heterogeneous melanin bleaching for systems containing 400 mM base, 2.5 mg mL⁻¹ Sepia melanin & 1.63 M H₂O₂ at pH 10 & 20 °C. (a) ammonia, 0 h, (b) MEA, 0 h, (c) ammonia, 12 h & (d) MEA, 12 h.

This observation suggests that on changing the base, any differences observed in melanin bleaching are more likely to be due to a change in diffusion rates of oxidants into hair fibres. This probably occurs because hair fibres are swollen to varying extents when the base is switched. However, as hair fibre swelling was not studied directly, there is a considerable possibility that other unforeseen physical factors may result in differing extents of melanin bleaching.

The results obtained from studying homogeneous model solutions show that there are no chemical reasons for the disparity observed in melanin bleaching systems, when MEA is used as a replacement for ammonia. In order to confirm that the results are applicable to real bleaching systems containing hair, hydrogen peroxide decomposition was studied for heterogeneous bleaching systems that contain pulverised hair fibres.

3.3.8 Hydrogen peroxide decomposition in solutions containing pulverised hair fibres

Hydrogen peroxide decomposition in the presence of pulverised hair fibres was studied, in order to confirm that chemical factors are not responsible for the differences observed in bleaching formulations, when the base is altered. By using pulverised hair fibres in bleaching solutions, it was thought that varying diffusion rates of hydrogen peroxide into hair fibres would not affect the rate of its decomposition to the same extent as they would for whole hair fibres. However, a more realistic bleaching environment is provided. It is evident from SEM images (not included) that cortex fibres become exposed during the process of hair pulverisation¹⁹⁰. Therefore, endogenous metal ions such as copper ions and iron ions, as well as a variety of keratinous proteins and melanin become accessible to the bulk bleaching solution. These bleaching systems therefore mimic the environment found within the hair cortex. It was of interest to see the effect of changing the base on the rate of peroxide decomposition for these compositions that were more realistic than the aqueous model formulations. It was thought that

the keratinous proteins or melanin inside the hair cortex may bind metals in some of these solutions, which may affect the chemistry of bleaching.

Initially, solutions containing 400 mM base, 1.3 mM EDTA, 2.5 mg mL⁻¹ pulverised hair and 0.979 M H₂O₂ at pH 10 & 20 °C (where the base is either MEA or NH₃), were compared to observe the effect of changing the base on peroxide decomposition. It was seen that negligible hydrogen peroxide decomposition occurred in both systems over the course of 120 minutes. This is consistent with the aqueous model systems, which also show low levels of peroxide decomposition, indicating that melanin and proteins do not compete significantly for metals in the presence of strong chelating ligands. These results confirm that peroxide decomposition is not affected in bleaching formulations containing strong ligands, such as EDTA, when the base is altered. This shows that physical factors remain the most likely causes of differences in melanin bleaching.

Decomposition of the peroxide species by pulverised hair fibres was also studied for ligand-free systems. There is a circumstantial theory that ligands cannot diffuse into hair fibres. As such it is possible that an environment similar to the ligand-free model system could exist inside the hair fibre. Therefore, it would be of interest to establish the effect of changing the base on hydrogen peroxide decomposition for such a system.

Oxygen evolution was monitored for solutions containing 400 mM base, 2.5 mg mL⁻¹ of pulverised hair fibres and 0.979 M H₂O₂ at pH 10 & 20 °C. Pulverised hair was used that contained natural levels of copper ions (13.0 ppm), as well as hair that was dosed with extra copper ions (218.1 ppm), in order to observe the effect of the copper concentration on the decomposition of peroxide species. Comparisons of the rates of decomposition in systems, where MEA and NH₃ were used as the base, are shown in *Figure 90*.

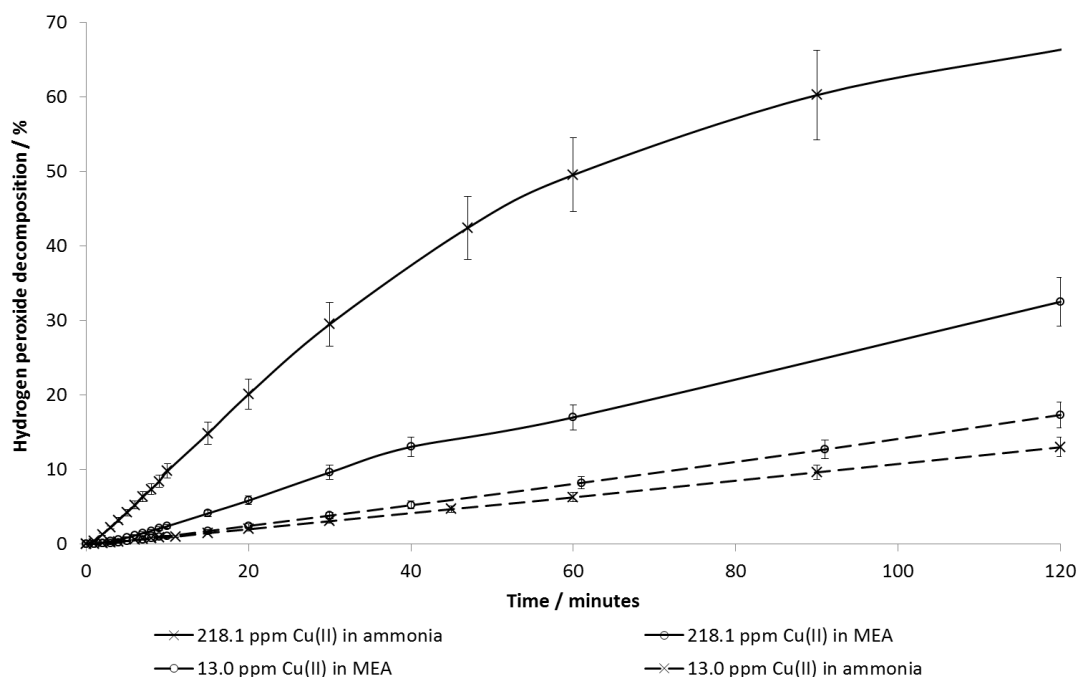


Figure 90: The effect of changing the base on hydrogen peroxide decomposition for systems containing 400 mM base, 2.5 mg mL^{-1} pulverised hair and $0.979 \text{ M H}_2\text{O}_2$ at pH 10 & $20 \text{ }^\circ\text{C}$.

For pulverised hair that was not dosed with additional copper ions, it can be seen that there is almost 10% more oxygen evolution in the MEA-based system when compared with the corresponding ammonia-based system. This does not represent the results for homogeneous model solutions, which demonstrate much greater peroxide decomposition for the ammonia-based systems. Due to the presence of keratinous proteins and melanin, which can bind metal ions in the absence of chelating ligands, it is difficult to stipulate exactly what causes the change in reactivity. It could be due to proteins within the hair binding some of the metal ions, whilst others remain bound to the base itself. This would lead to varying types and quantities of base-metal complexes in solution and could account for the differences that were observed.

When copper ion dosed pulverised hair was used, solutions that contain ammonia exhibited a greater rate of hydrogen peroxide decomposition. This is a similar

pattern to that with the homogeneous model systems (*Figure 62*) and to that with the whole hair-based compositions. Despite the greater copper ion concentration in the pulverised hair, the extent of decomposition is much less. It is also less than the amounts observed for the whole hair bleaching systems (*Figure 60*). This indicates that species in pulverised hair binds the copper ions and inhibits peroxide decomposition as a result. As discussed in chapter 2, melanin can bind metal ions. The resulting complexes affect hydrogen peroxide decomposition in varying ways, dependent on the type, concentration and oxidation state of the metal ion that is bound^{46, 158}. However, it appears from *Figure 43* that melanin-copper complexes do not inhibit the breakdown of hydrogen peroxide. They may actually accelerate the process. Keratin proteins are also potential chelants of these metals, and are more abundant in hair fibres than is melanin. Wool keratin-metal complexes have also been shown to slow down the breakdown of hydrogen peroxide¹⁹¹. This suggests that the inhibition of peroxide decomposition by pulverised hair fibres is more likely to be due to the sequestration of metals by keratin rather than by melanin. Due to the complex nature of these systems it is hard to prove this, as there may be other unforeseen factors involved.

As mentioned on page 105, pulverising hair fibres allows components within the hair, such as keratins and melanin, to become accessible to the bleaching solution. Ordinarily these components that make up the cortex are not immediately accessible to the bulk formulation. However, if the user has badly damaged hair or split ends, then the cortex is exposed to the formulation¹⁹². Thus, it was of interest to know the effect that these components have on hydrogen peroxide decomposition.

In order to confirm that one or more of these exposed components could inhibit hydrogen peroxide decomposition in bleaching systems, pulverised fibres were added to compositions containing whole hair, as well as model homogeneous solutions. A lower rate of oxygen evolution in systems containing pulverised hair would suggest that species within hair fibres could sequester redox metal ions. Therefore, to a solution containing 400 mM NH₃, 2.5 mg mL⁻¹ of whole hair fibres (13.0 ppm Cu(II)) and 0.979 M H₂O₂ at pH 10 & 20 °C, was added 1.25 mg mL⁻¹ of

pulverised hair fibres (13.0 ppm Cu(II)). The inhibition of hydrogen peroxide decomposition by pulverised hair is evident from the results shown in *Figure 91*.

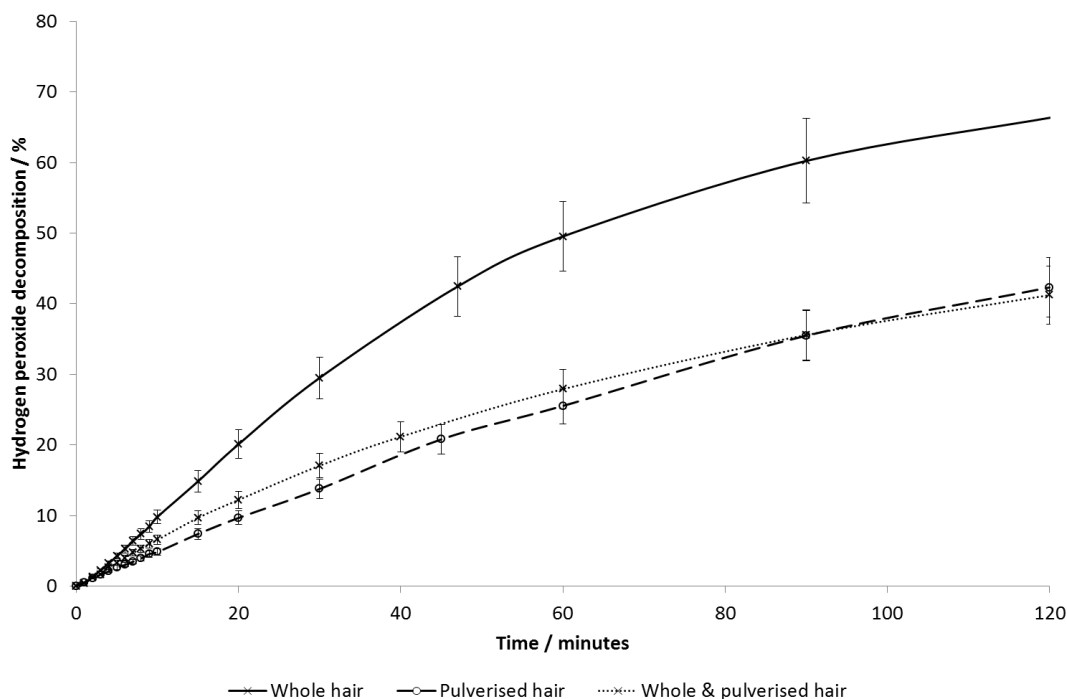


Figure 91: The effect of pulverised and whole hair fibres on hydrogen peroxide decomposition for systems containing 400 mM NH₃, 2.5 mg mL⁻¹ hair and 0.979 M H₂O₂ at pH 10 & 20 °C.

It can be seen that the rate and extent of hydrogen peroxide decomposition that was observed in whole hair bleaching systems is lowered substantially on the addition of 1.25 mg mL⁻¹ pulverised hair. In fact the rate of decomposition is identical to a system containing only 2.5 mg mL⁻¹ pulverised hair. This perhaps shows that the metal binding agent in the hair is present in excess, resulting in the formation of similar amounts of metal-complex regardless of the amount of pulverised hair used in these experiments. During 'real' hair colouring processes it is possible that if hair becomes damaged during treatment, the cortex can become exposed to the bleaching formulation. Thus, further hydrogen peroxide decomposition would be prevented, in a similar manner to the inhibition by

pulverised hair shown in *Figure 91*. In this way the hair would effectively prevent further damage to itself. However, this factor is outweighed by the fact that effective commercial formulations contain ligands that bind to any metal ions in the first instance, preventing hydrogen peroxide decomposition and thus hair fibre damage.

Furthermore, the inhibition of peroxide decomposition by pulverised hair is evident from the data in *Figure 92*. The addition of 2.5 mg mL^{-1} pulverised hair (13.0 ppm Cu(II)) to a solution containing 400 mM NH_3 , 0.02 mM Cu(II) and $0.979 \text{ M H}_2\text{O}_2$ at pH 10 & $20 \text{ }^\circ\text{C}$ results in a much lower rate of peroxide decomposition when compared with the equivalent system without the addition of any hair. A lower concentration of copper ions had to be used for this set of experiments, as the rate of peroxide decomposition is too fast in these ligand-free systems to obtain reliable results when a 0.18 mM copper ions solution was used.

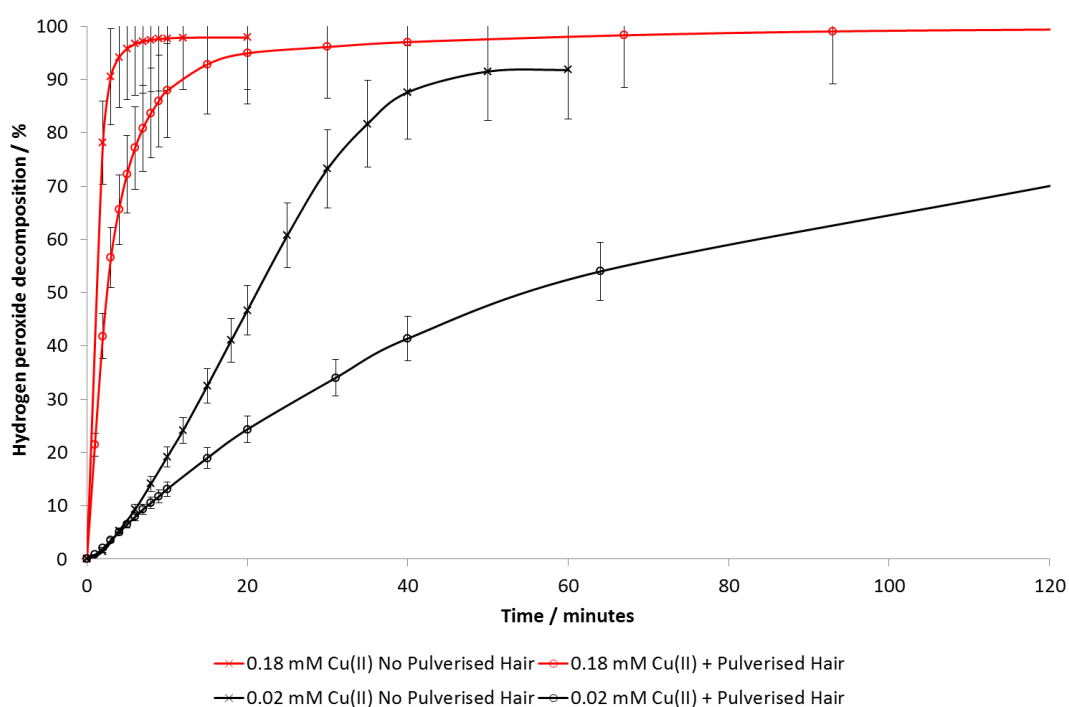


Figure 92: The effect of pulverised hair on the decomposition of hydrogen peroxide for systems containing 400 mM NH_3 , (n) mM Cu(II) , $0.979 \text{ M H}_2\text{O}_2$ and (2.5 mg mL^{-1} pulverised hair) at pH 10 & $20 \text{ }^\circ\text{C}$.

These results show that the extent of peroxide decomposition is generally lower for pulverised hair systems than for the equivalent homogeneous compositions and whole hair systems. This could be due to accessible keratinous proteins sequestering the redox active metal ions. For whole hair fibres, these proteins are trapped within the cortex of the fibre and so do not effect decomposition to the same extent.

For the ligand-free systems, differences were observed in peroxide decomposition when the base was changed from ammonia to MEA. This could again be due to the binding of metal ions by keratin. However, when EDTA was used there was found to be negligible peroxide decomposition, regardless of the base that was used. As most commercial hair bleaching formulations contain ligands such as EDTA, the latter experiment seems to confirm that any major differences in hair damage or melanin bleaching are not caused by changes in chemistry, for the conditions studied. However, as discussed in chapter 1, a wide range of conditions are used for different hair treatments. The temperature of colouring processes and the concentrations of the reagents are all variable. This could result in situations where the chemistry changes.

3.4 Conclusions

The aim of the research that is represented in this chapter was to establish reasons for the observed differences in hair bleaching systems, when MEA was used as a base in formulations as a replacement for ammonia. This was investigated primarily by measuring the extent of hydrogen peroxide decomposition and of hydroxyl radical production during the bleaching of whole and pulverised hair fibres, as well as for aqueous model systems.

During the bleaching of whole hair fibres, the peroxide decomposition was found to be greater in MEA systems, if the hair contained natural amounts of copper ions. However, when the hair fibres are treated with extra copper ions, it is in the ammonia-based formulations that more hydrogen peroxide decomposition occurs. This led to the investigation of model aqueous compositions to help in explaining why this was the case.

Hydrogen peroxide decomposition and hydroxyl radical production were monitored for various controlled homogeneous model bleaching solutions. Differences were observed for the ligand-free compositions and for the HEDP formulations. This was mainly due to the presence of different metal complexes in solution when the base was changed. For the 20 mM MEA system, which contained HEDP, a pH drop was responsible for the presence of different types of metal complex. This pH drop resulted from both HEDP degradation to form phosphate ions and MEA degradation to form acidic products. There was some evidence to suggest that formic acid is one of the major acids that is produced as a result of MEA degradation under these conditions.

MEA degradation was also observed when the conditions were changed to those of 400 mM MEA, ligand-free compositions. The main product of degradation in this case was thought to be HEI. However, the conditions of the reaction probably play a role in the final product(s) of MEA degradation, as it has been seen that the MEA : oxygen ratio determines which products of degradation form¹⁸⁵. Therefore, if solutions contain chelating ligands, which inhibit the decomposition of hydrogen

peroxide, the formation of different products is possible. Different colouring formulations contain different concentrations of base, depending on their intended use. This will also affect the MEA : oxygen ratio and thus the types of degradation product that are observed. Different degradation products may also form depending on the temperature of the treatment. During this study the temperature was kept constant at 20 °C. However, in the salon where higher temperatures are used, the products of MEA degradation may vary. It is also worth noting that during the investigations in this thesis, compositions were stirred constantly during reactions. This is not a representation of the hair colouring process, where solutions cannot be mixed thoroughly on the scalp. This fact, coupled with the diffusion of hydrogen peroxide into hair fibres, will result in varying concentrations of hydrogen peroxide throughout the hair fibre. Thus, there is the potential for a wide variety of MEA degradation products to form during salon treatments.

Formic acid has been shown to cause foaming in air-sparged solutions containing amines¹⁹³. Therefore, the degradation of MEA to produce formic acid may explain why foaming is observed in formulations that contain MEA. Foam is defined as a liquid phase that has a gas dispersed throughout it. Foaming is a physical factor dependent on the surface tension of the liquid-vapour interface. Therefore, the extent of foaming that occurs is dependent on the temperature of compositions and the concentration of MEA in the formulation. Anti-foaming agents, such as silicone polymers, can be used in formulations where excessive foaming is observed¹⁹⁴.

The suggested mechanism of MEA degradation, to form formic acid and HEI, involves the formation of carbon centred radicals, which would react with the proteins in hair fibres and lead to damage in MEA systems.

Despite the differences observed in ligand-free formulations and HEDP compositions, when the base was changed, peroxide decomposition did not vary when ligands such as EDTA or EDDS were used. The model formulations that contained these ligands are more representative of commercial bleaching formulations, as the concentrations of the base, ligand, metal ions and hydrogen

peroxide were chosen to mimic the conditions used to colour hair. As the temperature studied was 20 °C these compositions would be more comparable to home use colouring kits than salon treatments, where higher temperatures are often used to accelerate the colouring process. It should also be noted that the mixing of these model compositions was much more thorough than can be achieved by formulations that are applied to the scalp. Nevertheless, it can be inferred from the data in this chapter that differences observed in melanin bleaching, when the base is changed in commercial formulations, are unlikely to be due to any chemical factors that result in a change to the extent of hydrogen peroxide decomposition that occurs. Alternative causes for these differences that could be investigated are physical phenomena, such as changes to the extent of hair swelling and melanin solubilisation.

Homogeneous melanin bleaching formulations were studied and similar levels of bleaching were observed regardless of the base used. This confirmed the observations drawn from the majority of aqueous model systems, where peroxide decomposition is unchanged on altering the base. Solubilisation of heterogeneous melanin is usually a prerequisite for bleaching to occur at a higher rate. Replacing ammonia with MEA does not appear to affect this process, based on the visual appearance of heterogeneous melanin bleaching formulations (although more quantitative data is needed to confirm this). This suggests that varying rates of hydrogen peroxide diffusion into hair fibres are the main cause of differing bleaching extents when MEA is used in formulations. Access is likely to be affected by changes to the extent of hair fibre swelling, when the base is altered. This would lead to varying concentrations of hydrogen peroxide present in the cortex. Thus, the rate or extent of bleaching that occurs over comparable time periods would be affected.

A similar trend to the whole hair systems was evident when the effect of pulverised hair on hydrogen peroxide decomposition was studied for ligand-free systems. When hair contains copper atom amounts that are equivalent to the levels typically found in Asian countries, such as Japan (13.0 ppm samples)¹⁷⁶, solutions that contain MEA exhibit more peroxide decomposition than ammonia systems.

However, when the copper atom amount is increased to levels that are more representative of the Americas (218.1 ppm)¹⁷⁶, it is the ammonia-based compositions that result in more peroxide decomposition. This could be due to the formation of more copper-ammonia complexes at greater copper ion concentrations. These copper-ammonia complexes have been shown to be more effective at decomposing hydrogen peroxide than MEA complexes. Pulverised hairs have been shown to decrease the rate of peroxide decomposition, when compared with whole hair fibres or homogenous systems. When hair is pulverised, melanin and a variety of keratinous proteins become accessible to metal ions in the bleaching solutions, which can potentially bind redox metals. The possible formation of keratin-metal complexes could explain the observed behaviour, as it can be seen from the literature that these complexes can inhibit hydrogen peroxide decomposition¹⁹¹. These whole hair compositions and pulverised hair compositions are similar to commercial formulations in terms of the concentrations of base, metal ions and hydrogen peroxide used. However, differences in hydrogen peroxide decomposition were only evident for ligand-free formulations when the base was changed. Therefore, the differences that were observed above will not necessarily be observed in commercial formulations.

The extent to which metal atoms bind to keratin is controlled by various factors and can be determined approximately. However any remaining metal ions that are not bound to keratin or melanin are free to form complexes with the base. The convoluted nature of metal atom binding in hair fibres could explain the differences observed in peroxide decomposition when the base is varied. However, for pulverised hair bleaching formulations that contain EDTA, negligible peroxide decomposition was observed in both MEA-based formulations and NH₃-based formulations. This again suggests that the differences in melanin bleaching, observed when MEA formulations are used, are initially due to physical factors, such as lower rates of oxidant diffusion into hair fibres, as a result of less hair fibre swelling. This change in diffusion would result in varying concentrations of hydrogen peroxide in the hair cortex, leading to a chemical reason for the change in the extent of bleaching that is observed.

Chapter 4

Chapter 4 – The Mechanism of Hair Dye Primary Oxidation in Hair Fibres

4.1 Introduction

4.1.1 The mechanism of hair dye formation

The formation of dimeric and trimeric indamine dyes or indophenol dyes is the main reaction associated with the production of permanent hair dyes on human hair. It is known that the formation of such dyes is initially triggered by the oxidation of aromatic amines, such as *p*-phenylenediamine, to form reactive imine intermediates in the rate-determining step, as shown in *Figure 93*^{3, 195, 196}:

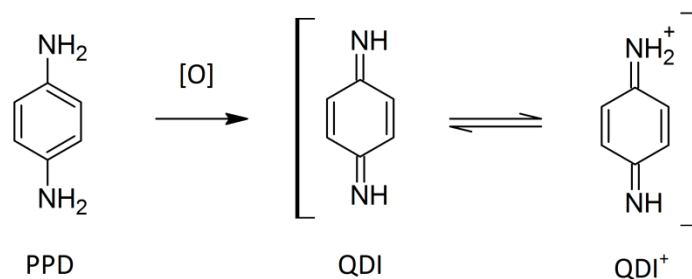


Figure 93: Oxidation of the aromatic amine PPD to QDI

This oxidation can occur in the presence of either redox active metal ions or redox active organic compounds^{197, 198}, as well as O₂ that comes into contact with such aromatic amines¹⁹⁹. The imine generated may then be subject to protonation although, as the conjugate acid (QDI⁺) has a pK_a of 5.75, the proportion present at the alkaline pH required for hair colouring is in the minority³. This step is followed by rapid coupling to specific meta- substituted aromatics, such as 3-aminophenol or 4-amino-2-hydroxytoluene. Further oxidation to generate indophenol or indamine

dye molecules that are responsible for the colour may then occur, as shown in the mechanism in *Figure 94*^{3, 196}:

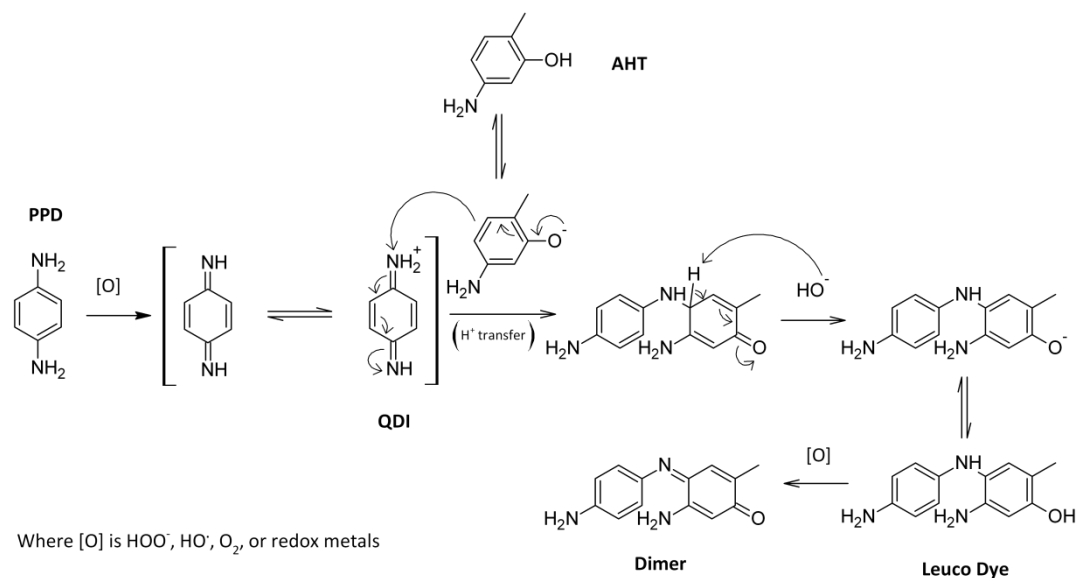


Figure 94: Mechanism to show the coupling of AHT to QDI to form indamine dye molecules

4.1.2 The chemistry behind the formation of dyes during hair colouring

For the application of permanent hair dyes, the oxidation of precursors in the dyeing solution is initially a problem due to large quantities of metal ions such as Cu(II) and Fe(III) that are present in water used to wash hair^{47, 200}. The metal ions bind to the surface of the hair and can catalyse the formation of hair dyes, outside the fibre. This is undesirable for the use as permanent hair dyes, as dyes that form outside hair fibres are easily washed out and the chosen colour will not be retained. In order to prevent the premature oxidation of precursors, ligands such as EDTA can be used⁵⁰. This effectively alters the redox potential of the metal atom centre and prevents metal-catalysed hydrogen peroxide decomposition and the initial oxidation of the aromatic amine from occurring before it has diffused into the hair fibre²⁰¹.

One theory is that the charge density on ligands such as EDTA is too high for them to diffuse into the hair fibres, while the dye precursors themselves are able to diffuse into the cortex of the fibre (*Figure 2*). It is here where the precursors can be oxidised by endogeneous metal ions^{47, 202} or potentially by redox active organic molecules within the hair fibre, to form permanent dye molecules inside the hair that cannot be washed or rinsed out in normal washing procedures.

Multiple literature citations suggest that it is the alkaline hydrogen peroxide that is responsible for the oxidation of dye precursors within the hair fibre^{4, 122, 203}. Alternatively, Corbett suggests that molecular oxygen, formed during the decomposition of hydrogen peroxide within the hair fibre, could be responsible for precursor oxidation^{3, 196}. However, it remains unclear what exactly is responsible for dye formation inside hair. Whilst working with aqueous dye formulations, it became apparent that the enzyme catalase might have a role to play in dye formation.

4.2 The effect of catalase on dye reagent coupling in aqueous systems to form dyes

Chapter 5 of this thesis describes the quantification of dye molecules formed in aqueous solutions by HPLC. To achieve this, samples were taken at time points during dye formation. As the HPLC analysis takes a substantial amount of time, it was thought to be desirable to prevent further dye formation or degradation once these samples have been taken. Catalase was used consistently throughout this project in order to decompose remaining hydrogen peroxide at the end point of Fenton and Fenton-like reactions. By decomposing the hydrogen peroxide it was thought that the main oxidant responsible for subsequent dye formation could be removed and the reaction may stop. This would enable the quantification of dye molecules at multiple time points throughout the reaction^{122, 203}.

Surprisingly, it was discovered on the addition of 0.1 mL of bovine liver catalase (20 – 50 mg mL⁻¹) (see chapter 7) to an aqueous system containing 400 mM NH₃, 1.3 mM EDDS, 0.18 mM Cu(II), 70 mM H₂O₂, 1 mM PAP and 1 mM AHT at pH 10 and 20 °C, that dye coupling was significantly accelerated. This is evident from *Figure 95*, for which PAP-AHT coupling was monitored at 550 nm by UV-vis spectroscopy. Upon addition of catalase at a reaction time of 30 minutes, a sharp increase in absorbance, due to increased dye formation, is apparent.

The base, EDDS and Cu(II) concentrations that were used throughout the study provided a comparable system to commercial formulations, for observing dye formation. However, the concentration of hydrogen peroxide and dye precursors is substantially lower as this provided a composition where the rate of reaction was not too fast to follow. Dyes were also not subject to an excessive amount of degradation by reactive oxygen species under these conditions. The reactions were controlled at a temperature of 20 °C, which is lower than the temperature used in dyeing procedures, due to the heat of the scalp. Therefore, the rates of dye formation were expected to be lower than for commercial formulations. However, the rates of formation could be accurately compared when the base was changed.

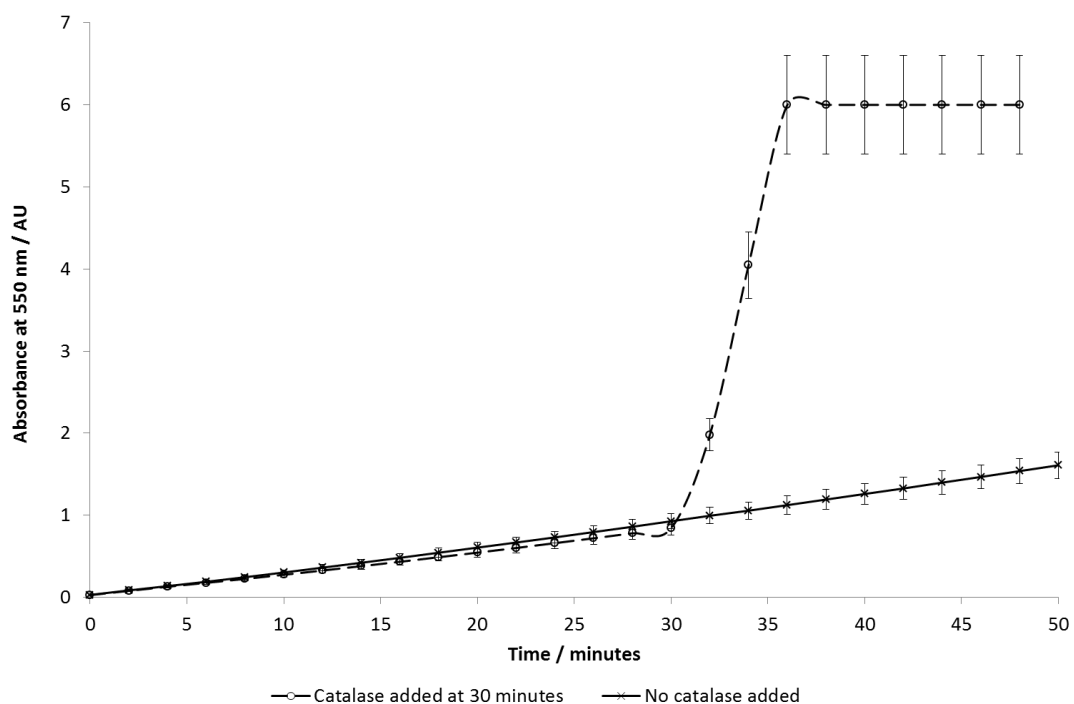


Figure 95: Graph to show the increase in dye coupling on addition of 0.1 mL catalase to the following composition: 400 mM NH_3 , 1.3 mM EDDS, 0.18 mM Cu(II) , 70 mM H_2O_2 , 1 mM PAP and 1 mM AHT at pH 10 and 20 °C.

When catalase was added to the aqueous dye bath at 30 minutes, the absorbance due to the dye produced increased almost instantaneously, due to increased oxidative dye coupling.

Catalase, which is also present in hair follicles²⁰⁴, is known for catalysing the oxidation of aromatic amines and phenols to the reactive intermediates, required for the formation of dye molecules²⁰⁵. The active sites of catalase consist of four porphyrin heme groups (Figure 96). Experimental evidence has shown that these iron atom centres are responsible for the oxidation of aromatics. Even when the enzyme is denatured, the oxidative activity of these centres on substrates remains²⁰⁵. This could be the reason for increased dye formation in the model formulations when catalase was added. However, this needed verifying (see page 164).

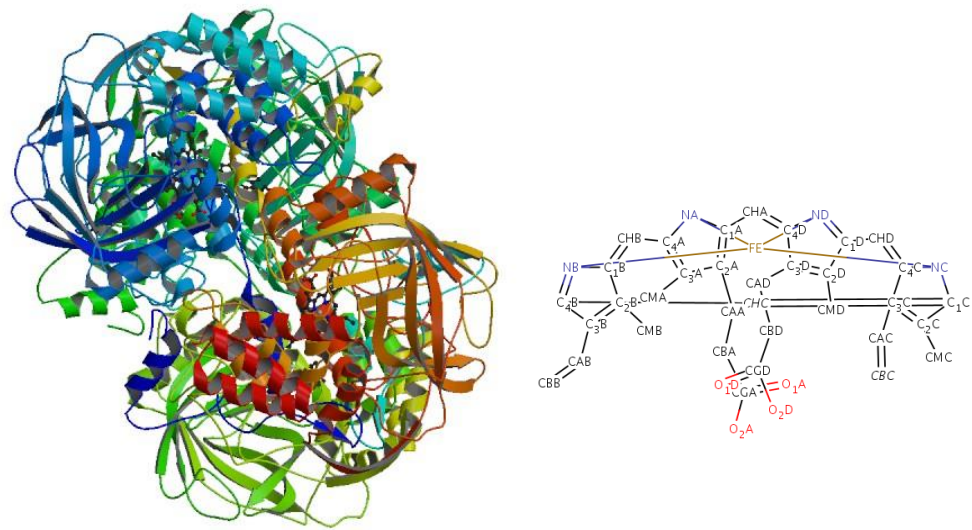


Figure 96: (Above left) the structure of human erythrocyte catalase (The four porphyrin heme groups are shown in blue). (Above right) the structure of each heme group^{206, 207}.

Catalase is thought to be present in the hair follicles to decompose any hydrogen peroxide that accumulates, via a non-radical pathway. This prevents free-radical mediated damage of melanocytes, which are responsible for producing the melanin that is found in hair fibres. It is thought that the presence of catalase in hair follicles could therefore be responsible for the prevention of hair greying.

4.3 Aims

Rapid dye precursor oxidation was observed directly in several aqueous dye systems containing catalase. This led to the investigation of what causes dye formation within hair fibres.

In order to probe the main species that is responsible for the oxidative dye formation in hair fibres, several areas were investigated. Firstly, the dye production in aqueous solutions was monitored in the presence of both pulverised hair and whole hair fibres. By using pulverised hair, diffusion of hair dye precursors into the hair fibre is no longer a factor. As a result, components within the hair fibre are more immediately accessible to the aqueous dye bath. The effect of oxidants on dye formation, within hair fibres, can thus be directly compared to the effect of oxidants that are accessible on the surface of whole hair fibres.

There are many possible potential oxidants of dyes within hair fibres, including redox active organic molecules, such as melanin¹⁹⁸, and redox metals. It was thought that the extent to which metals contribute to dye formation in hair fibres could be investigated. This could be done by comparing any differences in the rate of dye coupling for systems that contained demetallated hair and untreated hair. By treating pulverised hair with excess EDTA, the majority of endogenous metals should be removed. The effect that demetallated hair fibres have on dye coupling in aqueous solutions could then be investigated.

Finally, it was thought that if metal ions were found to be responsible, even if only in part, for dye formation in the hair, the effect of specific metal ions on primary oxidation could be investigated. It is known that Cu(II) and Fe(III) are the more abundant redox metal ions within the hair fibre. If pulverised hair samples were to be dosed with either of these metal ions, then the effects they have on dye coupling in aqueous systems could be compared.

4.4 Results & Discussion

4.4.1 The mechanism of dye formation by catalase

Several dyeing experiments were performed to establish why the addition of bovine liver catalase to aqueous dye baths causes such a dramatic increase in dye coupling. The general conditions used were 400 mM base, 1.3 mM EDDS, 0.18 mM Cu(II), 70 mM H₂O₂, 1 mM primary and 1 mM coupler, at pH 10 and 20 °C. The formation of dye was monitored using UV-vis spectroscopy, at a wavelength of 550 nm. 0.1 mL of bovine liver catalase (20 – 50 mg mL⁻¹) was then added at a reaction time of 30 minutes. The increase in dye formation in each of the compositions can be observed in *Figure 97*.

Each time, the base, coupler or primary was varied, whilst keeping their concentrations constant. The effects of altering these are shown in *Figure 97*. It was hoped that this approach would yield further information concerning the cause of rapid dye formation in the presence of catalase.

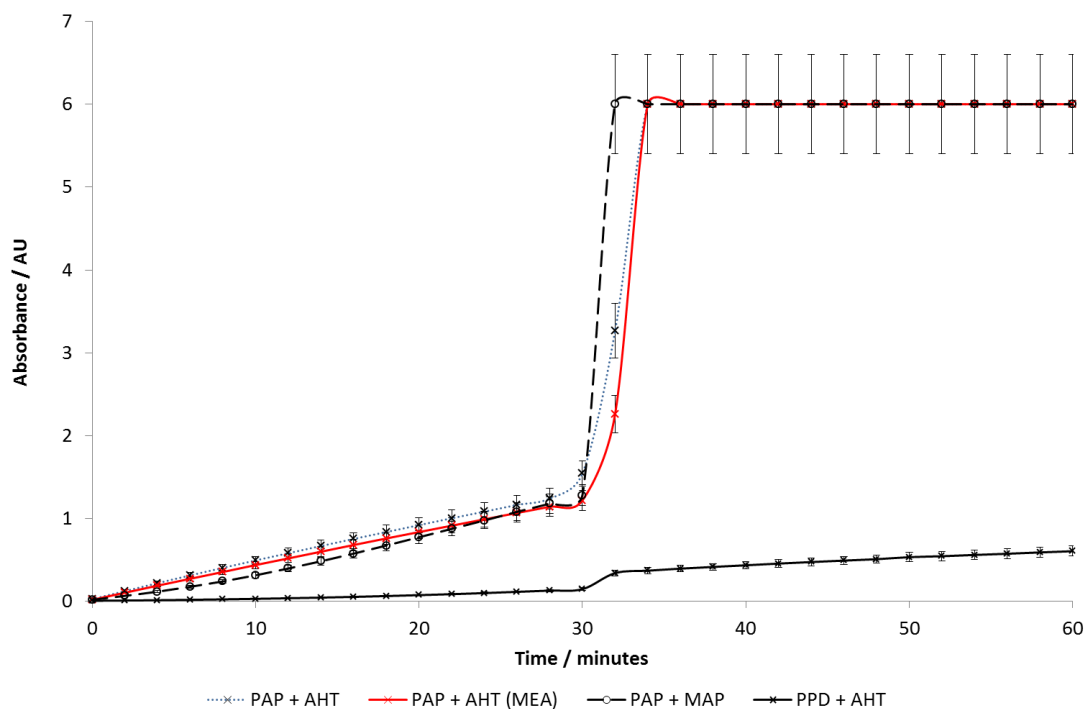


Figure 97: Graph to show the increase in dye reagent coupling on addition of 0.1 mL catalase to the following system: 400 mM base, 1.3 mM EDDS, 0.18 mM Cu(II), 70 mM H₂O₂, 1 mM primary and 1 mM coupler at pH 10 & 20 °C

Change of base

By changing the base from NH₃ to MEA, there was no significant change in the kinetics of dye coupling, showing that the same chemistry occurred regardless of which of these bases is used.

Change of coupler

When the coupler was changed from AHT to MAP, the kinetics of dye coupling were not altered significantly. This shows that the initial oxidation of primary is probably the step that is affected by the presence of catalase.

Change of primary

On changing the primary from PAP to PPD the kinetics of dye formation appeared to change substantially.

Initially, in the first 30 minutes of the reaction before catalase addition, dye formation is much slower than the equivalent PAP system. This may be because the oxidation of PPD to QDI is much slower than in the oxidation of PAP to quinone monoimine^{3, 208, 209}. However, it is worth noting that the molar absorbance coefficients of the dyes that are formed will be different when the primaries are changed. This will affect the intensity of the colour formed when different dye systems are studied.

Catalase addition does not appear to affect the rate of dye coupling in the PPD system as much as the PAP system. This has also been observed by Job and Dunford²¹⁰ who report that, for compounds with the same substituents, the rate of aromatic amine oxidation by peroxidase is lower than it is with phenol oxidation. The peroxidase activity by catalase was confirmed by removal of hydrogen peroxide from the dye bath. The effect of catalase on primary oxidation under these conditions is shown in *Figure 98*.

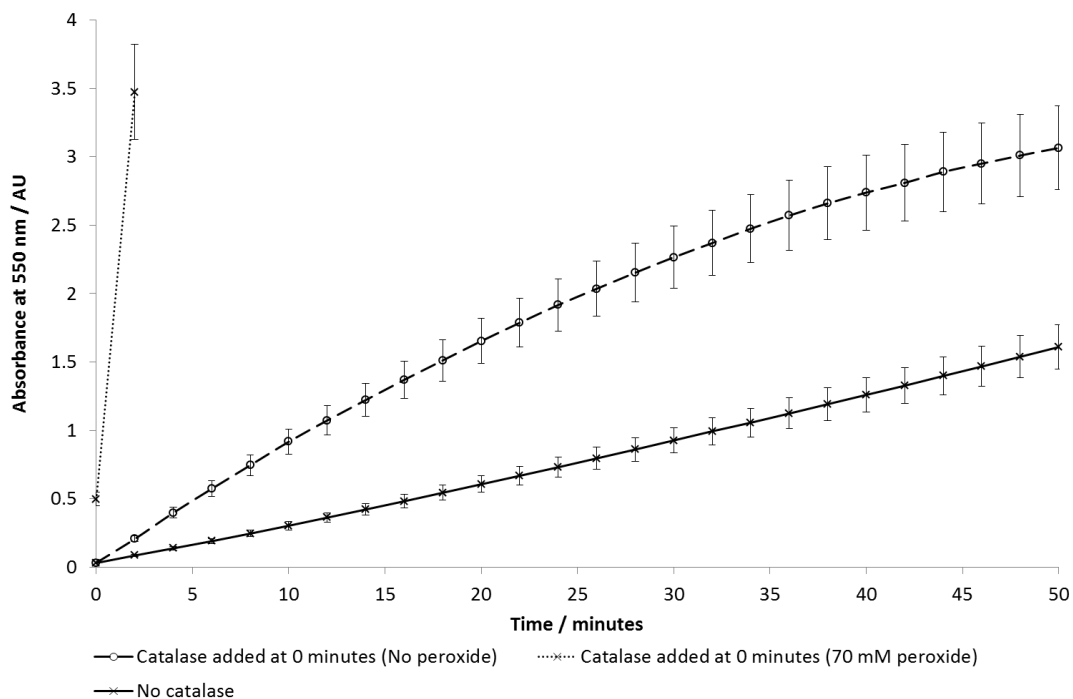
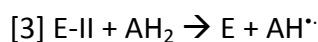
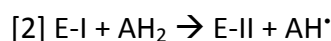
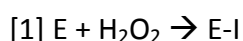


Figure 98: Graph to show the effect of 0.1 mL catalase on the coupling of PAP-AHT, with and without the hydrogen peroxide in the following system: 400 mM NH_3 , 1.3 mM EDDS, 0.18 mM Cu(II) , 0.07 M H_2O_2 , 1 mM PAP and 1 mM AHT at pH 10 & 20 °C.

On addition of catalase to a system containing no H_2O_2 , catalase causes a greater rate of oxidative dye coupling compared to the system, which contains H_2O_2 and no catalase. Presumably, this means that the heme centres in the catalase may contribute in some manner to oxidation of the primary.

Furthermore, it is apparent that when H_2O_2 is introduced to the system containing catalase, the rate of oxidation of PAP is much greater than for the system containing no H_2O_2 , indicating a reliance on the hydrogen peroxide. This suggests the mechanism of peroxidase activity by catalase is consistent with the work of Job and Dunford²¹⁰:



Here, E is the enzyme, E-I and E-II are different enzymatic intermediates, AH₂ is the aromatic substrate and AH[•] is the aromatic radical.

Keilin and Hartree also report this peroxidase activity by catalase²¹¹. It is therefore evident that this could be the dominant mechanism by which catalase oxidises primary intermediates.

The change in kinetics on changing the dye primary suggests that catalase is responsible for dye primary oxidation. The rate-determining step of the oxidative coupling is thus accelerated significantly and the rate of dye formation increases, as assessed by UV-vis spectroscopy.

Having confirmed that catalase accelerates dye formation in aqueous solutions, it was decided to investigate whether or not a similar process could occur inside hair fibres, due to the presence of catalase. It is known that human hair catalyses the formation of hair dyes via the oxidation of precursors, such as *p*-phenylenediamine, within the fibre, but it is not known exactly what is responsible for this dye formation. With this in mind, an investigation of several aspects of dye formation inside hair fibres was undertaken.

4.4.2 Comparison of whole hair and pulverised hair

Since it was hypothesised that catalase might be responsible for the oxidation of the primary component in the hair, a decision was taken to first observe the effect that pulverised hair would have on dye formation. By using pulverised hair, potential oxidants, which are present inside the hair fibre, are more immediately accessible to the oxidation of dye precursors. Their effect on dye formation can be monitored and compared to oxidants that are present on the surface of whole hair fibres.

An aqueous dye bath containing 400 mM NH₃, 1.3 mM EDDS, 0.18 mM Cu(II), 70 mM H₂O₂, 1 mM PAP and 1 mM AHT at pH 10 & 20 °C was set up and the reaction was monitored by UV-vis spectroscopy at 550 nm. At a reaction time of 25 minutes,

either pulverised or whole hair fibres were added to the dye bath for 1 minute. The solution was then centrifuged and the kinetics of dye formation in the supernatant solution was further studied by UV-vis. The results are shown in *Figure 99*.

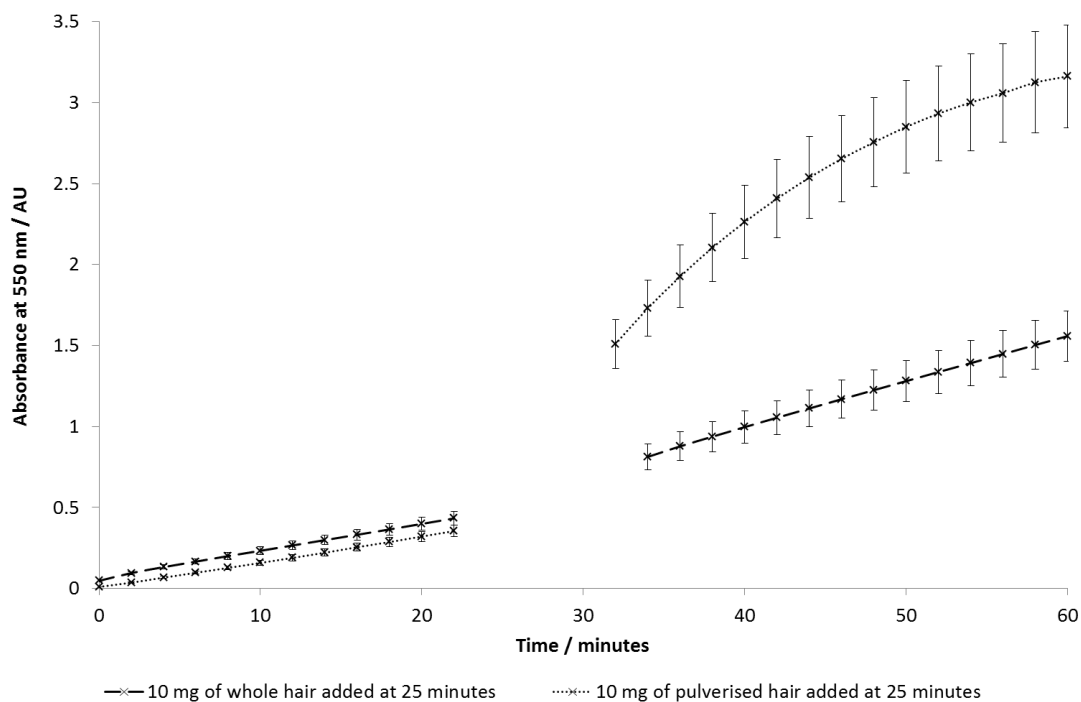


Figure 99: Graph to show the effect of adding pulverised hair or whole hair to an aqueous system containing 400 mM NH_3 , 1.3 mM EDDS, 0.18 mM Cu(II) , 70 mM H_2O_2 , 1 mM PAP and 1 mM AHT at pH 10 & 20 °C.

It is evident that the addition of pulverised hair to dye systems increases the rate of dye formation substantially, when compared to behaviour involving whole hair fibres. This may be due to the increased rate of primary oxidation, by an oxidant within the hair. Furthermore, pulverised hair is shown to be capable of accelerating dye formation in an aqueous dye bath that contains the ligand EDDS. This shows that the oxidant is potentially a strongly bound metal ion within the hair, or a redox active organic molecule, such as melanin.

More evidence was needed in attempts to confirm the identity of the oxidant responsible for this increased coupling. It was therefore decided to determine whether or not the oxidation of dyes within the hair fibre is due to metal atom centres or alternative oxidants, such as redox active organic molecules.

4.4.3 Dye precursor oxidation within hair fibres

Currently it is not clear what is responsible for the increased dye formation inside hair fibres. Bandrowski and Erdmann first observed oxidation of PPD in alkaline solutions^{212, 213}. It is also known that dye precursors in aqueous solution are oxidised by molecular oxygen^{199, 214}. The majority of the existing literature on dye formation in hair refers to both hydrogen peroxide and a base, such as ammonia, as being the cause of primary oxidation inside hair fibres^{50, 105, 215}.

However, these reasons would not explain why there is a large change in the kinetics of dye formation in aqueous systems on the addition of pulverised hair fibres, as shown in *Figure 99*. These data imply that an oxidant inside the fibre is likely to be responsible for the change in the kinetics. Redox-active organic molecules or a species with a metal atom centre are the more likely oxidation sources, as discussed below.

Melanin

It is possible that melanin, found within the cortex of the hair fibre plays a role in the oxidation of dye precursors, such as PPD. Melanin can exhibit redox behaviour^{197, 198} due to the reversible oxidation of dihydroxyindole units to the corresponding *o*-quinone (*Figure 31*). The conversion of these units is directly affected by the presence of metal cations, such as Fe(III).

When redox active metal ions bind to melanin^{155, 156, 164, 167, 216, 217} their redox potential is altered and the decomposition of hydrogen peroxide is affected as a

result. However, this event is highly dependent on the concentration and type of metal cation. Additionally, if iron atoms are bound to melanin, the oxidation state of the metal centre becomes an important factor, as discussed in chapter 2.

Different types of melanin have also been shown to exhibit different behaviour with regards to redox chemistry. For instance, pheomelanin has proven to be a pro-oxidant, capable of oxidising the very precursors from which it is synthesised³¹, whereas eumelanin has been shown to inhibit the formation of radical oxidants³².

The effect that melanin could have on hair dye formation is complicated and depends on metal atom concentrations and on the types of melanin that are present in the hair fibre, which varies from one person to another. Ultimately factors such as geography and ethnicity mean that this factor could vary considerably across the globe.

Keratin

There are multiple types of keratin protein present in human hair that are thought to bind to redox metal ions, primarily through their carboxylate groups²¹⁸. The presence of metal ions and hydrogen peroxide could also result in oxidation of cysteine residues of keratin, to form sulfonic acids, which would also have an affinity for metal ions^{50, 219}. The resulting keratin-metal atom complexes could be responsible for initial precursor oxidation. However, more likely, they effectively sequester metal ions and inhibit dye formation¹⁹¹.

Metal ion centres

Redox-active metal ions are also present in hair fibres. These can potentially lead to the oxidation of hair dye primaries. It is possible that the metal ions can either oxidise the primary species directly or can result in the catalytic decomposition of hydrogen peroxide to form radical species that may also be capable of oxidising the primary species⁴⁷.

4.4.4 EDTA treatment of pulverised hair

Firstly, it was decided to narrow down the list of potential oxidants within hair fibres to metal atom centres. In order to try and determine the effect that metal atoms have on the oxidation of dye primaries, it was decided to remove any metal centres from the pulverised hair, using a strong chelant. The effect of this treated hair on dye formation could then provide information concerning the importance of metal ions in catalysing dye production inside the hair fibre.

Pulverised hair was treated 3 times with 50 mM EDTA over a period of 48 hours. The hair was then rinsed extensively with deionised water to remove any excess EDTA. The pulverised hair was analysed using inductively coupled plasma mass spectrometry (ICP-MS) to determine the amount of metal ions that were removed from the hair. Approximately 40% of copper ions were removed. However, reliable data for the amount of iron ions that remained could not be obtained.

A dye bath was set up that contained 400 mM NH_3 , 1.3 mM EDDS, 0.18 mM Cu(II), 70 mM H_2O_2 , 1 mM PAP and 1 mM AHT at pH 10 & 20 °C. At a reaction time of 30 minutes, the rinsed pulverised hair was added and the kinetics of dye formation were monitored at 550 nm. The result is shown in *Figure 100*.

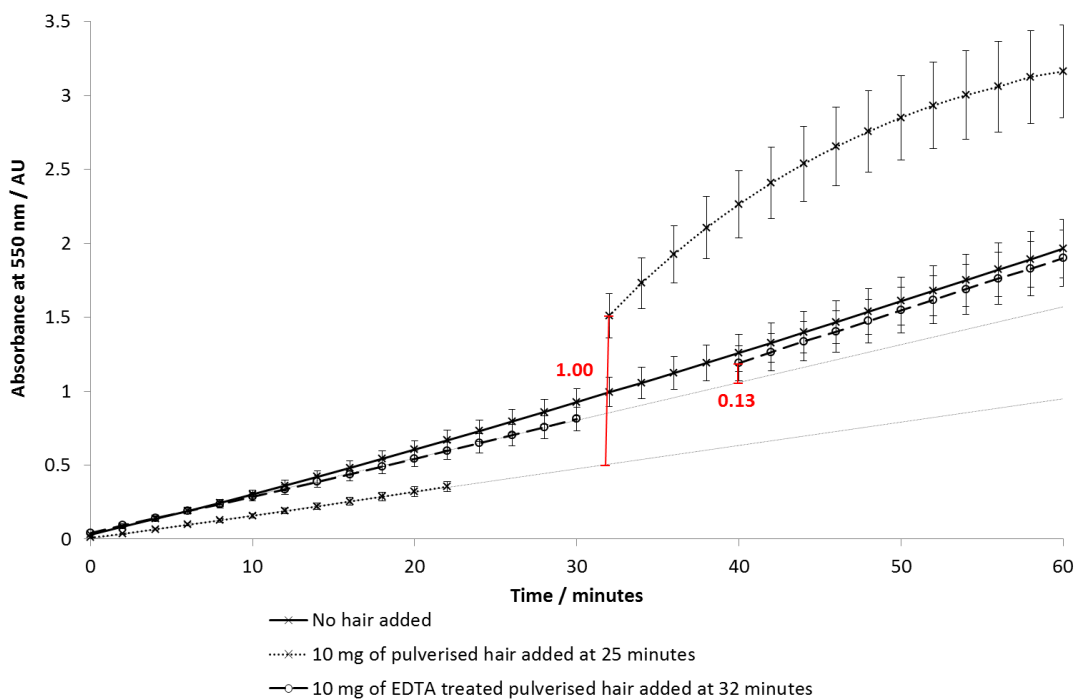


Figure 100: Graph to show the effect of pulverised hair and EDTA rinsed pulverised hair on the coupling of PAP-AHT in the following system: 400 mM NH_3 , 1.3 mM EDDS, 0.18 mM Cu(II), 0.07 M H_2O_2 , 1 mM PAP and 1 mM AHT at pH 10 & 20 °C.

It can be seen that there is some disparity between the initial rates of dye oxidation, before the addition of hair in some reactions. This is probably due to the fact that PAP begins to oxidise in water. It was necessary to dissolve the PAP in water before its addition to dye baths, to ensure that the dye solutions were homogeneous. As the time taken to dissolve PAP in water varied, it is possible that this had an effect on the amount of PAP that oxidised before the monitoring of the reaction, by UV-vis spectroscopy, began. This could have caused slight differences in the initial rate of dye formation.

Despite this, Figure 100 clearly shows that the initial rate of dye formation, presumably due to either molecular oxygen or the alkaline hydrogen peroxide, is not altered significantly on addition of the EDTA treated hair. After the addition of non-treated pulverised hair to dye baths, the change in absorbance was approximately 1. When the EDTA rinsed hair was added this change in absorbance

was only 0.13. Also, a very similar rate of reaction was observed to a system where no hair is added. The slight increase in the rate of dye formation that is observed in this case could potentially be due to the presence of redox active organic molecules in the hair, such as melanin¹⁹⁸. Alternatively, it could be due to metal ions that were not successfully removed from the pulverised hair.

These results indicate that metal ions are almost entirely responsible for dye formation inside the hair fibre, either directly or through peroxide decomposition to form reactive oxidation species such as the hydroxyl radical. It was considered to be of interest to identify which metal atom centre was predominantly responsible for the dye formation inside the hair. As discussed on page 161, the active sites of catalase consist of heme centres that contain iron atoms. If iron ions were identified as the main cause of increased dye formation inside hair, then this might indicate that catalase could be a potential oxidant of dye precursors in hair dye formulations.

4.4.5 Identifying the types of metal ions that are responsible for dye formation

By chelating metal atom species in hair fibres with EDTA it has been shown that metal atoms have a large impact on dye formation within hair fibres. The two metal atom types that are most likely to be responsible for accelerating dye formation in hair fibres are the redox-active Cu(II) and Fe(III) centres. EDTA does not have a specific preference for binding either copper(II) ($\text{LogK} = 18.78^{95, 130}$) or iron(III) ($\text{LogK} = 25.10^{95, 130}$). Therefore, when the hair fibres are washed with excess EDTA both of these metal atoms are removed from the fibre. Thus, it is not possible to establish whether or not it is Fe(III) or Cu(II), or both, that are responsible for accelerating dye formation.

It was thought that if Fe(III) was identified as the metal atom responsible for accelerating primary oxidation, this would provide supporting evidence for the possible involvement of catalase in the formation of dyes inside hair fibres.

It was therefore decided to use hair samples that had been dosed with a high concentration of copper ions, in order to determine the effect copper ion centres have on the rate of primary oxidation inside hair fibres. A solution containing 400 mM NH_3 , 1.3 mM EDDS, 0.18 mM Cu(II) , 70 mM H_2O_2 , 1 mM PAP and 1 mM AHT at pH 10 and 20 °C was stored for 25 minutes, before the addition of 10 mg pulverised hair that contained Cu(II) amounts of 218.0 ppm. The effect of hair containing either 218.0 and 13.1 ppm of Cu(II) on the rate of primary species oxidation is shown in *Figure 101*.

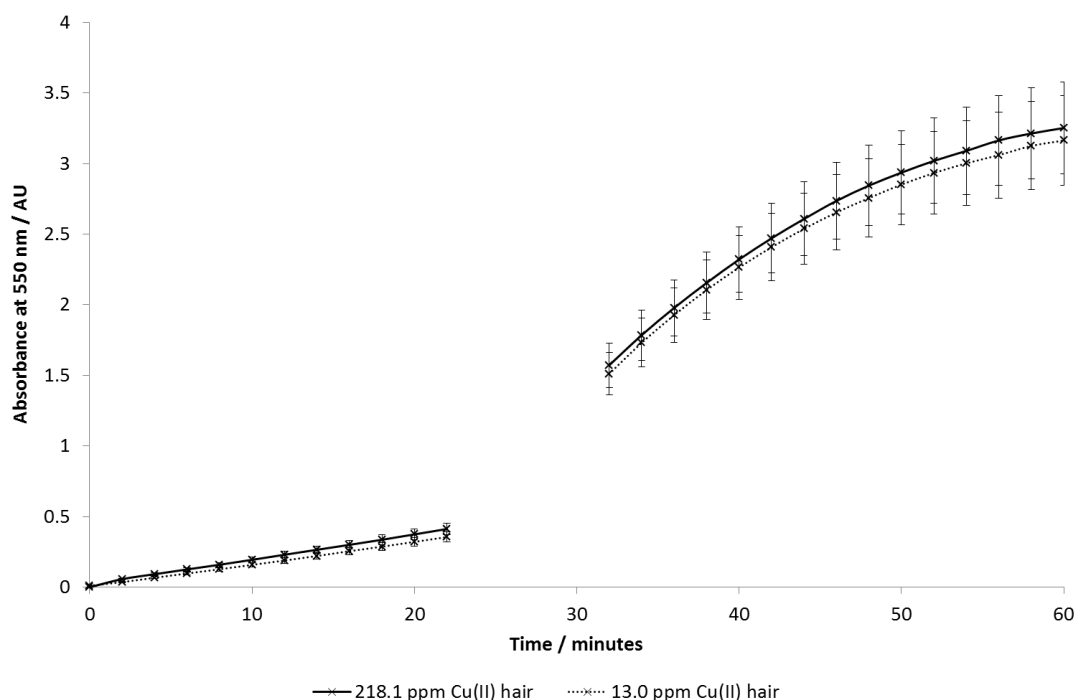


Figure 101: The rate of primary species oxidation in formulations containing 400 mM NH_3 , 1.3 mM EDDS, 0.18 mM Cu(II) , 70 mM H_2O_2 , 1 mM PAP and 1 mM AHT at pH 10 & 20 °C when 10 mg pulverised hair (218.0 or 13.1 ppm Cu(II)) is added at 25 minutes.

It is evident from *Figure 101* that regardless of the copper atom levels, when the hair samples are introduced to dye baths the increase in the rate of primary oxidation is similar. Increasing the copper atom concentration of the hair fibres

does not result in a significant increase of the rate of dye formation, although this does not rule out the possibility that copper contributes to primary oxidation within the hair fibre. This suggests that another type of redox metal atom plays a more important role in the formation of dye. Copper and iron are thought to be the most abundant redox metals within hair fibres (10.5 - 70.1 ppm and 7.12 - 26.7 ppm respectively^{47, 220}). ICP-MS data confirmed that the presence of iron atoms in these hair samples is approximately 35 ppm. Therefore, it could be inferred that iron atoms are the metal centre type that is predominantly responsible for the catalytic behaviour of pulverised hair in dye formation.

In order to confirm whether or not iron atom centres within the hair are mainly responsible for catalysing primary oxidation, it was decided to remove metals atoms from the hair fibres, using EDTA, and then dose the fibres with an excess of either Cu(II) or Fe(III). The relative effects that the dosed hair has on dye formation would provide further information on the roles of the redox metal atoms on primary oxidation within hair fibres.

Two samples of pulverised hair (10 mg) were washed with 0.1 M EDTA for 48 hours. The hair was then rinsed with deionised water to remove excess EDTA. One sample was dosed with 2 mM Cu(II), whilst the other was treated with 2 mM Fe(III) at pH 2 (to prevent precipitation of iron ions) for 2 hours. The samples were then washed with HCl (pH 2) to remove excess metal ions from solution, before being rinsed thoroughly with deionised water. ICP-MS showed that for Fe(III)-dosed hair the concentration of iron ions was 300 times greater than copper ions, whilst for Cu(II)-dosed hair the concentration of copper ions was only 50 times greater than iron ions. This suggests that iron ions are bound more easily in the hair fibres than copper ions, potentially due to the size of the cations affecting the stability of the complexes that are formed.

The dosed hair samples were added to solutions containing 400 mM NH₃, 1.3 mM EDDS, 0.18 mM Cu(II), 70 mM H₂O₂, 1 mM PAP and 1 mM AHT at pH 10 and 20 °C, at 25 minutes reaction time. The effect of each dosed hair sample is shown in *Figure 102*.

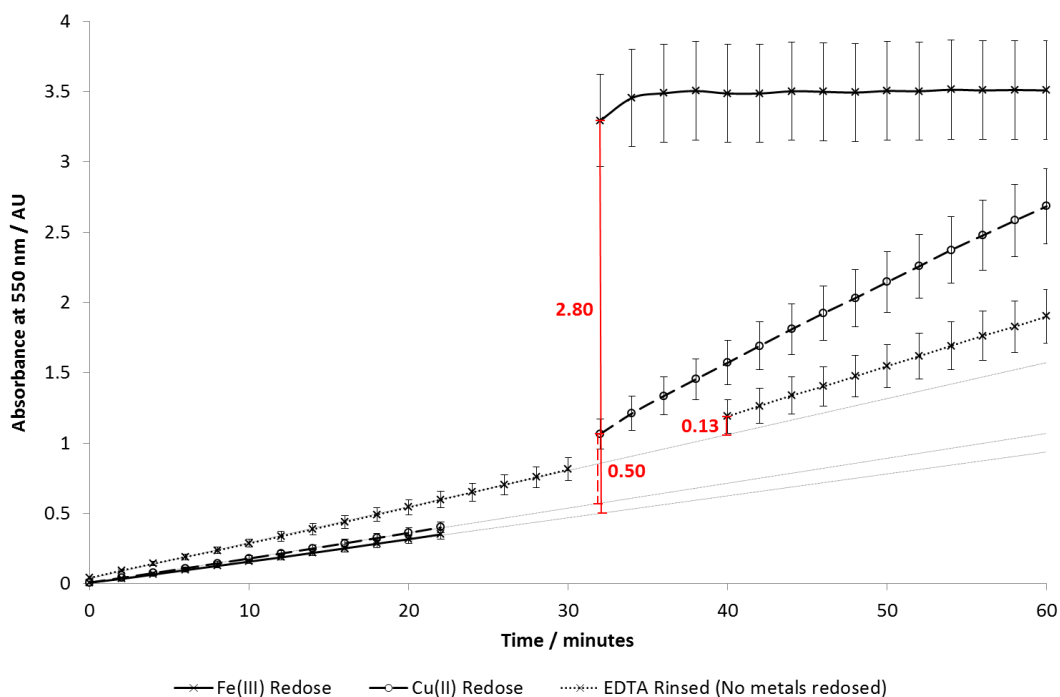


Figure 102: The effect of metal ion dosed pulverised hair fibres on primary oxidation in systems containing 400 mM NH_3 , 1.3 mM EDDS, 0.18 mM Cu(II) , 70 mM H_2O_2 , 1 mM PAP and 1 mM AHT at pH 10 & 20 °C.

It can be seen from the data in *Figure 102* that the pulverised hair samples that were only rinsed with EDTA do not significantly increase the rate of primary oxidation, as shown in *Figure 100*. This is due to the partial removal of metal atoms from the hair fibre. When the EDTA-treated hair samples are dosed with Cu(II) and added to dye baths there is an increase in the absorbance at 550 nm of approximately 0.5, presumably as a result of hair binding the redox-active metal. Dye formation also appears to continue after the addition of hair at a greater rate. Interestingly, when Fe(III) -dosed hair is added to dye baths there is almost a six fold increase in absorbance compared to that obtained with copper(II). This indicates that iron complexes are much more effective at catalysing dye formation within the hair fibres. This increase in dye formation, upon redosing the fibres with metal ions, could be due to the differing sizes of the Fe(III) and Cu(II) cations. When the hair is redosed with metal ions, the binding sites of enzymes or complexes within the hair

would then show a higher affinity for Fe(III) than for Cu(II). This would lead to greater uptake of iron ions upon redosing, leading to a higher rate of dye formation.

If present in hair fibres, catalase is an example of an enzyme with an iron atom type of centre that could potentially contribute to dye formation. This is not an unreasonable hypothesis as the oxidation of aromatic amines and phenols by catalase has been observed in other studies. No catalase was directly detected in the hair fibres. Claims that catalase is the main species that could be responsible for the catalysis of dye formation in hair are purely speculative at this stage.

4.5 Conclusions

It has been shown that catalase significantly increases the rate of dye formation in alkaline aqueous formulations, involving the reaction of precursors such as PAP, PPD, AHT and MAP. It has been postulated that this reaction could be of significance in the hair fibre, as it is known that hair follicles produce catalase²⁰⁴. Therefore, this may be the underlying cause for rapid permanent dye formation within hair fibres.

Pulverised hair accelerates the coupling of dye precursors to a much greater extent than whole hair fibres. Furthermore, this acceleration of dye coupling is in the presence of EDDS. Interestingly, when pulverised hair was pre-treated with EDTA for a substantial time period the acceleration of dye coupling was no longer observed. Firstly, this shows that metal atoms are responsible for the majority, if not all, of the dye formation inside hair fibres. It also indicates that the chelation of metal centres in the hair fibres is time dependent, perhaps because the metal atoms that oxidise the dye precursors are bound strongly within hair fibres. Alternatively, the diffusion of ligands into pulverised hair may be slow. This may help to explain why dye formation can occur in dye formulations inside hair fibres despite the presence of chelating agents.

Hair that was treated with extra copper atoms did not result in a faster oxidation of the dye primaries when added to dye baths. Furthermore, hair that was dosed with additional Fe(III) showed a significant increase in dye formation. This implies that iron(III) is the metal cation that is mainly responsible for the increase in the rate of dye formation within hair fibres

The literature shows that the iron-centred enzyme catalase can result in aromatic amine and phenol oxidation²⁰⁵. It may be possible that this species performs the same role inside hair. It is known that catalase is present in hair follicles. However, no catalase was detected in the hair fibres. It was realised that the presence or absence of catalase in hair fibres could be confirmed with further investigations that involve the direct detection of catalase by SDS-PAGE or by the comparison of Fe(III) EPR spectra for catalase and pulverised hair. If it was found to be present in hair

fibres, as it is in hair follicles, even in its denatured form, there is a strong possibility that it would be able to catalyse oxidative dye formation inside hair fibres.

Chapter 5

Chapter 5 – The effect of replacing ammonia with ethanolamine in dyeing formulations

5.1 Introduction

As mentioned in chapter 1, MEA is sometimes used as a replacement for ammonia in hair colouring formulations in order to improve the odour of the final products. Some circumstantial evidence, gathered by commercial producers of permanent hair dyes, suggests that replacing ammonia with MEA in hair dye formulations causes the final product to produce a non-identical colour result when applied to hair compared to the ammonia formulation⁴³. It is therefore necessary for companies to alter permanent oxidative dye formulations, by rebalancing the levels of primaries and couplers within the formula, that use MEA in order to achieve the same shade that is observed when ammonia is used. The chemical mechanisms responsible for the different colour formation with different bases are currently not understood.

The work in this chapter primarily focussed on investigating the underlying causes for the differences in colour result that are observed in oxidative dye formation when ethanolamine is used, at 20 °C. The mechanism for permanent dye formation was discussed in chapter 4. It relies on the oxidation of aromatic amines and phenols by hydrogen peroxide under alkaline conditions, forming polynuclear indamine or indophenol molecules. These molecules are responsible for the final colour that is observed when the product is applied. The general mechanism for the formation of binuclear and trinuclear indamine and indophenol molecules is discussed below.

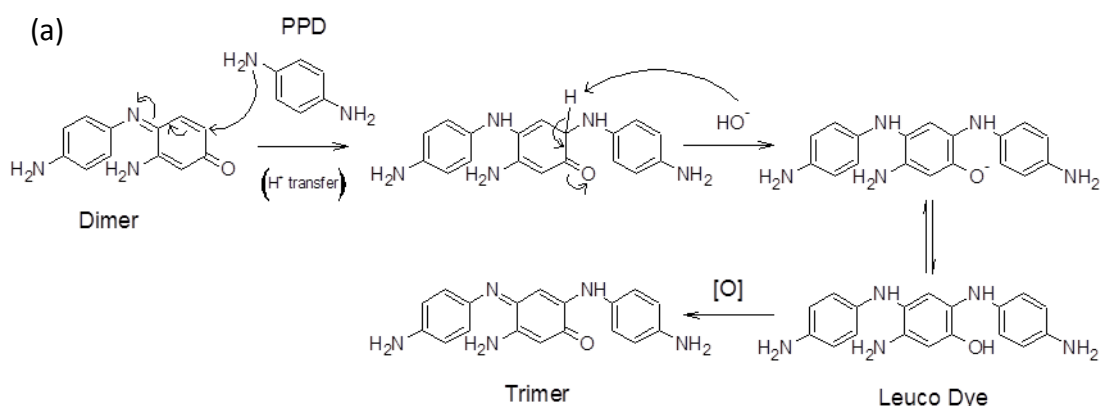
5.1.1 The mechanism of dye formation in binuclear systems

The mechanism of binuclear dye formation, relevant to hair colouration, was outlined in chapter 4. This occurs by the initial oxidation of a dye precursor, usually a *para*-substituted aromatic amine, to generate a reactive imine intermediate. This may then attack a *meta*-substituted phenol or aromatic amine, by electrophilic addition, to form a reactive leuco intermediate, which can then be further oxidised to give a binuclear dye compound^{3, 112}. This mechanism is displayed in *Figure 94*.

5.1.2 The mechanism of dye formation in trinuclear systems

It has been shown that binuclear dye compounds can be formed from couplers that have an appropriate functional group present in the 6 position of the ring, for example AHT. However, some couplers that are used in dye formulations, such as MAP, have the potential to form larger dye molecules such as trinuclear dye species, in addition to the formation of the dimer¹¹².

There are two possible mechanisms for trimer formation that are discussed in existing literature^{4, 112, 221-224}. Both of these mechanisms are outlined in *Figure 103*.



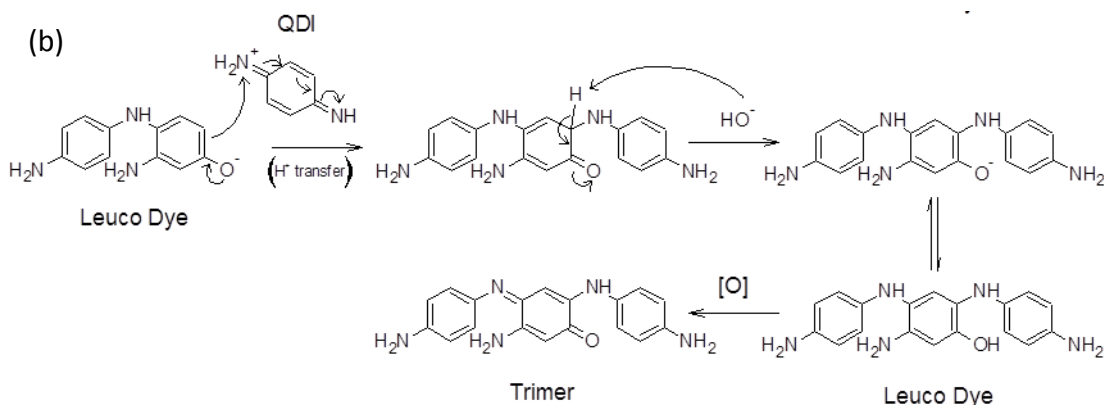


Figure 103: Possible mechanisms for the formation of trinuclear dye species from PPD and from MAP. (a) nucleophilic attack of PPD on a binuclear dye (b) electrophilic attack of QDI on a leuco dye intermediate.

The current literature gives mixed opinions on which of the above mechanisms is the most likely to occur in the formation of trinuclear dyes and larger dye compounds. In the review published by Lewis et. al, it is suggested that *mechanism b* is the route by which trimer formation occurs, based on earlier work^{4, 221-223}. This observation is based on the principle that the leuco dye intermediate is the subject of electrophilic attack by QDI, both of which are highly reactive intermediates.

However, Corbett has presented strong evidence to suggest that the main pathway of trimer formation is by *mechanism a*^{112, 224}, where it is the dimer that undergoes nucleophilic attack by PPD. If PPD was able to act as a nucleophile then MEA could react in a similar way and become involved in dye formation, potentially leading to molecules that result in a different colour. Corbett also suggests that systems with a slower rate of PPD consumption result in a higher ratio of trimer:dimer, since more PPD would be available to react with the dimer to form the trinuclear species by *mechanism a*. The colour of such a formulation would be a darker brown colour, as the PPD-MAP dimer is a red colour, whereas the PPD-MAP trimer is a dark brown. Both of these mechanisms may play a role during the formation of trimeric dye molecules. However, it is not known the extent to which each pathway would contribute to the process. The pathway could be influenced by several factors, such

as pH, temperature or the solvent. However, there have been no comprehensive studies aimed at identifying the effect that these variables have on the mechanism of dye formation.

When MEA is used in dye formulations, as opposed to ammonia, the final colour result may vary due to several factors, which may affect the formation of dyes by the mechanisms shown in *Figure 103*. These factors have been discussed in chapter 1. The most relevant issues to consider for the work in this chapter are, the effect MEA has on the pH of formulations, the effect MEA has on the diffusion of the active species into hair fibres and the nucleophilicity of the MEA.

5.2 Aims

Based on the observation by Godfrey et al, at Procter & Gamble that the final colour result of hair dye formulations differs when MEA is used as an alternative base to ammonia, it was decided to investigate several possible chemical reasons for these changes in colour formation.

Initially the rate of colour formation and the quantities of dyes that were formed in the aqueous solutions containing ammonia or ethanolamine were studied. It was realised that the molecules responsible for colour may take a different amount of time to form. This was investigated using HPLC and UV-vis spectroscopy. It was recognised that aqueous solutions would be an acceptable model for comparing ammonia-containing and ethanolamine-containing dyeing formulations, as both bases are fully soluble in water at 20 °C. The surface tension of MEA-water mixtures and ammonia-water mixtures, for the base concentrations used in the model compositions, are also comparable (67.24 mN m⁻¹ at 25 °C for MEA-water mixtures and 69.36 mN m⁻¹ at 20 °C for ammonia-water mixtures^{131, 132}).

Also of interest were the types of dye molecules produced when the base was altered. The possibility that alternative dye species may be formed in solution when ethanolamine is used, was also considered. This point was investigated using a combination of HPLC and HPLC-MS, to identify new peaks from MEA formulations that may correspond to new dye molecules. Finally, attempts were made to identify the mechanism of formation for any new species that may be formed, using MS.

5.3 Results & Discussion

5.3.1 Dye formation in aqueous MEA and NH₃ solutions

Varying the rates of dye production in formulations that contain MEA and ammonia could result in different quantities of dyes being produced, when the formulations are applied to hair for the same length of time, at the same temperature. This could result in changes to the final colour of hair formulations when the base is changed. It was therefore initially decided to monitor the quantities of dyes formed in aqueous solutions containing either MEA or ammonia.

Changing ammonia for MEA in colouring formulations could affect the extent of hair fibre swelling that occurs, which in turn will affect the rate of dye precursor diffusion into hair fibres. It was thus decided to study homogeneous aqueous systems. Under such conditions diffusion rates would no longer contribute to the amount of dyes formed. Any differences in the amount of dyes that are produced, when the base is altered, could therefore be attributed to changes in the chemistry behind dye formation. This had the added advantage of simplifying the analysis of dye solutions by UV-vis and HPLC.

Firstly, the relative rates of dye formation were studied using UV-vis spectroscopy. This was to gain an understanding of the effect of base on the rate of colour formation in solutions containing 400 mM of base, 1.3 mM EDDS, 0.18 mM Cu(II), 70 mM H₂O₂, 1 mM primary and 1 mM coupler at pH 10 & 20 °C (where primary is PPD or PAP, coupler is MAP or AHT and the base is MEA or NH₃).

EDDS is more commonly used in dye formulations due to its specificity for binding Cu(II) in the presence of calcium, in order to prevent the decomposition of hydrogen peroxide to give ROS, that may damage hair fibres⁵⁰. This model aqueous system is therefore representative of some commercial dye products. It also provided a rate of oxidative coupling that was not too fast, being able to be followed by HPLC. Additionally, the use of EDDS means Cu(II) will be bound

exclusively to the ligand rather than to the different bases, due to the relatively high stability constant of the $[\text{Cu}(\text{EDDS})]^{2-}$ complex (Table 11 and Figure 29).

Dye formation will thus occur due to the presence of alkaline hydrogen peroxide, the ROS from the decomposition of hydrogen peroxide by the Cu(II)-EDDS complex, or directly by the Cu(II) centre.

Metal-complex	Stability constant / logK
$[\text{Cu}(\text{NH}_3)_4]^{2+}$	12.5
$[\text{Cu}(\text{MEA})_4]^{2+}$	11.5
$[\text{Cu}(\text{EDDS})]^{2-}$	18.4

Table 11: The binding constants of some copper complexes^{95, 130}

Most commercial hair colouring formulations do not use fixed concentrations of base, which are then buffered to a specific pH. Instead, the appropriate base is added to the formulation until the desired pH is reached. This practice results in formulations that have varying concentrations of base, when ethanolamine is used instead of ammonia, due to their different pK_a values. Any differences in dye formation that occur when using commercial formulations could therefore be due to varying concentrations of base. To avoid this, the model formulations that were used in this study had fixed concentrations of base (400 mM MEA or NH_3), which were then buffered to pH 10. Dye formation was then monitored in model formulations that contained comparable concentrations of either ethanolamine or ammonia. Any differences in dye formation that were observed could thus be attributed to a change in the identity of the base, as opposed to a change in the concentration of the base.

UV-vis spectra were acquired for each formulation over a reaction time of 60 minutes. The rates of dye formation were monitored at the wavelength maximum

value in the visible region. This varied depending on the dye precursors used (PPD-MAP: 506 nm, PPD-AHT: 500 nm and PAP-AHT: 554 nm). Examples of the UV-vis spectra acquired from such dye coupling reactions are shown in *Figure 104*. The rate of dye formation at 20 °C for each of these systems is shown in *Figure 105*, for both the ammonia-based and the MEA-based formulations.

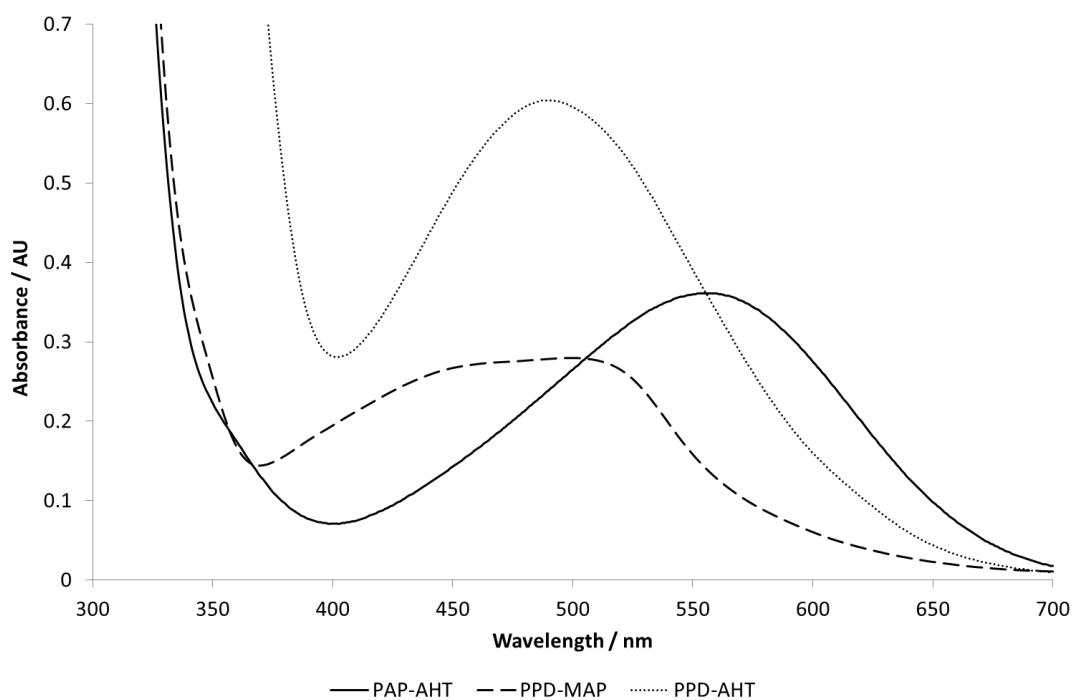


Figure 104: Examples of UV-vis spectra for the following dye formulations, 400 mM NH_3 , 1.3 mM EDDS, 0.18 mM Cu(II) , 70 mM H_2O_2 , 1 mM primary and 1 mM coupler at pH 10 & 20 °C.

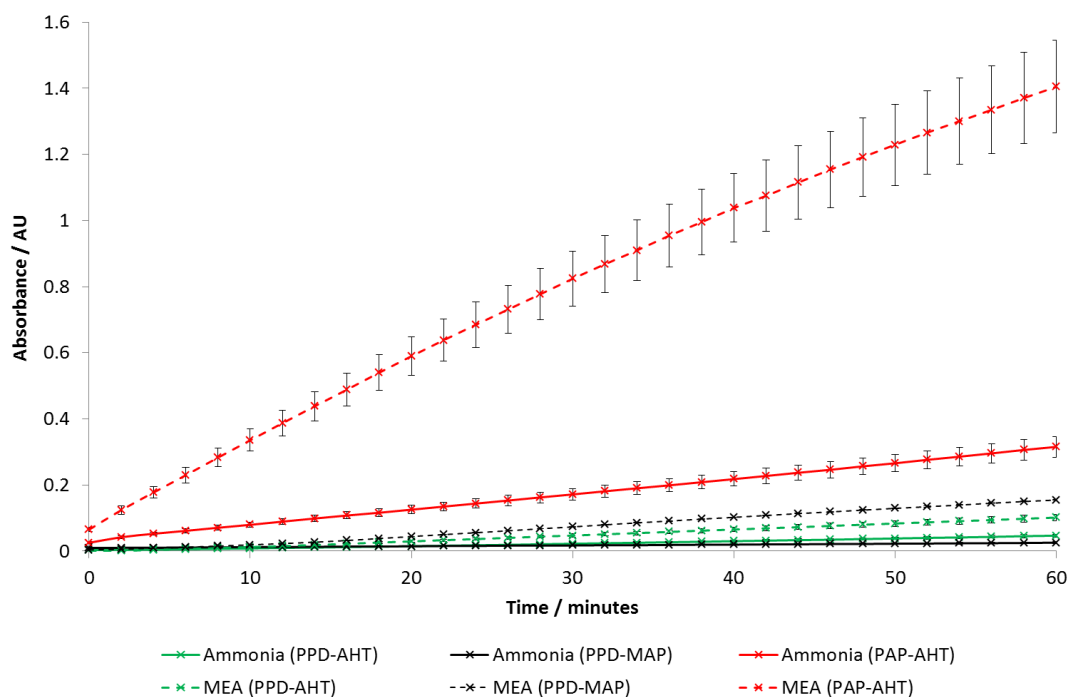


Figure 105: The relative rates of dye formation in aqueous dye baths containing 400 mM base, 1.3 mM EDDS, 0.18 mM Cu(II), 70 mM H₂O₂, 1 mM primary and 1mM coupler at pH 10 & 20 °C. (The base used is MEA or ammonia, the primary used is PAP or PPD and the coupler used is MAP or AHT).

From Figure 105, it appears that the formation of dyes in MEA-based formulations is much faster than the equivalent ammonia-based formulations. However, it is unclear why this is the case. In the presence of EDDS, at pH 10, the expected extent of hydrogen peroxide decomposition is similar for both systems, as shown in Table 9. There was no change in pH over the course of the reaction. Therefore, the types and ratios of the metal complexes should not vary between compositions. Additionally, the quantities of oxidants would not be expected to differ either. It was thus decided to use HPLC to study the consumption of precursors during oxidative dye formation. As mentioned previously, the idea was to separate the complex mixture of components so that individual molecules could be quantified during reactions. It was thought that this might provide more information regarding the extent of dye formation that occurs when the base is altered. It was also thought that any products from potential side reactions could be identified. New

products could help to explain the differences in the varying rates of colour formation, when the base is changed in these model formulations.

5.3.2 Consumption of dye couplers

The model dyeing solutions identified in the previous section were complex mixtures of molecules. Therefore, it was not facile to use UV-vis spectroscopy to monitor the quantity of individual components of these dye solutions, due to the overlapping UV-vis spectra of the molecules. It was envisaged that by using HPLC, individual components of the formulations could be separated out from the mixture. In this way the peak areas of dye couplers could be monitored during a reaction, to give more information on the state of dye production in ammonia-based formulations and MEA-based formulations.

Peak areas of dye couplers were compared for systems that contained 400 mM base, 1.3 mM EDDS, 0.18 mM Cu(II), 70 mM H₂O₂, 1 mM primary and 1 mM coupler, at pH 10 & 20 °C (where the primary is PPD or PAP, the coupler is MAP or AHT and the base is MEA or NH₃). The HPLC method that was used is discussed in chapter 7.

The coupling reaction could not be stopped at a desired time point using catalase to decompose hydrogen peroxide, as this dramatically increased the rate of dye formation, as discussed in chapter 4. Therefore, dye samples were injected for analysis by HPLC, without the addition of catalase, at reaction times of 30 and 120 minutes.

Using this method, a comparison of the quantities of precursors that are consumed gave an idea of the differences in the quantities of dyes formed when the base was altered from ammonia to ethanolamine. The results could be compared to the UV-vis data to establish whether or not different quantities of dyes were indeed produced during the reaction. If this was the case then this could be a reason for the change in colour observed when the base is altered in formulations.

Samples of various reaction mixtures that are outlined above were taken at time periods of 30 minutes and 2 hours and analysed by HPLC to provide chromatograms that were similar to the one in *Figure 106*, where PPD and MAP have been used. The identities of peaks and their elution times are listed in *Table 12*.

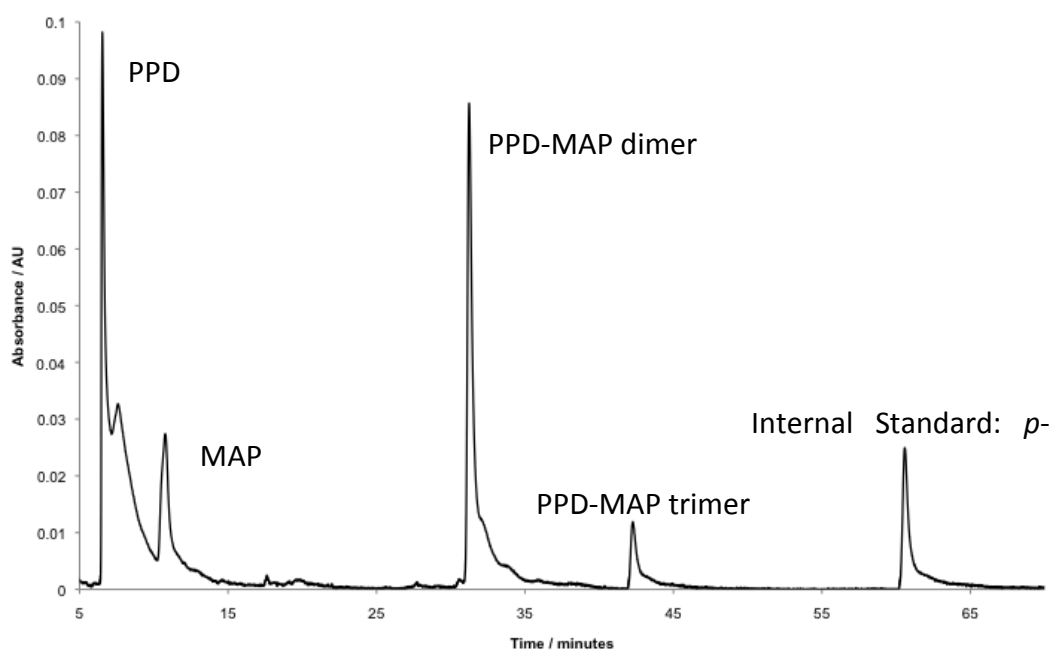


Figure 106: Chromatogram to show dye formation after 2 hours for the following system: 400 mM NH₃, 1.3 mM EDDS, 0.18 mM Cu(II), 70 mM H₂O₂, 1 mM PPD and 1 mM MAP at pH 10 & 20 °C.

Elution Time / minutes	Peak Identification
6.5	PPD
10.7	MAP
31.2	PPD-MAP dimer
42.2	PPD-MAP trimer
60.5	p-HBA

Table 12: The elution times and identities for the peaks of the chromatogram shown in Figure 106.

Peaks were identified by a combination of retention times, UV-spectra and mass spectra. Dye precursors were easily identified by their retention time. However, isolation of the dyes themselves was not facile. Therefore, it was thought to be simpler to identify the peaks that relate to the dye compounds by a combination of MS and UV-vis spectra. The spectra for the PPD-MAP dimer and trimer peaks are shown in *Figure 107*, *Figure 108*, *Figure 109* and *Figure 110*. UV-vis spectra were acquired using a diode array detector (DAD). Fractions were collected manually to obtain an ESI mass spectrum of the peaks at 31.2 and 42.2 minutes.

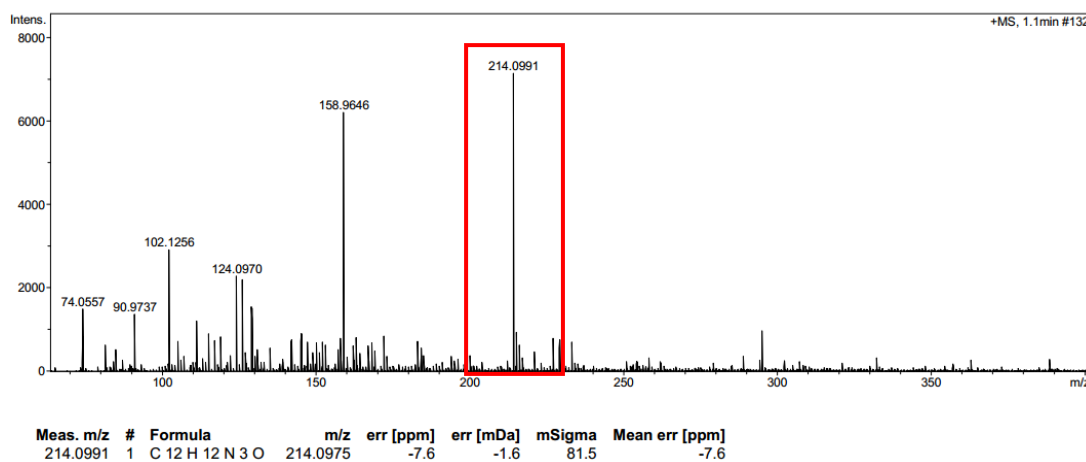


Figure 107: The ESI mass spectrum of the peak at 31.2 minutes.

The molecular ion peak at 214.0991 corresponds well to the molecular formula of the PPD-MAP dimer (C₁₂H₁₂N₃O). Various other peaks are apparent in these mass spectra, due to the low concentration of the dye and the presence of small amounts of contaminants from the HPLC buffer, for example triethylamine at 102.1256. The UV-vis spectrum confirms the presence of the dye with a peak in the visible region ($\lambda_{\text{max}} = 506 \text{ nm}$).

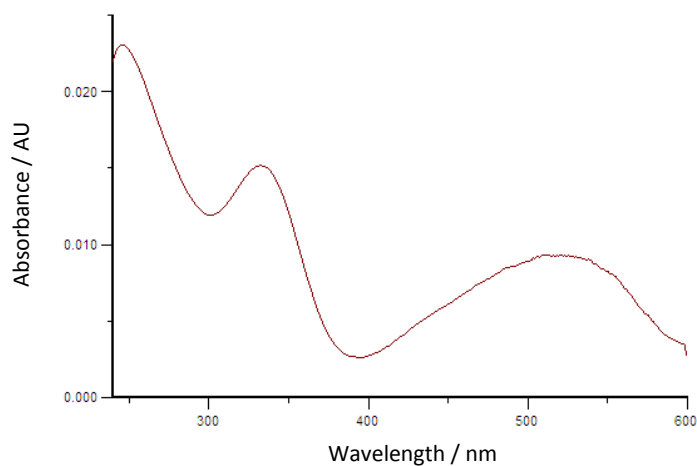


Figure 108: UV-vis spectrum of the peak at 31.2 minutes ($\lambda_{max} = 506$ nm).

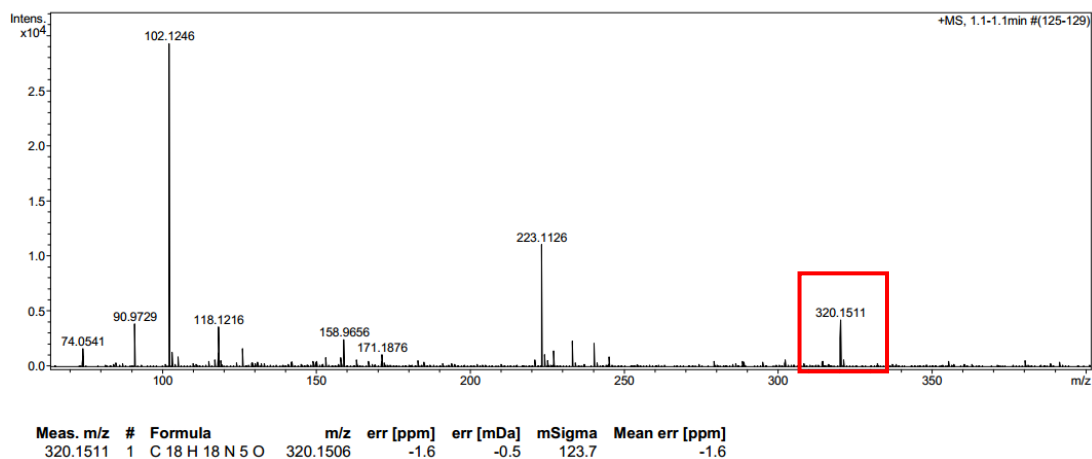


Figure 109: The ESI mass spectrum of the peak at 42.2 minutes.

The molecular ion peak at 320.1511 in *Figure 109* corresponds to the molecular formula of the PPD-MAP trimer (C₁₈H₁₈N₅O). The UV-vis spectrum is shown in *Figure 110*. The peaks for dyes formed in the compositions using the different precursors were identified by UV-vis spectroscopy and MS in a similar manner.

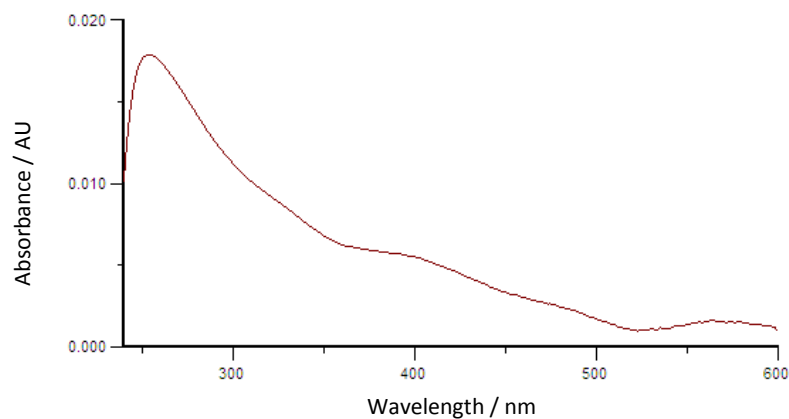


Figure 110: UV-vis spectrum of the peak at 42.2 minutes.

Splitting of the peak at 6.5 minutes in *Figure 106* is evident. However, the UV spectra indicate that they both originate as a result of the use of PPD. The HPLC buffer has a pH of 7 and the pK_a of PPD is 5.75³. Therefore, it is likely that a small amount of protonated PPD, as well as neutral PPD was present. Although the creation of the equilibrium between PPD and $PPDH^+$ is likely to be fast, this could potentially cause peak splitting due to the differing retention times of the two species.

For formulations in which AHT was used, the retention time of the coupler was significantly different to that of MAP. The formation of the trimeric dye molecule does not occur, due to the fact that the coupler is blocked in the 6 position of the ring. *Figure 111* shows the chromatogram that was obtained when AHT was used in conjunction with PPD. The relevant peaks and the elution times are shown in Table 13.

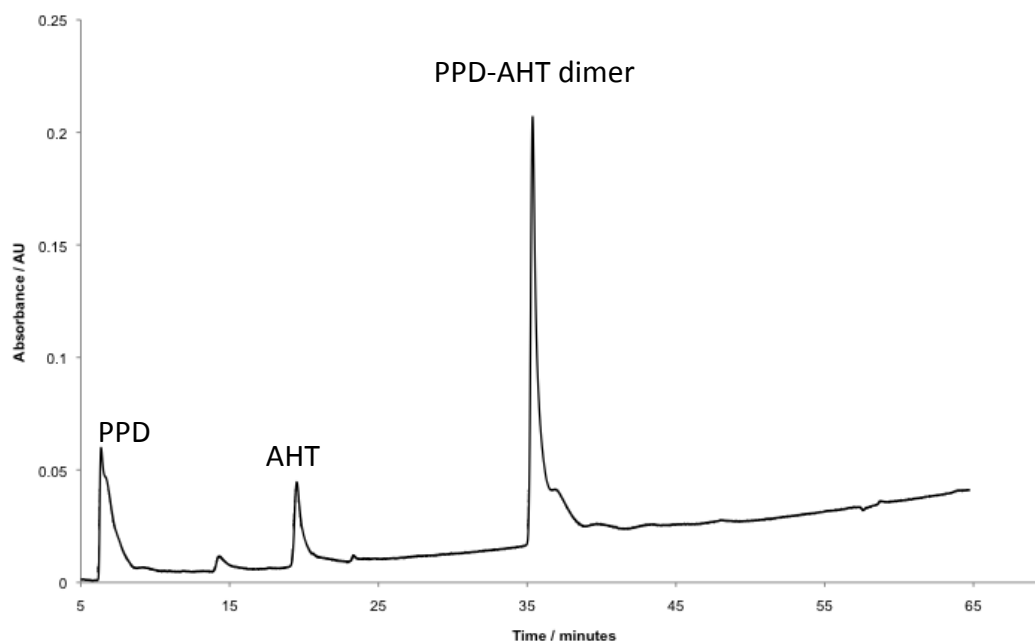


Figure 111: Chromatogram to show dye formation after 30 minutes for the following system: 400 mM NH_3 , 1.3 mM EDDS, 0.18 mM Cu(II) , 70 mM H_2O_2 , 1 mM PPD and 1 mM AHT at pH 10 & 20 °C.

The apparent peak at 15 minutes is just a disturbance in the baseline of the UV spectrum. The peaks at 6 and 35 minutes exhibit significant tailing. Again, as these compounds contain multiple primary amino groups and the mobile phase is buffered to pH 7. This could lead to a mixture of protonated and non-protonated amines, which elute at slightly different retention times and appear as tailing in the chromatogram. This could be resolved for such formulations by buffering the mobile phase to either a high pH or a low pH, but comparability with other dye compositions was required.

Elution Time / minutes	Peak Identification
6.3	PPD
19.4	AHT
35.3	PPD-AHT dimer

Table 13: The elution times and identities for the peaks of the chromatogram shown in Figure 111.

The peaks that correspond to the couplers (MAP or AHT) for these chromatograms were standardised externally and a calibration curve was constructed to assist with the determination of the quantity of coupler that was used in each dye formation reaction (*Figure 112 & Figure 113*). From this, an estimate of the quantities of dye formed in each reaction could be made, without providing specific information on the structure or number of dyes that were produced. This information is provided in *Figure 114* and *Figure 115*.

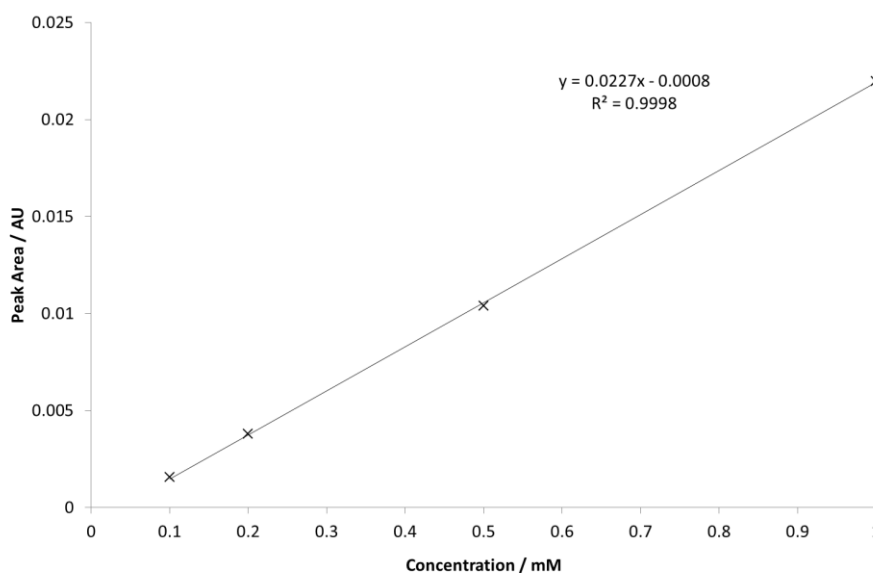


Figure 112: Calibration curve to show how the HPLC peak areas at ~11 minutes changes with concentration of the coupler MAP.

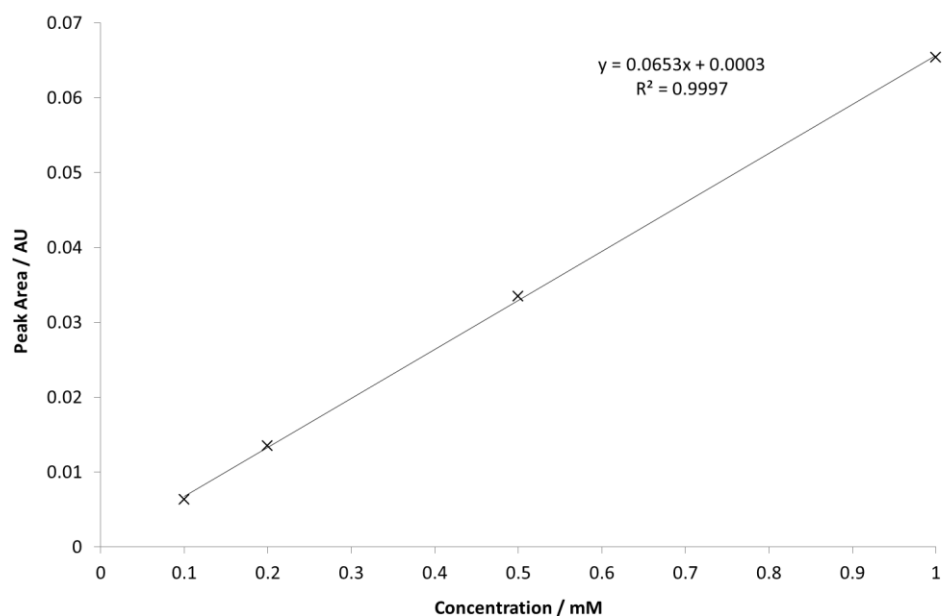


Figure 113: Calibration curve to show how the HPLC peak area at ~19 minutes changes with concentration of the coupler AHT.

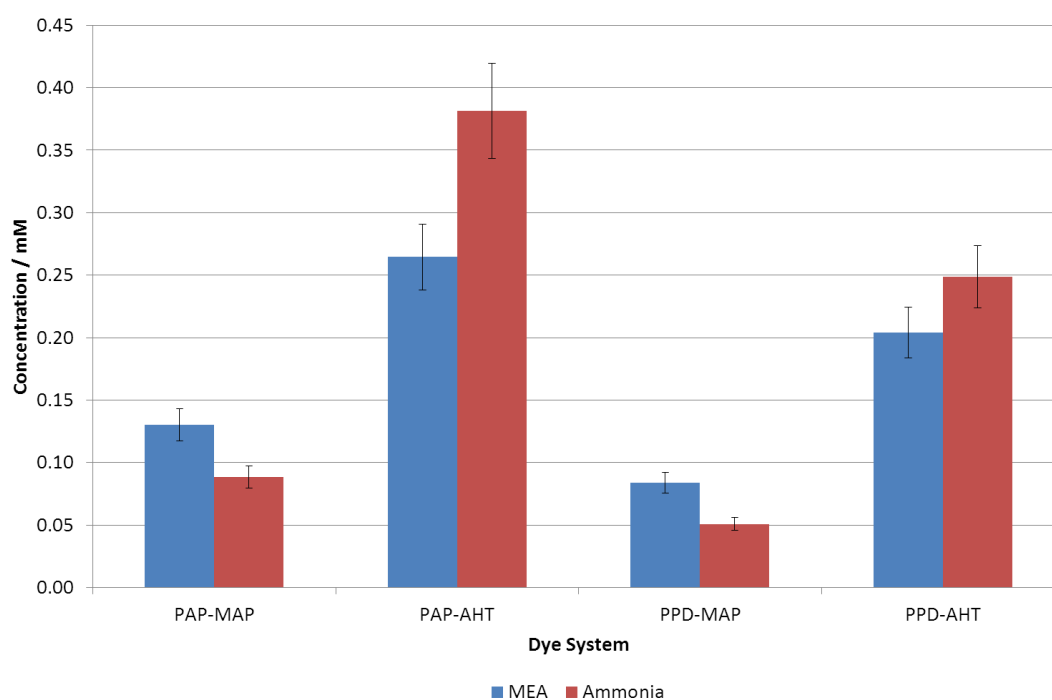


Figure 114: Chart to show a relative estimate of the amount of non-specific dye formed after 30 minutes of the following reaction: 400 mM base, 1.3 mM EDDS, 0.18 mM Cu(II), 70 mM H₂O₂, 1 mM primary and 1 mM coupler at pH 10 & 20 °C.

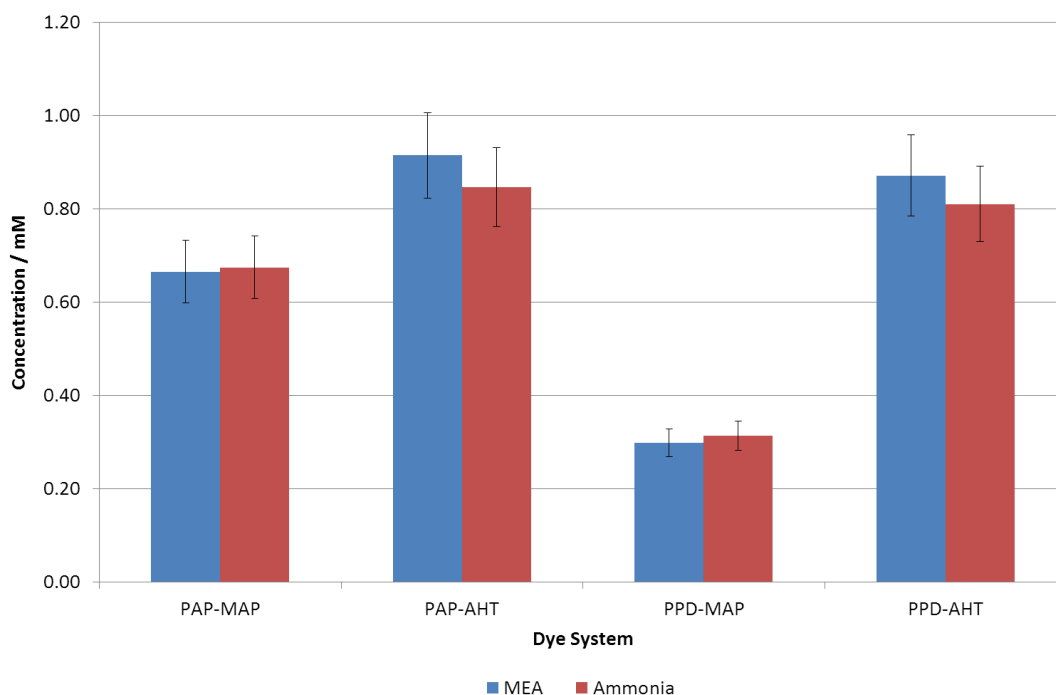


Figure 115: Chart to show a relative estimate of the amount of non-specific dye formed after 2 hours of the following reaction: 400 mM base, 1.3 mM EDDS, 0.18 mM Cu(II), 70 mM H₂O₂, 1 mM primary and 1 mM coupler at pH 10 & 20 °C.

For samples taken at both the 30 minutes reaction time and the 2 hours reaction time, the consumption of dye couplers appears to be comparable, on changing the base from ammonia to ethanolamine. Any variation is generally within experimental error of 10%, based on experimental repeats. Although some minor differences are apparent in the 30 minutes reaction time dataset, they do not indicate the level of disparity that is shown between MEA-based formulations and ammonia-based formulations when the rate of dye formation is monitored by UV-vis spectroscopy.

These HPLC results indicate that the quantities of couplers consumed do not vary significantly when the base is altered. This directly contradicts the results observed by UV-vis in the previous section, which indicate that the use of MEA results in higher rates of dye formation. The difference in colour between the two systems, despite the apparent similar rates of dye formation, could potentially be explained

by varying rates of dye degradation. It may be the case that there is more extensive dye degradation in the ammonia system than the MEA system.

As seen in chapter 3, the reaction of hydroxyl radical with MEA leads to the degradation of the MEA. At high concentrations of MEA, this could potentially be a mechanism by which dye molecules are protected from degradation by the hydroxyl radical. It should be noted that whilst rapid fading of the colour of dye solutions has been observed in systems which produce a high concentration of hydroxyl radicals, products of dye degradation have not been detected in this work. For copper ion-based formulations that contained EDDS, low levels of hydrogen peroxide decomposition were observed (*Table 9*). Therefore, the small amounts of hydroxyl radical that are generated will probably result in lesser amounts of dye degradation. This could explain why no products of degradation are observed in the chromatograms, as they may fall below the limit of detection. The limit of detection for the dye precursors is ~ 0.02 mM, based on the equation $3\sigma/S$, where σ is the standard deviation of response and S is the slope of the calibration curve. The products of dye degradation could also be smaller and more polar. This would result in them eluting too quickly to be detected by the HPLC method used.

Varying rates of dye degradation could help to explain why substantial differences in colour formation exist when the base used in dyeing formulations is changed from ammonia to MEA. However, as no direct evidence has been obtained to confirm this is the case, there may be other explanations for the apparent differences in the rate of dye formation when the base is altered, such as side reactions to give other products. In commercial formulations, effects such as temperature and localised pH will play a role in the rate of dye formation and fading. However, these factors will not contribute to the observed differences in the homogeneous model formulations, as the temperature was controlled at 20 °C and the pH was maintained through the use of the appropriate buffer solution.

Dye peaks could not be quantified reliably for several reasons, firstly, due to the potential degradation of dyes, as discussed above. The appearance of a new peak in MAP-based formulations, when MEA is used, further complicates the

chromatograms. This new peak overlaps with the dimer peak and indicates a change in product formation in these formulations. Additionally, due to the complex nature of the systems, dye molecules are difficult to isolate and are poorly soluble in aqueous media. Therefore, dye peaks could not be standardised.

It can be concluded from these results that the rate of dye formation does not change when the type of base is changed. Instead the apparent increase in the rate of colour production in the MEA system may be due to lesser amounts of dye degradation. Varying amounts of dye degradation, when the base type is altered, would have a significant effect on the overall amount of dye that remained in hair fibres when formulations are applied, thus changing the final shade result significantly. In addition to this increase in rate of colour production for MEA systems, the formation of an additional dye molecule in MAP systems was also investigated. This could be another factor that contributes to the change in colour result associated formulations that use MEA instead of ammonia.

5.3.3 The formation of an additional chromophore in the PAP-MAP-MEA formulation

As mentioned in the previous section, a new peak appeared in the chromatograms obtained for the PAP-MAP system when MEA was used. This peak could indicate the formation of a new dye in the presence of MEA. In addition to the factors discussed in the previous section, the formation of this new dye could also explain the differences in the colour of solutions containing PAP and MAP, when the base is altered. The chromatogram for a system containing 400 mM MEA, 1.3 mM EDDS, 0.18 mM Cu(II), 70 mM H₂O₂, 1 mM PAP and 1 mM MAP at pH 10 & 20 °C is shown in *Figure 116*. The new peak (1) is shown to elute at a similar time to that of the PAP-MAP dimer. Importantly, when the equivalent ammonia-containing formulation is studied by ESI-MS, there are no peaks to suggest that ammonia is incorporated into the structure of dye molecules (*Figure 130*).

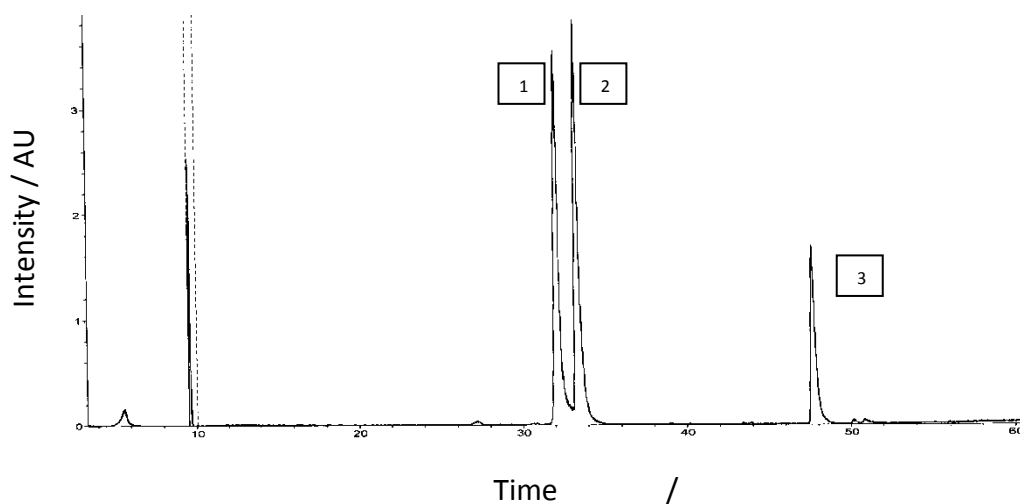


Figure 116: Chromatogram to show the dyes formed in the following system: 400 mM MEA, 1.3 mM EDDS, 0.18 mM Cu(II), 70 mM H₂O₂, 1 mM PAP and 1 mM MAP at pH 10 & 20 °C.

Peak	Time of Elution / minutes	Peak Identity
1	32.1	New peak
2	33.5	PAP-MAP dimer
3	47.9	PAP-MAP trimer

Table 14: The elution times and identities for the peaks of the chromatogram shown in Figure 116

The formation of the product responsible for this peak may help to explain the differences in colour, when MEA is used as a base. As such it was necessary to identify the structure of the product responsible for this peak and how it is formed.

5.3.4 Identification of a new dye in MAP systems when MEA was used as a base

Using the same method, HPLC-MS was employed to obtain a mass spectrum of the new peak in *Figure 116* that elutes at 32.1 minutes. This is shown in *Figure 117*.

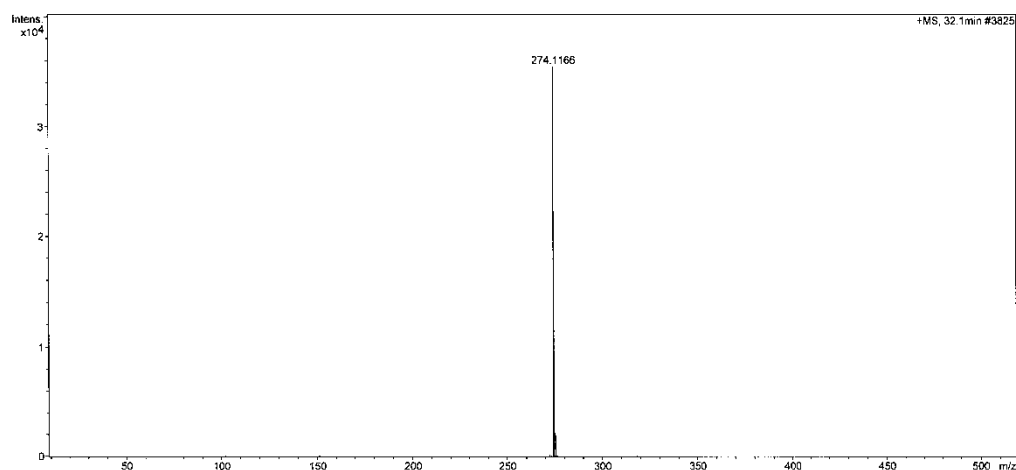


Figure 117: Mass spectrum of peak 1 from the chromatogram shown in Figure 116.

The molecular ion peak at 274.1166 indicates that the molecular formula could be $C_{14}H_{15}N_3O_3$. This formula could correspond to the structure shown in *Figure 118* that could form as a result of MEA becoming included in the structure of dye.

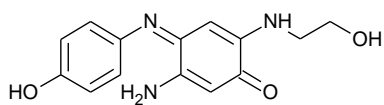


Figure 118: The possible structure of the dye formed in the PAP-MAP dyeing reaction when MEA is used as a base.

Whilst this structure is a good fit with the data obtained from MS, it was considered to be important to confirm this by further studies, including NMR, before a possible mechanism of formation could be investigated.

5.3.5 Analysis of the MEA incorporated dye (274)

In order to obtain further structural information on the dye that is postulated to contain MEA within its structure, the dye was synthesised using the following reaction conditions:

400 mM MEA, 1.3 mM EDDS, 0.18 mM Cu(II), 0.979 M H₂O₂, 37 mM PAP and 37 mM MAP at pH 10 & 20 °C.

These reaction conditions were used in order to generate the dye on a reasonable time scale, without it being subject to degradation by excess amounts of hydroxyl radicals. The only difference to the reactions that were studied by HPLC was that the concentrations of dye precursors were greater. This increase in concentration was to improve the mass of dye product obtained from the reaction. Although new peaks were detected in both the PPD and PAP systems when MAP was used, it was decided to investigate the PAP system, as oxidative coupling is much faster.

TLC was used to confirm that a known separation technique could be applied to separate dye molecule 274 from other dyes in this system²²⁵. Once confirmed, this separation, which involves the use of chloroform, ethyl acetate and ethanol (7:2:1) was scaled up for column chromatography. The product was further purified using preparatory TLC and the same solvent system. A proton NMR spectrum of the purified product, in CD₃OD, is shown in *Figure 119*.

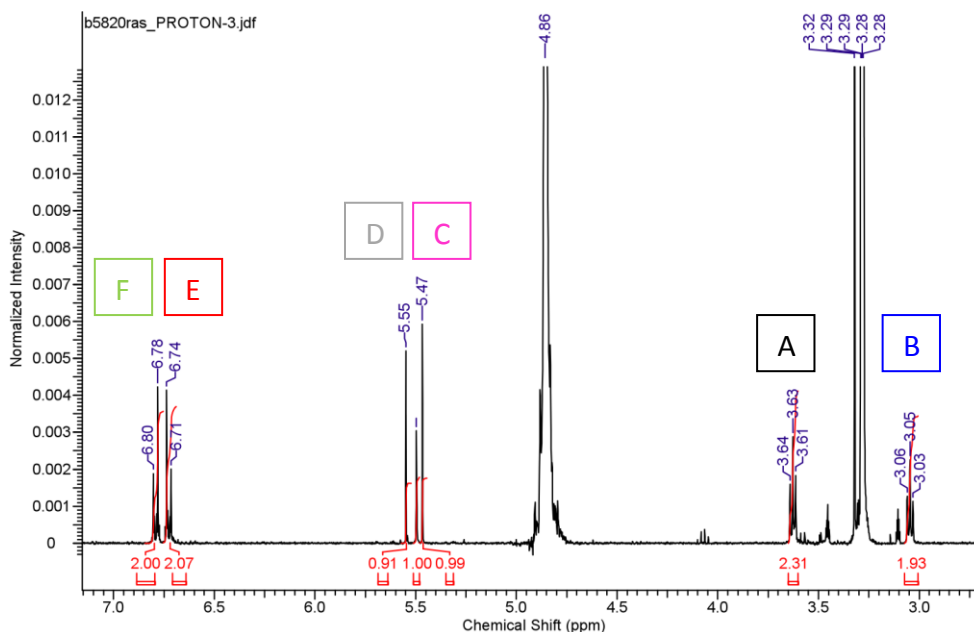


Figure 119: ^1H NMR spectrum for dye molecule 274

Despite showing multiple peaks that correspond to the solvents used for purification and the washing of the dye, the NMR shows 2 triplets (A and B) at 3.63 ppm and 3.05 ppm respectively, which correspond well to the section of the molecule that has originated from the hypothesised incorporation of MEA. These protons are labelled with the appropriate colours in the structure shown in Figure 120.

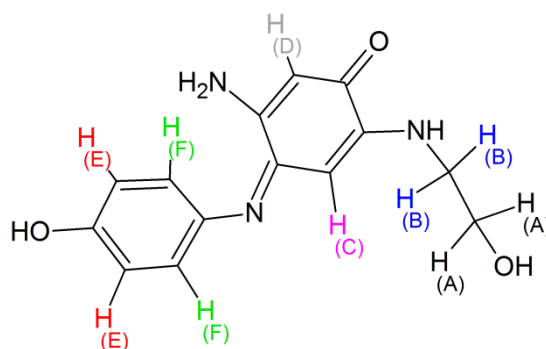


Figure 120: The proposed structure of the dye molecule 274

The NMR also shows 2 doublets at approximately 6.75 ppm (E & F) that are indicative of a 1-4 substituted aromatic, which also fits with the proposed structure.

There appears to be 3 signals at ~5.5 ppm, where there should only be two that correspond to the two protons on the quinonoid-like ring (C & D). The peak in the middle of these can be attributed to dichloromethane (DCM), which coincidentally integrates to one. As well as this there are also solvent signals at 4.86 ppm (bs) for water, 4.1 ppm (q) for ethyl acetate and 3.29 ppm (s) for methanol with satellite peaks. The integration of peak A appears to be greater than would be expected, probably due to an overlapping quartet at 3.65 ppm, due to the presence of ethanol²²⁶.

A cleaner sample was obtained and more data were collected by 2D NMR, to confirm whether or not the extra signal at 5.5 ppm could be due to DCM or part of the structure. Firstly, ¹H COSY was used to show protons that are in adjacent environments and hence are coupled to each other.

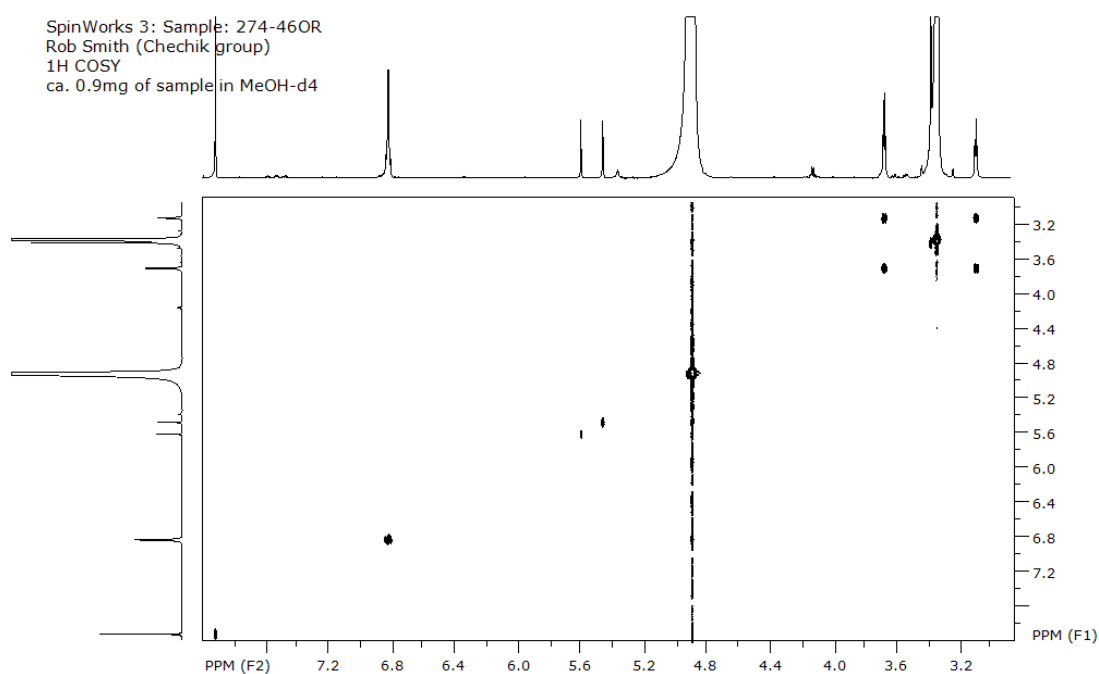


Figure 121: ¹H COSY spectrum for dye molecule 274

The only coupling expected and observed in *Figure 121* is between the triplets on the MEA incorporated section of the dye. The singlets on the quinonoid-like ring are not expected to couple and the aromatic region is shown as one signal. The extra signal present in this spectrum, at approximately 7.90 ppm can be attributed to the presence of chloroform²²⁶.

This is the extent of the information that can be obtained from proton NMR and ¹H COSY. However, more information would be required to confirm the structure and not enough of the sample could be isolated in order to obtain a ¹³C NMR. It was also necessary to use other techniques, such as HSQC and HMBC, to yield more information on the carbon environments in the structure of the molecule. ¹H-¹³C HSQC is a technique that gives information on carbon atoms that have hydrogen atoms attached directly. *Figure 122* shows the carbon atom signals detected by HSQC for each proton environment.

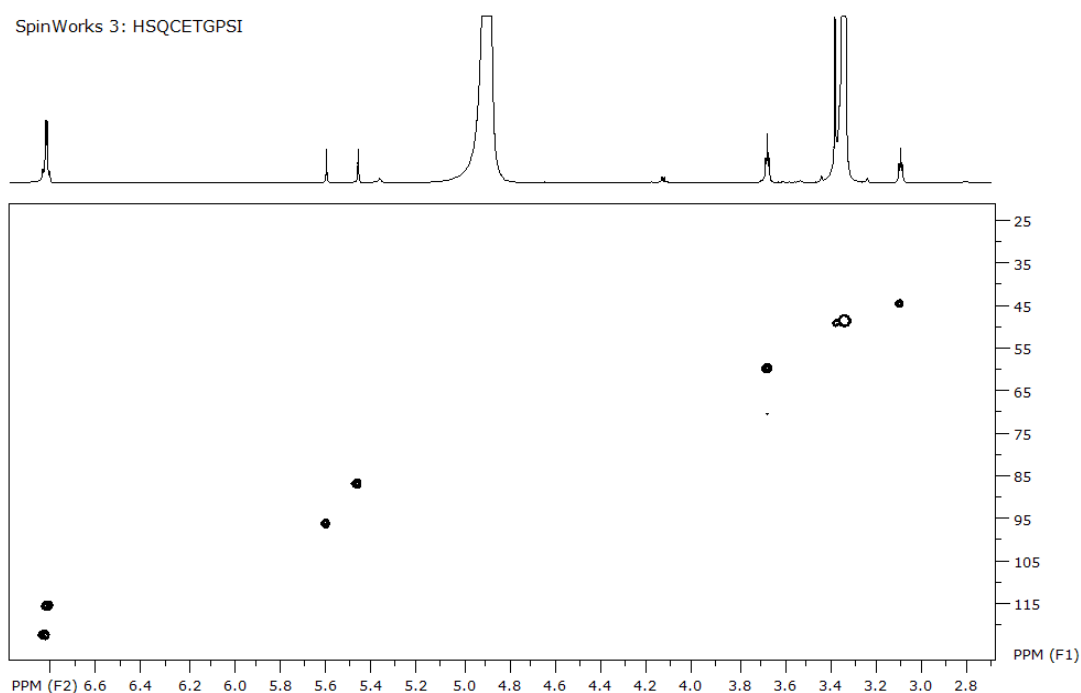


Figure 122: HSQC spectrum for dye molecule 274

HSQC shows that there are a total of 6 different carbon environments that are coupled to protons, (ignoring the peak at ~50 ppm for methanol). Since the aromatic ring is *para*-substituted, there are two equivalent carbons for each signal in this region, bringing the total number of carbons detected by HSQC to 8 out of the possible 14 for the postulated compound, (labelled 1-6 in *Figure 123*).

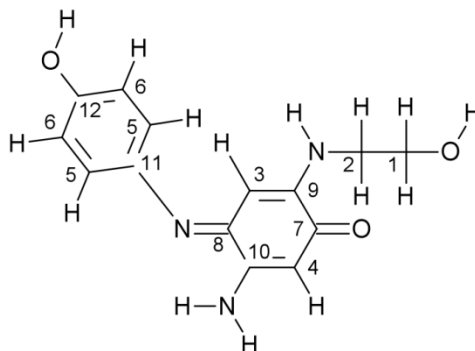


Figure 123: The proposed structure for dye molecule 274 with labelled carbons

Carbon	Shift / ppm
1	60
2	45
3	87
4	96
5 (x 2)	115
6 (x 2)	120

Table 15: The shifts for the carbons in dye molecule 274 as revealed by HSQC

This leaves carbons 7-12 within the dye molecule, which need to be defined. These carbons are all bonded to heteroatoms, with no protons directly attached, and so could potentially be detected by HMBC. This is a technique whereby carbons and protons that are separated by 2,3 and sometimes 4 bonds can be detected. Direct

^1H - ^{13}C interactions are not shown. The HMBC spectrum for dye molecule 274 is shown in *Figure 124*.

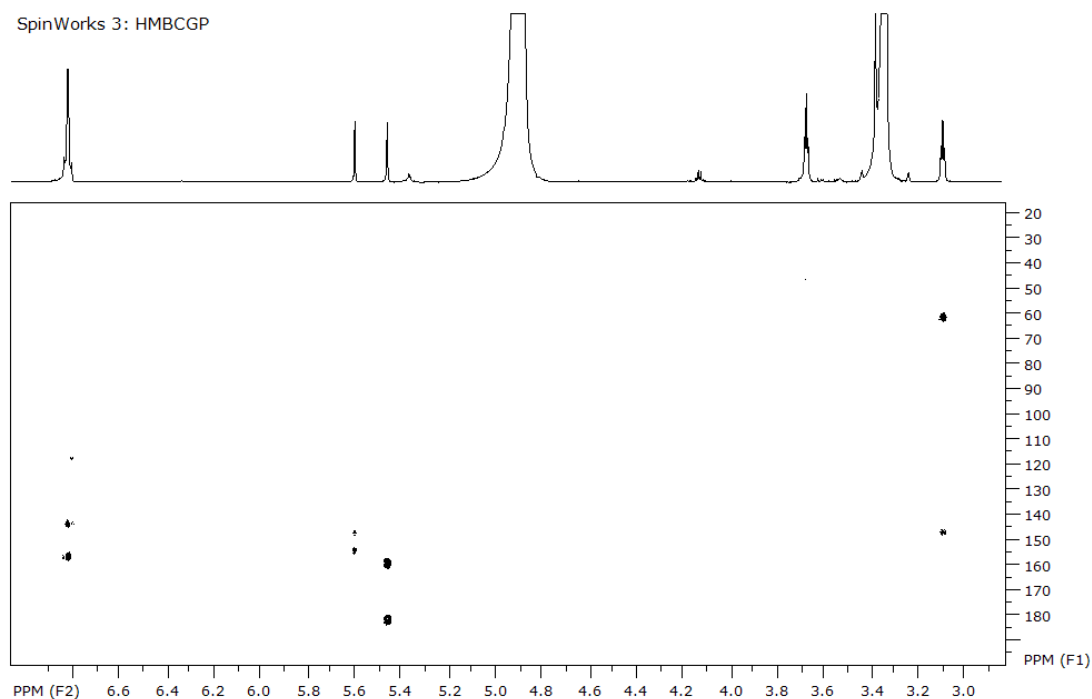


Figure 124: HMBC spectrum for dye molecule 274

The HMBC spectrum shows 6 new carbon signals (with chemical shifts different to those observed in the HSQC). These signals could correspond to the quaternary carbon atoms that are bonded to heteroatoms within the molecule. All the interactions observed from both HQSC and HMBC are shown in *Table 16*.

Proton	Shift / ppm	HSQC Carbon Interaction	HMBC Carbon Interaction(s)
A	3.63	1 (60 ppm)	2 (45 ppm)
B	3.10	2 (45 ppm)	1 (60 ppm), 9 (147 ppm)
C	5.47	3 (87 ppm)	7 (184 ppm), 8 (160 ppm), 9 (147 ppm)
D	5.55	4 (96 ppm)	9 (147 ppm), 10 (157 ppm)
E	6.74	5 (115 ppm)	11 (143 ppm), 12 (158 ppm), 5/6 (115/120 ppm)
F	6.78	6 (120 ppm)	11 (143 ppm), 12 (158 ppm), 5/6 (115/120 ppm)

Table 16: The HSQC and HMBC interactions with all proton environments for dye molecule 274

The total number of carbons observed by HSQC and HMBC match those for the postulated compound (*Figure 123*). HMBC interactions are evident between protons B and carbon 1, as well as between protons A and carbon 2, which are consistent with the MEA section of the molecule. There is also a weak interaction between protons B and the carbon adjacent to the nitrogen atom (9), showing that the MEA is attached to the quinonoid-like ring.

The aromatic signals couple to one another weakly (5 & 6) and also show coupling to two new carbon atoms, which can be assigned to the quaternary carbon atoms that are adjacent to the hydroxyl group (12) and the imine (11) on the PAP section of the molecule.

The proposal for the quinonoid-like ring is more complicated. The HMBC coupling between proton C with carbons 7, 8 (and weakly with 9), in addition to the coupling between proton D with carbons 9 and 10 indicate that the arrangement around this ring could be as postulated in *Figure 123* or alternatively as shown by the isomer in *Figure 125*.

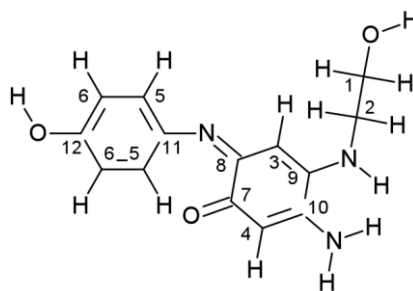


Figure 125: An alternative isomer for dye molecule 274

Despite failing to identify by NMR whether the dye structure is the *o*-iminoquinone or the *p*-iminoquinone, the basics of the structure have clearly been identified and MEA is definitely incorporated into the dye molecule.

It should also be noted that an MEA-incorporated dye is not observed in AHT systems, potentially due to the methyl group in the 6-position of AHT preventing MEA addition at this position. This would suggest that for MAP systems the structure in *Figure 123* is more likely, as the MEA would be free to attack the 6 position of MAP. This would explain why MEA inclusion is observed for MAP systems but not for those that use AHT.

The observation of this new dye in the PAP-MAP system led to the investigation of other compositions that might incorporate MEA into the formation of dyes.

5.3.6 Systems that incorporate MEA into dyes

Several different dye systems were studied by MS. Peaks were observed that could correspond to MEA incorporation, in a similar manner to the PAP-MAP system that was explored previously. The molecular ion peaks and proposed structures are shown in *Table 17* and *Table 18* (See Appendix for MS data). The equivalent dyeing formulations that contained ammonia were also studied, to confirm that these molecular ion peaks were present as a result of MEA. These spectra also ruled out

the possibility that ammonia behaves in a similar manner to MEA, with regards to incorporation into dye structures. The ESI-MS are also included in the appendix.

3-aminophenol

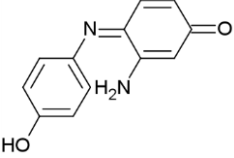
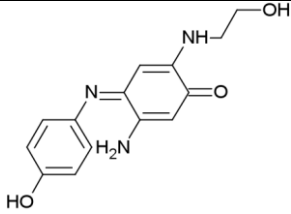
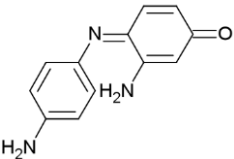
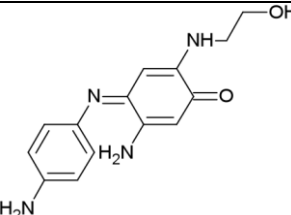
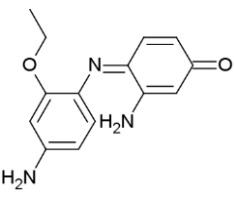
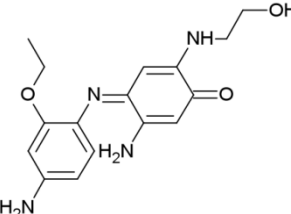
Precursor	Coupler	Dimer	MEA Incorporated
PAP	MAP		
Mass		214.07	273.11
PPD	MAP		
Mass		213.09	272.13
MBB	MAP		
Mass		257.12	316.15

Table 17: Proposed structures of dye products detected by MS on oxidation of dye systems containing MAP

1-Naphthol

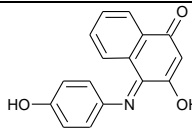
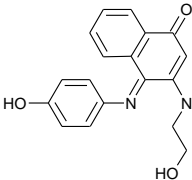
Precursor	Coupler	Hydroxylated	Mass
PAP	NAP		266.08
		MEA Incorporated	Mass
			308.12

Table 18: Proposed dye products detected by MS on oxidation of the precursors PAP and NAP

It was observed that MEA incorporation into the structure of dye molecules occurred when couplers were used that did not have functional groups in the 6-position. When couplers such as AHT were used, no peaks are seen in the MS that would indicate MEA inclusion in dye structures. This confirms that the structure of MEA incorporated dyes that is shown in *Figure 123* is most likely, as discussed previously on page 211. Additionally, the formulations that used naphthol as a coupler did not show that dimer molecules are produced. It is possible that a hydroxylated adduct of the dimer forms instead, due to the presence of the hydroxyl radical. A possible structure of this dye is shown in *Table 18*.

From the data collected, it is apparent that MEA is incorporated into dye structures in various products. However, it was considered to be necessary to show that the resulting dyes could be responsible for the different colours in formulations. This was achieved by observing the UV-vis spectra of the dyes in water. *Figure 126* and *Figure 127* represent the UV-vis spectra of PAP-MAP dimer and MEA incorporated PAP-MAP dimer, respectively. The spectrum for the PAP-MAP dimer shows one peak in the visible range with a λ_{max} of approximately 470 nm. There is also a shoulder in the absorbance at roughly 300 nm. For the MEA incorporated dye, the

peak in the visible region has shifted significantly, with the λ_{\max} now approximately 440 nm. A new peak is also apparent at $\lambda_{\max} = 340$ nm. This confirms that the dyes produced, as a result of MEA incorporation, are directly responsible for the different colours observed in these systems.

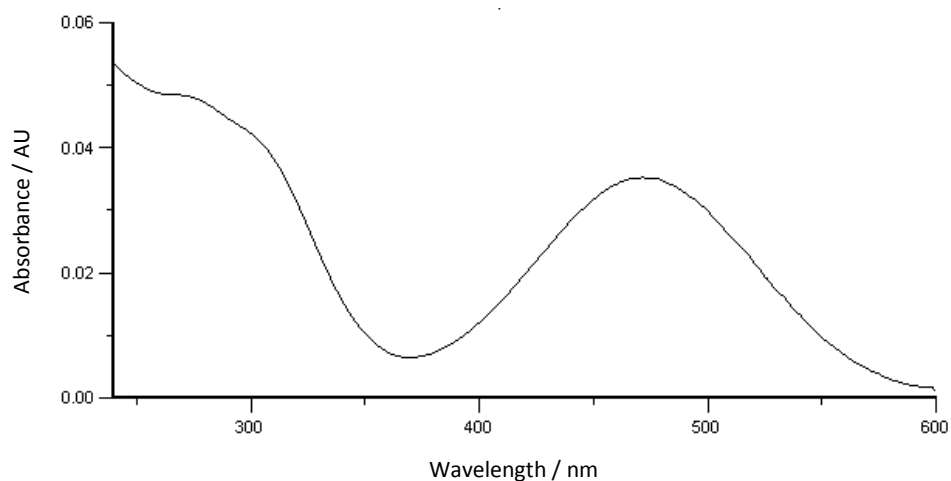


Figure 126: UV-vis spectrum for PAP-MAP dimer in H_2O .

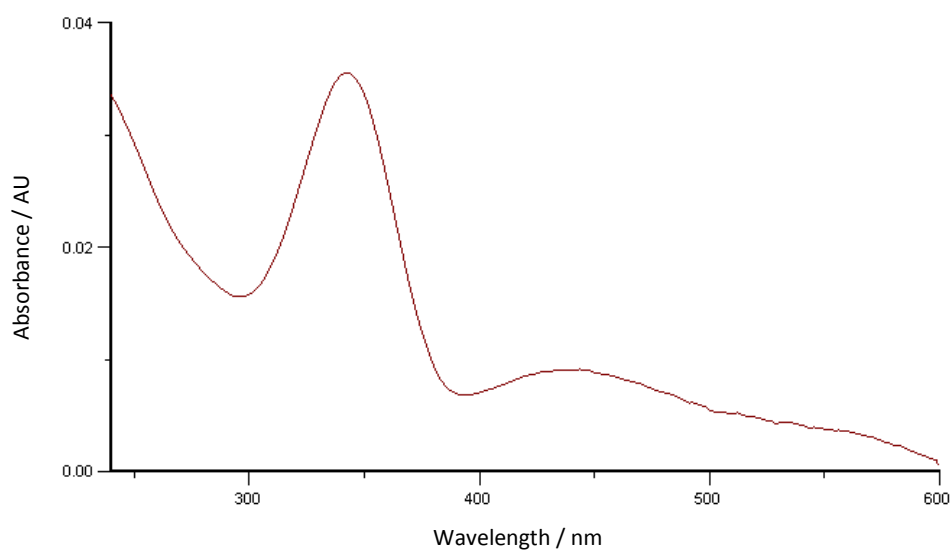


Figure 127: UV-vis spectrum of the MEA incorporated PAP-MAP dimer in H_2O .

These spectra confirm that the colour change in certain formulations could be due to the incorporation of MEA into the dye structures. Furthermore, although couplers such as 2-methyl-5-hydroxyethylaminophenol and 3-nitro-*p*-hydroxyethylaminophenol are used in permanent dye formulations, which lead to dye structures that are similar to the one shown in *Figure 123*, the inclusion of MEA during dye formation is not reported in the current literature.

Finally, having confirmed the incorporation of MEA into dye molecules for a variety of dyeing systems, it was of interest to attempt to identify the mechanism by which MEA can become included into the structures of dyes.

5.3.7 Mechanism of MEA incorporation

There were two possible mechanisms that were considered when studying how the inclusion of MEA into dye molecules might be possible. These mechanisms are similar to those discussed on page 184. Nucleophilic attack of MEA on the dimer, followed by further oxidation, can yield dye molecule 274, as shown in *Figure 128*. It is also possible that MEA could first be oxidised to give a protonated imine that could act as an electrophile and react with leuco dye to give the final dye product (*Figure 129*)^{227, 228}.

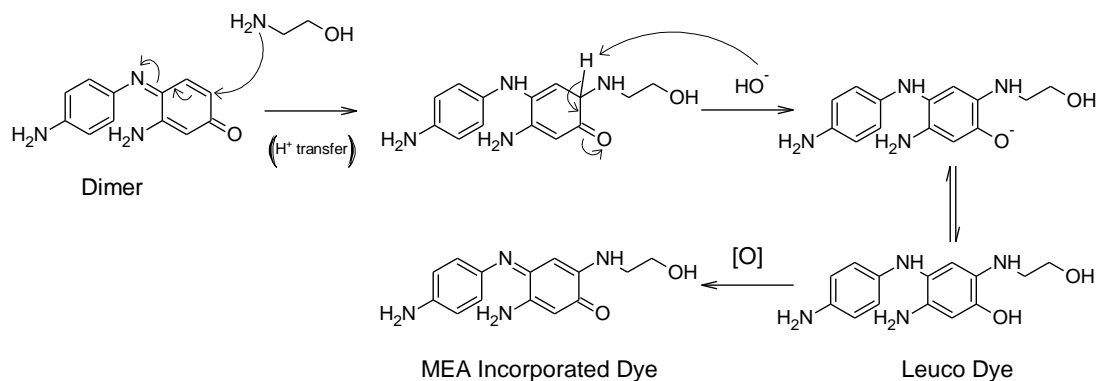
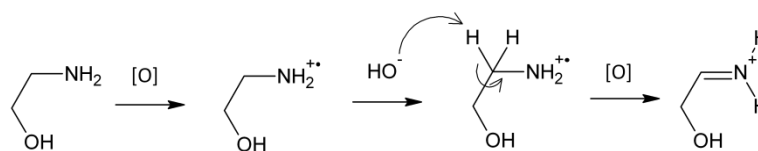


Figure 128: Mechanism to show the possible formation of dye molecule 274 by nucleophilic attack of MEA on PPD-MAP dimer.



Where [O] is Fe(III), Cu(II) or $\cdot\text{OH}$

Figure 129: Mechanism to show the possible generation of a protonated imine electrophile from MEA that could then react with leuco dye to give an MEA incorporated dye

Several experiments were set up in order to help determine the mechanism of MEA incorporation into the dye molecules, using MS. Firstly the dimer was generated using a system that did not contain MEA. The following conditions were used to generate the dimer on a reasonable time scale, without any excessive degradation of the dimer by the hydroxyl radical. Thus, NH_3 was used as the substitute for MEA.

400 mM NH_3 , 1.3 mM EDDS, 0.18 mM Cu(II), 70 mM H_2O_2 , 1mM PPD and 1 mM MAP, at pH 10 & 20 °C.

0.1 mL Catalase was added to the reaction mixture after 60 minutes in order to decompose hydrogen peroxide and the solution was left to stir overnight. The MS in *Figure 130* was obtained.

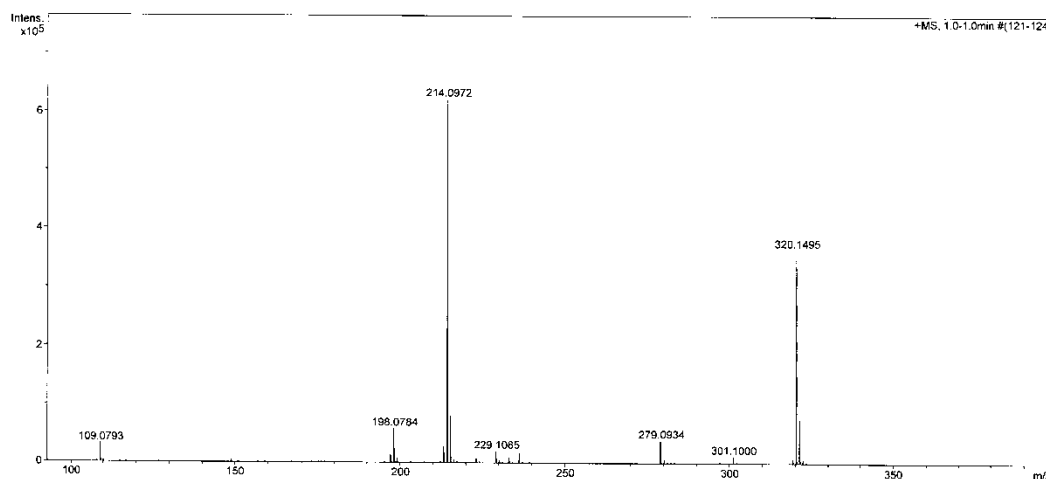


Figure 130: MS to show the formation of dyes in the following system: 400 mM NH₃, 1.3 mM EDDS, 0.18 mM Cu(II), 70 mM H₂O₂, 1 mM PPD and 1 mM MAP at pH 10 & 20 °C

The results show that there is formation of PPD-MAP dimer and trimer. Importantly no molecular ion peak is observed at 273 for the MEA incorporated dye, as expected in a system that does not use MEA as a base.

To this solution that contained the dimer was then added 800 mM MEA, the reaction was left to stir overnight. The MS in *Figure 131* was obtained.

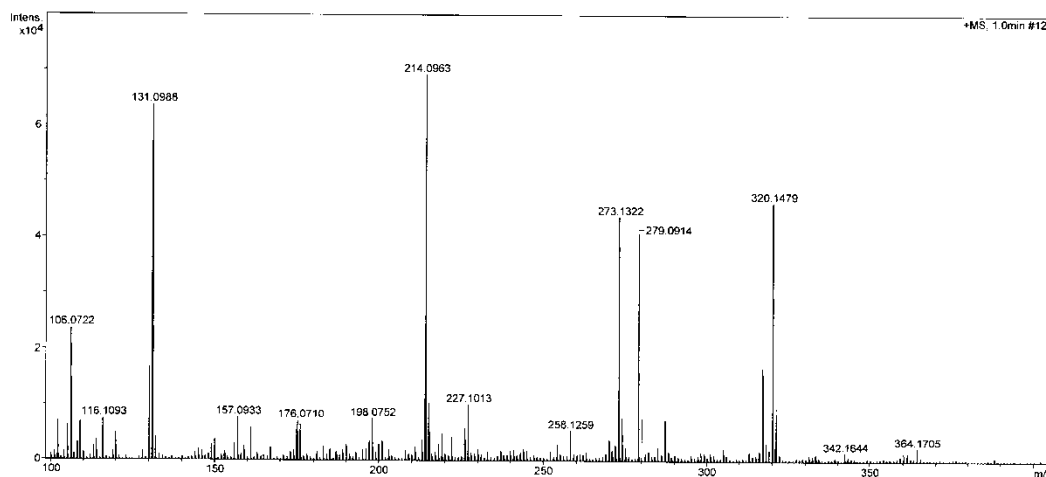


Figure 131: MS to show the formation of dyes in the following system: 400 mM NH₃, 1.3 mM EDDS, 0.18 mM Cu(II), 70 mM H₂O₂, 1 mM PPD and 1 mM MAP at pH 10 & 20 °C (+800 mM MEA)

The MS shows that there is a molecular ion peak at 273 that corresponds to MEA incorporated dye in the PPD-MAP system. The ratio of 273:214 (MEA dye: dimer) is roughly 0.6:1, showing that a substantial amount of MEA incorporated dye is formed, when left to react overnight. This suggests that when the dimer is formed independently of MEA and the reaction is stopped, MEA can then be added and still be incorporated into the dye. This information favours the mechanism of nucleophilic addition of MEA to dimer seen in *Figure 128*. In this instance all of the hydrogen peroxide was decomposed, so metal ions, such as Fe(III) or Cu(II) or oxygen could be responsible for the oxidation of MEA-leuco dyes to the final dyes.

5.4 Conclusions

The work described in this chapter was used to investigate possible reasons for the differences in colour formation in dyeing systems when MEA is used as a base as a replacement for ammonia.

The study of model aqueous dyeing formulations by UV-vis spectroscopy revealed that the rate of colour formation in the presence of MEA is greater than for the corresponding ammonia-based formulations. HPLC analysis of the same systems showed that there were no significant differences in the amounts of the dye couplers that were consumed during the reaction, when the base type is altered. This indicates that while there is unlikely to be a difference in the rate of dye formation, the rate of dye degradation could be greater in the ammonia system. This might be because MEA can act as a hydroxyl radical scavenger, preventing the degradation of dyes in MEA-based systems. This could potentially be the reason for the greater rate of colour formation observed in solutions containing MEA. If this effect occurs in real dyeing formulations, it could be a factor that contributes to the change in final shade of products that use MEA.

Alongside this difference in the rate of colour formation, another peak was apparent in the chromatograms that were obtained for the PAP-MAP system, when MEA was used as a base. Investigation of the source of this extra peak in this system led to the identification of a new dye that is formed by the inclusion of MEA into dye structures. The structure of this dye has been confirmed by MS and multiple NMR studies. This is shown in *Figure 123*.

The incorporation of MEA into the structure of dye molecules was investigated for several model aqueous compositions. It was found that it occurred when couplers were used that did not have functional groups in the 6-position, such as MAP and naphthol. The precursor that is used does not affect whether or not MEA incorporation occurs. MEA inclusion in dye structures results in the production of dyes with different electronic spectra to those produced in an ammonia system, thus altering the final shade of the formulation. It was also observed that ammonia

does not get incorporated into dye structures, in the same way that MEA does (*Figure 130*).

The primary mechanism for MEA incorporation into the dye molecules appears to be through the nucleophilic addition of MEA to pre-formed dimer molecules. It is not possible to rule out completely the possibility of MEA oxidation followed by electrophilic attack on the leuco dye intermediate. However, this work shows that the majority of MEA incorporation should occur by the former mechanism.

Nucleophilic attack of MEA on dimer molecules can compete with the nucleophilic attack of the unoxidised precursor onto the dimer. As a result, there would be a lower concentration of trimer in systems that incorporate MEA into the structure of dye molecules. This would affect the final concentration of dimer. As the MEA dye and trimer molecules are different shades, the final colour of dye formulations would vary due to the change in the ratios of the dyes formed in the presence of MEA. This could be the major reason for the differences in colour that are associated with the use of MEA in hair dye formulations containing certain couplers, in addition to the apparent increased rate of colour formation in the presence of MEA.

Chapter 6

Chapter 6 – Conclusions and Further Work

6.1 Summary

The principal aim of this study was to investigate the reasons for differences between hair colouring formulations that contain equivalent concentrations of MEA and ammonia. Additionally, the mechanisms of melanin bleaching and dye formation within hair fibres were studied.

Initially, the mechanism of soluble melanin bleaching was investigated using *Sepia* melanin sourced from cuttlefish. A correlation was observed between the concentration of the hydroxyl radicals and the extent of melanin bleaching that occurs. Bleaching in neutral solutions and in alkaline solutions showed that there was a relationship between the concentration of perhydroxyl anion and the extent of bleaching, for compositions with either a high hydroxyl radical flux or with a low hydroxyl radical flux. Furthermore, the rate of melanin bleaching due to the perhydroxyl anion was shown to be much greater for formulations in which the melanin was initially exposed to hydroxyl radicals. This evidence substantiates the mechanism of bleaching that was proposed by Korytowski⁴⁶, whereby single electron oxidants, such as the hydroxyl radical, can oxidise the DHI units in melanin to *o*-quinones. These *o*-quinone units are then broken down by the perhydroxyl anions.

Finally, during melanin oxidation it was proposed that ammonia is used purely to assist with the physical aspects of bleaching, as the rates of soluble melanin bleaching in both ammonia and sodium hydroxide were comparable. However, this does not exclude the possibility that the products of bleaching may vary when the base is changed.

After investigating the mechanism of melanin bleaching and the role of ammonia in oxidation, the effect of MEA on peroxide decomposition and on hair bleaching was studied. It is known from the literature that MEA causes more structural hair

damage and less melanin bleaching in hair bleaching systems. The chemical reasons for these differences were investigated.

Firstly, it was shown that whole hair fibres, containing natural levels of copper, result in more hydrogen peroxide decomposition in aqueous solutions of MEA when compared with aqueous solutions of ammonia. When the Cu(II) concentrations were increased, the ammonia-based compositions became more active in breaking down the peroxide group. This led to the investigation of homogenous model bleaching systems, to investigate the differences in chemistry that might cause changes in the extent of peroxide decomposition. It was found that the formation of different metal complexes in solution was the main reason for differences in the peroxide breakdown in aqueous solutions. This was either due to the different organic bases binding directly to the metal ions, or to a change in pH as result of the degradation of organic material. In real bleaching formulations that contain EDTA or EDDS, these are not factors that would arise.

MEA degraded under various conditions and the products of degradation varied in type and amount, depending on the conditions of the bleaching system. Formic acid and HEI are two of the major products that have been identified by this work (though there are multiple additional products that may form). Previous work has shown that production of formic acid can result in foaming of amine solutions. Foaming has been observed by Procter & Gamble when using MEA in hair bleaching systems, showing that MEA degradation may occur in real formulations. As discussed in chapter 3, various literature sources suggest that the oxidation of MEA occurs via a radical pathway, with the formation of carbon-centred radicals. These carbon-centred radicals may react with hair proteins and result in increased levels of hair damage in MEA systems.

The rate of soluble melanin bleaching in aqueous solutions of MEA and in ammonia-based aqueous solutions was also found to be comparable. This confirms that physical factors are primarily responsible for the differences in the level of bleaching observed in MEA systems. The most likely cause of this difference is the varying rate of the diffusion of hydrogen peroxide into the cortex (where melanin is

situated), as the solubilisation of heterogeneous melanin in MEA and ammonia solutions was also found to be similar.

Pulverised hair was used to replicate the environment found within the hair fibres, so that the effect of base on peroxide decomposition inside the hair could be studied. A similar pattern of peroxide decomposition was observed to the whole hair fibre systems, again due to the different complexes that are formed in solution, when the base is altered. However, less peroxide decomposition was evident in these systems than in the solutions that contained whole hair fibres. This is potentially due to the fact that when hair is pulverised, keratin is accessible and can bind metal ions. The possible formation of keratin-metal complexes may result in the inhibition of hydrogen peroxide decomposition. The complex nature of metal binding inside hair fibres results in varying extents of hydrogen peroxide decomposition in ligand-free systems. However, when chelants such as EDTA or EDDS are added, oxygen evolution becomes negligible during bleaching reactions. Therefore, the extent of hydrogen peroxide decomposition is unlikely to vary if the base is changed in commercial hair formulations that usually contain EDTA or EDDS.

As well as the differences that arise in the use of hair bleaching systems that are observed when ammonia is replaced with MEA, differences in model hair dyeing formulations were investigated. Firstly however, the mechanism of hair dye formation inside hair fibres was investigated, as it was not known exactly what was responsible for the oxidation of dye primaries inside hair. Additionally, it was discovered that catalase could accelerate the rate of dye formation in solutions dramatically, in the presence of hydrogen peroxide. Knowing that catalase is present in hair follicles it was decided to investigate whether this could be a potential species that accelerates dye formation in hair fibres. In order to do this pulverised hair was used in aqueous dye baths to mimic the environment inside hair fibres. It was found that metal atom centres in the hair are responsible for the acceleration of dye formation in hair fibres. Furthermore, there was evidence to suggest that Fe(III) complexes are the more likely cause of primary oxidation. However, further evidence is required to ascertain whether or not these Fe(III) centres are bound in an enzymatic environment, such as catalase. If the iron ions

were bound in such an environment, then the nature of the binding would also be of interest. Cu(II) and Fe(III) were evaluated as potential redox metal ions that could be responsible for dye precursors oxidation. It is possible that other redox metal ions, such as manganese, are present in the hair fibres in low concentrations and could contribute to dye oxidation¹⁷⁶. However, as the hair was always from the same source and treated in the same way, it can be assumed that the concentration of these redox metal ions is constant for the hair samples studied. Thus, they should not affect the findings of this study.

Differences in the final shade of hair dye formulations containing MEA were investigated by measuring the rate of dye formation in aqueous solutions. It was found that there were no major differences in the rates of dye formation. However, a lower rate of dye degradation in the MEA-based composition could result in an apparent increase in the overall rate of colour formation. When dyes were produced using MAP and naphthol couplers, it was discovered that MEA became incorporated into the structure of the dye molecules. The structure of an MEA dye formed in the PAP-MAP system was characterised and found to have a different UV-vis spectrum relative to that of dimer and trimer dyes that are formed in this system. Changes in the colour of MEA formulations are therefore a direct result of the formation of MEA-containing dyes. Additionally, the formation of MEA-incorporated dyes would affect the amounts of dimer and trimer that are present in MEA formulations, which would have the effect of altering the final shade of the formulation. The most likely mechanism of MEA-incorporation was considered to be that of nucleophilic addition of the MEA.

6.2 Concluding Remarks

6.2.1 The mechanism of hair bleaching and dyeing

Evidence has been obtained to show that the perhydroxyl anion and the hydroxyl radical are involved in the bleaching of soluble melanin, which suggests that melanin bleaching can occur in such compositions, via the mechanism postulated by Korytowski⁴⁶. However, the data acquired from bleaching systems at pH 7 shows that this may not be the only pathway of melanin oxidation during hair bleaching. Rapid melanin oxidation was evident at low perhydroxyl anion concentrations, where there was a high hydroxyl radical flux (*Figure 47*). Therefore, an alternative pathway of soluble melanin bleaching by hydroxyl radical alone has been proposed.

Currently, it is assumed that alkaline hydrogen peroxide is responsible for the rapid formation of hair dyes within hair fibres. This work has shown that endogenous iron atom centres are also vital for the formation of dyes within the hair shaft. The environment of the metal atom centres in which the acceleration of dye formation occurs is unknown. However, it has been speculated that the iron atoms could be bound in an enzymatic environment, such as catalase.

6.2.2 The Effect of MEA on hair colouring formulations

In conclusion, this work has shown that the chemistry of melanin bleaching does not change when MEA is used, as a replacement for ammonia, in model bleaching systems (for the concentration ranges studied). Therefore, a physical factor is presumably responsible for the lower extent of melanin bleaching observed in hair bleaching formulations that contain MEA. The most likely physical reason for this difference is the extent to which hair fibres are swollen when the base is changed. This would lead to varying diffusion rates of oxidants into the hair cortex where melanin is found.

By contrast, the chemistry of the behaviour of the “model” dyeing formulations changes significantly when ammonia is replaced with MEA. Firstly, the rate of colour formation increases in solutions that contain MEA. This is hypothesised to be due to a lesser amount of dye degradation in these systems. Varying rate of colour formation, based on changing dye degradation rates, is therefore a factor that could explain the disparity in the final shade of dye formulations, when the base is changed. Additionally, it has been confirmed that MEA becomes incorporated into the structure of dye molecules in model aqueous formulations, leading to the formation of different dye molecules. These dye molecules are also responsible for changes to the colour of aqueous model formulations that use MEA.

6.3 Further Work

The work undertaken goes some way to identifying and explaining the differences that emerge when ammonia is replaced with MEA in hair bleaching and dyeing formulations. Additionally, it provides some mechanistic insights into the mechanism of melanin bleaching and dye formation inside hair fibres. There are several areas where further research could provide more insights into the chemistry of bleaching and dyeing formulations that are based on the use of MEA.

During soluble melanin bleaching in ligand-free formulations, an absorbance at 400 nm was observed in the UV-vis spectra that could correspond to the build-up of *o*-quinone units in melanin, due to a high hydroxyl radical flux. By using in situ IR, an estimation of the relative amounts of *o*-quinone and DHI units can be made during this reaction. An increase in *o*-quinone units could provide further evidence for the mechanism of bleaching proposed by Korytowksi.

Melanin is known to degrade into various pyrroles. The types of pyrroles that form from the oxidation of melanin could vary depending on the conditions that are used for bleaching. Identification and quantification of the pyrrolic acids formed during

melanin degradation, under various conditions, may also provide further insights into the role of oxidants in the breakdown of the melanin.

MEA degradation during hair bleaching is also likely to result in a variety of products when the conditions are changed¹⁸⁵. Separation techniques could be used to identify and to quantify the degradation products formed under various bleaching conditions. This could help to identify the main cause of foaming when MEA is used in colouring systems. Carbon centred radical intermediates that are potentially formed during the degradation of MEA may also be detected and quantified by EPR. This may help to determine whether or not these radicals play a role in damaging hair fibres.

The formation of dye molecules within hair fibres is most likely due to the presence of iron(III) complexes within the hair fibre. Due to the fact that catalase is present in the hair follicles and can catalyse the oxidation of aromatic amines and phenols, it was postulated that the Fe(III) centres that are responsible for increased primary oxidation could be present within the enzyme catalase. However, the direct detection of catalase in hair fibres is needed in order to confirm this hypothesis.

MEA was also shown to become incorporated into the structure of dye molecules when used in model aqueous dyeing formulations. A variety of dye formulations that contain MEA can be investigated using the methods described in this work, in order to determine which other systems, if any, result in the inclusion of the base into dye molecules. In this way hair colourants containing MEA as a base could be shade formulated more easily.

Chapter 7

Chapter 7 – Experimental

7.1 Materials and chemicals

All chemicals were reagent grade and purchased from Sigma-Aldrich, unless stated otherwise. All solvents used were purchased from Fisher Scientific. Deuterated solvents were purchased from Sigma-Aldrich. Buffers for pH probe calibration were purchased from Fisher Scientific. AHT, AMC, DTS, HDP, MBB, MEA, 2-methyl resorcinol, 1-naphthol, PAP and resorcinol were kindly supplied by Procter & Gamble. Cuttlefish ink for the *Sepia* melanin preparation was purchased from www.frozenfishdirect.co.uk, supplied by Nortindol Sea Products S.L. The cuttlefish ink also contained E-466 thickener (sodium carboxymethyl cellulose).

Where water was used in reactions it was deionised water, from the University of York. Where water was used in HPLC methods, it was HPLC grade, supplied by Fisher Scientific.

An aqueous suspension of 20 – 50 mg mL⁻¹ catalase from bovine liver was used for this study, (10,000 – 40,000 units / mg protein), purchased from Sigma-Aldrich. Catalase was used throughout this study to decompose hydrogen peroxide in alkaline aqueous solutions, at room temperature. It is known that at alkaline pH catalase can denature. However, this is only partial denaturation at pH 10 (general conditions used throughout the study)²²⁹. Catalase only denatures fully above pH 12.²³⁰

NPDPA was originally synthesised by Kazim Naqvi of the Victor Chechik group, according to the synthesis of Singh and Hider¹⁰⁴.

The pulverised and whole hair samples were provided by Kerling International Haarfabrik GmbH, based in Germany. The samples were comprised of a blended source of natural female European human hair strands in different levels of shade, 3/0 to 9/0. Before it was used in studies, the hair strands were washed with

laboratory neutral shampoo and rinsed in water for varying time periods (0 minutes – 120 minutes), to change the level of copper within the hair. The Cu(II) ion content was then analysed, using ICP (See section 7.2 Instrumentation / techniques). The hair samples were not pre-treated with any colouring formulations. Pulverised hair samples were prepared using the same treated whole hair samples (The preparation procedure is described in section 7.2 Instrumentation / techniques).

7.2 Instrumentation / techniques

NMR – All 1D NMR spectra have been recorded using a JEOL ECX400 or JEOL ECS400 ($^1\text{H} = 400 \text{ MHz}$, $^{13}\text{C} = 100 \text{ MHz}$). Spectra were then analysed using ACDLABS 12.0 NMR Processor. ^1H NMR spectra were acquired using 64 scans and ^{13}C NMR using 1024 scans.

2D NMR (^1H COSY, HSQC and HMBC) were recorded using a Bruker AVII 700 (700 MHz). Spectra were analysed using SpinWorks.

MS – Mass spectra were obtained using a Bruker micrOTOF mass spectrometer. ESI positive is used in all cases, except where stated otherwise. Reports were exported to .pdf using MassLynx MS Software.

UV-Vis – Spectra were recorded using a Hitachi U-3000 spectrophotometer, in quartz cuvettes of pathlength 10 mm. Data were processed using Microsoft Excel.

HPLC – Separation of dye precursors and dyes was achieved using a Gilson 321 HPLC pump, with a 234 auto-sampler and a 170 DAD detector. Data acquired was processed using UniPoint version 3.0 software, Spectrum Viewer and Microsoft Excel. The following method, developed by Procter & Gamble, was used:

Column: C18 (ODS) (250 mm x 4.6 mm x 5 μm)

Eluent: 99% 20 mM ammonium formate (pH 7), 1% acetonitrile for 5 minutes, ramp to 50% ammonium formate, 50% acetonitrile over 45 minutes and hold for 10 minutes. The column is then equilibrated for 20 minutes with 99% ammonium formate, 1% acetonitrile.

Flow rate: 1 mL min⁻¹

HPLC-MS – Chromatograms were obtained using the same method and column as regular HPLC, with the exception of the buffer which was 10 mM ammonium formate (pH 7) and a lower flow rate of 0.2 mL min⁻¹.

EPR – Solutions of 20 mM NH₄OH, 0.18 mM Cu(II), 1.3 mM EDTA and/or 0.06 mg mL⁻¹ Sepia MFA at pH 10 were prepared. Spectra of the resulting Cu(II)-EDTA and Cu(II)-*Sepia* MFA complexes were acquired on a Bruker EMX spectrometer at 140 K with the following parameters:

Centre Field: 3062.79 G (Sweep width: 1600 G)

Time constant: 163.84 s

Received gain: 1.00237 x 10⁴

Modulation amplitude: 4 G

Microwave power: 5.024 mW

Elemental Analysis – The elemental composition of samples of *Sepia* melanin and MFA were acquired using an Exeter Analytical CE-440 Analyser. Mean values of % C, % H and % N were determined from 2 separate runs and compared to literature values.

pH – All pH measurements have been obtained using a Jenway 3505 pH meter, calibrated using buffers from Fisher (4, 7 and 9.2) on day of use.

ICP-MS – ICP analysis of Cu(II) ions in hair samples was acquired by Northumbria Water at the request of Procter & Gamble. Fe(III) amounts were analysed at the Trace Elemental Analysis Laboratory, University of Hull.

Hair Pulverisation – Treated whole hair samples were cryo-pulverised by Procter & Gamble, using a 6850 Freezer/Mill, filled with 15 L of liquid nitrogen. Hair samples were cut into pieces, placed in milling vials and loaded into the freezer. Milling parameters were:

Rate (Impact Frequency): 13

T1 (Grinding Time): 2 minutes

T2 (Re-Cooling Time): 2 minutes

T3: (Pre-Cooling Time): 2 minutes

This led to pulverised hair particles with a length ranging from a few nm to a maximum of 300 μm . At the time of publishing, the size distribution of the particles was unknown.

7.3 Preparation of buffer solutions containing either ammonia or ethanolamine

When studies were performed that used ammonia or ethanolamine buffer solutions, at pH 10, the concentration of each base was kept equivalent (usually at either 400 mM or 20 mM). The differing molar masses and densities of the bases were taken into account when preparing these solutions of equivalent concentration. The stock solutions were then buffered to pH 10, using ammonium chloride for the ammonia solutions or acetic acid for the ethanolamine solutions.

It was recognised that the concentration of free base varies upon changing the base from ammonia to ethanolamine, due to the small differences between the pK_a values of the two bases. However, it was determined, using the Henderson-Hasselbalch equation that this resulted in an insignificant difference in the concentration of free base present in each composition.

7.4 Isolation of *Sepia* melanin

Sepia melanin was isolated from 50 g of cuttlefish ink by stirring in 100 mL of 2 M HCl for 30 minutes at 20 °C. The resulting solution was then stored at 10 °C for 24 hours. This solution was then centrifuged at 3400 rpm for 40 minutes. The resulting pellet was washed three times with 0.5 M HCl, deionised water, acetone and finally with deionised water again. Any residual solvent was then removed on a rotary evaporator and then the product was kept under vacuum on a Schlenk line overnight. Approximately 5 g of melanin were isolated.

7.5 Conversion of *Sepia* melanin to *Sepia* MFA

300 mg of *Sepia* melanin were rehydrated in a few drops of deionised water overnight before the addition of 60 mL of 0.2 M NH_4OH , containing 326 mM H_2O_2 . As no additional metal ions were added to the solution, this provided a relatively mild oxidation, when compared with the bleaching studies in chapter 2. This solution was stirred for 60 minutes at 20 °C and quickly filtered to remove any *Sepia* melanin that had not been converted to MFA. The filtrate was then acidified to approximately pH 2 and centrifuged at 3400 rpm for 40 minutes. The pellet was then washed three times with 0.01 M HCl and 32 mM HCl in methanol until the washings were colourless. MFA was then washed once with anhydrous methanol, before it was placed on a rotary evaporator and stored under vacuum on a Schlenk line overnight. Approximately 100 mg of MFA were recovered.

7.6 Monitoring the bleaching of *Sepia* Melanin by UV-vis

The kinetics of *Sepia* melanin bleaching were observed by monitoring the absorbance of melanin between 800 – 300 nm, with readings taken at 0.5 nm intervals. Scans were made every 2 minutes over a reaction time of 2 hours at 20 °C. The decreasing absorbance at 532 nm was then plotted in a graph against time, using Microsoft Excel, to show the kinetics.

7.7 Monitoring the hydroxyl radical flux of Fenton-like systems

Hydroxylation of the colorimetric probe NPDPA was recorded by monitoring the absorbance between 600 – 200 nm, with readings taken every 2 nm. Scans were made every 2 minutes over a reaction time of 2 hours at 20 °C. The increasing absorbance at 430 nm was then plotted in a graph against time, using Microsoft Excel, to show the kinetics of hydroxyl radical production.

7.8 Determination of the hydrogen peroxide decomposition

Hydrogen peroxide decomposition was monitored by measuring the production of molecular oxygen in various Fenton(-like) reactions, throughout this work.

Oxygen production was monitored by the displacement of oxygen using the equipment shown in *Figure 132*.

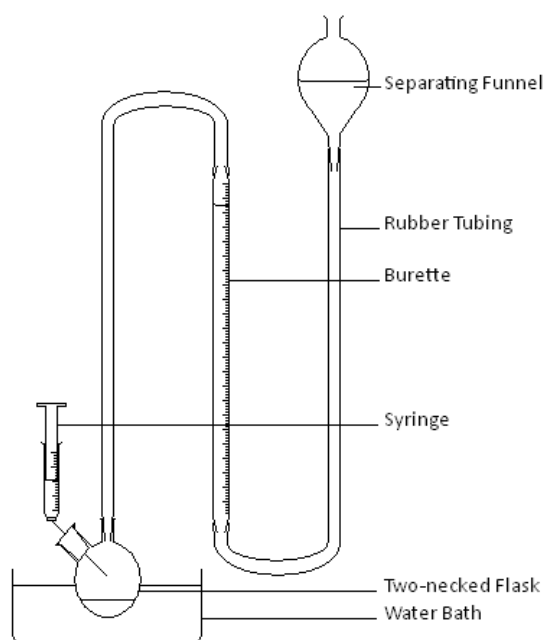


Figure 132: Diagram to show the experimental setup that was used to monitor hydrogen peroxide decomposition in Fenton(-like) reactions.

The reaction was setup inside the two-necked flask (with the exception of hydrogen peroxide). The rubber tubing was connected and a Suba-Seal ensured that the system was air-tight. The closed system was tested for leaks and the initial water level in the burette was recorded. Hydrogen peroxide was then injected, through the Suba-Seal, to initiate the reaction. During injection another needle was in place through the Suba-Seal, in order to displace air from the system and account for the added injection volume. This was left in place for a few seconds for the system to equilibrate before it was removed. The level of water in the burette was then monitored over the course of the reaction. When measuring the volume of water in the burette, it was considered to be important to keep the temperature constant at 20 °C. This was done using a stirrer hotplate and thermocouple. It was also important to ensure that the level of water in the separating funnel was at the same height as the level in the burette, so that pressure did not affect the reading²³¹.

The volume of oxygen that was recorded was then converted to moles and a molar ratio of 1:2 was applied, in order to determine the number of moles of hydrogen

peroxide that was decomposed. Using the initial number of moles of hydrogen peroxide, the percentage of hydrogen peroxide was determined for each time point. Graphs of time against the percentage hydrogen peroxide decomposition were then plotted, using Microsoft Excel.

The quantity of remaining hydrogen peroxide, as indicated by this water displacement method, was verified by iodometric titration, to ensure accuracy of the method²³². 25 mL of the diluted reaction mixture were added to 100 mL of 1 M sulphuric acid. To this 10 mL of 10% potassium iodide solution was added, followed by 3 drops of ammonium molybdate. This was then titrated against 0.1 M sodium thiosulfate and 2 mL of starch solution was used to clarify the endpoint. A blank determination was also run to improve the accuracy of the titration.

7.9 Verification of hydrogen peroxide concentrations by titration

After hydrogen peroxide decomposition was measured by oxygen evolution, the remaining hydrogen peroxide in solution was occasionally checked by iodometric titration. This was to ensure that the volume of oxygen produced during the break down of hydrogen peroxide represented the extent of decomposition that occurred. The procedure for iodometric titrations described by Vogel was followed, in order to determine the concentration of hydrogen peroxide²³². 2 mL of reaction solution was added gradually, whilst stirring, to a 10 mL solution of 10% potassium iodide and 100 mL 1 M H₂SO₄. To this was then added 3 drops of ammonium molybdate solution (3%). The final solution was then titrated against 0.1 M sodium thiosulfate immediately. 2 mL of starch solution was added when the colour of iodine was nearly discharged, to clarify the end point of the titration. Repeat titrations were performed until the readings were within 0.1 mL.

7.10 Phosphate ion analysis during the Fenton-like degradation of HEDP

Phosphate ion analysis was carried out using a method developed by Murphy and Riley²³³. A combined molybdenum reagent consisting of 2.5 N H₂SO₄, 4.85 mM ammonium molybdate, 30 mM ascorbic acid and 0.21 mM potassium antimonyl tartrate, was prepared prior to the analysis. Using this reagent, a calibration curve was created using samples with a phosphate ion concentration over the range of 0.25 – 1.25 ppm. In order to do this, a 40 mL sample of the required concentration phosphate standard was added to 8 mL of the combined reagent and made up to 50 mL. The combined mixture was shaken and left for 15 minutes before being studied by UV-vis spectroscopy. The absorbance at 882 nm, due to the resulting molybdenum blue complex, was used to construct the calibration curve. This was then used to determine the concentration of phosphate ions in solutions containing 20 mM MEA, 1.3 mM HEDP, 0.18 mM Cu(II) and 0.979 M H₂O₂ at pH 10, over the course of the Fenton-like reaction at 20 °C.

7.11 GC analysis MEA degradation products

Solutions containing 400 mM MEA, 0.18 mM Cu(II) and 0.979 M H₂O₂ at pH 10 were reacted for 120 minutes at 20 °C. 3.42 mM glycerol was added as an internal standard and a 1 in 4000 dilution in methanol was made. A 1 µL injection was then made onto a RTX-50 column (30 m x 0.32 mm x 1 µm). A HP 5890 Series II GC was used in conjunction with a HP 3396A Integrator, to obtain chromatograms using the conditions shown in *Table 19*.

Initial temperature / °C	100
Initial hold time / minutes	1
Ramp rate / °C min ⁻¹	20
Final temperature / °C	240
Final hold time / minutes	5
Injection temperature / °C	280
Detector Temperature / °C	250
Column head pressure / PSI	19
Flow rate / mL min ⁻¹	7

Table 19: The conditions used to obtain chromatograms for solutions of degraded MEA.

When GC-MS was used, chromatograms and EI mass spectra were acquired using a Waters GCT Premier Mass Spectrometer coupled to an Agilent 6890 GC. The conditions used were the same as those identified in *Table 19*, with the exception of a lower flow rate of 1 mL min⁻¹.

7.12 Binding Constants

Database 46: NIST Critically Selected Stability Constants of Metal Complexes, Version 8 was used to report all the binding constants in this work.

7.13 Speciation curves of metal complexes

HYDRA (Hydrochemical Equilibrium-Constant Database) was used to create input files for MEDUSA (Make Equilibrium Diagrams Using Sophisticated Algorithms) in order to create speciation curves. These curves show the metal complexes that are

present in a variety of infinitely dilute aqueous formulations of infinite dilution, between pH 1 – 14, at 25 °C. Procter & Gamble provided data plot files for the ligands and the bases used in this work. Speciation plot data was exported and processed using Microsoft Excel.

7.14 Monitoring dye formation in aqueous systems by UV-vis

1 mM PAP and 1 mM AHT was oxidised, at 20 °C, in the presence of 400 mM NH₃, 1.3 mM EDDS, 0.18 mM Cu(II) and 70 mM H₂O₂ at pH 10. The absorbance of these solutions was monitored between 700 – 200 nm, to show the kinetics of formation of PAP-AHT dimer.

Where experiments to observe the effect of hair or catalase are described, the above reactions were generally monitored for 30 minutes before the addition of either 0.1 mL of catalase or 10 mg of pulverised/whole hair, which was stirred for 1 minute before it was centrifuged at 3400 rpm for 5 minutes. The supernatant solution containing the dye was replaced in UV cuvettes and the monitoring of dye formation was continued between 700 – 200 nm, for a further 24 minutes at 20 °C. The absorbance at 550 nm was plotted against time in Microsoft Excel to show the kinetics of dye coupling.

7.15 HPLC analysis of dye formation

The following general reaction composition was studied in order to quantify dye production, using HPLC:

400 mM base, 1.3 mM EDDS, 0.18 mM Cu(II), 70 mM H₂O₂, 1 mM precursor and 1 mM coupler, at pH 10.

The base used was either MEA or NH₃. The precursors studied were PPD or PAP and the coupler was either AHT or MAP. The reaction mixture was stirred for 30 minutes

at 20 °C before the addition of 0.14 mM *p*-hydroxybenzoic acid as an internal standard. A partial loop injection of 90 µL was made at reaction times of 30 and 120 minutes. The HPLC method is described on page 231.

Chromatograms and UV spectra of peaks were processed using Gilson Unipoint Version 3.0 and Microsoft Excel. Peak areas of chromatograms were integrated using Spectrum Viewer Basic 2.6.3.

7.16 Separation of the MEA dye molecule in the PAP-MAP system

The PAP-MAP dimer that incorporates MEA was synthesised in a solution containing 400 mM MEA, 1.3 mM EDDS, 0.18 mM Cu(II), 0.979 M H₂O₂, 37 mM PAP and 37 mM MAP, at pH 10, for 14 hours at 20 °C. The reaction mixture was centrifuged at 3400 rpm for 20 minutes and the precipitate washed with methanol. Approximately 200 mg of precipitate was recovered. TLC of the precipitate, using 7 CHCl₃: 2 EtOAc: 1 EtOH²²⁵, revealed 3 major components at R_f values of 0, 0.3 and 0.5. Mass Spectrometric evaluation of the components showed these to be a mixture of larger oligomeric dyes, the MEA incorporated dye and PAP-MAP trimer respectively.

Flash column chromatography, using the same solvent system, was used initially to separate the MEA-incorporated dye at R_f = 0.3. Preparatory TLC, again using the same solvent system, was required for further purification, due to excessive tailing of the PAP-MAP trimer component at R_f = 0.5. Methanol was used to extract 0.9 mg of the purified MEA-incorporated dye molecule. This was re-dissolved in deuterated methanol for NMR analysis.

Appendix

MEA incorporation in dyeing systems (Chapter 5)

The MBB-MAP system

A reaction formulation containing 400 mM MEA, 1.3 mM EDDS, 0.18 mM Cu(II), 70 mM H₂O₂, 1 mM MBB and 1 mM MAP at pH 10 was left for 2 h at 20 °C. The ESI mass spectrum shown in *Figure 133* was acquired. The molecular ion peak at 258 is indicative of the MBB-MAP dimer and the peak at 317.1611 represents the MEA incorporated dye for this combination (structures shown in *Table 17*). Multiple unknown peaks have also been detected, which may be present due to the degradation of organic material, such as MEA or EDDS during this reaction.

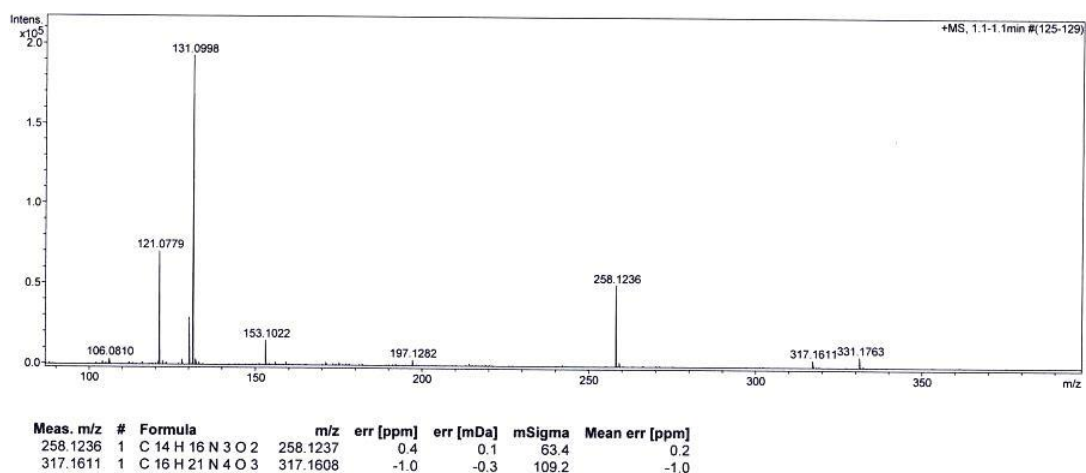


Figure 133: Mass spectrum for the product of a reaction solution containing 400 mM MEA, 1.3 mM EDDS, 0.18 mM Cu(II), 70 mM H₂O₂, 1 mM MBB and 1 mM MAP, at pH 10, after 2 h at 20 °C.

The PPD-MAP system

For a reaction containing 400 mM MEA, 1.3 mM EDDS, 0.18 mM Cu(II), 70 mM H₂O₂, 1 mM PPD and 1 mM MAP at pH 10, the ESI mass spectrum in *Figure 134* was acquired after 2 h of reaction at 20 °C. PPD-MAP dimer is responsible for the molecular ion peak at 214, whilst a small peak is present at 273, that corresponds to the MEA incorporated dye for this system. Again the structures of these dyes are shown in *Table 17*.

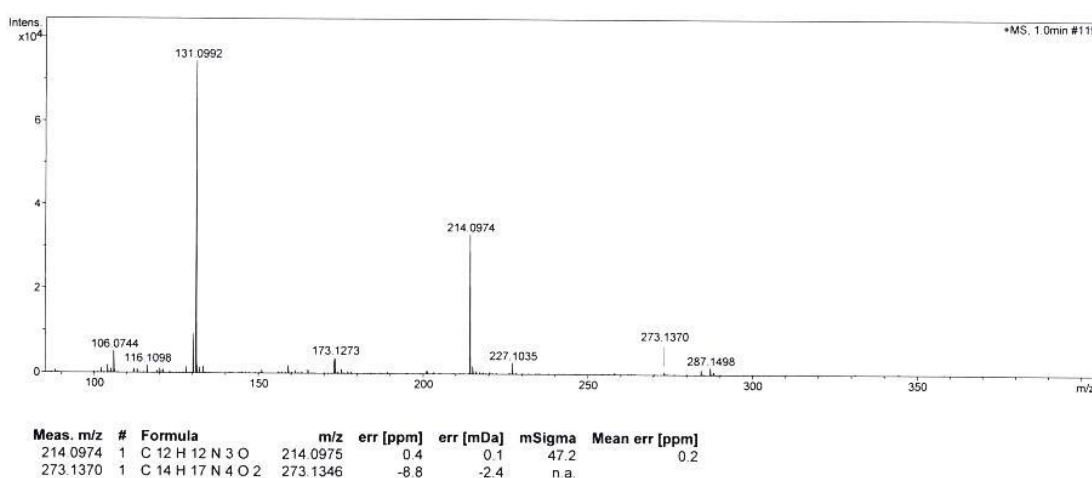


Figure 134: Mass spectrum for a reaction solution containing 400 mM MEA, 1.3 mM EDDS, 0.18 mM Cu(II), 70 mM H₂O₂, 1 mM PPD and 1 mM MAP, at pH 10, after 2 h at 20 °C.

Tandem mass spectrometry (MS/MS) was performed on the molecular ion peak of the MEA incorporated dye, to determine the fragment ions of this molecule (*Figure 135*). This was to gain further insight into the structure of the dye. The peak at 213.9 represents a fragment ion, with the loss of 60.1 from the dye, which corresponds to a loss of MEA from the original dye. This is further proof of the inclusion of MEA into dye molecules in the PPD-MAP system.

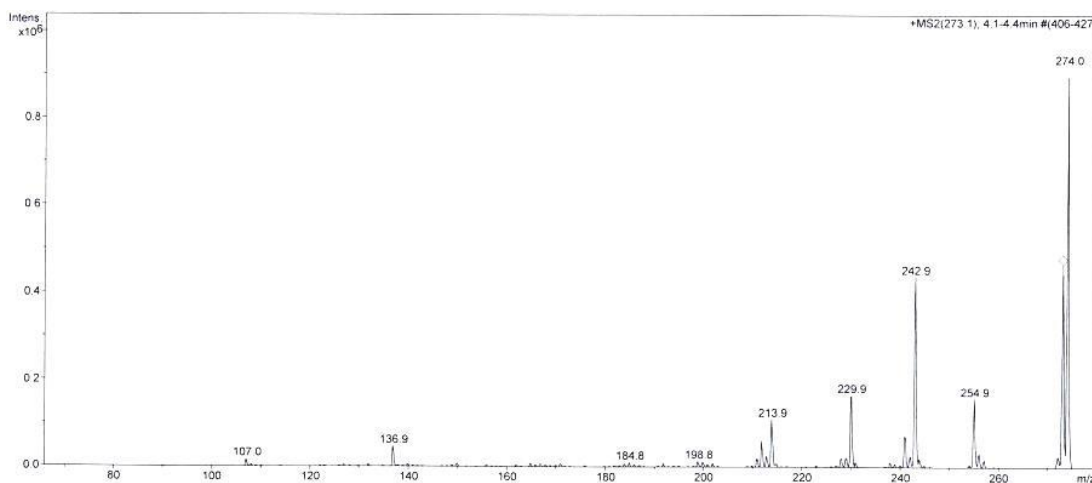


Figure 135: MS/MS of the molecular ion peak at 273.1370 shown in the mass spectrum in Figure 134.

The PAP-NAP system

A reaction containing 400 mM MEA, 1.3 mM EDDS, 0.18 mM Cu(II), 70 mM H₂O₂, 1 mM PAP and 1 mM naphthol (NAP) at pH 10 was left for 2 h at 20 °C, an ESI mass spectrum of the solution was acquired (Figure 136). Interestingly, no PAP-NAP dimer is observed under these conditions, but a hydroxylated adduct of the dimer could be responsible for the peak at 266. Additionally, the peak at 309 could represent a PAP-NAP dimer that incorporates MEA into the structure. The structures of both these postulated molecules are shown in Table 18. However, it is not known if the structures shown are the correct isomers.

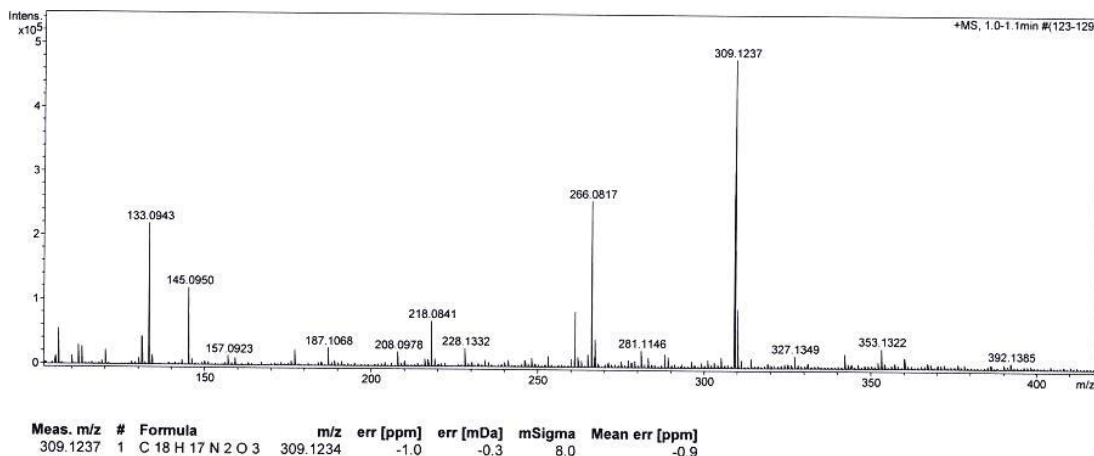


Figure 136: Mass spectrum for a reaction solution containing 400 mM MEA, 1.3 mM EDDS, 0.18 mM Cu(II), 70 mM H₂O₂, 1 mM PAP and 1 mM NAP, at pH 10, after 2 h at 20 °C.

The Corresponding ESI spectra for equivalent ammonia-containing formulations

When ammonia was used in equivalent dyeing formulations, as opposed to MEA, there was no evidence of peaks that corresponded to the incorporation of ammonia into the dye structures. There was also no evidence of peaks that corresponded to MEA-incorporated dyes, as seen in *Figure 137*, *Figure 138* and also in *Figure 130*.

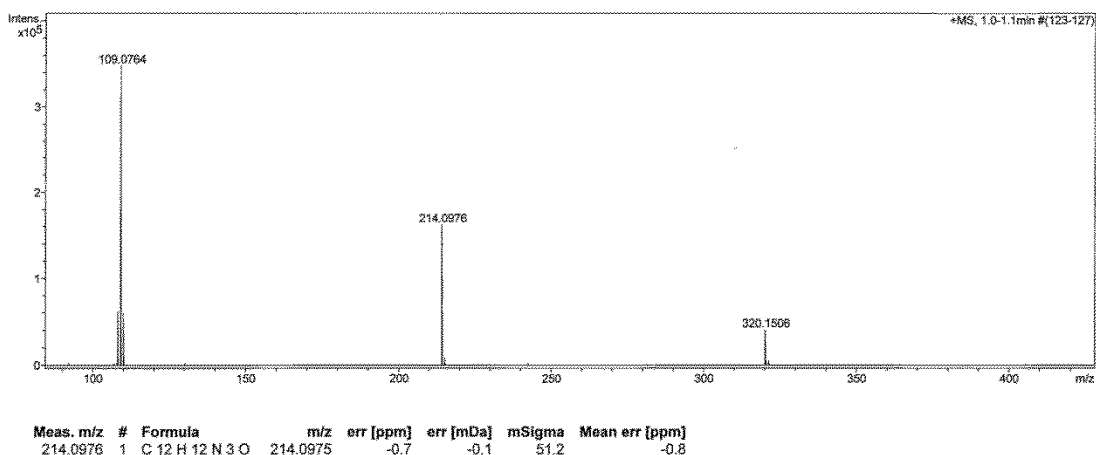


Figure 137: Mass spectrum for a reaction solution containing 400 mM NH_3 , 1.3 mM EDDS, 0.18 mM Cu(II), 70 mM H_2O_2 , 1 mM PPD and 1 mM MAP, at pH 10, after 2 h at 20 °C.

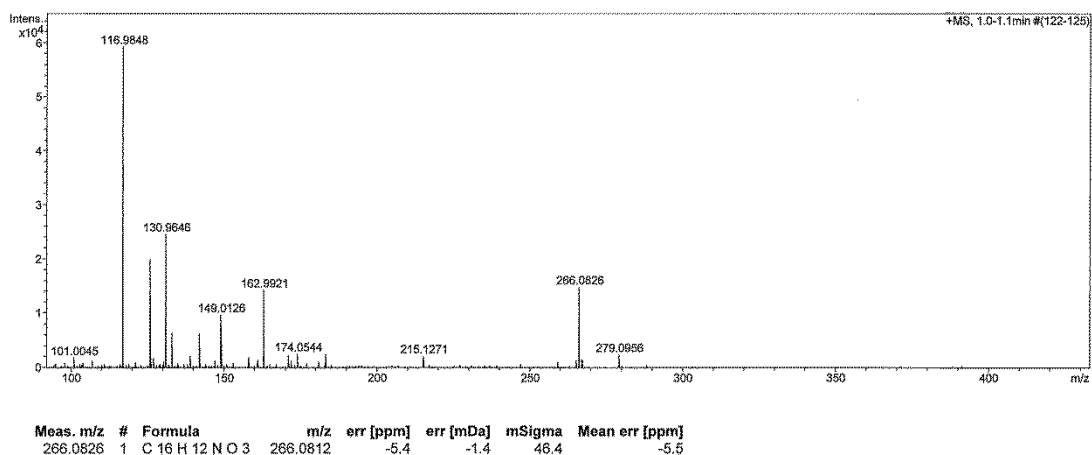


Figure 138: Mass spectrum for a reaction solution containing 400 mM NH_3 , 1.3 mM EDDS, 0.18 mM Cu(II), 70 mM H_2O_2 , 1 mM PAP and 1 mM NAP, at pH 10, after 2 h at 20 °C.

Abbreviations

[O]	Oxidising agent
°C	Degrees Celsius
°C min ⁻¹	Degrees Celsius per minute
¹³ C	Carbon-13
1D	One Dimensional
¹ H	Proton
2D	Two Dimensional
A	Hyperfine tensor (parallel region)
A _∞	Hyperfine tensor (perpendicular region)
AHT	5-amino- <i>o</i> -cresol
AMC	4-amino- <i>m</i> -cresol
ATR	Attenuated Total Reflectance
AU	Arbitrary Units
bs	Broad singlet
COSY	Correlation Spectroscopy
DAD	Diode Array Detector
DCA	Dichloroacetic acid
DCM	Dichloromethane
DFT	Density functional theory
DHI	5,6-dihydroxyindole
DHICA	5,6-dihydroxyindole-2-carboxylic acid
DMPO	5,5'-dimethyl-1-pyrroline-N-oxide
DTPMP	Diethylenetriamine penta(methylene phosphonic acid)
DTS	2,5-diaminotoluene sulfate
EDDS	Ethylenediamine- <i>N,N'</i> -disuccinic acid
EDTA	Ethylenediaminetetraacetic acid
EI	Electron Ionisation
EPR	Electron Paramagnetic Resonance
ESI	Electro Spray Ionisation

FT-IR	Fourier Transform - Infra Red
G	Gauss
g	Grams
GC	Gas Chromatography
GC-EI	Gas Chromatography Electron Ionisation
h	Hour
HDP	1-hydroxyethyl-4,5-diaminopyrazole
HEDP	Etidronic acid
HEI	1-(2-hydroxyethyl)imidazole
HMBC	Heteronuclear multiple bond correlation
HPLC	High Performance Liquid Chromatography
HPLC-MS	High Performance Liquid Chromatography - Mass Spectrometry
HSQC	Heteronuclear single quantum coherence
ICP-MS	Inductively Coupled Plasma Mass Spectrometry
INEPT	Insensitive nuclei enhanced by polarization transfer
IR	Infra-Red
K	Kelvin
kPa	kilopascals
MAP	<i>m</i> -aminophenol
MBB	1,4-diamino-2-methoxymethyl-benzene
MCR1	Melanocortin 1 receptor
MEA	Monoethanolamine
MFA	Melanin free acid
mg	milligrams
mg mL ⁻¹	milligrams per millilitre
MHz	Mega Hertz
mL min ⁻¹	millilitres per minute
mm	millimetre
mM	millimolar
MS	Mass Spectrometry

mW	milli Watt
NAP	1-naphthol
nm	nanometres
NMR	Nuclear Magnetic Resonance
NPDPA	5,5'-[(5-nitro-1,3-phenylene)diimino]bis(5-oxopentanoic acid)
ODS	Octadecyl silica
PAP	<i>p</i> -aminophenol
PDCA	Pyrrole-2,3-dicarboxylic acid
pH	power of Hydrogen
<i>p</i> -HBA	<i>p</i> -hydroxybenzoic acid
pKa	Acid dissociation constant
PPD	<i>p</i> -phenylenediamine
ppm	Parts per million
PSI	Pounds per square inch
PTCA	Pyrrole-2,3,5-tricarboxylic acid
QDI	Quinonediimine intermediate
R _f	Retardation factor
ROS	Reactive oxygen species
rpm	Revolutions per minute
s	second
SDS-PAGE	Sodium dodecyl sulfate polyacrylamide gel electrophoresis
SEM	Scanning Electron Microscopy
TEMPO	2,2,6,6-tetramethylpiperidine-1-oxyl
TLC	Thin Layer Chromatography
UV-Vis	Ultra Violet - Visible
V	Volts
λ _{max}	wavelength maximum
μm	micrometre

List of References

1. P. Walter, et al., *Nano Letters*, **2006**, 6, (10), 2215-2219.
2. P&G:Beauty&Grooming, *Hair color History*, <http://www.pgbeautyscience.com/hair-color-history.php>, Accessed 11/08/14, 2014.
3. J. F. Corbett, *J Soc Cosmet Chem*, **1984**, 35, (6), 297-310.
4. D. Lewis, J. Mama and J. Hawkes, *Materials*, **2013**, 6, (2), 517-534.
5. P. Yesudian, *Int J Trichology*, **2011**, 3, (2), 69.
6. D. J. Tobin, Biology of Hair Follicle Pigmentation, in *Hair Growth and Disorders*, eds. U. Blume-Peytavi, et al., Springer Berlin Heidelberg, **2008**, pp. 51-74.
7. P&G:Beauty&Grooming, *Hair Structure*, <http://pgbeautyscience.com/hair-structure.php>, Accessed 11/08/14, 2014.
8. L. J. Wolfram, *J Am Acad Dermatol*, **2003**, 48, (6), 106-114.
9. L. N. Jones and D. E. Rivett, *Micron*, **1997**, 28, (6), 469-485.
10. C. R. Robbins, *Chemical and physical behavior of human hair*, 3rd ed. edn., Springer-Verlag, New York ; London, **1994**.
11. J. A. Swift, *Nature*, **1964**, 203, 976-977.
12. E. K. Nishimura, *Pigm Cell Melanoma R*, **2011**, 24, (3), 401-410.
13. A. Slominski, et al., *J Invest Dermatol*, **2005**, 124, (1), 13-21.
14. A. J. Thody, et al., *J Investig Dermatol*, **1991**, 97, (2), 340-344.
15. G. Prota, *J Invest Dermatol*, **1980**, 75, (1), 122-127.
16. S. Ito and K. Wakamatsu, *Photochem Photobiol*, **2008**, 84, (3), 582-592.
17. N. Kollias, et al., *J Photoch Photobio B*, **1991**, 9, (2), 135-160.
18. N. Flanagan, et al., *Hum Mol Genet*, **2000**, 9, (17), 2531-2537.
19. S. Ito, *Pigm Cell Res*, **2003**, 16, (3), 230-236.
20. P. Prem, et al., *J Cosmet Sci*, **2003**, 54, (4), 395-409.

21. H. Ozeki, S. Ito and K. Wakamatsu, *Pigm Cell Res*, **1996**, 9, (2), 51-57.
22. K. Wakamatsu, et al., *J Neurochem*, **2003**, 86, (4), 1015-1023.
23. K. Wakamatsu and S. Ito, *Pigm Cell Res*, **2002**, 15, (3), 174-183.
24. A. Napolitano, et al., *Tetrahedron*, **1995**, 51, (20), 5913-5920.
25. S. Ito, et al., *Pigm Cell Melanoma R*, **2011**, 24, (4), 605-613.
26. A. R. Katritzky, et al., *Pigm Cell Res*, **2002**, 15, (2), 93-97.
27. B. B. Adhyaru, et al., *Magn Reson Chem*, **2003**, 41, (6), 466-474.
28. P. Thureau, et al., *Chem-Eur J*, **2012**, 18, (34), 10689-10700.
29. G. Prota, *Pigm Cell Res*, **1997**, 10, (1-2), 5-11.
30. G. W. Zajac, et al., *BBA-Gen Subjects*, **1994**, 1199, (3), 271-278.
31. L. Panzella, et al., *Pigm Cell Melanoma R*, **2014**, 27, (2), 244-252.
32. E. S. Krol and D. C. Liebler, *Chem Res Toxicol*, **1998**, 11, (12), 1434-1440.
33. A. Napolitano, et al., *Pigm Cell Melanoma R*, **2014**, 27, (5), 721-733.
34. T. Sarna, *J Photoch Photobio B*, **1992**, 12, (3), 215-258.
35. H. Fedorow, et al., *Prog Neurobiol*, **2005**, 75, (2), 109-124.
36. V. Dias, E. Junn and M. M. Mouradian, *Journal of Parkinson's Disease*, **2013**, 3, (4), 461-491.
37. W. Korytowski, T. Sarna and M. Zareba, *Arch Biochem Biophys*, **1995**, 319, (1), 142-148.
38. M. Sasaki, et al., *NeuroReport*, **2006**, 17, (11).
39. L. J. Wolfram and L. Albrecht, *J Soc Cosmet Chem*, **1987**, 38, (3), 179-191.
40. D. H. Johnson, *Hair & Hair Care*, Marcel Dekker, **1997**.
41. L. J. Wolfram, K. Hall and I. Hui, *J Soc Cosmet Chem*, **1970**, 21, (13), 875-900.
42. K. W. Herrmann, *Trans Faraday Soc*, **1963**, 59, 1663-1671.
43. A. D. Bailey, G. Zhang and B. P. Murphy, *J Cosmet Sci*, **2014**, 65, (1), 1-9.
44. A. N. Syed, W. W. Habib and A. M. Kuhajda, *Water-soluble polymers in hair care - Prevention and repair of damage during hair relaxing*, Plenum Press Div Plenum Publishing Corp, New York, **1998**, pp. 231-244.

45. M. G. Evans and N. Uri, *Trans Faraday Soc*, **1949**, 45, 224-230.
46. W. Korytowski and T. Sarna, *J. Biol. Chem.*, **1990**, 265, (21), 12410-12416.
47. S. Godfrey, et al., *Int J Cosmetic Sci*, **2013**, 35, (3), 264-271.
48. K. E. Smart, et al., *J Cosmet Sci*, **2009**, 60, (3), 337-345.
49. R. E. Noble, *Sci Total Environ*, **1999**, 239, (1-3), 189-193.
50. J. M. Marsh, et al., *Int J Cosmetic Sci*, **2008**, 30, (5), 383-383.
51. J. M. Marsh, et al., *Int J Cosmetic Sci*, **2014**, 36, (1), 32-38.
52. H. J. H. Fenton, *J Chem Soc Trans*, **1894**, 65, 899-910.
53. F. Haber and J. Weiss, *P Roy Soc Lond A Mat*, **1934**, 147, (861), 332-351.
54. F. Haber and R. Willstätter, *Ber Dtsch Chem Ges*, **1931**, 64, (11), 2844-2856.
55. W. G. Barb, et al., *Trans Faraday Soc*, **1951**, 47, 462-500.
56. K. Barbusinski, *Ecol Chem Eng S*, **2009**, 16, (3), 347-358.
57. S. X. Chen and P. Schopfer, *Eur J Biochem*, **1999**, 260, (3), 726-735.
58. C. Leeuwenburgh, et al., *Am J Physiol*, **1998**, 274, (2), 453-461.
59. T. C. Squier, *Exp Gerontol*, **2001**, 36, (9), 1539-1550.
60. K. R. Naqvi, et al., *Int J Cosmetic Sci*, **2013**, 35, (1), 41-49.
61. W. C. Bray and M. H. Gorin, *J Am Chem Soc*, **1932**, 54, 2124.
62. A. N. Pham, et al., *J Catal*, **2013**, 301, 54-64.
63. L. Deguillaume, M. Leriche and N. Chaumerliac, *Chemosphere*, **2005**, 60, (5), 718-724.
64. S. J. Hug and O. Leupin, *Environ Sci Technol*, **2003**, 37, (12), 2734-2742.
65. W. H. Koppenol and J. F. Liebman, *J Phys Chem*, **1984**, 88, (1), 99-101.
66. W. Freinbichler, et al., *J Inorg Biochem*, **2009**, 103, (1), 28-34.
67. A. Masarwa, et al., *Coordin Chem Rev*, **2005**, 249, 1937-1943.
68. S. Rachmilovich-Calis, et al., *Chem-Eur J*, **2009**, 15, (33), 8303-8309.
69. C. Walling, in *Oxidases and related redox systems*, eds. T. E. King, et al., University Park Press, **1973**, pp. 85-97.

70. M. J. Burkitt, *Free Radical Res Com*, **1993**, 18, (1), 43-57.
71. P. Wardman and L. P. Candeias, *Radiat Res*, **1996**, 145, (5), 523-531.
72. F. Buda, et al., *Chem-Eur J*, **2001**, 7, (13), 2775-2783.
73. C. E. Cooper, Chapter 3 Ferryl iron and protein free radicals, in *New Comprehensive Biochemistry*, eds. A. R.-E. Catherine and H. B. Roy, Elsevier, **1994**, vol. 28, pp. 67-111.
74. C. Rovira and I. Fita, *J Phys Chem B*, **2003**, 107, (22), 5300-5305.
75. A. Ivancich, et al., *Biochemistry*, **1997**, 36, (31), 9356-9364.
76. O. Horner, et al., *J Biol Inorg Chem*, **2007**, 12, (4), 509-525.
77. W. Freinbichler, et al., *J Inorg Biochem*, **2008**, 102, (5-6), 1329-1333.
78. B. S. Berlett and E. R. Stadtman, *J. Biol. Chem.*, **1997**, 272, (33), 20313-20316.
79. O. Smithies, *Science*, **1965**, 150, (3703), 1595-1598.
80. C. Robbins, *J Soc Cosmet Chem*, **1971**, 22, (6), 339-348.
81. P. J. Hogg, *Trends Biochem Sci*, **2003**, 28, (4), 210-214.
82. J. P. Danehy and V. J. Elia, *J Org Chem*, **1971**, 36, (10), 1394-1398.
83. J. Nachtigal and C. Robbins, *Text Res J*, **1970**, 40, (5), 454-457.
84. M. S. Jeong, et al., *J Dermatol*, **2010**, 37, (10), 882-887.
85. M. L. Tate, et al., *J Soc Cosmet Chem*, **1993**, 44, (6), 347-371.
86. C. R. Robbins and R. J. Crawford, *J Soc Cosmet Chem*, **1991**, 42, (1), 59-67.
87. S. Croft, et al., *J Chem Soc Perk T 2*, **1992**, (2), 153-160.
88. D. P. Griffiths, *Trying to decrease the decomposition rates of peracids (and H₂O₂) by solution-phase metal ions*, University of York, **2004**.
89. S. G. Bratsch, *J Phys Chem Ref Data*, **1989**, 18, (1), 1-21.
90. B. H. J. Bielski, et al., *J Phys Chem Ref Data*, **1985**, 14, (4), 1041-1100.
91. B. Morgan and O. Lahav, *Chemosphere*, **2007**, 68, (11), 2080-2084.
92. P. Salgado, et al., *J Chil Chem Soc*, **2013**, 58, (4), 2096-2101.
93. C. W. Jones, *Applications of Hydrogen Peroxide and Derivatives*, Royal Society of Chemistry, **1999**.

94. T. Kocha, et al., *BBA-Protein Struct M*, **1997**, 1337, (2), 319-326.
95. S. R. D. Program, *NIST critically selected stability constants of metal complexes database*, **2004**, National Institute of Standards and Technology, U.S. Dept. of Commerce, Gaithersburg, MD.
96. D. R. Lide, *CRC Handbook of Chemistry and Physics*, 73rd edn., CRC Press, **1993**.
97. K. R. Naqvi, *Role of transition metal ions in oxidative hair colouring*, University of York, **2014**.
98. L. Li, et al., *Anal Chim Acta*, **2004**, 512, (1), 121-124.
99. G. Applerot, et al., *RSC Adv*, **2012**, 2, (6), 2314-2321.
100. M. Yun, *Nitroxides in Mechanistic Studies: Ageing of Gold Nanoparticles and Nitroxide Transformation in Acids*, University of York, **2010**.
101. R. Richmond, et al., *Anal Biochem*, **1981**, 118, (2), 328-335.
102. D. Vione, et al., *Environ Chem Lett*, **2010**, 8, (1), 95-100.
103. M. Sahni and B. R. Locke, *Ind Eng Chem Res*, **2006**, 45, (17), 5819-5825.
104. S. Singh and R. C. Hider, *Anal Biochem*, **1988**, 171, (1), 47-54.
105. H. H. Tucker, *J Soc Cosmet Chem*, **1967**, 18, (10), 609-628.
106. A. W. Holmes, *J Soc Cosmet Chem*, **1964**, 15, 595-608.
107. F. Kind, K. Scherer and A. J. Bircher, *J Dtsch Dermatol Ges*, **2012**, 10, (8), 572-577.
108. K. S. Chugh, G. H. Malik and P. C. Singhal, *J Med*, **1982**, 13, (1-2), 131-137.
109. S. Handa, R. Mahajan and D. De, *Indian J Dermatol Ve*, **2012**, 78, (5), 583-590.
110. M. V. R. Velasco, et al., *Braz J Pharm Sci*, **2009**, 45, (1), 153-162.
111. T. Förster and M. J. Schwuger, Correlation between adsorption and the effects of surfactants and polymers on hair, in *Interfaces in Condensed Systems*, ed. G. H. Findenegg, Steinkopff, **1990**, vol. 83, pp. 104-109.
112. J. F. Corbett, *J Chem Soc Perk T 2*, **1972**, (5), 539-548.
113. J. F. Corbett, *J Soc Cosmet Chem*, **1973**, 24, 103-134.
114. R. L. Siegrist, M. Crimi and T. J. Simpkin, *In Situ Chemical Oxidation for Groundwater Remediation*, Springer, **2011**.

115. A. Sigel and H. Sigel, *Metal Ions in Biological Systems, vol. 36, Interrelations Between Free Radicals and Metal Ions in Life Processes*, Taylor & Francis, **1999**.
116. M. Masarwa, et al., *J Am Chem Soc*, **1988**, 110, (13), 4293-4297.
117. P. G. Beauty, *Clairol Nice n Easy Colorblend Foam MSDS*, [http://www.clairol.co.uk/m/docs/new/Clairol Nice n Easy Colorblend Foam %289-11%29.pdf](http://www.clairol.co.uk/m/docs/new/Clairol%20Nice%20n%20Easy%20Colorblend%20Foam%20MSDS.pdf), Accessed 18/02/2015.
118. Clairol, *How to color your hair at home with Nice'n Easy*, <https://www.youtube.com/watch?v=pwqWfeVAhfM>, Accessed 18/02/2015.
119. H. K. Hall, *J Am Chem Soc*, **1957**, 79, (20), 5441-5444.
120. F. Fujita, et al., *Int J Cosmetic Sci*, **2010**, 32, (3), 217-224.
121. J.-A. Seo, et al., *J Dermatol Sci*, **2012**, 66, (1), 12-19.
122. O. J. X. Morel and R. M. Christie, *Chem Rev*, **2011**, 111, (4), 2537-2561.
123. T. A. Wilson, *University of Illinois Bulletin*, **1925**, 22.
124. S. Kapteina, et al., *J Chem Eng Data*, **2005**, 50, (2), 398-402.
125. K. Kishore, G. R. Dey and T. Mukherjee, *Res Chem Intermediat*, **2005**, 31, (9), 875-884.
126. S. Mahapatra and R. S. Subrahmanya, *P Indian AS-Math Sci*, **1963**, 58, (3), 161-176.
127. R. B. King, *Mol Phys*, **2002**, 100, (10), 1567-1577.
128. R. Englman, *The Jahn-Teller Effect in Molecules and Crystals*, John Wiley & Sons Ltd, Wiley Monographs in Chemical Physics, **1972**.
129. O. G. Holmes and D. S. McClure, *J Chem Phys*, **1957**, 26, (6), 1686-1694.
130. R. M. Smith and A. E. Martell, *Critical Stability Constants*, **1989**.
131. G. Vázquez, et al., *J Chem Eng Data*, **1997**, 42, (1), 57-59.
132. H. H. King, J. L. Hall and G. C. Ware, *J Am Chem Soc*, **1930**, 52, (12), 5128-5135.
133. S. K. Singh, *Handbook on Cosmetics (Processes, Formulae with Testing Methods)*, NIIR Project Consultancy Services, **2010**.
134. I. A. Cody, et al., *J Inorg Nucl Chem*, **1970**, 32, (10), 3263-3269.

135. B. P. Murphy, Hair Colorants, in *Poucher's Perfumes, Cosmetics and Soaps*, ed. H. Butler, Kluwer Academic Publishers, London, 10th edn., **2000**, pp. 307-324.
136. M. L. Kremer, *J Phys Chem A*, **2003**, 107, (11), 1734-1741.
137. M. Scalzo, et al., *Int J Cosmetic Sci*, **2010**, 32, (3), 234-235.
138. The DOW Chemical Company, *DOW Ethanolamines Overview Brochure*, **2003**.
139. A. Melinder, *Thermophysical Properties of Aqueous Solutions Used as Secondary Working Fluids*, Royal Institute of Technology, KTH, **2007**.
140. Y.-M. Tseng and A. R. Thompson, *J Chem Eng Data*, **1964**, 9, (2), 264-267.
141. MettlerToledo, *Ammonia Refractometry concentration table (+20 °C)*, http://us.mt.com/us/en/home/supportive_content/application_editorials/Ammonia_re_e.html, Accessed 25/02/2015.
142. S. Ito and K. Fujita, *Anal Biochem*, **1985**, 144, (2), 527-536.
143. S. Ito and K. Wakamatsu, *Pigm Cell Res*, **2003**, 16, (5), 523-531.
144. C. R. Borges, et al., *Anal Biochem*, **2001**, 290, (1), 116-125.
145. J. C. Arnaud and P. Bore, *J Soc Cosmet Chem*, **1981**, 32, (3), 137-152.
146. S. Ghiani, et al., *Magn Reson Chem*, **2008**, 46, (5), 471-479.
147. S. Aime, et al., *Pigm Cell Res*, **1991**, 4, (5-6), 216-221.
148. R. R. Grinstead, *Biochemistry*, **1964**, 3, (9), 1308-1314.
149. A. Napolitano, et al., *Tetrahedron*, **1996**, 52, (26), 8775-8780.
150. T. Matsuura, *Tetrahedron*, **1977**, 33, (22), 2869-2905.
151. G. Gellerstedt, H.-L. Hardell and E.-L. Lindfors, *Acta Chem Scand*, **1980**, B34, 669-673.
152. W. Korytowski, et al., *Biochim Biophys Acta*, **1986**, 882, (2), 145-153.
153. W. S. Lee, *Int J Trichology*, **2009**, 1, (2), 94-99.
154. W. Korytowski, et al., *Photochem Photobiol*, **1987**, 45, (2), 185-190.
155. W. Froncisz, T. Sarna and J. S. Hyde, *Arch Biochem Biophys*, **1980**, 202, (1), 289-303.
156. B. Szpoganicz, et al., *J Inorg Biochem*, **2002**, 89, (1-2), 45-53.

157. M. Zareba, et al., *BBA-Mol Basis Dis*, **1995**, 1271, (2-3), 343-348.
158. B. Pilas, et al., *Free Radical Bio Med*, **1988**, 4, (5), 285-293.
159. L. Hong and J. D. Simon, *J Phys Chem B*, **2007**, 111, (28), 7938-7947.
160. L. K. Charkoudian and K. J. Franz, *Inorg Chem*, **2006**, 45, (9), 3657-3664.
161. L. Que and R. Y. N. Ho, *Chem Rev*, **1996**, 96, (7), 2607-2624.
162. E. J. Land and M. Ebert, *Trans Faraday Soc*, **1967**, 63, 1181-1190.
163. J. Fossey, D. Lefort and J. Sorba, *Free Radicals in Organic Chemistry*, Wiley, **1995**.
164. C. C. Felix, et al., *J Am Chem Soc*, **1978**, 100, (12), 3922-3926.
165. B. Ensing, et al., *Phys Chem Chem Phys*, **2002**, 4, (15), 3619-3627.
166. M. Magarelli, P. Passamonti and C. Renieri, *Rev CES Med Vet y Zootec*, **2010**, 5, (2), 18-28.
167. Y. Liu, et al., *Pigm Cell Res*, **2004**, 17, (3), 262-269.
168. B. G. Malmström and T. Vänngård, *J Mol Biol*, **1960**, 2, (2), 118-124.
169. D. Kivelson and R. Neiman, *J Chem Phys*, **1961**, 35, (1), 149-155.
170. K. R. Naqvi, J. Marsh and V. Chechik, *Dalton T*, **2014**, 43, (12), 4745-4751.
171. S. Nagakura and A. Kuboyama, *J Am Chem Soc*, **1954**, 76, (4), 1003-1005.
172. B. Poeggeler, et al., *Ann NY Acad Sci*, **1994**, 738, (1), 419-420.
173. B. Iddon, et al., *J Chem Soc B*, **1971**, 1887-1892.
174. D. Kenneally, Cunningham, H., *Hair Color Research Update*, http://www.pgbeautyscience.com/assets/files/research_updates/P&G_ResearchUpdate_Hair_Color.pdf, Accessed 17.07.14.
175. E. I. Valko and G. Barnett, *J Cosmet Sci*, **1952**, 3, (2), 108-117.
176. Y. Takagi, et al., *Bull Environ Contam Toxicol*, **1986**, 36, (1), 793-800.
177. K. C. Francis, D. Cummins and J. Oakes, *J Chem Soc Dalton*, **1985**, (3), 493-501.
178. W. Huang, et al., *Environ Sci Technol*, **2013**, 47, (4), 1952-1959.
179. R. J. Watts, et al., *J Hazard Mater*, **1999**, 69, (2), 229-243.

180. R. E. Hinchee, D. C. Downey and P. K. Aggarwal, *J Hazard Mater*, **1991**, 27, (3), 287-299.
181. K. A. Barrett and M. B. McBride, *Environ Sci Technol*, **2005**, 39, (23), 9223-9228.
182. K. E. Schwarzans, *Angew Chem Int Edit*, **1970**, 9, (12), 946-953.
183. R. B. Lauffer, *Chem Rev*, **1987**, 87, (5), 901-927.
184. C. Gouedard, et al., *Int J Greenh Gas Con*, **2012**, 10, 244-270.
185. G. S. Goff and G. T. Rochelle, *Ind Eng Chem Res*, **2004**, 43, (20), 6400-6408.
186. M. T. Johansen, *Degradation of Amines*, Norwegian University of Science and Technology, **2013**.
187. W. H. Dennis, L. A. Hull and D. H. Rosenblatt, *J Org Chem*, **1967**, 32, (12), 3783-3787.
188. I. G. R. Gutz, *CurTiPot*, Universidade de Sao Paulo, **2010**.
189. A. J. Sexton and G. T. Rochelle, *Ind Eng Chem Res*, **2010**, 50, (2), 667-673.
190. V. Sendyureva, *Unpublished Data*, Procter & Gamble, **2014**.
191. K. Fukatsu, *Text Res J*, **1989**, 59, (7), 405-410.
192. P&G:Beauty&Grooming, *Hair Damage*, <http://pgbeautyscience.com/hair-damage.php>, Accessed 17/02/2015, 2015.
193. R. C. Pauley, R. Hashemi and S. Caothien, *Analysis of Foaming Mechanisms in Amine Plants*, Pauley Gas Conditioning, Pall Corporation., American Institute of Chemical Engineer's Summer Meeting, **1988**.
194. E. D. Goddard and J. V. Gruber, *Principles of polymer science and technology in cosmetics and personal care*, CRC Press, **1999**.
195. J. F. Corbett, *J Chem Soc B*, **1969**, 207-212.
196. J. F. Corbett, *J Soc Cosmet Chem*, **1969**, 20, (4), 253-263.
197. W. D. Bush, et al., *P Natl Acad Sci USA*, **2006**, 103, (40), 14785-14789.
198. S. Gidanian and P. J. Farmer, *J Inorg Biochem*, **2002**, 89, (1-2), 54-60.
199. J. F. Corbett, *J Soc Cosmet Chem*, **1972**, 23, (11), 683-693.
200. T. A. Hinnners, et al., *Environ Health Persp*, **1974**, 8, 191-199.
201. T. Ozawa, A. Hanaki and K. Onodera, *Biochem. Int.*, **1991**, 24, (4), 661-667.

202. V. Valkovic, *Human Hair: Trace-element levels*, CRC Press, **1988**.
203. J. F. Corbett, *J Soc Dyers Colour*, **1976**, 92, (8), 285-303.
204. J. M. Wood, et al., *Faseb J*, **2009**, 23, (7), 2065-2075.
205. V. D. Artemchik, V. P. Kurchenko and D. I. Metelitsa, *Biochemistry-Moscow+*, **1985**, 50, (5), 698-705.
206. T. P. Ko, et al., *Acta Crystallogr D*, **2000**, 56, (2), 241-245.
207. F. C. Bernstein, et al., *J Mol Biol*, **1977**, 112, 535.
208. K. C. Brown and J. F. Corbett, *J Soc Cosmet Chem*, **1979**, 30, (4), 191-211.
209. R. M. Christie and O. J. X. Morel, The Coloration of Human Hair, in *The Coloration of Wool and other Keratin Fibres*, John Wiley & Sons, Ltd, **2013**, pp. 357-391.
210. D. Job and H. B. Dunford, *Eur J Biochem*, **1976**, 66, (3), 607-614.
211. D. Keilin and E. F. Hartree, *Biochem J*, **1955**, 60, (1-4), 310-325.
212. E. Bandrowski, *Ber.*, **1894**, 27, 480.
213. E. Erdmann, *Ber.*, **1904**, 37, 2906-2913.
214. J. F. Corbett, *Rev Prog Coloration*, **1973**, 4, (1), 3-7.
215. M. Dolinsky, et al., *J Soc Cosmet Chem*, **1968**, 19, (6), 411-422.
216. W. S. Enochs, et al., *Radiology*, **1997**, 204, (2), 417-423.
217. B. Larsson and H. Tjälve, *Acta Physiol Scand*, **1978**, 104, (4), 479-484.
218. R. E. Guthrie and S. H. Laurie, *Aust J Chem*, **1968**, 21, (10), 2437-2443.
219. U. Jakob, Reichmann, D., *Oxidative Stress and Redox Regulation*, 1 edn., Springer, **2013**.
220. V. Valkovic, *Human Hair II: Trace Element Levels*, CRC Press, **1988**.
221. S. C. Rastogi, et al., *Contact Dermatitis*, **2006**, 55, (2), 95-100.
222. SCCP, *Exposure to Reactants and Reaction Products of Oxidative Hair Dye Formulations*, **2005**.
223. H. H. Tucker, *Am Perf Cosm* **1968**, 83, 59-62.
224. J. F. Corbett, *Dyes Pigments*, **1999**, 41, (1-2), 127-136.

225. M. J. Shah, *J Soc Cosmet Chem*, **1977**, 28, (5), 259-271.
226. H. E. Gottlieb, V. Kotlyar and A. Nudelman, *J Org Chem*, **1997**, 62, (21), 7512-7515.
227. S. Chi and G. T. Rochelle, *Ind Eng Chem Res*, **2002**, 41, (17), 4178-4186.
228. L. A. Hull, et al., *J Phys Chem*, **1969**, 73, (7), 2142-2146.
229. W. W. Sułkowski and M. Bartoszek, *Pol J Environ Stud*, **2006**, 15, (4A), 41-43.
230. A. Takeda, et al., *J Biochem*, **1983**, 93, (4), 967-975.
231. C. E. Huckaba and F. G. Keyes, *J Am Chem Soc*, **1948**, 70, (4), 1640-1644.
232. A. I. Vogel, *A text-book of quantitative inorganic analysis, including elementary instrumental analysis*, Longman, **1962**.
233. J. Murphy and J. P. Riley, *Anal Chim Acta*, **1962**, 27, 31-36.